이학박사 학위논문

Effects of warming, prey, and predators on the distributions of mixotrophic dinoflagellates in Korean coastal waters and development of an automatic system for cultivating dinoflagellates on a 100-L scale

온난화, 먹이, 포식자가 혼합영양성 와편모류의 한국 연안 분포에 미치는 영향과 100리터급 와편모류 자동배양시스템 개발

2023 년 8 월

서울대학교 대학원
지구환경과학부

유 지 현

Effects of warming, prey, and predators on the distributions of mixotrophic dinoflagellates in Korean coastal waters and development of an automatic system for cultivating dinoflagellates on a 100-L scale

지도 교수 정 해 진

이 논문을 이학박사 학위논문으로 제출함

2023년 5 월

서울대학교 대학원
지구환경과학부
유 지 현

유지현의 이학박사 학위논문을 인준함

2023 년 7 월

위 원 장 _____(인)

부위원장 _____(인)

위 원 _____(인)

위 원 _____(인)

위 원 _____(인)

Abstract

Effects of warming, prey, and predators on the distributions of mixotrophic dinoflagellates in Korean coastal waters and development of an automatic system for cultivating dinoflagellates on a 100-L scale

Ji Hyun You
Oceanography
School of Earth and Environmental Sciences
College of Natural Sciences
Seoul National University

Mixotrophic dinoflagellates are one of the major components of marine ecosystems and are involved in global biogeochemical cycles as primary producers, prey, predators, and symbionts. Thus, the population dynamics of these organisms are closely linked to those of their prey and predators. Furthermore, they sometimes dominate in plankton assemblages and cause harmful algal blooms or red tides. Therefore, understanding the distributions of mixotrophic dinoflagellates is both ecologically and commercially important. The distributions of mixotrophic dinoflagellates are expected to change if global warming continues. These distribution changes will also have an impact on the distributions of their prey and predators. Thus, to predict the distribution change of mixotrophic dinoflagellates, the environmental factors affecting their growth and mortality should be investigated. The ecological factors influencing distributions of mixotrophic dinoflagellates include the availability of prey or nutrients, light intensity, water temperature, salinity, and predators. In this thesis, effects of warming, prey, and predators on mixotrophic dinoflagellates with different ecophysiological characteristics, namely, *Gymnodinium smaydae* and *Biecheleria cincta*, as well as on the phototrophic dinoflagellates, namely, *Scrippsiella* spp. were investigated. Furthermore, a new automatic system for cultivation of mixotrophic and heterotrophic dinoflagellates on a 100-L scale was developed using their ecophysiological characteristics.

In Chapter 2, to investigate the spatiotemporal distributions of the

mixotrophic dinoflagellates *B. cincta* and *G. smaydae* in Korean coastal waters and predict their distribution changes under global warming conditions, surface waters collected from 27 stations in Korean coastal waters during 2015–2018 were analyzed using the quantitative real-time polymerase chain reaction method. Through field observations, the presence of *B. cincta* and *G. smaydae* at each station was predicted when the temperature increased by 2, 4, and 6℃ compared with the water temperature at each station during 2015–2018. During the period from 2015 to 2018, *B. cincta* was detected at 13 stations and was present throughout all four seasons. *B. cincta* was detected at the highest number of stations (8 stations) in summer. However, its highest abundance was found in autumn at a water temperature of 25.1℃. During the experimental period, *G. smaydae* was detected at 24 stations and was present throughout all four seasons. Although it was present during all four seasons, it was detected at the highest number of stations (21 stations) in summer. Moreover, its highest abundance was found in summer at a water temperature of 23.8℃. Under ocean warming conditions, *B. cincta* was expected to not survive at some stations when the temperature increased by 2, 4, and 6℃ in summer and when it increased by 6℃ in autumn. However, *G. smaydae* was expected to not survive at some stations only in summer when the temperature increased by 2, 4, and 6℃. *B. cincta* had a narrow distribution in Korean coastal waters and was expected to be more vulnerable to temperature changes compared with *G. smaydae*.

In Chapter 3, to investigate warming effects on two mixotrophic dinoflagellates *B. cincta* and *G. smaydae*, their autotrophic and mixotrophic growth and ingestion rates at temperatures of 5–35℃ were determined. To measure their mixotrophic growth and ingestion rates, *B. cincta* and *G. smaydae* were provided with the raphidophyte *Heterosigma akashiwo* and the dinoflagellate *Heterocapsa rotundata*, respectively, as prey. At temperatures of 5–35℃, *B. cincta* and *G. smaydae* did not grow autotrophically. However, *B. cincta* and *G. smaydae* grew mixotrophically at temperaures of 15–25 and 10–32℃, respectively. Furthermore, their highest mixotrophic growth rates were found at 25℃. The narrow survival range of water temperature of *B. cincta* compared with that of *G. smaydae* can explain the narrower distribution and vulnerability of the former to temperature changes in the field. Thus, the results of Chapter 3 support the field observations of the two species in Chapter 2.

In Chapter 4, to investigate effects of predators on *G. smaydae*, whether common heterotrophic protists can feed on *G. smaydae* was explored and the growth and ingestion rates of certain predators feeding on *G. smaydae* were determined. *Oxyrrhis marina*, *Gyrodinium dominans*, *G. moestrupii*, and *Pelagostrobilidium* sp. fed on *G. smaydae* but *Polykrikos kofoidii* and *Oblea rotunda* did not feed on this dinoflagellate. *G. smaydae* supported the positive growth rates of *O. marina* and *G. dominans*, but the growth rates of both predators were lower than those feeding on other prey species. Therefore, *O. marina* and *G. dominans* may be effective predators of *G. smaydae*, but *G. smaydae* may not be the preferred prey for supporting the high growth of the predators compared with other prey species, as inferred from a literature survey. However, *B. cincta* was a prey species that supported the relatively high growth rates of *O. marina* and *Strobilidium* sp. according to previous studies. Therefore, the population dynamics of *G. smaydae* may have less impact on that of the predator *O. marina* compared with that of *B. cincta*.

In Chapter 5, to investigate effects of prey availability on the phototrophic *Scrippsiella* species, the mixotrophic ability of *S. donghaiensis*, *S. lachrymosa*, *S. masanensis*, *S. plana*, and *S. ramonii* after adding 15 potential prey items was explored. In addition, whether the mixotrophic dinoflagellate *S. acuminata* can feed on the fluorescently labeled microspheres (FLM) and heterotrophic bacteria (FLB) was investigated. *Scrippsiella* species are commonly found in marine ecosystems and sometimes cause harmful red tides. Although research on factors affecting the growth of *Scrippsiella* species, such as light, water temperature, and predators, has been consistently conducted, more studies are required on the mixotrophic abilities and prey species. The results of Chapter 5 show that the five *Scrippsiella* species did not feed on any potential prey, indicating a lack of mixotrophy. However, *S. acuminata* was observed to ingest both FLM and FLB, indicating its expanded prey spectrum. These results lowered the proportion of mixotrophic species relative to the total number of tested *Scrippsiella* species for mixotrophy from 100 to 29–38%. Owing to its mixotrophic ability, *S. acuminata* occupies an ecological niche that is distinct from that of *S. donghaiensis*, *S. lachrymosa*, *S. masanensis*, *S. plana*, and *S. ramonii*.

In Chapter 6, to academically and commercially utilize the cultures of useful mixotrophic and heterotrophic dinoflagellates, new cultivation systems

for the mixotrophs *G. smaydae* and *B. cicnta* and heterotrophs *G. dominans*, *P. kofoidii*, and *Noctiluca scintillans* on a 10-L or 100-L scale were developed. Mixotrophic and heterotrophic dinoflagellates are valuable owing to their abilities to produce useful materials and control the population of red tide-forming species. All species used in these experiments can controll red tide-forming species or produce valuable substances, such as omega-3 fatty acids and bioluminescent materials. However, their ecological and physiological characteristics make their cultivation challenging, limiting research and commercial applications. Thus, to cultivate useful mixotrophic and heterotrophic organisms, it is important to understand their ecophysiological characteristics with engineering techniques. To develop the systems, the optimal prey species were selected and the growth and ingestion rates of each predator on the optimal prey were explored. In addition, the intervals and amounts of prey addition were investigated using the growth rates of prey and predators. The cultivation system was scaled up from 10- to 100-L with the addition of a newly developed software. Using these systems, *G. smaydae*, *B. cincta*, *G. dominans*, *P. kofoidii*, and *N. scintillans* were successfully cultivated. Mass cultures produced in the developed system are free from contamination and thus, can be used for various experiments and commercialization purposes.

Overall, in this thesis, I explored effects of warming, prey, and predators on mixotrophic dinoflagellates through field observations and laboratory experiments. These dinoflagellates responded differently to the ecological factors, indicating their different distributions and ecological niches in marine ecosystems. Furthermore, I developed the automatic system for cultivating mixotrophic and heterotrophic dinoflagellates based on their ecophysiological features, thereby enabling diverse experiments. Therefore, by investigating the ecophysiological characteristics of mixotrophic dinoflagellates, this thesis contributes to a better understanding of the structure and function of marine ecosystems and their utilization for research and commercial purposes.

Keyword: Climate change, Ecophysiology, Marine ecosystem, Mass cultivation, Plankton, Protist, Red tide, Trophic mode

Student Number: 2017-22349

Table of Contents

List of Tables

List of Figures

Chapter 1. Introduction

1.1. Backgrounds

The ocean covers approximately 70% of Earth's surface and contains approximately 97% of Earth's water. Thus, the ocean plays an important role in the global cycling of materials. Marine ecosystems comprise the space, inorganic materials and energy occupying the space, and organisms living in the space (Jeong et al. 2022). Inorganic materials are sometimes incorporated into organic materials inside organisms that are then transferred to their predators by feeding. The organic materials are also released to the ambient waters after death. These processes are called the function of the ecosystem. Therefore, the function of the ecosystem is mainly performed through photosysnthesis, predator-prey relationships, and release of organic materials.

Dinoflagellates are one of the major components of marine ecosystems (Shields 1994; Carlos et al. 2000; Lewis et al. 2001; Jeong et al. 2010b, 2016; Park et al. 2011, 2013a; Turner et al. 2012; Hehenberger et al. 2019; Lee et al. 2020a; You et al. 2020a). They have three trophic modes, namely, autotrophy, mixotrophy (which includes kleptoplastidy), and heterotrophy. Autotrophic dinoflagellates play diverse roles as primary producers and prey, whereas heterotrophic dinoflagellates act as predators and prey for higher trophic levels. Mixotrophic dinoflagellates conduct all three roles, namely, primary producers, prey, and predators. Thus, the distributions of mixotrophic dinoflagellates are closely related to those of their prey and predators. Therefore, investigating the distributions of mixotrophic dinoflagellates and related environmental factors is crucial to understand the structure and functions of marine ecosystems.

Temperature is one of the major abiotic factors affecting the survival and growth, and in turn the distribution of mixotrophic dinoflagellates (Jeong et al. 2018). Each dinoflagellate species has an optimal temperature that supports their maximum growth rates, as well as lowest and highest temperatures required for survival. The response of dinoflagellates to temperature changes can be expressed as growth rates, which can affect the

distribution of dinoflagellates. Recently, owing to global warming, marine organisms face various environmental changes. These environmental changes exceed the resistance of marine organisms to change, thereby changing the distributions of many marine organisms. Therefore, it is important to investigate the response of marine organisms to changes in abiotic and biotic factors at the species level, considering the aforementioned situations. The autotrophic growth rates of mixotrophic dinoflagellates influenced by changes in water temperature have been extensively studied. However, mixotrophic growth rates of the dinoflagellates in response to changes in water temperature are scarcely investigated. To understand the distribution of mixotrophic dinoflagellates under changing water temperature, both autotrophic and mixotrophic growth rates should be considered (Lee et al. 2020b, You et al. 2020b, 2023a).

Prey and predators are major biotic factors that affect the population dynamics of mixotrophic dinoflagellates (e.g., Jeong et al. 2015). Although some mixotrophic dinoflagellates show enhanced growth when they have access to prey species, they show little to no growth in the absence of prey (Jeong et al. 2016). Therefore, it is important to explore the diversity of prey species that a mixotrophic dinoflagellate can feed on and determine its growth rate with and without prey. Furthermore, to assess the impact of predation on dinoflagellate populations, the kind of predators that can feed on the dinoflagellate and the growth and ingestion rates of predators of the dinoflagellate should be determined. In particular, heterotrophic dinoflagellates and ciliates are known to be effective predators of many phototrophic dinoflagellates (Kamiyama and Matsuyama 2005, Turner 2006). In addition, the predation impacts of heterotrophic protists are usually much greater than those of metazooplankton (Lee et al. 2017, Lim et al. 2017). Therefore, exploring predation by common heterotrophic protistan predators of a target dinoflagellate is also an important step in understanding the population dynamics of the dinoflagellate (Jeong at al. 2018c, You et al. 2020a, 2023b).

Owing to their ecological and physiological characteristics, mixotrophic and heterotrophic dinoflagellates have many benefits for living organisms, such as humans and animals. They produce useful materials, such as fatty

acids, amino acids, pigments, and bioluminescent compounds. Moreover, they often have significant grazing impact on phytoplankton species, implying that they can delay or control red tides or harmful algal blooms. In particular, they can be potentially used as biological controls of red tides or harmful algal blooms. However, most mixotrophic and heterotrophic dinoflagellates have preferred prey and different growth and ingestion rates depending on the prey species. Therefore, for their mass culture, the prey species and growth and ingestion rates on the prey species should be explored. The intervals and amounts of prey addition should be chosen using the growth and ingestion rates. Moreover, the growth and ingestion rates under abiotic factors, such as water temperature and light conditions, should also be investigated (Lim et al. 2020, You et al. 2022). These ecological and physiological characteristics of mixotrophic and heterotrophic dinoflagellates make mass cultivation challenging, which limits their research and commercial utilization.

In this thesis, the effects of abiotic (water temperature) and biotic (prey and predators) factors on the growth of mixotrophic dinoflagellates were explored to understand their distributions in marine ecosystems (**Figure 1.1**). Comparing the differences resulting from the ecophysiological characteristics of mixotrophic dinoflagellate species provides insights into their distributions and ecological niches. Therefore, two mixotrophic dinoflagellates, *Biecheleria cincta* and *Gymnodinium smaydae*, were selected for this study: the former feeds on diverse prey species but has moderate growth rates; and the latter feeds on certain prey species but has very high growth rates. Moreover, understanding the mixotrophic ability of species within the same genus is important for revealing their ecological niches and evolutionary trends. Thus, the dinoflagellate genus *Scrippsiella*, which includes major species causing red tides, was selected to investigate the impact of prey availability. Based on the results obtained from these studies, an automatic system for cultivating mixotrophic and heterotrophic dinoflagellates on a 100-L scale was developed and the useful dinoflagellates were successfully cultivated (**Figure 1.1**). Consequently, this thesis will contribute to a better understanding of the distribution patterns of mixotrophic dinoflagellates and their utilization (**Figure 1.1**).

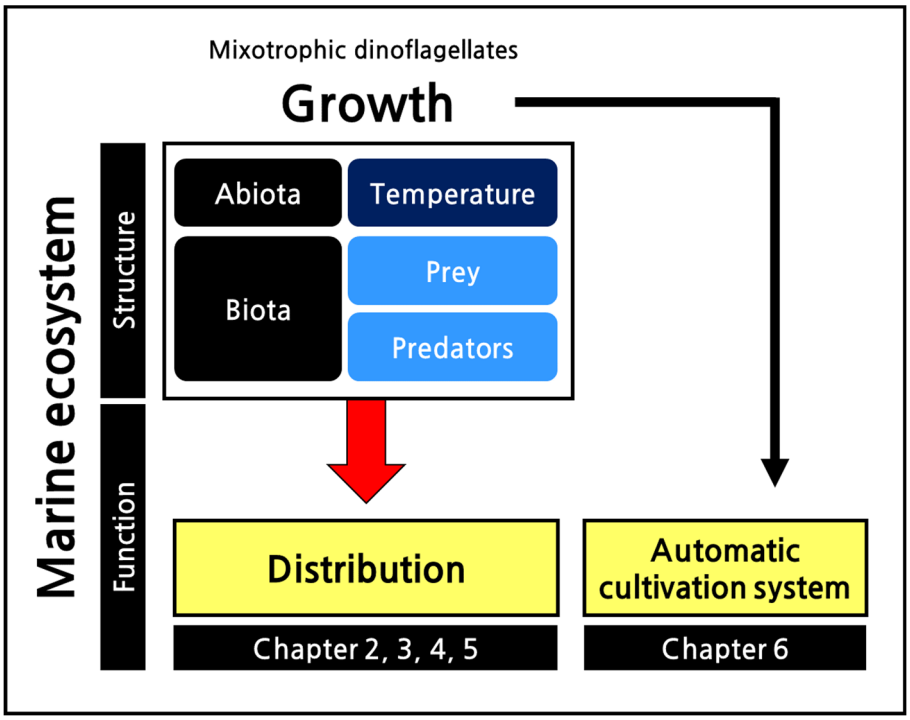

Figure 1.1. Thesis frame. To understand the structures and functions of marine ecosystems, mixotrophic dinoflagellates, which are one of the major components, were studied in this thesis. Among the factors affecting the distributions of mixotrophic dinoflagellates, warter temperature, prey, and predators were selected, and the effects of these factors on the survival and growth of mixotrophic dinoflagellates were explored in Chapters 2–5. In addition, to academically and commercially utilize the usefulness of dinoflagellates, an automatic cultivation system on a 100-L scale was developed in Chapter 6.

1.2. Research Aims

The overall objectives of my doctoral thesis were to: (a) investigate the effects of physical (water temperature) and biological (prey and predators) factors on the distributions of marine mixotrophic dinoflagellates; and (b) develop an automatic cultivation system on a 100-L scale for mixotrophic and heterotrophic dinoflagellates using their growth and ingestion rates feeding on the optimal prey (**Table 1.1**). The objectives of each chapter were as follows:

Chapter 2:

- To explore the spatiotemporal distributions of the mixotrophic dinoflagellates *Biecheleria cincta* and *Gymnodinium smaydae* in Korean coastal waters.
- To predict the distribution changes of *B. cincta* and *G. smaydae* under conditions of ocean warming.

Chapter 3:

- To determine the autotrophic and mixotrophic growth rates of the dinoflagellate *B. cincta* as a function of water temperature.
- To determine the autotrophic and mixotrophic growth rates of the dinoflagellate *G. smaydae* as a function of water temperature.

Chapter 4:

- To investigate whether heterotrophic protists can feed on the mixotrophic dinoflagellate *G. smaydae*.
- To determine the growth and ingestion rates of the heterotrophic dinoflagellates *Gyrodinium dominans* and *Oxyrrhis marina* and the ciliate *Pelagostrobilidium* sp. as a function of *G. smaydae* concentration.

Chapter 5:

- To explore whether each of the five *Scrippsiella* species is able to feed on potential prey species.

- To expand a prey spectrum of the mixotrophic dinoflagellate *Scrippsiella acuminata*.

Chapter 6:

- To develop a 10-L semi-continuous system and scale it up to a 100-L automatic system for cultivating useful mixotrophic and heterotrophic dinoflagellates.
- To test whether the developed systems can cultivate the mixotrophic dinoflagellates *G. smaydae* and *B. cincta* and the heterotrophic dinoflagellates *G. dominans*, *Polykrikos kofoidii*, and *Noctiluca scintillans*.

Chapter 7 combined the results of Chapters 2–6 and provided a comprehensive understanding of the distributions of mixotrophic dinoflagellates under current and global warming conditions, as well as the necessity of the automatic cultivation system for future research and commercial utilization.

Table 1.1. Summary of research aims.

Ch.	Major content	Aim	Ecological level	Cause	
				Physical factor	Biological factor
2	Ecophysiology	● To explore the spatiotemporal distributions of the mixotrophic dinoflagellates *Biecheleria cincta* and *Gymnodinium smaydae* in Korean coastal waters. ● To predict the distributions of *B. cincta* and *G. smaydae* under ocean warming conditions.	Species	Temperature	
3	Ecophysiology	● To determine the autotrophic and mixotrophic growth rates of the dinoflagellates *B. cincta* and *G. smaydae* as a function of water temperature.	Species	Temperature	Prey
4	Ecophysiology	● To investigate whether heterotrophic protists can feed on the mixotrophic dinoflagellate *G. smaydae*. ● To determine the growth and ingestion rates of the heterotrophic dinoflagellates *Gyrodinium dominans* and *Oxyrrhis marina* and the ciliate *Pelagostrobilidium* sp. as a function of *G. smaydae* concentration.	Species		Predator
5	Ecophysiology	● To explore whether each of five *Scrippsiella* species is able to feed on any of potential prey items.	Species		Prey

		● To investigate whether the mixotrophic dinoflagellate *S. acuminata* is able to feed on heterotrophic bacteria and microspheres (diameter= 2 μm).		
6	Ecophysiology, Application	● To develop cultivation systems for mixotrophic and heterotrophic dinoflagellates on 10-L (semi-continuous sytem) and 100-L scales (automatic system). ● To test whether the developed systems can cultivate the mixotrophic dinoflagellates *G. smaydae* and *B. cincta* and the heterotrophic dinoflagellates *G. dominans*, *Polykrikos kofoidii*, and *Noctiluca scintillans*.	Species	Temperature Prey Light

Chapter 2.
Spatiotemporal distributions of the mixotrophic dinoflagellates *Biecheleria cincta* and *Gymnodinium smaydae* under current temperature and global warming conditions*

2.1. Introduction

Phototrophic dinoflagellates that are autotrophic or mixotrophic species are major components of marine ecosystems and they play diverse roles as primary producers, predators, prey, parasites, and symbiotic partners (Shields 1994; Carlos et al. 2000; Lewis et al. 2001; Jeong et al. 2010b, 2016; Park et al. 2011, 2013b; Turner et al. 2012; Hehenberger et al. 2019; Lee et al. 2020a; You et al. 2020a). If a phototrophic dinoflagellate is an exclusively autotrophic species, it plays the roles of primary producer and prey, but if it is a mixotrophic species, it plays the roles of primary producer, prey, and predator (Jeong et al. 2010a, b, 2015). Phototrophic dinoflagellates often dominate plankton assemblages and cause red tides or harmful algal blooms (Campbell et al. 2010; Jeong et al. 2021). Thus, the distribution of a phototrophic dinoflagellate is important in understanding the structure and function of marine planktonic communities and to minimize losses due to red tides or harmful algal blooms.

Seawater temperature in coastal regions has increased due to global warming (Cox et al. 2000; Trenberth et al. 2007; IPCC 2021). Elevated temperature affects primary production at the community level and growth and survival of marine organisms at the species level (Grzebyk and Berland 1996; Brierley and Kingsford 2009; Koprivnikar et al. 2010; Kim et al. 2011;

* This chapter has been published in Marine Biology and Algae.
Lee, S. Y., Jeong, H. J.*, Ok, J. H., Kang, H. C. & **You, J. H**. 2020. Spatio-temporal distributions of the newly described mixotrophic dinoflagellate *Gymnodinium smaydae* in Korean coastal waters. Algae, 35:225–236.
You, J. H., Jeong, H. J.*, Ok, J. H., Kang, H. C., Park, S. A., Eom, S. H., Lee, S. Y. & Kang, N. S. 2023. Effects of temperature on the autotrophic and mixotrophic growth rates of the dinoflagellate *Biecheleria cincta* and its spatiotemporal distributions under current temperature and global warming conditions. Mar. Biol., 170:15.

Gao et al. 2012; Pistevos et al. 2015; You et al. 2020b). If an organism is a key species or plays diverse roles as a primary producer and predator in food webs, its growth and survival could affect the structure and function of the community (Petchey et al. 1999; Turner et al. 2000; Moline et al. 2004; Wiklund et al. 2009). Therefore, the effects of water temperature on the distribution of the species should be investigated at the species level.

The dinoflagellates *Biecheleria cincta* and *Gymnodinium smaydae* are heterotrophy-dominant mixotrophic dinoflagellates (Kang et al. 2011; Lee et al. 2014a; Jeong et al. 2021). The dinoflagellate genus *Biecheleria* was newly established from the genus *Woloszynskia*, based on its very unusual morphology and ultrastructure and molecular data (Moestrup et al. 2009). The heterotrophic dinoflagellates *Gyrodinium* spp., *Polykrikos kofoidii*, and *Oxyrrhis marina*, and the ciliate *Strobilidium* sp. were known to feed on *B. cincta* WCSH0906 (Yoo et al. 2013). The dinoflagellate *Gymnodinium smaydae*, belonging to the family Gymnodiniaceae, was newly described in 2014 (Kang et al. 2014). Some heterotrophic protists such as the common heterotrophic dinoflagellates *Oxyrrhis marina* and *Gyrodinium dominans* and the naked ciliate *Pelegostrobilidium* sp. are able to feed on *G. smaydae* (Jeong et al. 2018c; Chapter 4). Thus, *B. cincta* and *G. smaydae* plays diverse roles in marine ecosystems (Kang et al. 2011; Yoo et al. 2013; Lee et al. 2014a; Jeong et al. 2018c). However, the nationwide distributions of *B. cincta* and *G. smaydae* have not yet been investigated. Furthermore, the distribution change of *B. cincta* and *G. smaydae* under global warming condition have not been predicted.

A dinoflagellate was isolated from Shiwha Bay, Korea, in 2010 and established as a clonal culture. To identify the taxonomic position of this dinoflagellate, molecular and morphological analyses under a light microscope, field emission scanning electron microscope (FE-SEM), and transmission electron microscope (TEM) were conducted. Based on these molecular and morphological analyses, the dinoflagellate was identified as *B. cincta*, with a similar description of the holotype of *B. cincta* (Siano et al. 2009). The strain was named *B. cincta* BCSH1005, based on morphological and genetic characterizations of *B. cincta* BCSH1005 described in the present study. In this study, the spatial and temporal distributions of *B. cincta*

BCSH1005 and *G. smaydae* GSSH1005 at 27 stations along the Korean coasts were investigated 16 times seasonally during 2015–2018 using the molecular method of the real-time polymerase chain reaction (qPCR). Cells of *B. cincta* BCSH1005 and *G. smaydae* GSSH1005 were too small to distinguish this species from similar species in fixed samples (12–15 μm in cell length); thus, the qPCR method was used. The specific primer-probe set for detecting *B. cincta* BCSH1005 was newly designed and established in this study. Using the data on the spatiotemporal distributions of *B. cincta* BCSH1005 and *G. smaydae* GSSH1005 during 2015–2018, their presences at each station were predicted when the temperature increased by 2, 4, and 6℃ compared to the water temperature at each station during 2015–2018. This research lays the groundwork for understanding the distributions of *B. cincta* BCSH1005 and *G. smaydae* GSSH1005 under current temperature and global warming conditions.

2.2. Materials and Methods

2.2.1. Preparation of experimental organisms

A clonal culture of *B. cincta* BCSH1005 was originally isolated from Shiwha Bay in May 2010 when water temperature and salinity were 17.8℃ and 27.9, respectively. A dense culture (ca. 3,000 cells mL^{-1}) of *B. cincta* BCSH1005 was transferred every week to a 270-mL culture flask containing a fresh culture of *H. akashiwo* HAKS9905 (ca. 30,000 cells mL^{-1}) in 0.2-μm filtered sea water. All flasks were placed on a shelf at 20℃ under an illumination of 20 μmol photons m^{-2} s^{-1} from cool-white fluorescent light with a 14:10 h Light-Dark (L:D) cycle.

A clonal culture of *G. smaydae* GSSH1005 was originally isolated from Shiwha Bay in May 2010 when water temperature and salinity were 17.8℃ and 27.9, respectively. A dense culture (ca. 5,000 cells mL^{-1}) of *G. smaydae* GSSH1005 was transferred every week to a 270-mL culture flask containing a fresh culture of *Heterocapsa rotundata* (ca. 50,000 cells mL^{-1}) in 0.2-μm filtered sea water. All flasks were placed on a shelf under same conditions mentioned above.

2.2.2. Morphology of *Biecheleria cincta* BCSH1005

The general morphology of living and fixed cells of *B. cincta* BCSH1005 was investigated using an inverted microscope (Axiovert 200M; Carl Zeiss, Göttingen, Germany) at a magnification of 1,000 × or 400 ×. Image-analysis software (ZEN3.0 Pro; Carl Zeiss) with a digital camera connected to the inverted microscope was used to measure the length and width of living and fixed cells of *B. cincta* BCSH1005.

For FE-SEM observation, 10-mL aliquots of cultures (approximately 8 × 10^3 cells mL^{-1}) were fixed for 10 min in osmium tetroxide (OsO_4) at a final concentration of 1% (v/v). The fixed cells were collected on 3-μm pore size polycarbonate (PC) membrane filters (Whatman Inc., Kent, UK). Residual salts in the filters were removed by washing three times in 50% filtered

seawater diluted with distilled water. Dehydration of the filters was conducted using a graded ethanol series (10, 30, 50, 70, 90, and 100% ethanol) and followed by two changes in 100% ethanol. The filters were dried using a critical point dryer (EM CPD300; Leica, Wetzlar, Germany). The dried filters were mounted on an aluminum stub (Electron Microscopy Sciences, Hatfield, PA, USA) using copper conductive double-sided tape (Ted Pella, Redding, CA, USA) and coated with gold using an ion sputter coater (MC1000; Hitachi, Tokyo, Japan). A high resolution Sigma 500/VP FE-SEM (Carl Zeiss) was used to observe cell-surface morphologies.

For TEM observation, cells of *B. cincta* BCSH1005 were transferred to a 10-mL test tube and fixed in 2.5% glutaraldehyde (v/v; final concentration) for 1.5 h. Test-tube contents were placed in a 10-mL centrifuge tube and concentrated at 1,610 × g for 10 min using a Centrifuge VS-5500 (Vision, Bucheon, Korea). Subsequently, the pellet was transferred into a 1.5-mL test tube and washed in 0.2-M sodium cacodylate buffer at pH 7.4. The washed pellet was post-fixed for 90 min in 1% (w/v) OsO_4 in deionized H_2O and then embedded in agar. Dehydration of the pellet was carried out using an ethanol series of 50, 60, 70, 80, 90, and 100% and completed in the two changes in 100% ethanol. The dehydrated pellet was embedded in Spurr's resin (Electron Microscopy Sciences) and then sectioned using EM UC7 ultramicrotome (Leica). Finally, the sectioned sample was stained with 3% (w/v) aqueous uranyl acetate and lead citrate and observed using Sigma 500/VP TEM (Carl Zeiss).

2.2.3. DNA sequencing and phylogenetic analysis

Ten cells were isolated from a *B. cincta* BCSH1005 culture and added into a 0.2-mL PCR tube with 38.75-μL deionized sterile distilled water (DDW). PCR amplification was conducted with adding a mixture of 1-μL dNTP mix, 0.25-μL F-StarTaq DNA polymerase, 5-μL 10X F-StarTaq buffer (BioFACT Co., Ltd., Daejeon, Korea), and 2-μL of each primer needed for amplification of the ribosomal DNA (rDNA) of small subunit (EukA, G17F, G18R, and ITSR2), large subunit (ITSF2, D1R, LSU500R, and 1483R), and internal transcribed spacers (G17F, ITSR2, ITSF2, and LSU500R) regions to

the test tube (**Table 2.1**). The PCR thermal profile on AllInOneCycler (Bioneer, Daejeon, Korea) consisted of the following three steps: DNA denaturation (95℃ for 2 min), primer annealing (38 cycles at 95℃ for 20 s, the annealing temperature for 40 s, and 72℃ for 1 min), and DNA extension (72℃ for 5 min). An AccuPrep DNA Purification Kit (Bioneer) was used to purify the PCR products, and an ABI 3730XL DNA Analyzer (Applied Biosystems, Foster City, CA, USA) to perform sequencing. Using ContigExpress (Infomax, Frederick, MD, USA), sequences were aligned and manually edited.

Large subunit (LSU) and internal transcribed spacers (ITS; including ITS1, 5.8S rDNA, and ITS2) rDNA sequences of *B. cincta* BCSH1005, other *B. cincta* strains, and related dinoflagellates in the order Suessiales obtained from GenBank were aligned (MEGA v4; Tamura et al. 2007) to obtain the phylogenetic tree. The LSU and ITS rDNA phylogenetic trees were constructed using a Bayesian analysis (the default GTR + G + I model in MrBayes v3.1; Ronquist and Huelsenbeck 2003) and maximum likelihood analysis (the default GTRGAMMA model in RAxML 7.0.3 program; Stamatakis 2006).

2.2.4. Collection of field samples and hydrological properties

Field samples were collected using a clean bucket from the surface waters of 27 stations in Korean coastal waters, including those of Jeju Island, 16 times seasonally from April 2015 to October 2018 (**Figure 2.1**): seven stations were in the West Sea of Korea; nine stations were in the South Sea; six stations in the East Sea; and five stations were near Jeju Island.

For qPCR, cells in 50–300 mL of the surface water samples collected from each station at each time were obtained by filtering through a 25-mm GF/C filter (Whatman Inc.) and the filter was stored at ca. -20℃ in a cooler filled with dry ice until transported to the laboratory.

The data on the major environmental parameters such as salinity, water temperature, chlorophyll-a (chl-a), dissolved oxygen (DO), silicate (SiO_2),

phosphate (PO_4), and nitrite plus nitrate (NO_2+NO_3, hereafter NO_3) at 27 stations were obtained from Kang et al. (2019).

2.2.5. Design of a primer-probe set for *Biecheleria cincta* BCSH1005

For qPCR, a primer-probe set for *B. cincta* BCSH1005 was designed by aligning ITS sequences of *B. cincta* BCSH1005 and other related dinoflagellates (the order Suessiales) which were obtained from GenBank. The procedures for the design of the primer-probe set were described in detail in Lee et al. (2017b).

The specificity of the designed primers and probe for *B. cincta* BCSH1005 was tested using each DNA extract of *B. cincta* BCSH1005, other related dinoflagellates species, and the prey species (**Table 2.2**). The qPCR to test the specificity of the primer-probe set was conducted using the steps modified from Lee et al. (2017b). The qPCR assay was conducted using Rotor-Gene Q (Qiagen, Hilden, Germany) according to Lee et al. (2017b).

2.2.6. Quantification of the abundance of *Biecheleria cincta* BCSH1005 and *Gymnodinium smaydae* GSSH1005 in field using qPCR

Using the DNA extracted from 15–30 mL of a dense *B. cincta* BCSH1005 culture (targeting 100,000 cells in the final elution volume of 100 μL), a standard curve for quantifying the abundance of *B. cincta* BCSH1005 was obtained. To prepare six different DNA concentrations (1, 10, 100, 1,000, 10,000 and 100,000 cells), the extracted DNA was serially diluted by adding predetermined volumes of DDW to 1.5-mL tubes. The qPCR assay to generate the standard curve of *B. cincta* BCSH1005 was conducted as described above. The standard curve of *G. smaydae* GSSH1005 was obtained form Lee and You et al. (2020).

The DNA extract of a field water sample was used as a template, while only DDW was used as a non-template control, a DDW plus reaction mix as a negative control, and the DNA extract of cells of a *B. cincta* BCSH1005 or *G. smaydae* GSSH1005 culture as positive and standard controls. To ensure the accuracy of results, quadruple templates from each DNA sample were amplified. This analysis could detect a minimum of one cell of the target species per reaction and a minimum of 0.3 cells mL^{-1} in a reaction, considering the filtered seawater volume (50–300 mL).

2.2.7. *Biecheleria cincta* BCSH1005 and *Gymnodinium smaydae* GSSH1005 distribution prediction under ocean warming condition

To predict the distribution of *Biecheleria cincta* BCSH1005 and *Gymnodinium smaydae* GSSH1005 under ocean warming conditions, data on the spatial and temporal distributions of *B. cincta* BCSH1005 and *G. smaydae* GSSH1005 obtained from the present study and data on the water temperatures obtained from Kang et al. (2019) were used.

During the study period, *B. cincta* BCSH1005 appeared at the water temperatures of 8.6–25.4℃. Thus, this range was used as a criterion for the survival of *B. cincta* BCSH1005 under ocean warming conditions. In addition, *G. smaydae* GSSH1005 appeared at the water temperatures of 7.6–28.0℃. Thus, this range was used as a criterion for the survival of *G. smaydae* GSSH1005 under ocean warming conditions. The water temperatures at certain stations, where *B. cincta* BCSH1005 or *G. smaydae* GSSH1005 was detected at least once during the study period, were increased by 2, 4, and 6℃ in each season; spring, summer, autumn, and winter.

2.2.8. Statistical analysis

To investigate any one-to-one statistical relationships between environmental parameters (water temperature, salinity, chl-a, DO, NO_3, PO_4,

or SiO_2) and field abundance of *B. cincta* BCSH1005 or *G. smaydae* GSSH1005, correlation analyses were conducted. All statistical analyses were conducted with SPSS ver. 25 (IBM-SPSS Inc., Armonk, NY, USA) at a significance level of 0.05.

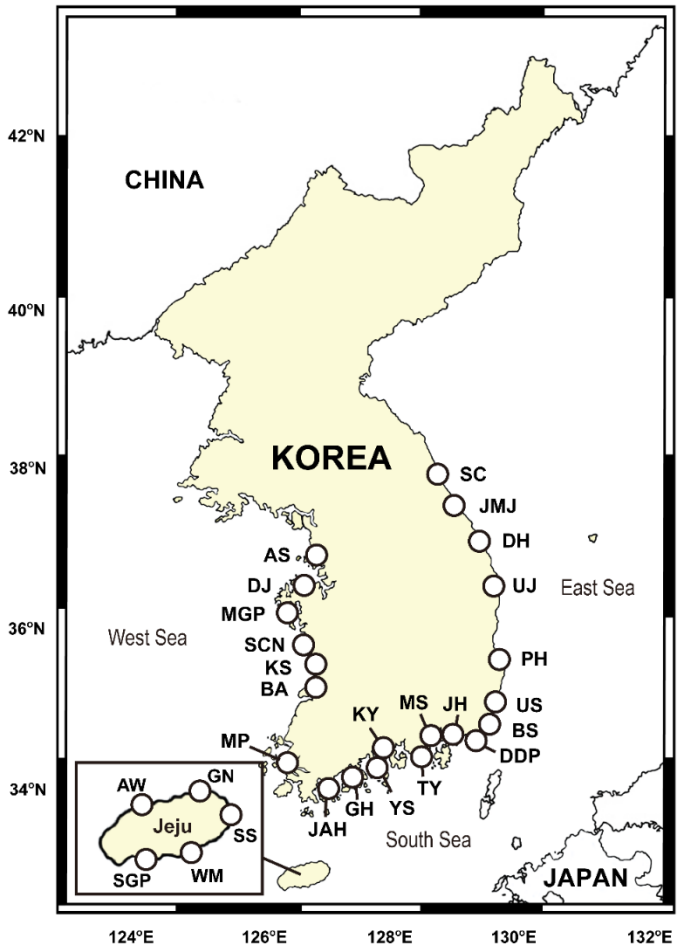

Figure 2.1. The sampling stations in Korean coastal waters from April 2015 to October 2018. Six stations [Sokcho (SC), Jumunjin (JMJ), Donghae (DH), Uljin (UJ), Pohang (PH), and Ulsan (US)] in the East Sea; nine stations [Busan (BS), Dadaepo (DDP), Jinhae (JH), Masan (MS), Tongyoung (TY), Kwangyang (KY), Yeosu (YS), Goheung (GH), and Jangheung (JAH)] in the South Sea; seven stations [Mokpo (MP), Buan (BA), Kunsan (KS), Seocheon (SCN), Mageompo (MGP), Dangjin (DJ), and Ansan (AS)] in the West Sea; five stations [Gimnyeong (GN), Seongsan (SS), Wimi (WM), Seogwipo (SGP), and Aewol (AW)] in Jeju Island.

Table 2.1. Oligonucleotide primers used to amplify the small subunit (SSU), internal transcribed spacers (ITS; including ITS1, 5.8S, and ITS2), and large subunit (LSU) of ribosomal DNA and the specific primers and Taq-Man probe used to determine the abundance of *Biecheleria cincta* BCSH1005 using qPCR.

Target gene	Analysis	Primer/Probe name	Sequence (5′–3′)		Reference
SSU	PCR	EUKA	Forward	CTG GTT GAT CCT GCC AG	(1)
		G17F	Forward	ATA CCG TCC TAG TCT TAA CC	(2)
SSU-ITS	PCR	G18R	Reverse	GCA TCA CAG ACC TGT TAT TG	(2)
		ITSR2	Reverse	TCC CTG TTC ATT CGC CAT TAC	(2)
ITS-LSU	PCR	ITSF2	Forward	TAC GTC CCT GCC CTT TGT AC	(2)
		LSU500R	Reverse	CCCTCATGGTACTTGTTTGC	(2)
	qPCR	BCSH1005_F	Forward	GCA GCT TCT GCA ACT TGT GA	(3)
		BCSH1005_R	Reverse	TTG CTG ACC TGA CTT CAT GC	(3)
		BCSH1005_P	Probe	[FAM] AAC ACG ACT CTC TTT GAG TCT CCC ATG [BHQ1]	(3)
		GSSH1005_F	Forward	GCC AAC TCA CTG AGC ATT TCT A	(4)
		GSSH1005_R	Reverse	CAT GCG CCA AGC TAT TGG AAA G	(4)
		GSSH1005_P	Probe	[FAM] TGC GCT TTA AGT TGC GCC AGT TG [BHQ1]	(4)
LSU	PCR	D1R	Forward	ACC CGC TGA ATT TAA GCA TA	(5)
		1483R	Reverse	GCT ACT ACC ACC AAG ATC TGC	(5)

(1) Medlin et al. 1988; (2) Litaker et al. 2003; (3) This study; (4) Lee and You et al. 2020; (5) Scholin et al. 1994

Table 2.2. List of species used to verify the specificity of the primer-probe set for *Biecheleria cincta* BCSH1005 and quantitative real-time polymerase chain reaction results. NA, not available; +, detected; -, not detected.

Taxon	Species	Strain name	Origin	Result
Dinoflagellate, Suessiales	*Biecheleria cincta*	BCSH1005	Shiwha bay, Korea	+
Cryptophyte, Pyrenomonadales	*Rhodomonas salina*	RS	NA	-
Cryptophyte, Pyrenomonadales	*Teleaulax amphioxeia*	TSGS0202	Buan, Korea	-
Dinoflagellate, Amphidiniales	*Amphidinium carterae*	SIO PY-1	USA	-
Dinoflagellate, Gymnodiniales	*Gymnodinium smaydae*	GSSH1005	Shiwha bay, Korea	-
Dinoflagellate, Gymnodiniales	*Gyrodinium dominans*	GDJK1907	Jeongok, Korea	-
Dinoflagellate, Gymnodiniales	*Paragymnodinium shiwhaense*	PSSH0605	Shiwha bay, Korea	-
Dinoflagellate, Peridiniales	*Heterocapsa rotundata*	HRSH1201	Shiwha bay, Korea	-
Dinoflagellate, Suessiales	*Biecheleriopsis adriatica*	BATY06	Tongyoung, Korea	-
Dinoflagellate, Suessiales	*Ansanella granifera*	AGSW10	Shiwha bay, Korea	-
Dinoflagellate, Suessiales	*Pelagodinium bei*	RCC3593	English channel	-
Dinoflagellate, Suessiales	*Yihiella yeosuensis*	YYYS1405	Yeosu bay, Korea	-
Dinoflagellate, Suessiales	*Effrenium voratum*	SVFL1	Jeju Island, Korea	-
Dinoflagellate, Suessiales	*Fugacium* sp.	CCMP2455	Caribbean sea	-
Dinoflagellate, Thoracosphaerales	*Luciella masanensis*	LMJH1607	Jinhae, Korea	-
Dinoflagellate, Thoracosphaerales	*Pfiesteria piscicida*	CCMP2091	North Carolina, USA	-
Prymnesiophyte, Isochrysidales	*Isochrysis galbana*	IG	NA	-
Rhaphidophyte, Chattonellales	*Heterosigma akashiwo*	HAKS9905	Kunsan, Korea	-

2.3. Results

2.3.1. Brief morphological and genetic description of *Biecheleria cincta* BCSH1005

The morphological characteristics of *B. cincta* BCSH1005 observed using light microscopy (**Figure 2.2a–e**) and SEM (**Figure 2.2f–i**) in the present study were very similar to those of the holotype of *B. cincta* [the Naples strain (MC716-B6) of Siano et al. (2009); **Figure 2.2**]. The length and width of live cells of *B. cincta* BCSH1005 (n=30), 17.2 ± 0.3 μm and 15.8 ± 0.3 μm, respectively, were slightly larger than those of the holotype.

The morphological characteristics of the holotype of *B. cincta* observed using TEM had not been reported yet, and thus, those of *B. cincta* BCSH1005 were described in the present study. Cells of *B. cincta* BCSH1005 had the nucleus, fibrous vesicle, chloroplasts, Golgi apparatus, eyespot, lipid body, mitochondria, pyrenoid, pusule system, and starch (**Figure 2.2j–m**). The eyespot had a stack of cisternae containing brick-like materials, indicating that this eyespot was type E, a generic character of the genus *Biecheleria* (**Figure 2.2l–m**; Moestrup et al. 2009). Cells of *B. cincta* BCSH1005 had a peduncle, indicating that this strain is a mixotrophic dinoflagellate (**Figure 2.2n**).

The genetic characteristics of *B. cincta* BCSH1005 analyzed in the present study were also similar to those of the holotype of *B. cincta* (**Figure 2.3, 2.4**; Siano et al. 2009). The LSU rDNA sequence of *B. cincta* BCSH1005 was different from that of the holotype by 3 bp. The small subunit (SSU) rDNA and ITS sequences of the holotype of *B. cincta* had not been reported yet. In the present study, the SSU rDNA and ITS sequences were reported.

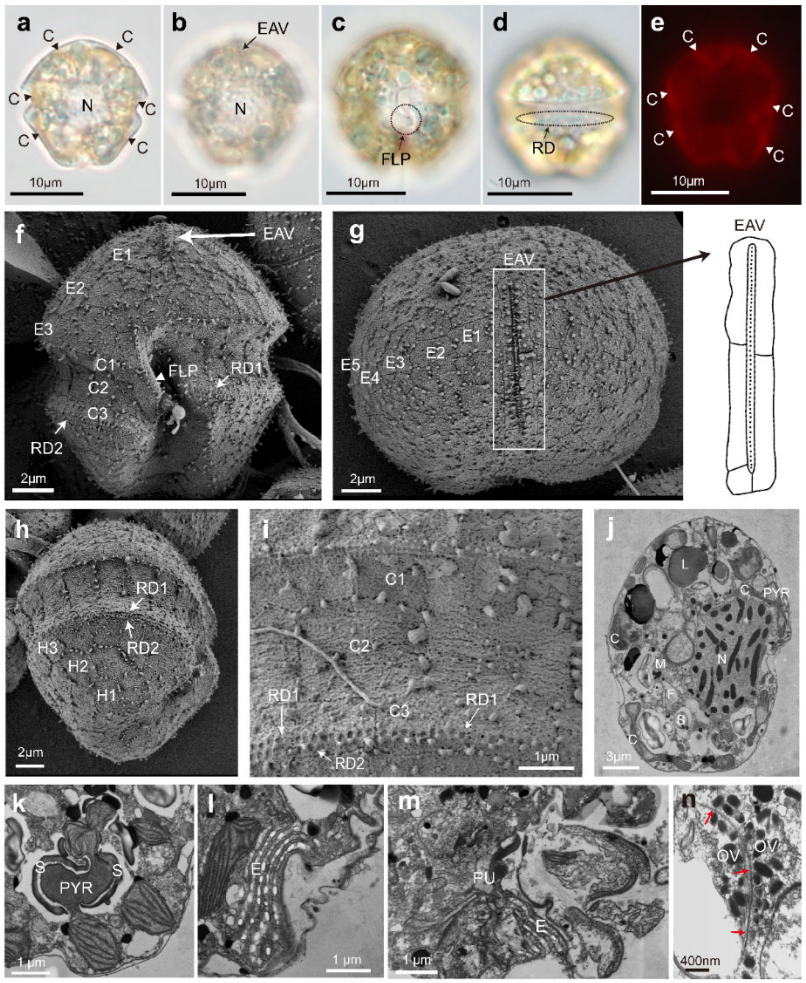

Figure 2.2. Micrographs of *Biecheleria cincta* BCSH1005 taken by light microscopy (a–d); epifluorescence microscopy (e); SEM (f–i); TEM (j–n). (a) dorsal view showing the nucleus (N) in the middle of the cell and brownish-yellow chloroplasts (C; arrowheads) distributed at the cell periphery. (b, c) ventral view showing an elongate apical vesicle (EAV; arrow) and finger-like protrusion (FLP; dashed circle). (d) dorsal view showing rounded depressions (RDs; dashed circle). (e) cell showing several C (arrowheads) by epifluorescence. (f, g), ventral and apical view showing three to five latitudinal rows (E1–E3 in f, E1–E5 in g) of amphiesmal vesicles (AVs) on the episome; three rows of AVs on the cingulum (C1–C3); a narrow EAV ornamented with a central row of approximately 55 small knobs. (h) right side view of cell showing three rows (H1–H3) of AVs on the hyposome and two rows of RDs (RD1 and RD2). Some cells had three, four, or five rows of AVs

on the hyposome. (i) three rows of AVs on the cingulum (C1–C3) and two rows of RDs (RD1 and RD2). (j) major cell components: nucleus (N), chloroplast (C), fibrous vesicle (F), lipid body (L), mitochondria (M), pyrenoid (PYR), and starch (S). (k) multiply-stalked PYR covered by S shed of *B. cincta* BCSH1005. (l) cross-section indicating the eyespot vesicles (E) containing crystalline bricks. (m) pusule system (PU) near the E. (n) microtubular strand (red arrows) and the opaque vesicles (OV) indicating the presence of a peduncle.

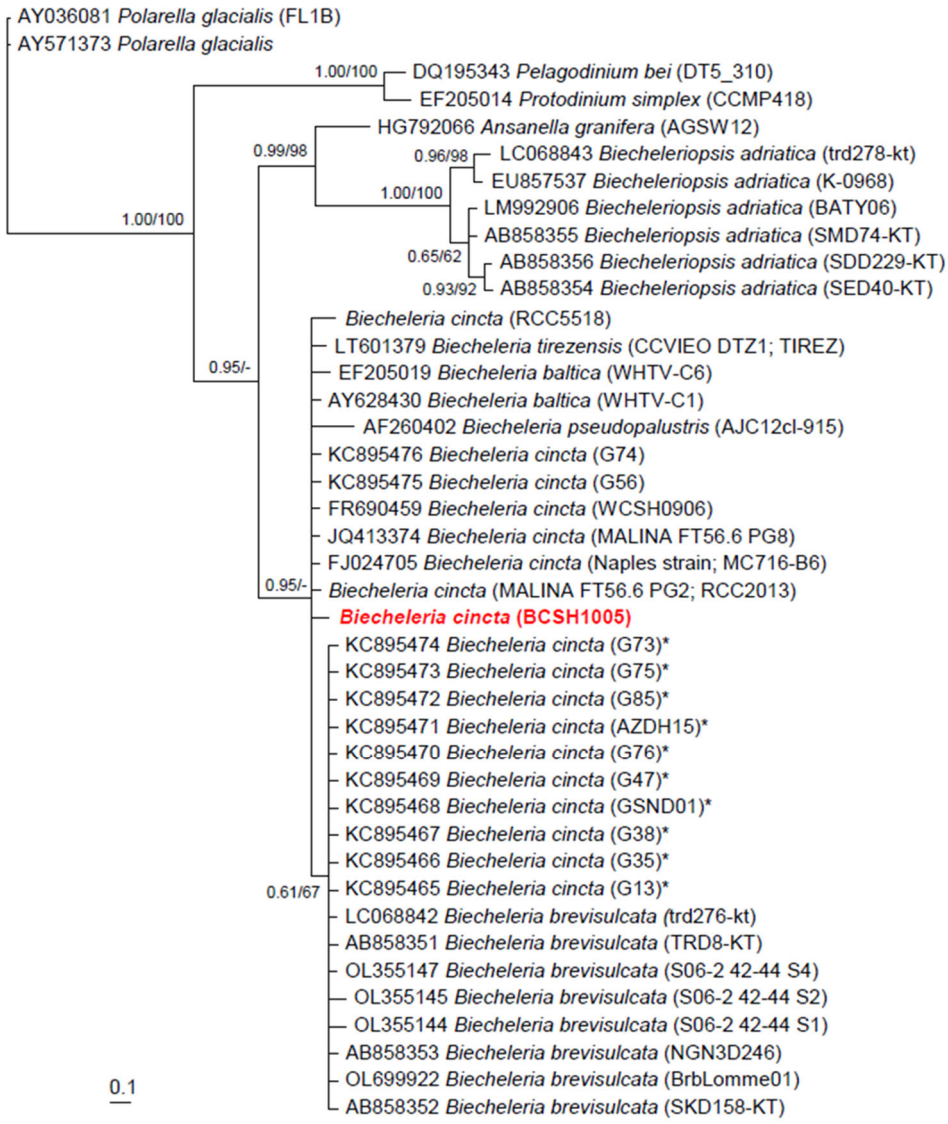

Figure 2.3. Consensus Bayesian tree based on 673-bp aligned positions of large subunit regions (LSU). *Polarella glacialis* was an outgroup. The number of character changes, proportional to branch lengths, indicate the maximum likelihood bootstrap values (right) and Bayesian posterior probability (left); posterior probabilities ≥ 0.5 are shown; the species name was followed by the strain names of each species. *Those strains belonged to *Biecheleria cincta* ribotype B (Luo et al. 2013), before *B. brevisulcata* was newly established (Takahashi et al. 2014).

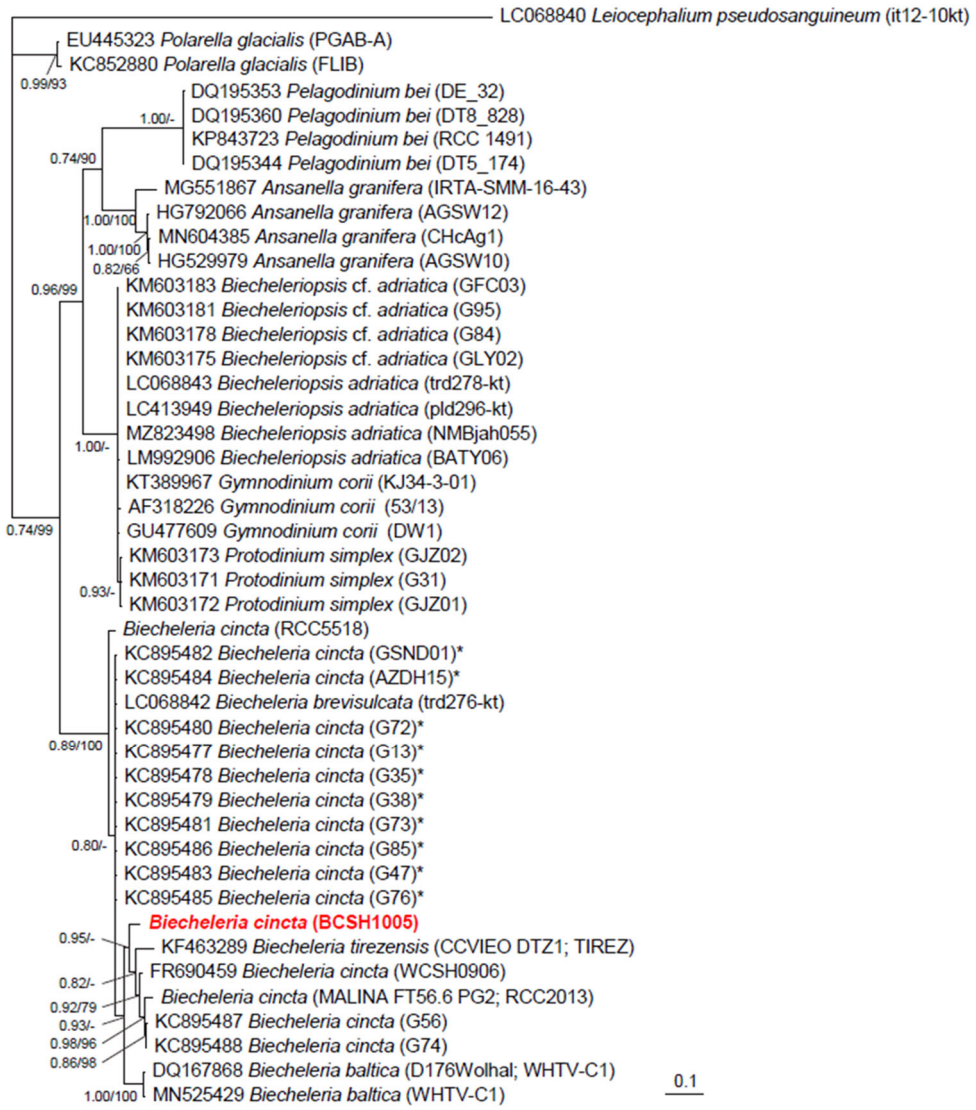

Figure 2.4. Consensus Bayesian tree based on 752-bp aligned positions of the internal transcribed spacer regions (ITS). *Leiocephalium pseudosanguineum* was an outgroup. The number of character changes, proportional to branch lengths, indicate the maximum likelihood bootstrap values (right) and Bayesian posterior probability (left); posterior probabilities ≥ 0.5 are shown; the species name was followed by the strain names of each species. *Those strains belonged to *Biecheleria cincta* ribotype B (Luo et al. 2013), before *B. brevisulcata* was newly established (Takahashi et al. 2014).

2.3.2. Spatial and temporal distributions of *Biecheleria cincta* BCSH1005

The specificity of the primer-probe set for *B. cincta* BCSH1005 established in the present study was tested using *B. cincta* BCSH1005 and other 17 microalgal species (**Table 2.2**). Cells of *B. cincta* BCSH1005 were only positively detected, while other species were not detected (**Figure 2.5**).

The abundance of *B. cincta* BCSH1005 was quantified in the water samples collected from 27 stations during the study period, and its distribution was investigated (**Figure 2.6**). During the study period, the cells of *B. cincta* BCSH1005 were detected from 13 stations among 27 sampling stations. However, *B. cincta* BCSH1005 was not found in the waters off Sokcho, Donghae, and Pohang in the East Sea of Korea; Yeosu, Kwangyang, Goheung, and Jangheung in the South Sea; Ansan, Seocheon and Dangjin in the West Sea; and Seogwipo, Wimi, Seongsan, and Gymnyeong near Jeju Island. The highest abundance of *B. cincta* (13.00 cells mL^{-1}) was found at the Tongyoung station, and the second-highest abundance (7.36 cells mL^{-1}) was found at the Jinhae station in the South Sea.

Cells of *B. cincta* BCSH1005 were found during all four seasons; these included three stations in spring; eight stations in summer; five stations in autumn; and only one station in winter (**Figure 2.6**). The highest and the second-highest abundances of *B. cincta* BCSH1005 (13.00 and 7.36 cells mL^{-1}, respectively) were found in autumn of 2015 (**Figure 2.6c**). When compared based on seasons in 2015–2018, the highest abundance of *B. cincta* BCSH1005 was 0.01 cells mL^{-1} in spring (**Figure 2.6a**), 0.64 cells mL^{-1} in summer (**Figure 2.6b**), 13.00 cells mL^{-1} in autumn (**Figure 2.6c**), and 0.02 cells mL^{-1} in winter (**Figure 2.6d**).

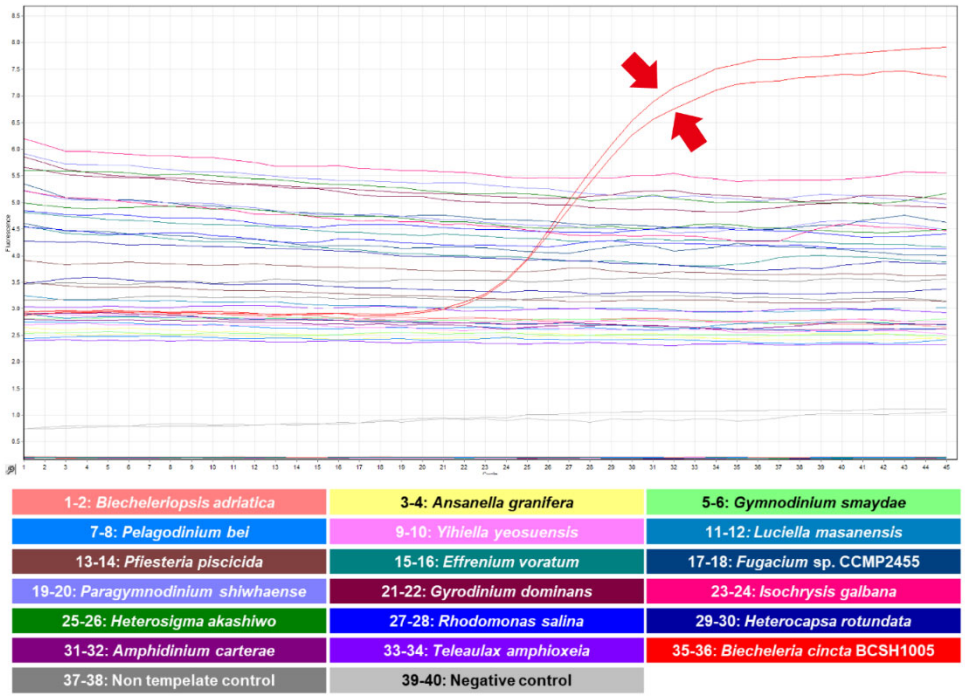

Figure 2.5. Specificity test for designed primers and probe for *Biecheleria cincta* BCSH1005. An amplification plot was generated through a test run as a duplicate of samples from *B. cincta* BCSH1005; they include the following: six Suessiales species (*Biecheleriopsis adriatica*, *Ansanella granifera*, *Pelagodinium bei*, *Yihiella yeosuensis*, *Effrenium voratum*, and *Fugacium* sp.), five mixotrophic or heterotrophic dinoflagellate species (*Gymnodinium smaydae*, *Gyrodinium dominans*, *Paragymnodinium shiwhaense*, *Luciella masanensis*, and *Pfiesteria piscicida*), six prey species (*Rhodomonas salina*, *Teleaulax amphioxeia*, *Amphidinium carterae*, *Heterocapsa rotundata*, *Isochrysis galbana*, and *Heterosigma akashiwo*), non-template controls, and negative controls. The plots of the amplification obtained from each sample were the results of the generated polymerase chain reaction product according to the fluorescence intensity. Red arrows represent the amplification results of *B. cincta* BCSH1005.

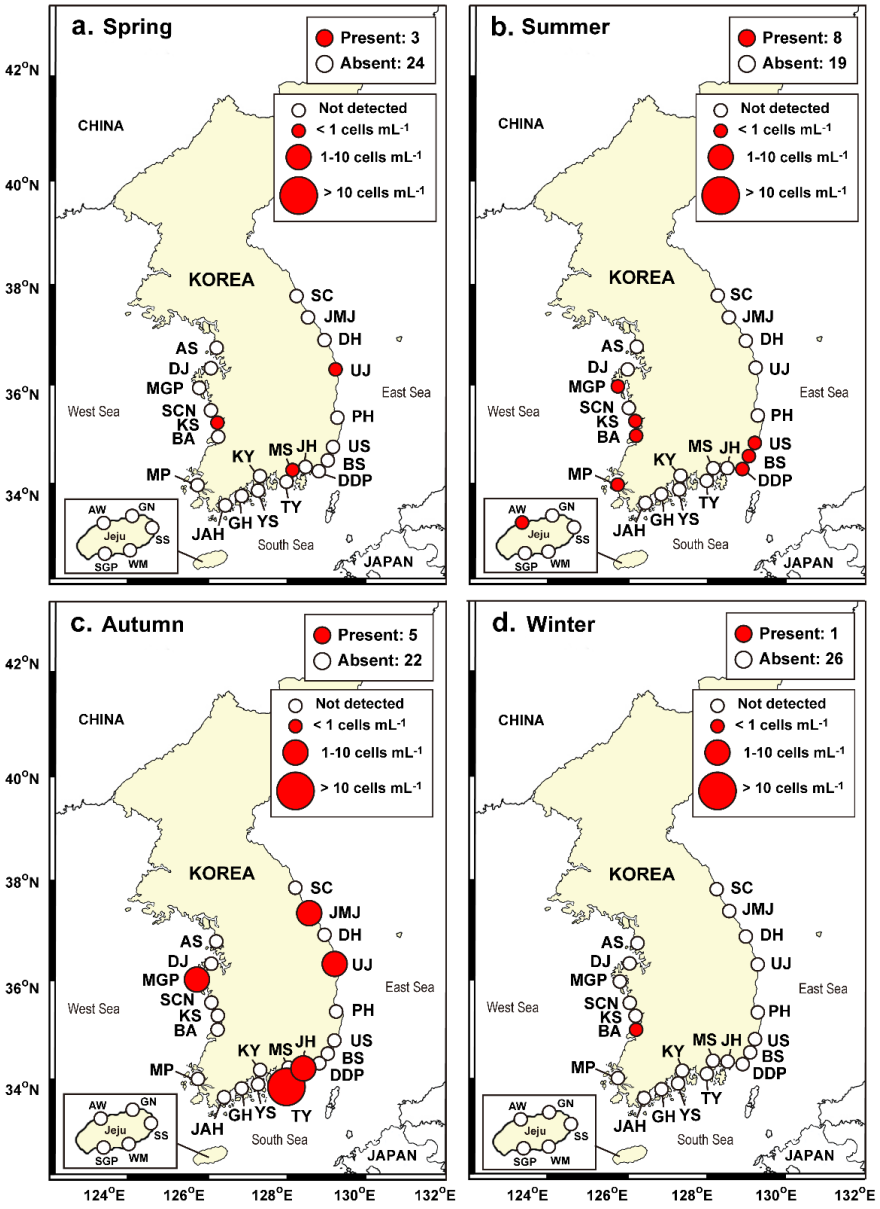

Figure 2.6. Map showing the spatial and temporal distribution of *Biecheleria cincta* BCSH1005 in Korean coastal waters in spring (a), summer (b), autumn (c), and winter (d) from April 2015 to October 2018. Red closed circles: the stations where *B. cincta* BCSH1005 was present. White closed circles: the stations where *B. cincta* BCSH1005 was not present. The size of the red circles: the abundance of *B. cincta* BCSH1005 (cells mL^{-1}). Abbreviations for station names are shown in **Figure 2.1**.

2.3.3. Spatial and temporal distributions of *Gymnodinium smaydae* GSSH1005

The abundance of *G. smaydae* GSSH1005 was quantified in the water samples collected from 27 stations during the study period, and its distribution was investigated (**Figure 2.7**). During the study period, the cells of *G. smaydae* GSSH1005 were detected from 24 stations among 27 sampling stations. However, *G. smaydae* GSSH1005 was not found in the waters off Ulsan in the East Sea of Korea; Kwangyang and Goheung in the South Sea. The highest abundance of *G. smaydae* GSSH1005 (18.5 cells mL^{-1}) was found at the Jinhae station, and the second-highest abundance (13.6 cells mL^{-1}) was found at the Seongsan station near Jeju Island.

Cells of *G. smaydae* GSSH1005 were found during all four seasons; these included 10 stations in spring; 21 stations in summer; 10 stations in autumn; and only one station in winter (**Figure 2.7**). The highest abundances of *G. smaydae* GSSH1005 (18.5 cells mL^{-1}) was found in summer 2017 (**Figure 2.7b**) and the second-highest abundances (13.6 cells mL^{-1}) was were found in autumn 2015 (**Figure 2.7c**). When compared based on seasons in 2015–2018, the highest abundance of *G. smaydae* GSSH1005 was 2.9 cells mL^{-1} in spring (**Figure 2.7a**), 18.5 cells mL^{-1} in summer (**Figure 2.7b**), 13.6 cells mL^{-1} in autumn (**Figure 2.7c**), and 0.3 cells mL^{-1} in winter (**Figure 2.7d**).

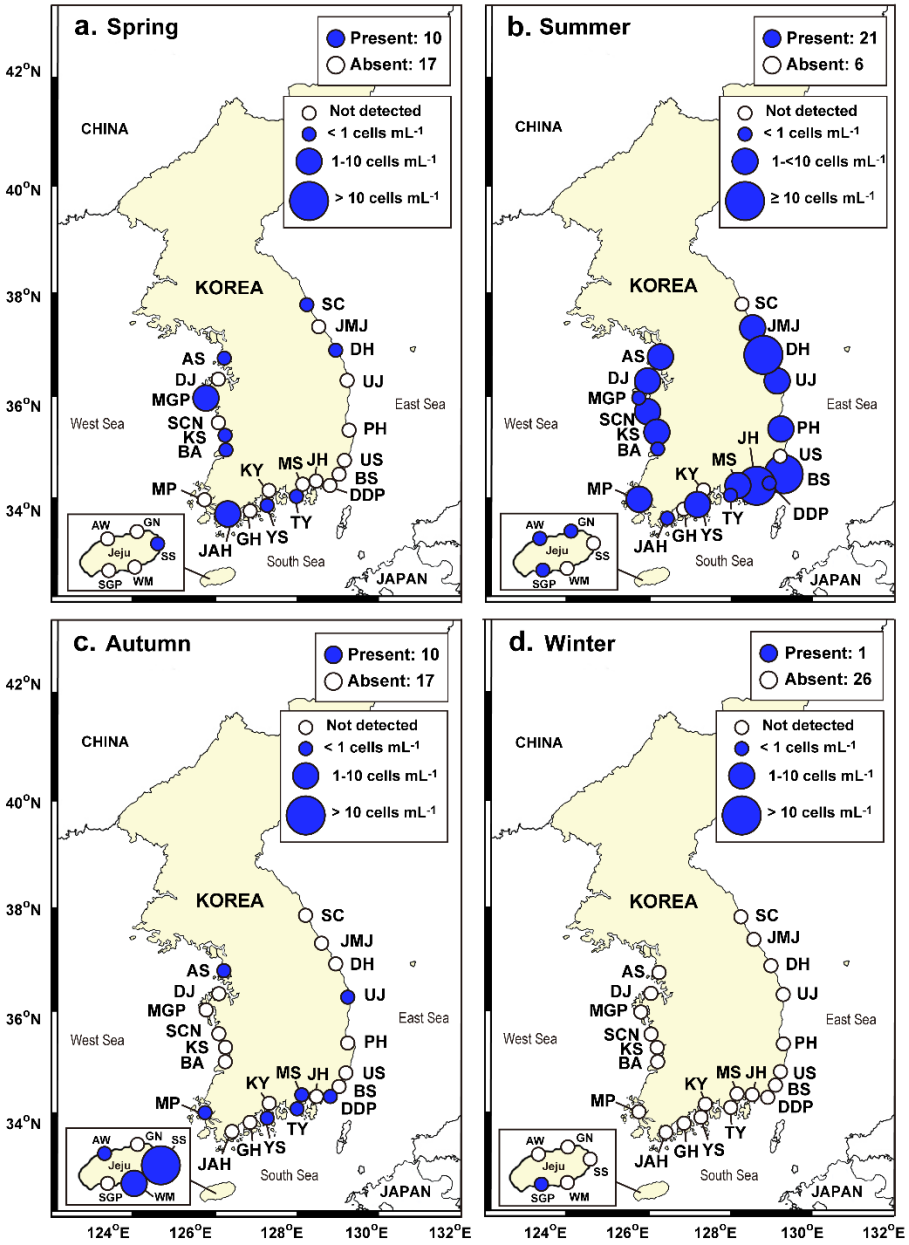

Figure 2.7. Map showing the spatial and temporal distribution of *Gymnodinium smaydae* GSSH1005 in Korean coastal waters in spring (a), summer (b), autumn (c), and winter (d) from April 2015 to October 2018 (redrawn from Lee and You et al. 2020). Blue closed circles: the stations where *G. smaydae* GSSH1005 was present. White closed circles: the stations where *G. smaydae* GSSH1005 was not present. The size of the blue circles: the abundance of *G. smaydae* GSSH1005 (cells mL^{-1}). Abbreviations for station names are shown in **Figure 2.1**.

2.3.4. Hydrographic and biological properties

During the study period, *B. cincta* BCSH1005 was detected when the water temperature range was 8.6–25.4℃, the salinity range was 12.3–35.6, concentrations of DO were 3.9–11.4 mg L^{-1}, and concentrations of chl-a were 0.2–8.7 μg L^{-1} (**Table 2.3**, **Figure 2.8**). Furthermore, *B. cincta* BCSH1005 was detected when the concentrations of NO_3, PO_4, and SiO_2 were ND–96.2, ND–2.7, and ND–273.1 μM, respectively (**Table 2.3**, **Figure 2.8**). The highest abundance of *B. cincta* BCSH1005 was found when the water temperature was 25.1℃, salinity was 32.0, DO was 5.5 mg L^{-1}, chl-a was 2.7 mg L^{-1}, NO_3 was 4.0 μM, PO_4 was 0.6 μM, and SiO_2 was 43.4 μM.

During the study period, *G. smaydae* GSSH1005 was detected when the water temperature range was 7.6–28.0℃, the salinity range was 9.6–34.1, concentrations of DO were 1.7–13.1 mg L^{-1}, and concentrations of chl-a were ND–127.0 μg L^{-1} (**Table 2.4**, **Figure 2.9**). Furthermore, *G. smaydae* GSSH1005 was detected when the concentrations of NO_3, PO_4, and SiO_2 were ND–106.0, ND–3.4, and ND–448.4 μM, respectively (**Table 2.4**, **Figure 2.9**). The highest abundance of *G. smaydae* GSSH1005 was found when the water temperature was 23.8℃, salinity was 28.3, DO was 10.8 mg L^{-1}, NO_3 was 12.5 μM, PO_4 was 1.7 μM, and SiO_2 was 41.0 μM (Lee and You et al. 2020).

Spearman's rank correlation showed that the abundance of *B. cincta* BCSH1005 was significantly affected by water temperature (**Table 2.3**). However, the other remaining environmental parameters were not significantly correlated with the abundance of *B. cincta* BCSH1005 (**Table 2.3**). Furthermore, the Pearson's correlation analysis showed that the abundance of *G. smaydae* was significantly and positively correlated with water temperature (**Table 2.4**). However, there were no significantly correlations between the abundance of *G. smaydae* and water salinity, concentrations of nutrients, or DO concentration (**Table 2.4**).

Table 2.3. Ranges of the environmental parameters in Korean coastal waters from April 2015 to October 2018 (A) and when cells of *Biecheleria cincta* BCSH1005 were detected (B) and the relationships between the abundance of *B. cincta* BCSH1005 and the environmental parameters (C). Data on the parameters were obtained from Kang et al. (2019). T, water temperature; DO, dissolved oxygen; chl-*a*, chlorophyll-*a*; ND, not detectable.

		T (°C)	Salinity	DO (mg L^{-1})	chl-*a* (μg L^{-1})	NO_3 (μM)	PO_4 (μM)	SiO_2 (μM)
(A)	The study period	0.23–28.00	ND–35.57	0.18–14.79	ND–127.00	ND–149.04	ND–6.31	ND–453.40
(B)	*Biecheleria cincta* was detected	8.60–25.40	12.32–35.57	3.85–11.43	0.19–8.66	ND–96.21	ND–2.66	ND–273.05
(C)	Spearman rank correlation coefficients (r)	0.508*	0.035	-	-	-0.132	-0.200	-0.063
	Pearson's correlation coefficients (r)	-	-	-0.228	-	-	-	-

* $p < 0.05$

Table 2.4. Ranges of the environmental parameters in Korean coastal waters from April 2015 to October 2018 (A) and when cells of *Gymnodinium smaydae* GSSH1005 were detected (B) and the relationships between the abundance of *G. smaydae* GSSH1005 and the environmental parameters (C). Data on the parameters were obtained from Kang et al. (2019). T, water temperature; DO, dissolved oxygen; chl-*a*, chlorophyll-*a*; ND, not detectable.

		T (℃)	Salinity	DO (mg L^{-1})	chl-*a* (μg L^{-1})	NO_3 (μM)	PO_4 (μM)	SiO_2 (μM)
(A)	The study period	0.23–28.00	ND–35.57	0.18–14.79	ND–127.00	ND–149.04	ND–6.31	ND–453.40
(B)	*Gymnodinium smaydae* was detected	7.6–28.0	9.6–34.1	1.7–13.1	ND–127.00	ND–106.0	ND–3.4	ND–448.4
(C)	Pearson's correlation coefficients (r)	0.156**	-0.028	0.013	0.427**	0.013	0.001	-0.007

* $p < 0.05$, ** $p < 0.01$

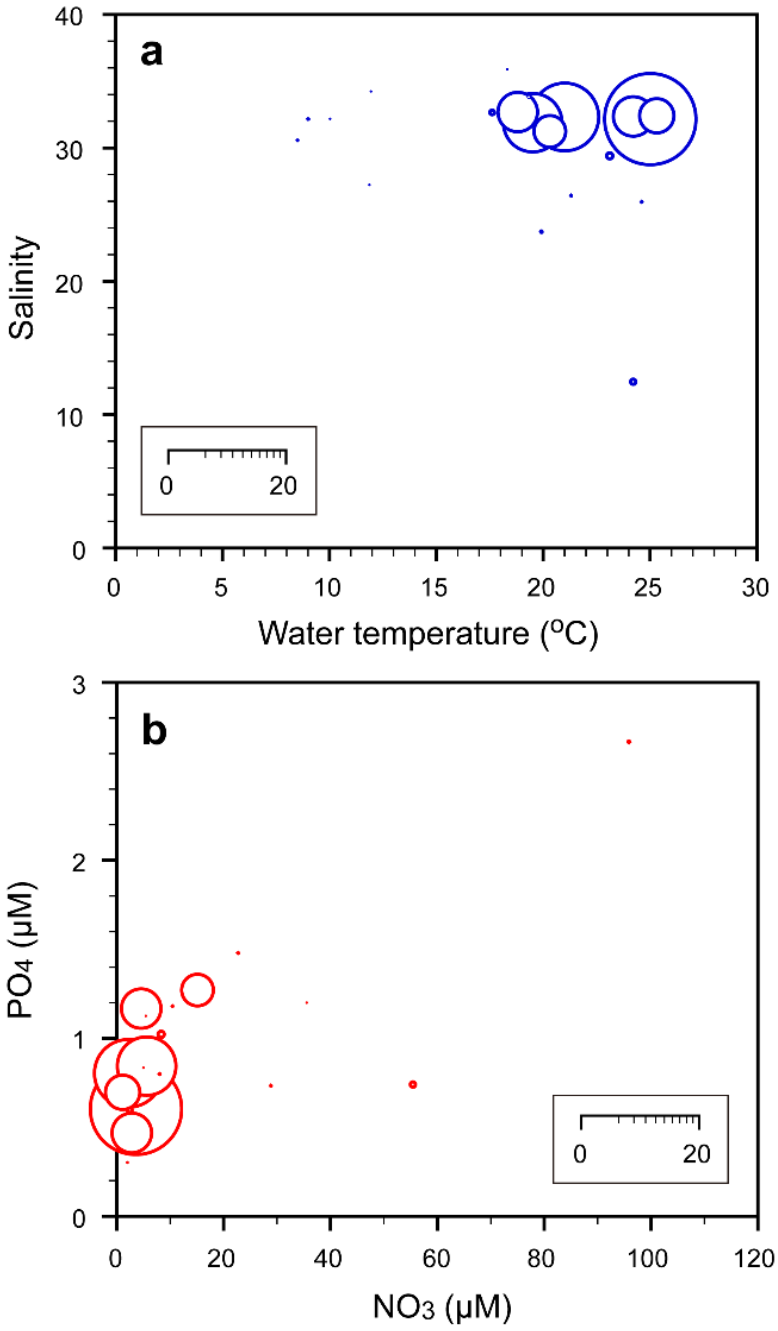

Figure 2.8. Abundances (cells mL^{-1}) of *Biecheleria cincta* BCSH1005 as a function of salinity and water temperature (a) and those as a function of PO_4 and NO_3 concentrations (b) at all the stations during 2015–2018. The size of circles: the abundance of *B. cincta* BCSH1005.

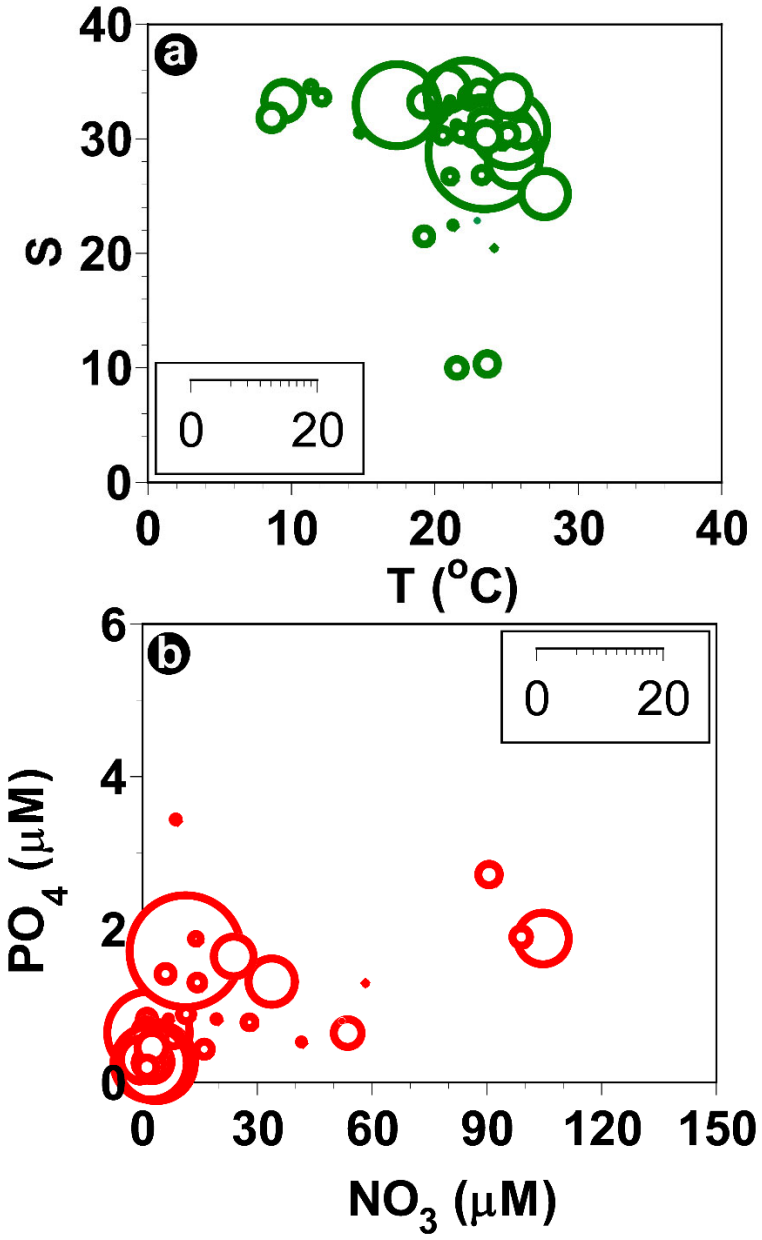

Figure 2.9. Abundances (cells mL^{-1}) of *Gymnodinium smaydae* GSSH1005 as a function of salinity and water temperature (a) and those as a function of PO_4 and NO_3 concentrations (b) at all the stations during 2015–2018. The size of circles: the abundance of *G. smaydae* GSSH1005 (Lee and You et al. 2020).

2.3.5. *Biecheleria cincta* BCSH1005 distribution prediction under ocean warming condition

At the 27 stations, the water temperature in spring during 2015–2018 was 7.4–18.4℃, and *B. cincta* BCSH1005 was only detected at three stations; these included one station each in the West, the South, and the East Seas of Korea (**Figure 2.10**). Under +2, +4, and +6℃ conditions, the distribution of *B. cincta* BCSH1005 was not expected to be different from that in 2015–2018 (**Figure 2.10**).

The water temperature in summer during 2015–2018 was 10.5–28.0℃, and *B. cincta* BCSH1005 was detected at eight stations; these included four stations in the West Sea, two stations in the South Sea, and one station each in the East Sea and near Jeju Island (**Figure 2.11**). Under +2℃ condition, *B. cincta* BCSH1005 was predicted to be present at six stations; these included two stations each in the West and the South Seas and one station each in the East Sea and near Jeju Island (**Figure 2.11**). Under +4℃ condition, *B. cincta* BCSH1005 was predicted to be present at five stations; these included one station each in the West and the East Seas and Jeju Island and two stations in the South Sea (**Figure 2.11**). Under +6℃ condition, *B. cincta* BCSH1005 was predicted to be present at three stations, including one station in the East Sea and two stations in the South Sea (**Figure 2.11**).

The water temperature in autumn during 2015–2018 was 16.7–27.9℃, and *B. cincta* BCSH1005 was detected at five stations: these included two stations each in the East and the South Seas, and one station in the West Sea (**Figure 2.12**). Under +2 and +4℃ conditions, the distributions of *B. cincta* BCSH1005 were not expected to be different from those in 2015–2018 (**Figure 2.12**). However, under +6℃ condition, *B. cincta* BCSH1005 was predicted to be present at three stations, including two stations in the East Sea and one station in the West Sea (**Figure 2.12**).

The water temperature in winter during 2015–2018 was 0.2–18.6℃, and *B. cincta* BCSH1005 was detected at only one station in the West Sea. Under +2, +4, and +6℃ conditions, the distribution of *B. cincta* BCSH1005 was not expected to be different from that in 2015–2018 (**Figure 2.13**).

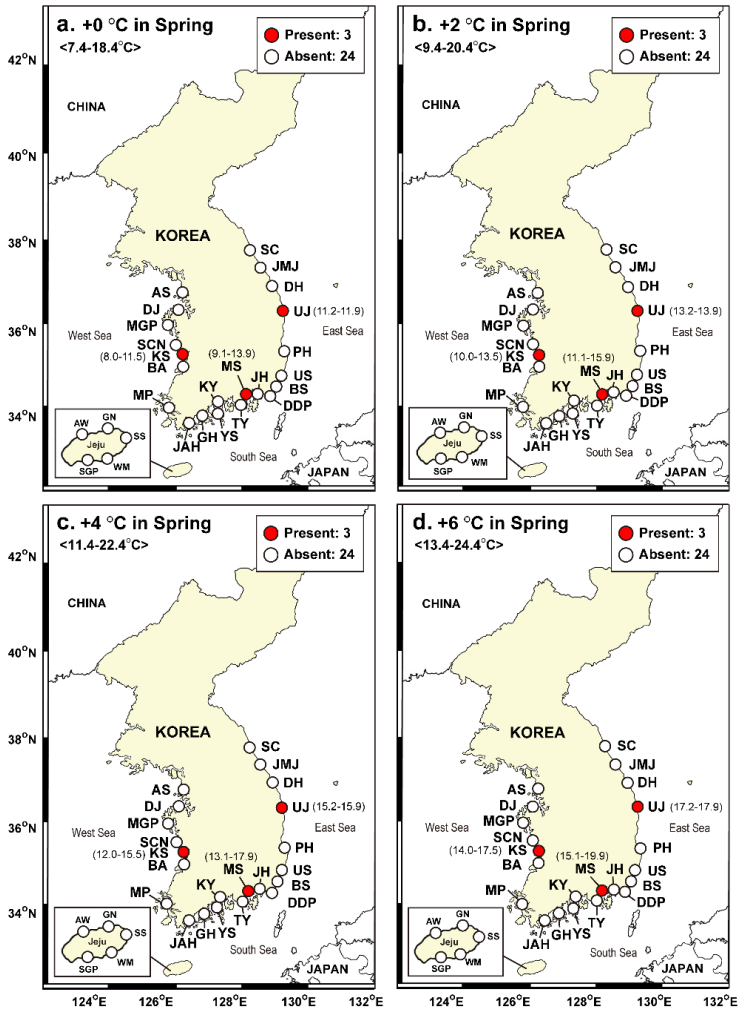

Figure 2.10. The results of the distribution of *Biecheleria cincta* BCSH1005 in Korean coastal waters in spring under increased water temperature conditions predicted using data from the distribution of *B. cincta* BCSH1005 and water temperature during 2015–2018 in the region. (a), absence (white closed circles) or presence (red closed circles) of *B. cincta* BCSH1005 at the ranges of water temperatures (parenthesis next station name) during the study period. (b–d), prediction of the distribution of *B. cincta* BCSH1005 under the +2℃ (b), +4℃ (c), and +6℃ (d) temperature conditions. Numbers in the box: the number of stations at which *B. cincta* BCSH1005 was expected to be present or absent. The range in parentheses at the upper left: the water temperature ranges during the study period and under the +2℃ (b), +4℃ (c), and +6℃ (d) conditions in spring season. Abbreviations for station names are shown in **Figure 2.1**.

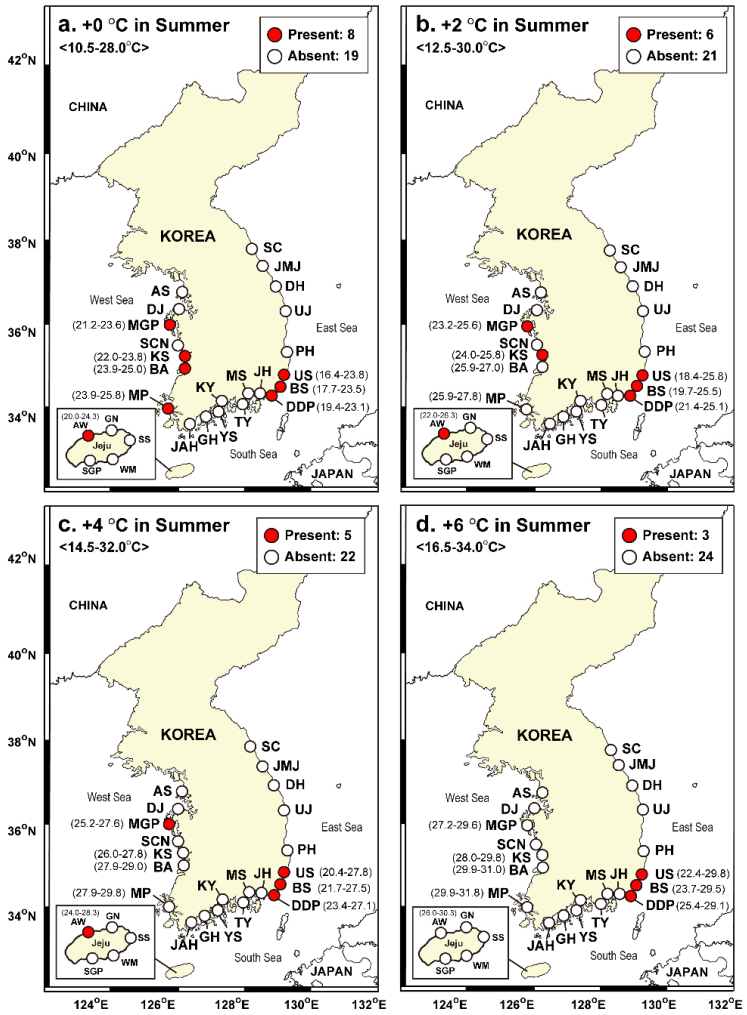

Figure 2.11. The results of the distribution of *Biecheleria cincta* BCSH1005 in Korean coastal waters in summer under increased water temperature conditions predicted using data from the distribution of *B. cincta* BCSH1005 and water temperature during 2015–2018 in the region. (a), absence (white closed circles) or presence (red closed circles) of *B. cincta* BCSH1005 at the ranges of water temperatures (parenthesis next station name) during the study period. (b–d), prediction of the distribution of *B. cincta* BCSH1005 under the +2°C (b), +4°C (c), and +6°C (d) temperature conditions. Numbers in the box: the number of stations at which *B. cincta* BCSH1005 was expected to be present or absent. The range in parentheses at the upper left: the water temperature ranges during the study period and under the +2°C (b), +4°C (c), and +6°C (d) conditions in summer season. Abbreviations for station names are shown in **Figure 2.1**.

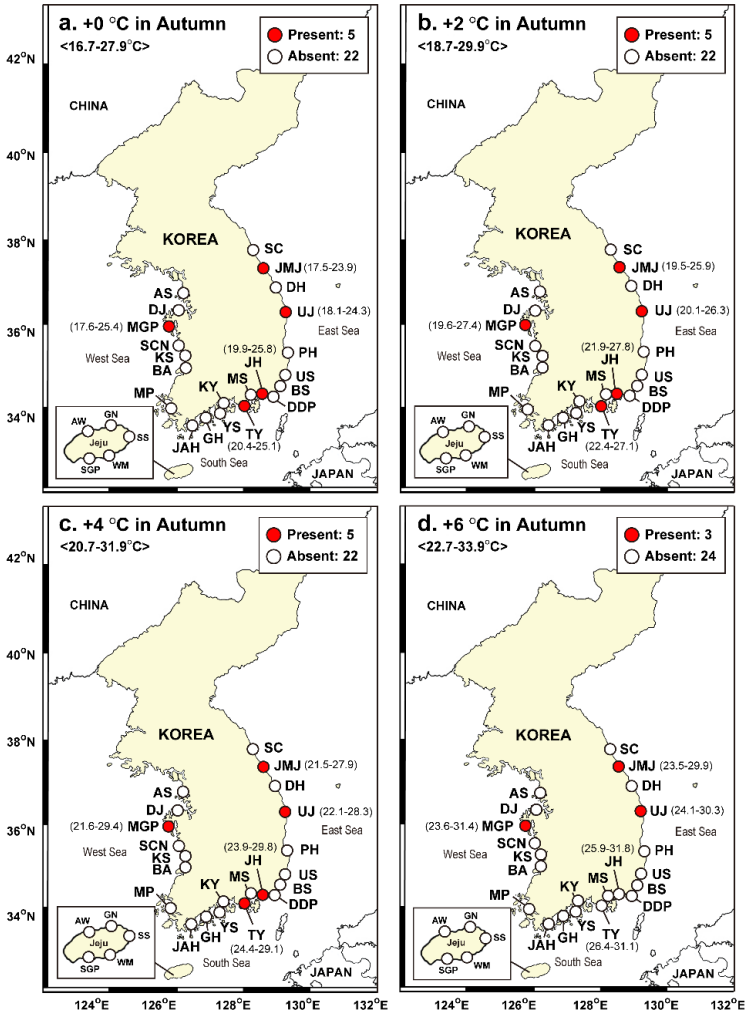

Figure 2.12. The results of the distribution of *Biecheleria cincta* BCSH1005 in Korean coastal waters in autumn under increased water temperature conditions predicted using data from the distribution of *B. cincta* BCSH1005 and water temperature during 2015–2018 in the region. (a), absence (white closed circles) or presence (red closed circles) of *B. cincta* BCSH1005 at the ranges of water temperatures (parenthesis next station name) during the study period. (b–d), prediction of the distribution of *B. cincta* BCSH1005 under the +2°C (b), +4°C (c), and +6°C (d) temperature conditions. Numbers in the box: the number of stations at which *B. cincta* BCSH1005 was expected to be present or absent. The range in parentheses at the upper left: the water temperature ranges during the study period and under the +2°C (b), +4°C (c), and +6°C (d) conditions in autumn season. Abbreviations for station names are shown in **Figure 2.1**.

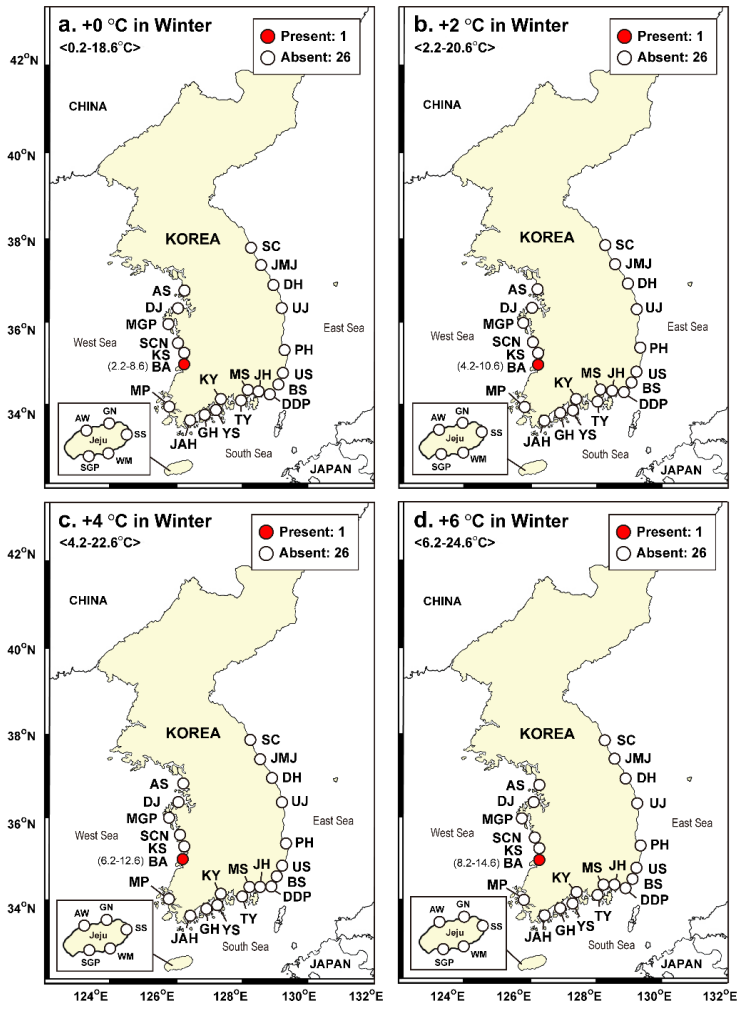

Figure 2.13. The results of the distribution of *Biecheleria cincta* BCSH1005 in Korean coastal waters in winter under increased water temperature conditions predicted using data from the distribution of *B. cincta* BCSH1005 and water temperature during 2015–2018 in the region. (a), absence (white closed circles) or presence (red closed circles) of *B. cincta* BCSH1005 at the ranges of water temperatures (parenthesis next station name) during the study period. (b–d), prediction of the distribution of *B. cincta* BCSH1005 under the +2°C (b), +4°C (c), and +6°C (d) temperature conditions. Numbers in the box: the number of stations at which *B. cincta* BCSH1005 was expected to be present or absent. The range in parentheses at the upper left: the water temperature ranges during the study period and under the +2°C (b), +4°C (c), and +6°C (d) conditions in winter season. Abbreviations for station names are shown in **Figure 2.1**.

2.3.6. *Gymnodinium smaydae* GSSH1005 distribution prediction under ocean warming condition

At the 27 stations, the water temperature in spring during 2015–2018 was 7.4–18.4℃, and *G. smaydae* GSSH1005 was detected at 8 stations; these included three station each in the West and the South Seas, and two stations in the East Seas of Korea (**Figure 2.14a**). Under +2, +4, and +6℃ conditions, the distribution of *G. smaydae* GSSH1005 was not expected to be different from that in 2015–2018 (**Figure 2.14b–d**).

The water temperature in summer during 2015–2018 was 10.5–28.0℃, and *G. smaydae* GSSH1005 was detected at 21 stations; these included seven stations in the West Sea, seven stations in the South Sea, four station in the East Sea, and three stations near Jeju Island (**Figure 2.15a**). Under +2℃ condition, *G. smaydae* GSSH1005 was predicted not to be different from that in 2015–2018 (**Figure 2.15b**). However, under +4℃ condition, *G. smaydae* GSSH1005 was predicted to be present at 20 stations; these included six station in the West, seven stations in the South Sea, four stations in the East Seas, and three stations near Jeju Island (**Figure 2.15c**). Under +6℃ condition, *G. smaydae* GSSH1005 was predicted to be present at 12 stations, these included one station in the West, four stations each in the East and South Seas, and three stations near Jeju Island (**Figure 2.15d**).

The water temperature in autumn during 2015–2018 was 16.7–27.9℃, and *G. smaydae* GSSH1005 was detected at 10 stations: these included two stations in the East Seas, four stations in the South Seas, one station in the West Sea, and three stations near Jeju Island (**Figure 2.16a**). Under +2, +4, +6℃ conditions, the distributions of *G. smaydae* GSSH1005 were not expected to be different from those in 2015–2018 (**Figure 2.16b-d**).

The water temperature in winter during 2015–2018 was 0.2–18.6℃, and *G. smaydae* GSSH1005 was detected at only one station near Jeju Island (**Figure 2.17a**). Under +2, +4, and +6℃ conditions, the distribution of *G. smaydae* GSSH1005 was not expected to be different from that in 2015–2018 (**Figure 2.17b–d**).

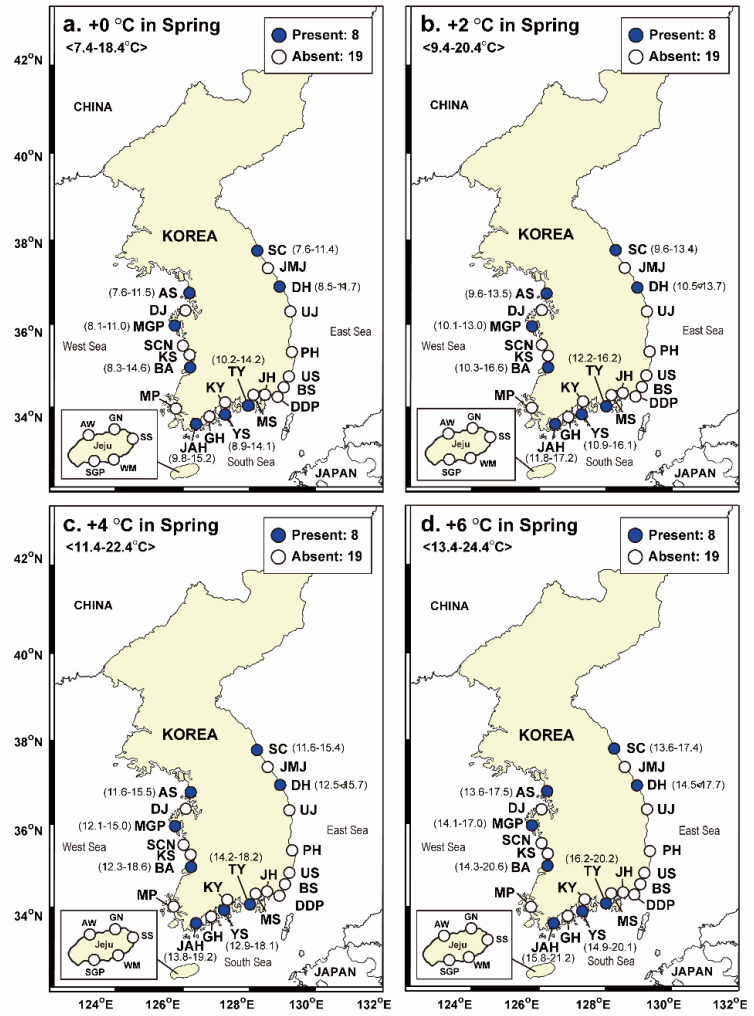

Figure 2.14. The results of the distribution of *Gymnodinium smaydae* GSSH1005 in Korean coastal waters in spring under increased water temperature conditions predicted using data from the distribution of *G. smaydae* GSSH1005 and water temperature during 2015–2018 in the region. (a), absence (white closed circles) or presence (blue closed circles) of *G. smaydae* GSSH1005 at the ranges of water temperatures (parenthesis next station name) during the study period. (b–d), prediction of the distribution of *G. smaydae* GSSH1005 under the +2℃ (b), +4℃ (c), and +6℃ (d) temperature conditions. Numbers in the box: the number of stations at which *G. smaydae* GSSH1005 was expected to be present or absent. The range in parentheses at the upper left: the water temperature ranges during the study period and under the +2℃ (b), +4℃ (c), and +6℃ (d) conditions in spring season. Abbreviations for station names are shown in **Figure 2.1**.

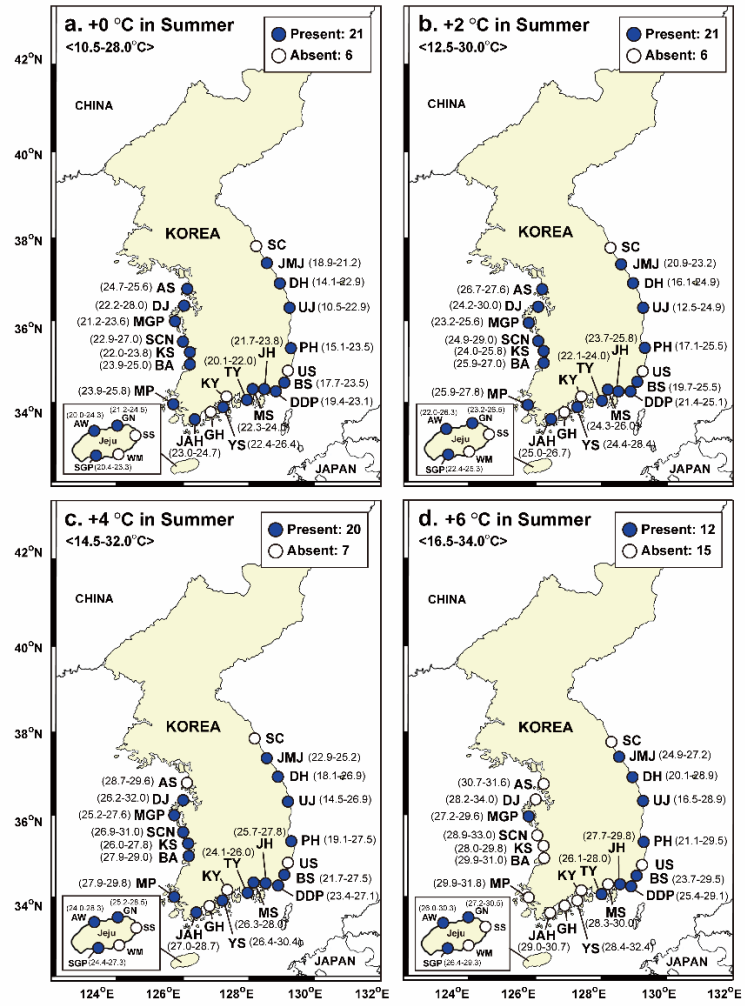

Figure 2.15. The results of the distribution of *Gymnodinium smaydae* GSSH1005 in Korean coastal waters in summer under increased water temperature conditions predicted using data from the distribution of *G. smaydae* GSSH1005 and water temperature during 2015–2018 in the region. (a), absence (white closed circles) or presence (blue closed circles) of *G. smaydae* GSSH1005 at the ranges of water temperatures (parenthesis next station name) during the study period. (b–d), prediction of the distribution of *G. smaydae* GSSH1005 under the +2℃ (b), +4℃ (c), and +6℃ (d) temperature conditions. Numbers in the box: the number of stations at which *G. smaydae* GSSH1005 was expected to be present or absent. The range in parentheses at the upper left: the water temperature ranges during the study period and under the +2℃ (b), +4℃ (c), and +6℃ (d) conditions in summer season. Abbreviations for station names are shown in **Figure 2.1**.

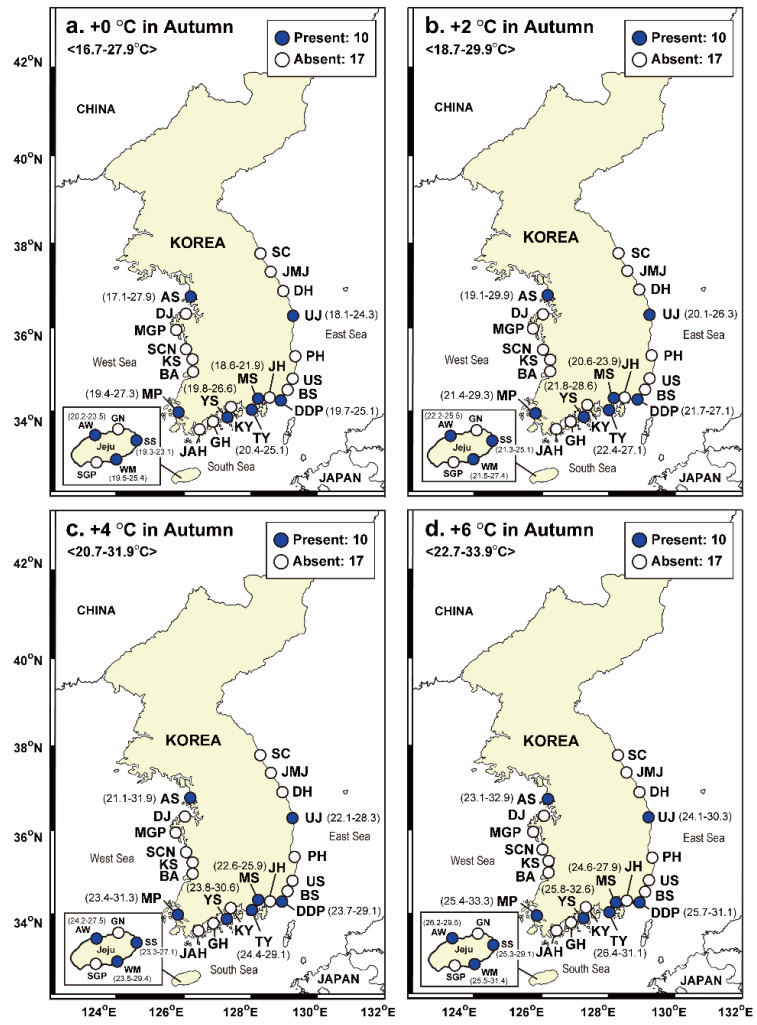

Figure 2.16. The results of the distribution of *Gymnodinium smaydae* GSSH1005 in Korean coastal waters in autumn under increased water temperature conditions predicted using data from the distribution of *G. smaydae* GSSH1005 and water temperature during 2015–2018 in the region. (a), absence (white closed circles) or presence (blue closed circles) of *G. smaydae* GSSH1005 at the ranges of water temperatures (parenthesis next station name) during the study period. (b–d), prediction of the distribution of *G. smaydae* GSSH1005 under the +2℃ (b), +4℃ (c), and +6℃ (d) temperature conditions. Numbers in the box: the number of stations at which *G. smaydae* GSSH1005 was expected to be present or absent. The range in parentheses at the upper left: the water temperature ranges during the study period and under the +2℃ (b), +4℃ (c), and +6℃ (d) conditions in autumn season. Abbreviations for station names are shown in **Figure 2.1**.

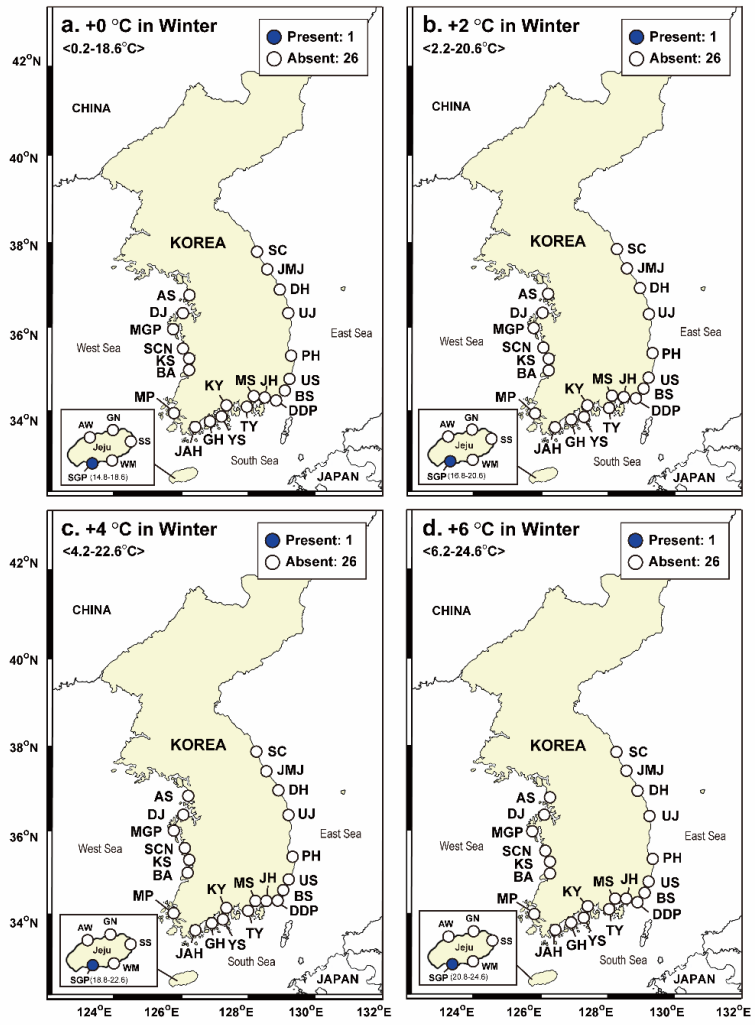

Figure 2.17. The results of the distribution of *Gymnodinium smaydae* GSSH1005 in Korean coastal waters in winter under increased water temperature conditions predicted using data from the distribution of *G. smaydae* GSSH1005 and water temperature during 2015–2018 in the region. (a), absence (white closed circles) or presence (blue closed circles) of *G. smyadae* GSSH1005 at the ranges of water temperatures (parenthesis next station name) during the study period. (b–d), prediction of the distribution of *G. smyadae* GSSH1005 under the +2℃ (b), +4℃ (c), and +6℃ (d) temperature conditions. Numbers in the box: the number of stations at which *G. smyadae* GSSH1005 was expected to be present or absent. The range in parentheses at the upper left: the water temperature ranges during the study period and under the +2℃ (b), +4℃ (c), and +6℃ (d) conditions in winter season. Abbreviations for station names are shown in **Figure 2.1**.

2.4. Discussions

2.4.1. Taxonomy of *Biecheleria cincta* BCSH1005

Many strains of *B. cincta* have been reported (Siano et al. 2009; Kang et al. 2011; Balzano et al. 2012; Luo et al. 2013; Gérikas Ribeiro et al. 2020). However, these strains are genetically divergent and form several clades. Thus, it is necessary to confirm that a target strain matches the original description of the holotype of *B. cincta* in morphology and genetics. The LSU rDNA sequence of *B. cincta* BCSH1005 was 0.4 % (3 bp) different from that of the holotype of *B. cincta* [the Naples strain (MC716-B6) of Siano et al. 2009]. The morphology of *B. cincta* BCSH1005 is also very similar to that of *B. cincta* MC716-B6 (Siano et al. 2009). Thus, *B. cincta* BCSH1005 is confirmed to be the holotype of *B. cincta*. The ITS rDNA sequence of the holotype has not been reported yet. In the phylogenetic tree based on ITS sequences, *B. cincta* WCSH0906, RCC2013, G56, and G74 form a clade with *B. cincta* BCSH1005. Therefore, there is a high similarity between *B. cincta* BCSH1005 and these strains of *B. cincta*.

2.4.2. Spatial and temporal distributions of *Biecheleria cincta* and *Gymnodinium smaydae*

Cells of *B. cincta* BCSH1005 did not survive mixotrophically at ≤ 10℃ and ≥ 30℃ and autotrophically at all tested water temperatures (Chapter 3). When the mixotrophic growth rates were interpolated, they were zero at 12.6 and 26.4℃ (Chapter 3). However, in the water samples seasonally collected from the study area during the study period, cells of *B. cincta* BCSH1005 were detected at 8.6–25.4℃. Therefore, the lowest water temperature (8.6℃) at which *B. cincta* BCSH1005 cells were present in Korean coastal waters was lower than the lowest water temperature (12.6℃) at which *B. cincta* BCSH1005 cells survived in the laboratory experiments; however, the highest water temperature (25.4℃) at which *B. cincta* BCSH1005 cells were present in Korean coastal waters is similar to the highest water temperature (26.4℃) at which *B. cincta* BCSH1005 cells survived in the laboratory experiments.

Although the mixotrophic growth rates of *B. cincta* BCSH1005 were negative at ≤ 10℃, the rates were -0.3 to -0.2 d^{-1}, and the mixotrophic growth rates at ≥ 30℃ were < -1 d^{-1} (Chapter 3). Thus, some cells of *B. cincta* BCSH1005 are likely to survive at 8.6℃ but not at ≥ 30℃.

Gymnodinium smaydae cells were present at most stations in summer but were present at only one station in winter. This study clearly showed that *G. smaydae* had a wide spatial distribution but a strong seasonality in Korean waters. The species was known as a predator of *Heterocapsa* spp. And *Scrippsiella acuminata* (Lee et al. 2014a). *Heterocapsa minima* is known to be present in 26 of the 28 stations evaluated in Korean waters (Lee et al. 2019d) and *S. acuminata* also has a wide distribution in Korean waters (Kim et al. 2019). In addition, red tides caused by *H. steinii* (= *H. triquetra*) or *Heterocapsa* sp. have been observed in Korea (National Institute of Fisheries Science 2020, National Institute of Biological Resources 2020). Therefore, high prey availability may be partially responsible for the wide distribution of *G. smaydae* in Korean coastal waters.

The mixotrophic growth rates of *G. smaydae* on *H. rotundata* were positive at 10–32℃, but negative at ≤ 8℃ (You et al. 2020b; Chapter 3). During the period of this study, *G. smaydae* was present in Korean coastal waters at 7.6–28.0℃, although the range of water temperatures at all stations was 0.2–28.0℃. Therefore, *G. smaydae* is not likely to survive in water temperatures of < 7–8℃. In winter, *G. smaydae* was only found in waters at Seogwipo, where the water temperature was 15.1℃. Thus, a water temperature >10℃ in winter may have allowed *G. smaydae* to survive in the water at Seogwipo. You et al. (2020b) also reported that the maximum mixotrophic growth rate was observed at 25℃ (Chapter 3). During this study period, the water temperature at which the highest abundance of *G. smaydae* was found was 23.8℃. Therefore, results of the laboratory experiments were consistent with those of the field observations, indicating that *G. smaydae* preferred temperatures of approximately 25℃.

The highest and second-highest abundances of *B. cincta* BCSH1005 during the study period were observed at 21.1–25.1℃ during the autumn. The maximum mixotrophic growth rate of *B. cincta* BCSH1005 in the laboratory

experiment was 25℃ (Chapter 3). Therefore, the highest abundance of *B. cincta* BCSH1005 may be affected by water temperature. Similarly, among the heterotrophy-dominant mixotrophic or kleptoplastidic dinoflagellates of which predation contribution to total growth rate ($PredC^{TGR}$) is > 60% (Jeong et al. 2021), *G. smaydae*, *Paragymnodinium shiwhaense*, *Shimiella gracilenta*, and *Yihiella yeosuensis* showed that the highest abundances were found at 18–25℃ in Korean coastal waters and their maximum mixotrophic growth rates on the optimal prey were achieved at 25℃ in laboratory experiments (Kang et al. 2013; Jeong et al. 2018b; Jang and Jeong 2020; Kang et al. 2020; Lee et al. 2020b; You et al. 2020b; Ok et al. 2021, 2022). Therefore, these heterotrophy-dominant mixotrophic or kleptoplastidic dinoflagellates are likely to be abundant in Korean coastal waters at similar times. Furthermore, *B. cincta* is known to feed on the dinoflagellates *Amphidinium carterae* and *Heterocapsa rotundata*, the cryptophytes *Rhodomonas salina* and *Teleaulax* sp., the prymnesiophyte *Isochrysis galbana*, the euglenophyte *Eutreptiella gymnastica*, and the rhaphidophyte *H. akashiwo* (Kang et al. 2011). Cells of *P. shiwhaense* also feed on all of these prey species, except for *E. gymnastica* (Yoo et al. 2010). Therefore, under similar water-temperature conditions, *B. cincta* and *P. shiwhaense* may compete with each other for common prey species (this study; Yoo et al. 2010; Kang et al. 2011; Jeong et al. 2018b). Meanwhile, *S. gracilenta*, *G. smaydae*, and Y. *yeosuensis* are known to feed on only one or two species among the prey species mentioned above; *G. smaydae* feed on only *I. galbana* and *H. rotundata*, *S. gracilenta* on *T. amphioxeia* and *R. salina*, and *Y. yeosuensis* on *T. amphioxeia* (Lee et al. 2014a; Jang et al. 2017b, c; Ok et al. 2021). Therefore, *B. cincta*, *P. shiwhaense*, *S. gracilenta*, and *Y. yeosuensis* may compete for *T. amphioxeia*, whereas *B. cincta*, *G. smaydae*, and *P. shiwhaense* may compete for *I. galbana* and *H. rotundata* under the similar water-temperature conditions. In addition, when *R. salina* is present under similar water-temperature conditions, *B. cincta*, *P. shiwhaense*, and *S. gracilenta* may compete for prey.

2.4.3. *Biecheleria cincta* BCSH1005 and *Gymnodinium smaydae* GSSH1005 distribution prediction under ocean warming condition

The spatiotemporal distributions of *B. cincta* BCSH1005 and *G. smaydae* GSSH1005 in Korean coastal waters were predicted to be largely affected by the elevated water temperatures; those of *B. cincta* in summer and autumn and those of *G. smaydae* in summer. Under 6℃-elevated water temperature in summer, *B. cincta* BCSH1005 cells in the waters off southeastern Korea were expected to survive, but not survive in the waters off the other regions. In addition, under 6℃-elevated water temperature in summer, *G. smaydae* GSSH1005 cells were expected to survive in the waters off eastern Korea including the southeastern coast and Jeju Island. During the summer season, water temperatures in the East Sea of Korea is lower than those in other regions due to upwelling phenomenon and the southward cold current (e.g. North Korea cold current; Lee et al. 2003; Park and Kim 2010a; Choi 2015; Hahm et al. 2019). Thus, the cold current and upwelling lower surface water temperatures, and *B. cincta* BCSH1005 and *G. smaydae* GSSH1005 cells may survive.

During 1968–2018, the mean surface water temperature in Korean coastal waters increased by 1.23℃, which was approximately twice the increase in global mean surface water temperature (Lee and Park 2019; Han and Lee 2020; NOAA National Centers for Environmental information 2022). Furthermore, in recent decades, the occurrence of extreme sea-surface temperature (SST), such as hot SST in summer and cold SST in winter, has increased (Lee and Park 2019; Han and Lee 2020). Therefore, *B. cincta* BCSH1005 and *G. smaydae* GSSH1005 may have difficulty in surviving in future summers.

Chapter 3.
Effects of temperature on the autotrophic and mixotrophic growth rates of the dinoflagellates *Biecheleria cincta* and *Gymnodinium smaydae*[*]

3.1. Introduction

Mixotrophic dinoflagellates are able to simultaneously conduct feeding and photosynthesis (Stoecker 1999; Jeong et al. 2010a, b; Hansen 2011). Interest in mixotrophic dinoflagellates is increasing because they play diverse roles in marine ecosystems as primary producers, prey, predators, symbiotic partners, and parasites (Skovgaard 1996; Menden-Deuer et al. 2005; Adolf et al. 2006; Shumway et al. 2006; Skovgaard et al. 2012; Turner et al. 2012; Harvey et al. 2013; Jeong et al. 2015; Johnson 2015; LaJeunesse et al. 2018) and have excessive DNA that may be attributed to the horizontal gene transfers by feeding (Holm–Hansen 1969; Allen et al. 1975; Fagan et al. 1998; Keeling and Palmer 2008; Johnson 2011). However, of approximately 1,200 phototrophic dinoflagellates, < 10 % have been assessed for mixotrophy (Bockstahler and Coats 1993; Jacobson and Anderson 1996; Stoecker et al. 1997; Jeong et al. 2005a, b, c, 2016; Burkholder et al. 2008; Lim et al. 2018b, 2019a). Furthermore, only a small portion of the mixotrophic dinoflagellates have been analyzed to determine whether environmental factors, such as temperature and light intensity, affect their rates of growth and ingestion (Skovgaard 1996; Hansen and Nielsen 1997; Berge et al. 2008; Jeong et al. 2018b; Lim et al. 2019b; Ok et al. 2019). During the past decade, several new species and genera of mixotrophic dinoflagellates have been described (Kang et al. 2014; Lee et al. 2014a; Lim et al. 2015a, b; Jang et al. 2017b, c; Yokouchi et al. 2018). Understanding the role of a newly-described

[*] This chapter has been published in Marine Biology.
You, J. H., Jeong, H. J.*, Lim, A. S., Ok, J. H. & Kang, H. C. 2020. Effects of irradiance and temperature on the growth and feeding of the obligate mixotrophic dinoflagellate *Gymnodinium smaydae*. Mar. Biol., 167:64.
You, J. H., Jeong, H. J.*, Ok, J. H., Kang, H. C., Park, S. A., Eom, S. H., Lee, S. Y. & Kang, N. S. 2023. Effects of temperature on the autotrophic and mixotrophic growth rates of the dinoflagellate *Biecheleria cincta* and its spatiotemporal distributions under current temperature and global warming conditions. Mar. Biol., 170:15.

mixotrophic dinoflagellate in marine ecosystems requires the determination of its prey and predators, effects of environmental factors on its growth and ingestion rates, and its distribution.

The dinoflagellates *Biecheleria cincta* and *Gymnodinium smaydae* are heterotrophy-dominant mixotrophic dinoflagellates (Kang et al. 2011; Jeong et al. 2021). The dinoflagellate *B. cincta* can feed on algal species that had equivalent spherical diameters (ESDs) ≤ 12. 6 μm, exceptions being the diatom *Skeletonema costatum* and the dinoflagellate *Prorocentrum cordatum* (Kang et al. 2011). In addition, the common heterotrophic dinoflagellates *Gyrodinium* spp., *Oxyrrhis marina*, and *Polykrikos kofoidii*, and the ciliate *Strobilidium* sp. were able to feed on *B. cincta* (Yoo et al. 2013). In addition, the dinoflagellate *G. smaydae* was described as a new species in 2014 and discovered to be mixotrophic (Kang et al. 2014; Lee et al. 2014a). This species can feed only on the thecate dinoflagellates *Heterocapsa rotundata*, *Heterocapsa steinii*, and *Scrippsiella acuminata*, among the tested 19 algal prey species, and can divide approximately three times per day when fed on the optimal prey *H. rotundata* (Lee et al. 2014a). Furthermore, *G. smaydae* was occasionally shown to have a considerable grazing impact on the population of co-occurring *H. rotundata* in Shiwha Bay (Lee et al. 2014a). The heterotrophic dinoflagellates *O. marina*, *Gyrodinium* spp., and the ciliate *Pelagostrobilidium* sp. are known to feed on *G. smaydae* (Chapter 4). Thus, *B. cincta* and *G. smaydae* play diverse roles as primary producers, prey, and predators in marine ecosystems (Kang et al. 2011; Yoo et al. 2013). Therefore, understanding the population dynamics of *B. cincta* and *G. smaydae* requires determination of its autotrophic and mixotrophic growth and ingestion rates under diverse environmental conditions.

Water temperature is major physical parameter affecting the growth and survival of phototrophic dinoflagellates (Ogata et al. 1987; Ono et al. 2000; Baek et al. 2008; López-Rosales et al. 2014). Temperature generally increases respiration which provides energy, but low or high temperature extremes often cause death in dinoflagellates (Baek et al. 2008; Xu et al. 2010; Kibler et al. 2012; Lim et al. 2019b). Water temperature changes seasonally and vertically in many marine environments (Richardson et al. 1983; Seip and Reynolds 1995; Lalli and Parsons 1997; Staehr and Sand–Jensen 2006). In

general, migratory dinoflagellates experience a wide range of water temperatures (Hasle 1950; Kamykowski and Zentara 1977; Blasco 1978; Kamykowski 1981; Whittington et al. 2000). The maximum swimming speeds of *B. cincta* and *G. smaydae* are approximately 378 and 700 μm s^{-1}, respectively; thus, theoretically, they can descend to 14 and 25 m from the surface after travelling for 10 h (Kang et al. 2011; Lee et al. 2014a). Thus, *B. cincta and G. smaydae* are also expected to experience a wide range of water temperatures in a day. Global warming is known to directly or indirectly affect seawater temperature (Levitus et al. 2005; Ding et al. 2007; IPCC 2007). A change in water temperature due to global warming may affect the growth and survival of *B. cincta* and *G. smaydae* as well as its distribution.

In this study, the growth and ingestion rates of *B. cincta* on *Heterosigma akashiwo* and *G. smaydae* on *H. rotundata* with (i.e., mixotrophic growth) and without added prey (autotrophic growth) were determined as a function of water temperature (5–35℃). These data were used to determine whether the autotrophic or mixotrophic growth rate of *B. cincta* and *G. smaydae* is affected by water temperature, whether the ingestion rates of *B. cincta* on *H. akashiwo* and *G. smaydae* on *H. rotundata* are affected by the temperature, and whether a particular water temperature causes a negative growth rate in *B. cincta* and *G. smaydae*. In this study, the terminology “autotrophic” rather than “phototrophic” was used against “mixotrophic” because both “autotrophic” and “mixotrophic” are “phototrophic”. The results of the present study provide a basis for understanding the effects of water temperature on the eco-physiological characteristics and population dynamics of *B. cincta* and *G. smaydae*.

3.2. Materials and Methods

3.2.1. Preparation of experimental organisms

A clonal culture of *B. cincta* BCSH1005 was originally isolated from Shiwha Bay in May 2010 at 17.8℃ and a salinity of 27.9, respectively. A dense culture (ca. 3,000 cells mL^{-1}) of *B. cincta* BCSH1005 was transferred every week to a 270-mL culture flask containing freshly *H. akashiwo* HAKS9905 cells (ca. 30,000 cells mL^{-1}) in 0.2-μm filtered sea water. All flasks were placed on a shelf at 20℃ under an illumination of 20μmol photons m^{-2} s^{-1} from cool-white fluorescent light with a 14:10 h Light-Dark cycle.

A non-axenic clonal culture of *G. smaydae* GSSH1005, which was isolated from Shiwha Bay, Korea, during May 2010, was used. A dense culture (ca. 20,000 cells mL^{-1}) of *G. smaydae* was transferred every three days to a 270-mL flask containing fresh culture of *H. rotundata* HRSH1201 (ca. 100,000 cells mL^{-1}). The flask was maintaied under the same conditions mentioned above. The ESD of *G. smaydae* GSSH1005 was obtained from Lee et al. (2014a).

3.2.2. Temperature effects on the growth and ingestion rates of *Biecheleria cincta* BCSH1005

The experiment (Expt) 1 was designed to determine the autotrophic and mixotrophic growth and ingestion rates of *B. cincta* BCSH1005 feeding on *H. akashiwo* as a function of water temperature (**Table 3.1**). A single high-*H. akashiwo* abundances saturating growth and ingestion rates of *B. cincta* WCSH0906, respectively, were selected to avoid prey restriction (Kang et al. 2011).

In Expt 1, target water temperatures were 5, 10, 15, 20, 25, 30, and 35℃. In the preliminary test, *B. cincta* BCSH1005 did not grow with the prey cells at 5–10 and 30–35℃. Therefore, for the experiments at 5–10 and 30–35℃, *B. cincta* BCSH1005 cultures were acclimatized as described in **Figure 3.1**. During the pre-incubation period (for 9 d), the abundances of *B. cincta* BCSH1005 and *H. akashiwo* were determined every day.

Table 3.1. Experimental design and actual initial concentration (cells mL^{-1}) of the prey (*Heterosigma akashiwo*) and predator (*Biecheleria cincta* BCSH1005) in Expt 1 and the prey (*Heterocapsa rotundata*) and predator (*Gymnodinium smaydae* GSSH1005) in Expt 2. Light intensity was maintained at 20 μmol photons m^{-2} s^{-1} in Expt 1 and 58 μmol photons m^{-2} s^{-1} in Expt 2. T, water temperature (℃).

Expt No.	Conditions		Prey concentration	Predator concentration
1	T	5, 10, 15, 20, 25, 30, 35	9,778 / 9,766 / 9,705 / 9,871 / 8,756 / 9,876 / 9,563	435 / 435 / 443 / 453 / 390 / 401 / 419
2	T	5, 6, 8, 10, 15, 20, 25, 30, 32, 35	17,699 / 15,255 / 17,459 / 18,379 / 19,611 / 20,545 / 24,501 / 22,587 / 16,085 / 18,148	33 / 44 / 44 / 48 / 77 / 68 / 65 / 62 / 46 / 43

For each target temperature, the initial concentrations of *B. cincta* BCSH1005 and *H. akashiwo* in triplicate 42-mL experimental (*B. cincta* BCSH1005 plus *H. akashiwo* cells), triplicate-prey control (only *H. akashiwo* cells), and triplicate-predator control bottles (only *B. cincta* BCSH1005 cells) were established as in **Table 3.1**. To ensure similar water conditions in the bottles, filtered water from the predator or prey cultures was added to the prey or predator control bottles as in previous studies (Jeong et al. 2006, 2007; Yoo et al. 2009, 2015; Lee et al. 2014b). Ten mL of F/2-Si medium and freshly-filtered seawater were added to all bottles which were then capped. The bottles were placed in each of the seven temperature chambers and incubated for 2 d at 20 μmol photons m^{-2} s^{-1} of light-emitting diode (LED) in a 14:10 h L:D cycle. To determine the actual initial abundances of the predator and prey in the experiments, 5-mL aliquots were obtained from each bottle and fixed with final 5 % Lugol's acidic solution and similarly, 10-mL aliquots after 2-d incubation were obtained and fixed. The abundances of *B. cincta* BCSH1005 and *H. akashiwo* were determined by counting all or more than 200 cells in Sedgewick-Rafter counting chambers. After subsampling at the beginning of the experiment, the bottles were fully refilled with filtered seawater and capped. In the calculations of growth and ingestion rates, dilution effects due to refilling were considered.

The specific growth rate of *B. cincta* BCSH1005 was calculated as:

$$\mu = \frac{\mathrm{Ln}\,(B_t / B_0)}{t}$$

, where B_0 is the initial abundance of *B. cincta* BCSH1005 and B_t is the final abundance after t days.

The ingestion rate of *B. cincta* BCSH1005 feeding on *H. akashiwo* was calculated using the modified equations of Frost (1972) and Heinbokel (1978). The carbon content per cell of *B. cincta* BCSH1005, 0.31 ng C $cell^{-1}$, was estimated from the volume of live cells (Menden-Deuer and Lessard 2000), and that of *H. akashiwo*, 0.1 ng C $cell^{-1}$, was obtained from Kang et al. (2011). The ingestion rate of *B. cincta* BCSH1005 at 35℃ was not provided in the present study because all cells of *B. cincta* BCSH1005 were observed not to

survive at this temperature, in order to avoid an overestimate of its ingestion rate.

3.2.3. Temperature effects on the growth and ingestion rates of *Gymnodinium smaydae* GSSH1005

In preliminary tests, *G. smaydae* GSSH1005 did not grow at 5, 6, 8, and 35°C. The Expt 2 was designed accordingly, with appropriate acclimation periods as shown in **Figure 3.2**. The specific autotrophic and mixotrophic growth and ingestion rates of *G. smaydae* on *H. rotundata* were determined above described at different temperatures (**Table 3.1**). The possible effects of prey concentration on the growth and ingestion rates were avoided by providing high prey concentrations at which the growth and ingestion rates of *G. smaydae* on *H. rotundata* were saturated (Lee et al. 2014a); both rates were saturated at ≥ 3,500 cell mL^{-1} *H. rotundata* concentrations.

A dense culture of *G. smaydae* (ca. 5,000–10,000 cells mL^{-1}) growing on *H. rotundata* was transferred to each of two or four 250-mL PC bottles. A dense culture of *H. rotundata* (ca. 100,000 cells mL^{-1}) growing in F/2-Si medium was also transferred to each of two or four 250-mL bottles. The target temperatures were established in two or four temperature-controlled chambers. A bottle each containing *G. smaydae* and *H. rotundata* were placed in one of the two or four chambers inside which a target temperature was established.

Considering that preliminary tests had shown that *G. smaydae* did not grow at 5, 6, and 8°C, *G. smaydae* and *H. rotundata* were each incubated at 15°C for 2 days and then acclimated at 10°C for 5 days (**Figure 3.2**). Subsequently, the bottles for the 5, 6, and 8°C experiments were acclimated at the target temperature for 2 days. This gradual acclimation was conducted to avoid any shock that may occur when a large temperature change occurs rapidly. In preparation for Expt 3, the cultures in the bottles were acclimated at each of 15, 20, and 25°C and 58μmol photons m^{-2} s^{-1} on a 14:10 h light-dark cycle for 9 days. For the experiments at 30°C, the bottle containing *G. smaydae* cells maintained at 20°C was gradually acclimated at 25°C for 7

days and then at 30°C for 2 days. The preliminary tests had also shown that *G. smaydae* cells died at 35°C; therefore, shorter acclimation periods were used. For tests at 32 and 35°C, bottles containing *G. smaydae* were first acclimated at 25°C for 2 days, then at 30°C for 5 days. Then the *G. smaydae* cultures were acclimated to the target temperatures of 32 or 35°C for 2 days (**Figure 3.2**). For the experiment at 15°C, the cultures were acclimated at 20°C for 1 day and then incubated at 15°C without further acclimation. At 2- or 3-d intervals after this pre-incubation started, 5-mL aliquots were obtained from each bottle incubated at the target temperature and fixed with 5% acidic Lugol's solution; subsequently, the abundance of *G. smaydae* and *H. rotundata* was measured.

For Expt 2, the initial concentrations of *G. smaydae* and *H. rotundata* were established as described above. Triplicate 42-mL experimental bottles, prey control bottles, and predator control bottles were set up for each target temperature. The experimental procedure was the same as that for Expt 1. The bottles were incubated for 2 days at each temperature in target chambers irradiated at 58 μmol photons m^{-2} s^{-1} by LED on a 14:10 h Light-Dark cycle. These light conditions supported the maximum mixotrophic growth rate of *G. smaydae* on *H. rotundata* in You et al. (2020b). The specific growth and ingestion rates of *G. smaydae* were calculated as described above.

3.2.4. Statistical analysis

To investigate the effects of water temperature on autotrophic and mixotrophic growth and ingestion rates of *B. cincta* BCSH1005 feeding on *H. akashiwo* and *G. smaydae* GSSH1005 on *H. rotundata*, univariate analyses and post-hoc tests were conducted. Also, to determine whether there were significant differences between the autotrophic and mixotrophic growth rates of *B. cincta* BCSH1005 and *G. smaydae* GSSH1005 at the same water temperatures, an independent-sample t test or Mann-Whitney U test was performed. All statistical analyses were conducted with SPSS ver. 25 (IBM-SPSS Inc., Armonk, NY, USA) at a significance level of 0.05. The detailed methods for statistical analyses are presented in **Table 3.2**.

Table 3.2. Methods of statistical analysis in this study. AGR, autotrophic growth rate; MGR, mixotrophic growth rate; IR, ingestion rate; T, water temperature (℃); O, a variance satisfied the condition; X, a variance did not satisfy the condition; -, not tested or not available.

a. A significant effect on the AGR, MGR, and IR of *Biecheleria cincta* BCSH1005 and *Gymnodinium smaydae* GSSH1005 by the T.

Normality (Shapiro-Wilk's W test)	Homogeneity (Levene's test)	Methods		References
		Univariate analysis	Post-hoc test	
O	O	One-way ANOVA	Tukey's HSD test	Tukey 1953; Levene 1961; Shapiro and Wilk 1965
X	-	Kruskal-Wallis test	Mann-Whitney U test with Bonferroni correction	Mann and Whitney 1947; Kruskal and Wallis 1952; Dunn 1961; Levene 1961; Shapiro and Wilk 1965

b. A significant difference between the AGR and MGR of *B. cincta* BCSH1005 and *G. smaydae* GSSH1005; between zero and its IR at the same T.

Normality (Shapiro-Wilk's W test)	Methods	References
O	Independent samples t test	Shapiro and Wilk 1965
X	Mann-Whitney U test	Mann and Whitney 1947; Shapiro and Wilk 1965

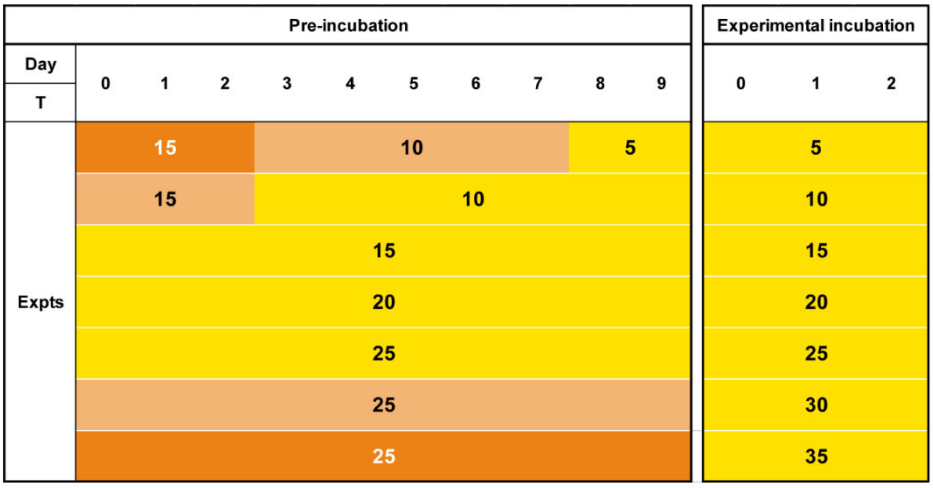

Figure 3.1. Information on the periods of the pre-incubation and experimental incubation for the experimental organism, *Biecheleria cincta* BCSH1005. Target experimental temperatures: 5, 10, 15, 20, 25, 30, and 35℃.

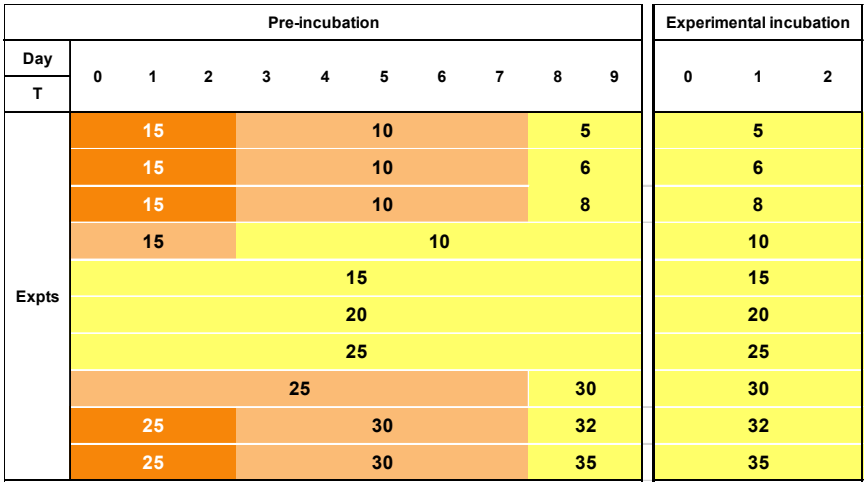

Figure 3.2. Information on the periods of the pre-incubation and experimental incubation for the experimental organism, *Gymnodinium smaydae* GSSH1005. Target experimental temperatures: 5, 6, 8, 10, 15, 20, 25, 30, 32, and 35℃.

3.3. Results

3.3.1. Temperature effects on the growth and ingestion rates of *Biecheleria cincta* BCSH1005

Cells of *B. cincta* BCSH1005 did not grow autotrophically at the tested range of water temperatures (**Figure 3.3**). The autotrophic growth rates ranged from -6.09 ± 0.01 to -0.09 ± 0.03 d^{-1}. The rates increased at 5–15℃ but decreased at 20–35℃ (**Figure 3.3**). Water temperature significantly affected the autotrophic growth rates (One-way ANOVA, **Table 3.3**).

The mixotrophic growth rates of *B. cincta* BCSH1005 feeding on *H. akashiwo* were positive at 15–25℃ but negative at 5–10℃ and at 30–35℃ (**Figure 3.3**). The mixotrophic growth rates continuously increased at 5–25℃ but decreased at 30–35℃. The maximum mixotrophic growth rate was 0.26 ± 0.003 d^{-1} at 25℃. Water temperature significantly affected the mixotrophic growth rates (Kruskal-Wallis test, **Table 3.3**). The mixotrophic growth rates of *B. cincta* BCSH1005 were significantly greater than the autotrophic growth rates at 15–30℃ but not higher at 10℃ (one-tailed t test, Mann-Whitney U test; **Table 3.3**).

The ingestion rates of *B. cincta* BCSH1005 feeding on *H. akashiwo* at 5–15℃, 0.22–0.24 ng C $predator^{-1}$ d^{-1}, were similar, 0.40 ng C $predator^{-1}$ d^{-1} at 25℃ but 0.26 ng C $predator^{-1}$ d^{-1} at 30℃ (**Figure 3.4**). However, in statistic tests, water temperature did not significantly affect the ingestion rates at 5–30℃ (Kruskal-Wallis test, **Table 3.3**). At 5, 10, and 30℃, low predator abundances due to cell death (i.e., negative mixotrophic growth rate) were likely to overestimate the ingestion rates.

Table 3.3. Results of the statistical analyses for water temperature effects on the autotrophic and mixotrophic growth and ingestion rates of *Biecheleria cincta* BCSH1005 feeding on *Heterosigma akashiwo*. AGR, autotrophic growth rate; MGR, mixotrophic growth rate; IR, ingestion rate; T, water temperature (℃).

a. A significant effect on AGR, MGR, and IR by the T.					
Variances	Range of T	Methods		Results	
		Univariate analysis	Post-hoc test	Univariate analysis	Post-hoc test
AGR	5–35	One-way ANOVA	Tukey's HSD test	F (6, 14) = 16308.71, $P < 0.001$	5 (a); 10 (a); 15 (a); 20 (b); 25 (c); 30 (d); 35℃ (d)
MGR	5–35	Kruskal-Wallis test	Mann-Whitney U test with Bonferroni correction	$H6 = 19.66$, $P = 0.003$	5 (a, b); 10 (a, b); 15 (a, b); 20 (a, b); 25 (a); 30 (a, b); 35℃ (b)
IR	5–30	Kruskal-Wallis test	Mann-Whitney U test with Bonferroni correction	$H5 = 10.31$, $P = 0.07$	Not divided

IR	15–25	Kruskal-Wallis test	Mann-Whitney U test with Bonferroni correction	$H2 = 7.26$, $P = 0.03$	Not divided

b. The MGR significantly higher than AGR at the same T.

Variances	T	Methods	Results
Between AGR and MGR	5	One-tailed t test	$t4 = -2.30$, $P = 0.04$
	10	Mann-Whitney U test	$Z = -0.22$, $P = 0.41$
	15	Mann-Whitney U test	$Z = -1.99$, $P = 0.02$
	20	One-tailed t test	$t4 = 51.00$, $P < 0.001$
	25	One-tailed t test	$t4 = 43.12$, $P < 0.001$
	30	One-tailed t test	$t4 = 29.54$, $P < 0.001$

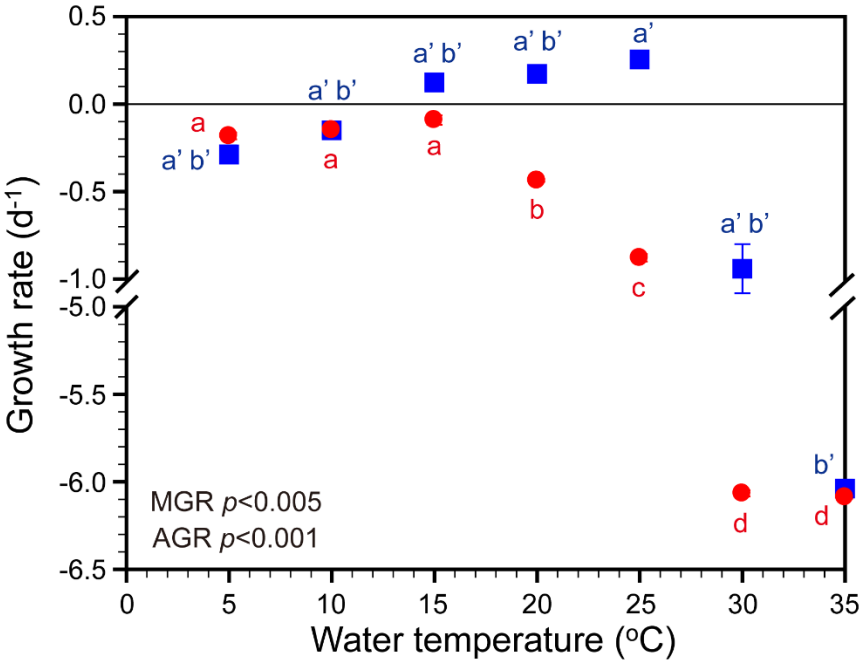

Figure 3.3. Specific autotrophic growth rates (AGRs) of *Biecheleria cincta* BCSH1005 (red circles) and mixotrophic growth rates (MGRs) of *B. cincta* BCSH1005 on *Heterosigma akashiwo* (blue squares) as a function of water temperature. Symbols indicate treatment means ± 1 standard error. Significantly distinct groups based on post-hoc test of one-way ANOVA in AGR and Kruskal-Wallis test in MGR: AGR by Tukey's HSD post-hoc test, 5 (a); 10 (a); 15 (a); 20 (b); 25 (c); 30 (d); and 35°C (d); MGR by Mann-Whitney U comparison with Bonferroni correction post-hoc test, 5 (a'b'); 10 (a'b'); 15 (a'b'); 20 (a'b'); 25 (a'); 30 (a' b'); and 35°C (b').

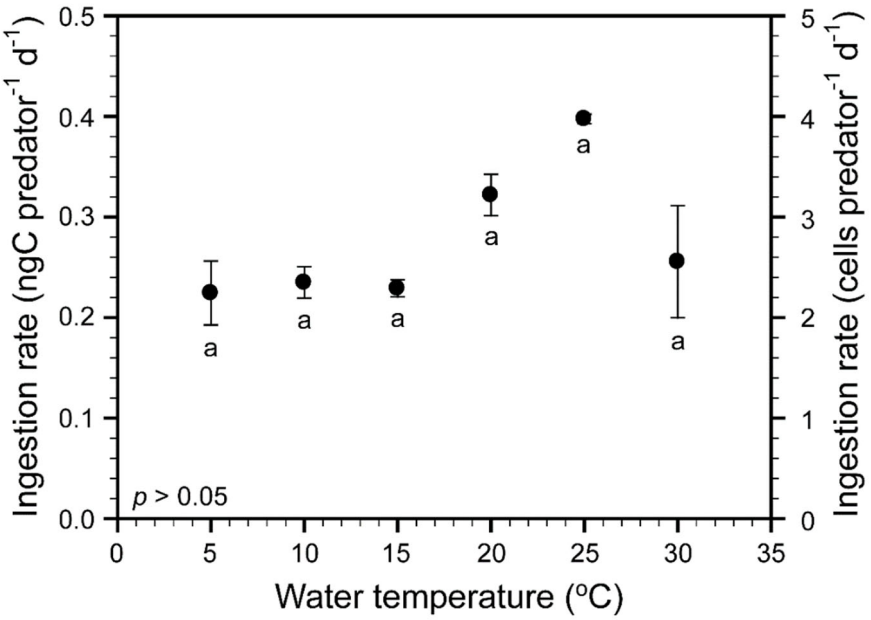

Figure 3.4. Ingestion rates of *Biecheleria cincta* BCSH1005 feeding on *Heterosigma akashiwo* as a function of water temperature. Symbols indicate treatment means ± 1 standard error. They were not significantly different based on Kruskal-Wallis test; however, the ingestion rates at 15–25℃, at which positive mixotrophic growth rates of *B. cincta* BCSH1005 was supported, were significantly different based on Kruscal-Wallis test. Ingestion rate at 35℃ was omitted because of all negative values.

3.3.2. Temperature effects on the growth and ingestion rates of *Gymnodinium smaydae* GSSH1005

The autotrophic growth rates of *Gymnodinium smaydae* increased from -0.54 d^{-1} at 5°C to -0.05 d^{-1} at 20°C, but decreased to -0.35 to -0.52 d^{-1} at 30–35°C (**Figure 3.5**). The autotrophic growth rates were significantly affected by water temperature (one-way ANOVA) and were divided into three different temperature groupings (Tukey HSD post-hoc test, $p < 0.05$; **Table 3.4**, **Figure 3.5**).

The mixotrophic growth rates of *G. smaydae* at 5–35℃ ranged from -0.64 to 1.55 d^{-1} with a maximum at 25℃ (**Figure 3.5**). The rates were significantly affected by temperature (Welch's one-way ANOVA; **Table 3.4**); the rates were subdivided into seven different temperature groupings (Games-Howell post-hoc test; **Table 3.4**, **Figure 3.5**).

The effects of temperature were significantly different between the autotrophic and mixotrophic growth rates of *G. smaydae* (MANOVA, Pillai's Trace = 1.635, $F(9,20) = 9.95$, $p < 0.001$). At 5, 8, and 35℃, the autotrophic and mixotrophic growth rates of *G. smaydae* were not significantly different (**Table 3.4**). However, at 6℃ and from 10 to 32℃, the autotrophic and mixotrophic growth rates of *G. smaydae* were significantly different (**Table 3.4**).

The ingestion rates of *G. smaydae* feeding on *H. rotundata* at 5–35℃ ranged from 0 to 4.2 ng C $predator^{-1}$ d^{-1} with a maximum at 32℃ (**Figure 3.6**). Ingestion rates at 5, 6, 8, and 35℃ have been omitted from the figure. They were unusually high because the cell concentrations of the predator at these temperatures were very low owing to cell death. The ingestion rates were significantly affected by water temperature (one-way ANOVA, **Table 3.4**) and were divided into three different temperature groupings (Tukey HSD post-hoc test; **Table 3.4**, **Figure 3.6**). The ingestion rates of *G. smaydae* on *H. rotundata* were significantly higher than those at zero at all water temperatures except at 15℃ (one–tailed t test, $t4 = 5.74$, $P = 0.003$ at 10℃; $t2 = 1.99$, $p = 0.092$ at 15℃; $t2 = 3.42$, $p = 0.038$ at 20℃; $t4 = 4.04$, $p = 0.008$ at 25℃; $t2 = 4.72$, $p = 0.021$ at 30℃; $t4 = 13.07$, $p < 0.001$ at 32℃).

Table 3.4. Results of the statistical analyses for water temperature effects on the autotrophic and mixotrophic growth and ingestion rates of *Gymnodinium smaydae* GSSH1005 feeding on *Heterocapsa rotundata*. AGR, autotrophic growth rate; MGR, mixotrophic growth rate; IR, ingestion rate; T, water temperature (℃).

a. A significant effect on AGR, MGR, and IR by the T.					
Variances	Range of T	Methods		Results	
		Univariate analysis	Post-hoc test	Univariate analysis	Post-hoc test
AGR	5–35	One-way ANOVA	Tukey's HSD test	F (9, 20) = 5.87, $p < 0.001$	5 (a); 6 (a, b, c); 8 (a, b); 10 (a, b, c); 15 (b, c); 20 (c); 25 (b, c); 30 (a); 32 (a, b); 35℃ (a, b, c)
MGR	5–35	Welch's one-way ANOVA	Games-Howell post-hoc test	F (9,7.659) = 742.03, $p < 0.001$	5 (a′); 6 (b′); 8 (a′b′c′); 10 (c′d′); 15 (d′e′); 20 (f′); 25 (g′); 30 (e′); 32 (e′f′); 35℃ (b′)

IR	10–32	One-way ANOVA	Tukey's HSD test	F (5,12) = 13.81, p < 0.001	10 (ab); 15 (a); 20–25 (ab); 30 (bc); and 32℃ (c).

b. The MGR significantly higher than AGR at the same T.

Variances	T	Methods	Results
Between AGR and MGR	5	One-tailed t test	$t4 = -1.974$, $p = 0.120$
	6	One-tailed t test	$t4 = 3.163$, $p = 0.034$
	8	One-tailed t test	$t4 = 0.175$, $p = 0.870$
	10	One-tailed t test	$t4 = 9.221$, $p = 0.001$
	15	One-tailed t test	$t4 = 4.590$, $p = 0.010$
	20	One-tailed t test	$t4 = 19.178$, $p < 0.001$
	25	One-tailed t test	$t4 = 30.368$, $p < 0.001$
	30	One-tailed t test	$t4 = 8.759$, $p = 0.001$
	35	One-tailed t test	$t4 = 2.717$, $p = 0.053$

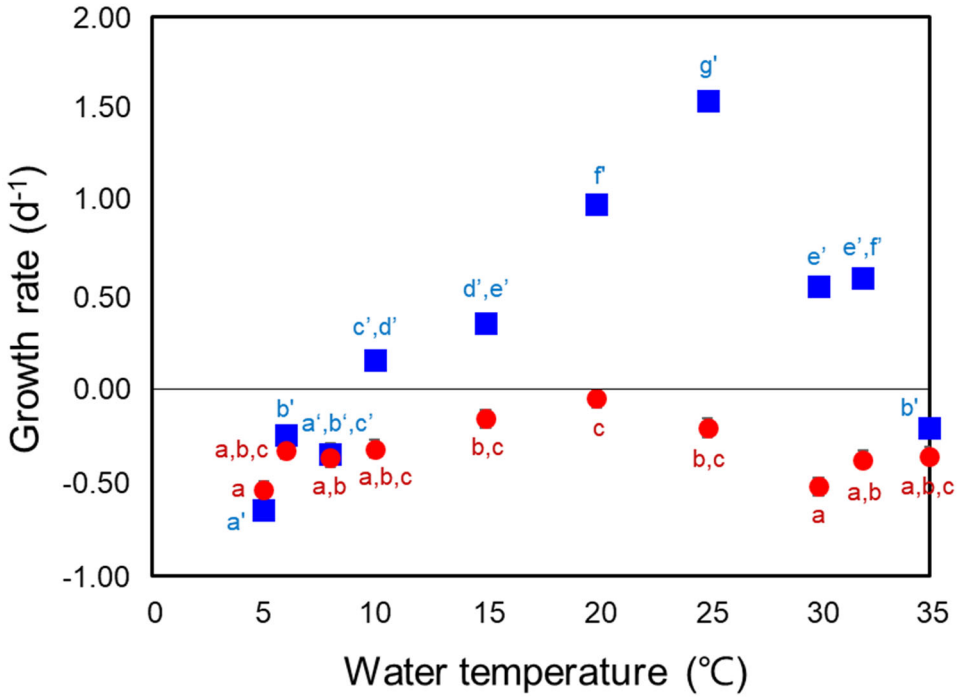

Figure 3.5. Specific autotrophic growth rates of *Gymnodinium smaydae* (red circles) and mixotrophic growth rates of *G. smaydae* on *Heterocapsa rotundata* (blue squares) as a function of water temperature. Symbols represent treatment means ± 1 SE. Significantly different groups based on post-hoc test of ANOVAs: autotrophic growth rate by Tukey HSD post-hoc test, 5 (a); 6 (abc); 8 (ab); 10 (abc); 15 (bc); 20 (c); 25 (bc); 30 (a); 32 (ab); and 35 ºC (abc); mixotrophic growth rate by Games-Howell post-hoc test, 5 (a'); 6 (b'); 8 (a'b'c'); 10 (c'd'); 15 (d'e'); 20 (f'); 25 (g'); 30 (e'); 32 (e'f'); and 35°C (b').

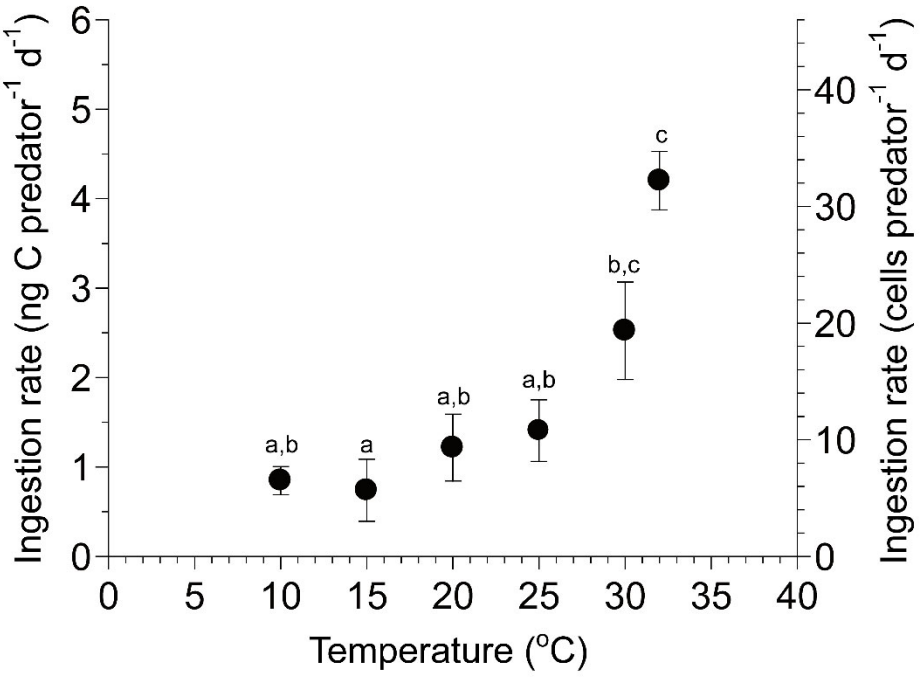

Figure 3.6. Ingestion rates of *Gymnodinium smaydae* on *Heterocapsa rotundata* as a function of water temperature. Data at which the mixotrophic growth rates of *G. smaydae* were negative were omitted because of the overestimation of the ingestion rates. Symbols represent treatment means ± 1 SE. Significantly different groups based on Tukey HSD post-hoc test of one-way ANOVA: 10 (ab); 15 (a); 20, 25 (ab); 30 (bc); and 32°C (c).

3.4. Discussions

3.4.1. Temperature effects on the growth and ingestion of the mixotrophic dinoflagellate *Biecheleria cincta* BCSH1005

Biecheleria cincta BCSH1005 did not survive autotrophically at 5–35℃ in the present study, but they survived by feeding on *H. akashiwo* at 15–25℃. Furthermore, both mixotrophic growth and ingestion rates of *B. cincta* BCSH1005 on *H. akashiwo* increased with increasing water temperature from 15 to 25℃. Thus, a combination of feeding and water temperature may both affect the survival and growth rate of *B. cincta* BCSH1005. Similarly, both the mixotrophic growth and ingestion rates of the mixotrophic dinoflagellate *Paragymnodinium shiwhaense* and the kleptoplastidic dinoflagellate *Shimiella gracilenta* increased with increasing water temperature from 5 to 20 or 25℃, respectively (Jeong et al. 2018b; Ok et al. 2022). However, the mixotrophic growth rates of the kleptoplastidic dinoflagellate *Gymnodinium smaydae* and the mixotrophic dinoflagellates *Takayama helix* and *Yihiella yeosuensis* increased at the water temperatures in which their ingestion rates did not increase (Ok et al. 2019; Kang et al. 2020; You et al. 2020b). Unlike *B. cincta* BCSH1005, *P. shiwhaense*, and *S. gracilenta* whose survival and growth rates are affected by both feeding and water temperature, the mixotrophic growth rates of *G. smaydae*, *T. helix*, and *Y. yeosuensis* are likely to be mainly affected by water temperature.

Biecheleria cincta BCSH1005 had the maximum autotrophic growth rate at 15℃, whereas it had both maximum mixotrophic growth and ingestion rates at 25℃. Therefore, feeding caused a considerable difference between maximum autotrophic and mixotrophic growth rates. Similarly, *S. gracilenta* had the maximum autotrophic growth rate at 20℃ but its maximum mixotrophic growth and ingestion rates at 25℃ (Ok et al. 2022). The water temperatures at which the maximum autotrophic growth rates of *Alexandrium pohangense*, *T. helix*, and *Y. yeosuensis* were achieved were somewhat different from those of the maximum mixotrophic growth rates; however, their maximum autotrophic growth rates were not clearly higher than the second and third-highest autotrophic growth rates at nearby water temperatures (Lim et al. 2019b; Ok et al. 2019; Kang et al. 2020).

3.4.2. Temperature effects on the growth and ingestion of the mixotrophic dinoflagellate *Gymnodinium smaydae* GSSH1005

The present study showed that *G. smaydae* GSSH1005 grew at 10–32℃ when prey was added, but not without prey. Thus, the data from this strain indicate that *G. smaydae* can grow mixotrophically at a wide range of water temperatures, but not autotrophically.

The maximum autotrophic growth rate of *G. smaydae* GSSH1005 was achieved at 20℃, whereas the maximum mixotrophic growth rate was noted at 25℃ (**Figure 3.5**). Hence, 20℃ seems to be an optimal temperature for the growth of *G. smaydae* when prey cells are not available. However, the ingestion rate at 25℃ (1.4 ng C predator^{-1} d^{-1}) was higher than that at 20℃ (1.2 ng C predator^{-1} d^{-1}). Thus, higher carbon acquisition from prey cells at 25℃ is likely to cause a higher growth rate than that at 20℃, and thus the optimal temperature for supporting the highest mixotrophic growth rate was observed at 25℃. The range of mixotrophic growth rates at 10–32℃ (0.16–1.55 d^{-1}) was considerably wider than that of the autotrophic growth rates (-0.05 to -0.52 d^{-1}). Thus, mixotrophy may increase the sensitivity of *G. smaydae* to temperature changes. Enzymes related to feeding may be more sensitive to temperature changes than those related to photosynthesis.

Relatively few studies have investigated the survival or growth rates of mixotrophic dinoflagellates under both autotrophic and mixotrophic conditions as a function of temperature (Lim et al. 2019b; Ok et al. 2019), whereas many studies have conducted such investigations under autotrophic conditions (Matsuoka et al. 1989; Grzebyk and Berland 1996; Band-Schmidt et al. 2004; Kim et al. 2004; Magaña and Villareal 2006; Nagasoe et al. 2006; Matsubara et al. 2007; Baek et al. 2008; Laabir et al. 2011). At 30–32℃, the growth rate of *G. smaydae* GSSH1005 was negative under autotrophic condition, but became positive under mixotrophic condition. This pattern is different from that of *T. helix* CCMP 3082 and *A. pohangense* PHAlex1409 (Lim et al. 2019b; Ok et al. 2019); the growth rates of *T. helix* at 25–28℃ under both autotrophic and mixotrophic conditions were positive, but became negative at 30℃. Furthermore, the growth rates of *A. pohangense* at 20–30℃ under both autotrophic and mixotrophic conditions were positive, but became

negative at 32–35℃. Thus, among these three mixotrophic dinoflagellates, *G. smaydae* is the only one in which mixotrophic growth changes from negative to positive at a certain temperature. Thus, mixotrophy might be a survival strategy of *G. smaydae* at high temperatures. Furthermore, *G. smaydae* can survive at 32℃, but *T. helix*, *A. pohangense*, and *P. shiwhaense* cannot (Jeong et al. 2018b; Lim et al. 2019b; Ok et al. 2019). Thus, high temperature may affect the causative species of blooms and may also be a driving force for the succession of dominant mixotrophic dinoflagellates.

In 2008–2012, water temperatures at the surface of Shiwha Bay were 0.2–28.4℃, but those from November to March were 0.2–8.9℃ (Kang et al. 2013). Thus, based on the data from this strain, *G. smaydae* can grow in April–November if *H. rotundata* or other suitable prey is available. However, global warming can cause the elevation of water temperature in the bay, and in particular, heat waves in summer may accelerate the elevation of water temperature (Lee et al. 2019b). The water temperatures at a depth of 1 m in the bay in the summer of 2018 increased up to 31.5℃ (MEIS). Therefore, *G. smaydae* may have an advantage in outgrowing *T. helix*, *A. pohangense*, and *P. shiwhaense* during the global warming period and/or heat wave year. Moreover, a maximum of 6℃ elevation by 2100 is expected, according to the Intergovernmental Panel on Climate Change report (IPCC, 2013). The data from this study indicate that *G. smaydae* cannot survive at 35℃. Thus, if the water temperature becomes ≥ 35℃ due to global warming or heat waves, *G. smaydae* may also not survive in the surface water. These data also indicate that *G. smaydae* can survive at depth, but its growth can be reduced because of light limitation. Over the coming several decades, water temperature at Shiwha Bay is expected to change largely because it is a small water body (Lee et al. 2019b). Therefore, the distribution of *G. smaydae* in the bay in the near future needs to be explored. Furthermore, to our knowledge, only one strain of *G. smaydae* has been reported. Responses by other strains of *G. smaydae* to light intensity and temperature may be different from those by *G. smaydae* GSSH1005. Thus, if another strain of *G. smaydae* is developed, it would be necessary to explore the differences in the responses.

Chapter 4.
Feeding by common heterotrophic protists on the mixotrophic alga *Gymnodinium smaydae* (Dinophyceae), one of the fastest growing dinoflagellates*

4.1. Introduction

Dinoflagellates are ubiquitous protists in marine environments (e.g., Dodge and Priddle 1987). In marine ecosystems, they have diverse ecological roles as one of the major primary producers (Zhang et al. 1999, Hinder et al. 2012), predators of bacteria, phytoplankton, heterotrophic protists, and metazoans (Burkholder et al. 2008, Jeong et al. 2008, Nishitani et al. 2008, Johnson 2015), and prey for other dinoflagellates, ciliates, and metazoans (Stoecker and Sanders 1985, Hansen 1992, Kamiyama and Matsuyama 2005, Turner and Borkman 2005). Furthermore, they often form red tides or harmful algal blooms, which cause human illness and large scale mortality of fin fish and shellfish (Stoecker 1999, Menden-Deuer and Montalbano 2015, Wolny et al. 2015). To understand the role of a dinoflagellate in marine ecosystems, and minimize the damage due to red tides or harmful blooms dominated by this dinoflagellate, interactions between the dinoflagellate and its potential prey and predators and its population dynamics should be explored.

In the population dynamics of a dinoflagellate, growth and mortality due to predation are the most important factors (e.g., Jeong et al. 2015). To assess predation impact on populations of the dinoflagellate, the kind of predators that are able to feed on the dinoflagellate, and growth and ingestion rates of predators on the dinoflagellate should be determined. In particular, heterotrophic dinoflagellates (HTDs) and ciliates are known to be effective predators on many phototrophic dinoflagellates (Kamiyama and Matsuyama 2005, Turner 2006). Furthermore, the predation impacts of heterotrophic

* This chapter has been published in Journal of Phycology.
Jeong, H. J.*, **You, J. H.**, Lee, K. H., Kim, S. J. & Lee, S. Y. 2018. Feeding by common heterotrophic protists on the mixotrophic alga *Gymnodinium smaydae* (Dinophyceae), one of the fastest growing dinoflagellates. J. Phycol., 54:734–743.

protists are known to be usually much greater than that of metazooplankton (Lee et al. 2017a, Lim et al. 2017). Thus, exploring predation by common heterotrophic protistan predators on a target dinoflagellate is one of the most important steps in understanding the population dynamics of the dinoflagellate.

Recently, a new phototrophic dinoflagellate *Gymnodinium smaydae* (Gymnodiniaceae) was isolated from the waters of Shiwha Bay, Korea and a clonal culture was established (Kang et al. 2014). The size of this dinoflagellate (6–11 μm long and 5–10 μm wide) is almost the smallest among species in the genus *Gymnodinium* so far reported (Kang et al. 2014, Lee et al. 2014a). Recently, this dinoflagellate was revealed to be mixotrophic, that is, it can conduct photosynthesis and ingest prey simultaneously (Lee et al. 2014a); it fed on only thecate dinoflagellates *Heterocapsa* spp. and *Scrippsiella acuminata*. *G. smaydae* can divide approximately three times per day when fed on *Heterocapsa rotundata*, and thus it is one of the fastest growing dinoflagellates so far reported (Lee et al. 2014a). Furthermore, based on the calculated grazing coefficients for *G. smaydae* on co-occurring *H. rotundata* in Shiwha bay, it was suggested that *G. smaydae* can sometimes have a considerable grazing impact on the prey population (Lee et al. 2014a). Although the maximum mixotrophic growth rate of *G. smaydae* is high, its *in situ* growth rate is likely to be affected by predation. Thus, if there are effective predators of this dinoflagellate, populations of *G. smaydae* could be considerably reduced. However, if there is no effective predator, the population of this dinoflagellate may grow well and become abundant without the high mortality due to predation.

In this study, feeding by the HTDs *Gyrodinium dominans* (Gymnodiniaceae), *Gyrodinium moestrupii*, *Oblea rotunda* (Diplopsalidaceae), *Oxyrrhis marina* (Oxyrrhinaceae), and *Polykrikos kofoidii* (Gymnodiniaceae), and the naked ciliate *Pelagostrobilidium* sp. (Strobilidiidae) on *Gymnodinium smaydae* was investigated. These heterotrophic protists were selected as potential predators because they are known to be commonly found in many marine environments (Strom and Buskey 1993, Claessens et al. 2008, Watts et al. 2010, Calbet et al. 2013, Tillmann and Hoppenrath 2013, Yoo et al. 2013). Furthermore, they have

diverse feeding mechanisms; *Gyrodinium* spp., *O. marina*, and *Pelagostrobilidium* sp. directly engulf whole prey cells, *P. kofoidii* engulfs prey cells after capturing them using the nematocyst-taeniocyst complex, while *O. rotunda* feeds on prey cells using the pallium (feeding veil). However, peduncle feeders such as *Pfiesteria* spp., *Stoeckeria* spp., and *Luciella* spp., were not tested because it is impossible to distinguish them from another peduncle feeder *G. smaydae* under a light microscope (Shumway et al. 2006, Lee et al. 2014a). In addition, growth and ingestion rates of the effective predators *O. marina*, *G. dominans*, and *Pelagostrobilidium* sp. on *G. smaydae* in response to prey concentration were also determined. Moreover, to understand the relative nutritional value of *G. smaydae* for *O. marina*, the maximum growth and ingestion rates of *O. marina* on *G. smaydae* were compared to those on other prey items. The results of the present study provide a basis for understanding the interactions between *G. smaydae* and heterotrophic protists, and also the ecological roles of *G. smaydae* in marine planktonic food webs.

4.2. Materials and Methods

4.2.1. Preparation of experimental organisms

A clonal culture of *G. smaydae*, which was isolated from Shiwha Bay, Korea (37°180 N, 126°360 E), during May 2010 and established following two serial single-cell isolations, was used. Approximately 90 mL of a dense culture (ca. 20,000 cells mL^{-1}) of *G. smaydae* were transferred every 3 d to a 270 mL flask of a fresh culture of *H. rotundata* containing ca. 100,000 cells mL^{-1}. The flask was placed on a shelf at 20°C under an illumination of 20 μmol photons m^{-2} s^{-1} cool-white fluorescent light in a 14:10 h Light-Dark cycle. For the isolation and culture of the HTD predators *Gyrodinium dominans* (equivalent spherical diameter of this irregularly shaped organism [i.e., the diameter of a sphere of equivalent volume] = 20.0 μm), *Gyrodinium moestrupii* (22.3 μm), *Oblea rotunda* (21.6 μm), *Oxyrrhis marina* (15.6 μm), and *Polykrikos kofoidii* (43.5 μm), plankton samples were collected with water samplers from the coastal waters off Masan, Jinhae, Kunsan, and Jangheung, Korea during 2001–2016.A clonal culture of each species was established by using two serial single cell isolations (**Table 4.1**).

For the isolation and culture of the ciliate *Pelagostrobilidium* sp., plankton samples were collected with a 20 μm mesh net, from the waters of Tongyoung, Korea, in August 2017 (**Table 4.1**). A clonal culture of *Pelagostrobilidium* sp. was established using two serial single-cell isolations. Cells of *Pelagostrobilidium* sp. were transferred to 270 mL flasks of fresh cultures of *Prorocentrum cordatum* containing ca. 90,000 cells mL^{-1} every day. The flasks were placed on a shelf at 20°C, under the illumination conditions described above.

The carbon contents of the HTDs and the ciliate were estimated from the cell volume, according to the procedure of Menden-Deuer and Lessard (2000). The cell volumes of the predators were obtained from Yoo et al. (2013) for *G. dominans*, *G. moestrupii*, and *P. kofoidii*; Jeong et al. (2008) for *O. marina*; and Ok et al. (2017) for *O. rotunda*. The cell volume of *Pelagostrobilidium* sp. was measured in this study (**Table 4.2**).

Table 4.1. Conditions for the isolation and maintenance of the experimental organisms.

Organisms	Type	FM	Location	Time	T	S	Prey species
Predators							
Gyrodinium dominans	HTD	EG	Shiwha Bay, Korea	Nov 2011	19.7	31.0	*Amphidinium carterae*
Oxyrrhis marina	HTD	EG	Kunsan, Korea	May 2001	16.0	27.7	*Amphidinium carterae*
Gyrodinium moestrupii	HTD	EG	Kunsan, Korea	Oct 2009	21.2	31.0	*Alexandrium minutum*
Oblea rotunda	HTD	PA	Jinhae Bay, Korea	Apr 2015	12.6	31.2	*Amphidinium carterae*
Pelagostrobilidium sp.	NC	FF	Tongyoung, Korea	Aug 2017	27.2	31.5	*Prorocentrum cordatum*
Polykrikos kofoidii	HTD	EG	Jangheung Bay, Korea	Jul 2016	23.6	26.4	*Scrippsiella acuminata*
Prey							
Gymnodinium smaydae	MTD	PD	Shiwha Bay, Korea	May 2010	19.0	27.7	*Heterocapsa rotundata*

FM, feeding mechanisms; T, temperature; S, salinity; HTD, heterotrophic dinoflagellate; NC, naked ciliate; EG, engulfment feeder; PA, pallium feeder; FF, filter feeder; PD, peduncle feeder.

Table 4.2. Feeding occurrence of heterotrophic protists on *Gymnodinium smaydae*.

Potential predators	CV	IPC (cells mL^{-1})	By potential predators		By *G. smaydae*	
			Physical attack	Successful capture	Physical attack	Successful capture
Heterotrophic dinoflagellates						
Gyrodinium dominans	2.0	2000	O	O*	X	X
Oxyrrhis marina	2.0	2000	O	O	X	X
Gyrodinium moestrupii	3.0	200	O	O*	X	X
Oblea rotunda	5.3	250	X	X	O	?
Polykrikos kofoidii	43.0	70	O	X	X	X
Naked ciliate						
Pelagostrobilidium sp.	23.0	5	O	O	X	X

The initial concentration of *G. smaydae* was 10,000 cells mL^{-1}; CV, cell volume ($\times 10^3$ μm^3); IPC, Initial predator concentration; O, observed; X, not observed; ?, deployment of a peduncle by a predator cell on a prey cell was clearly observed, but transfer of materials from the prey cell to the predator cell through the peduncle was not clearly observed; *, rarely captured.

4.2.2. Interactions between *Gymnodinium smaydae* and heterotrophic protists

Experiment (Expt) 1 was designed to investigate the interactions between *G. smaydae* and each of the heterotrophic protists after cells of *G. smaydae* were added to bottles containing cells of the target heterotrophic protist (**Table 4.2**). In this experiment, whether the target heterotrophic protist is able to feed on *G. smaydae*, or vice versa, was examined. A dense culture of a target heterotrophic protist was transferred to a 270-mL polycarbonate (PC) bottle when the prey cells were no longer detectable in the ambient water and the protoplasm of the heterotrophic protist cells. The cells in three 1-mL aliquots from the bottle were counted using a compound microscope to determine the concentrations of predator cells.

A dense culture (ca. 20,000 cells mL^{-1}) of *G. smaydae* was added to one 42-mL PC bottle containing each HTD and one well of a 6-well plate chamber containing ciliates (see **Table 4.2** for the final concentration of each component). One predator-control bottle or one well of the chamber (without *G. smaydae*) and one prey-control bottle or one well of the chamber (without heterotrophic protist) were set up for each experiment. The bottles were placed on a plankton wheel rotating at 0.9 rpm (equivalent to 0.00017 × g), and the plate chamber containing ciliates was placed on a shelf. The bottles and the plate chamber were incubated at 20°C under an illumination of 20 μmol photons m^{-2} s^{-1} of cool white fluorescent light on a 14 :10 h Light-Dark cycle.

Three-milliliter aliquots were removed from each bottle after 2, 6, 24, and 48 h incubations and then transferred to new 6-well plate chambers. Approximately 20 cells of each predator in the plate chambers at each interval were observed under a dissecting microscope (or inverted microscope) at a magnification of × 20–63 to determine whether the predator was able to feed on *G. smaydae*. Cells of predators containing ingested *G. smaydae* cells were photographed on covered glass slides using a digital camera (Zeiss AxioCam HRc5; Carl Zeiss Ltd., Gottingen, Germany) attached to a microscope at a magnification of × 200–1,000. In addition, the behaviors of more than 30

target predator cells were monitored using an inverted epifluorescence microscope equipped with differential interference contrast at a magnification of × 100–400. The feeding process of each of these heterotrophic protists on *G. smaydae* was recorded using a video analyzing system (Sony DXC-C33; Sony Co., Tokyo, Japan), and also captured using a digital camera. The attack by *G. smaydae* on *O. rotunda* was examined and recorded in the same manner as described above.

4.2.3. Growth and ingestion rates of heterotrophic protists feeding on *Gymnodinium smaydae* as a function of prey concentration

In Expt 1, *G. dominans*, *G. moestrupii*, *O. marina*, and *Pelagostrobilidium* sp. were revealed to feed on *G. smaydae*. Of these predators, *O. marina* was observed to grow feeding on *G. smaydae*, and feeding by *G. dominans* and *Pelagostrobilidium* sp. on *G. smaydae* was frequently observed. Thus, the growth and ingestion rates of *O. marina*, *G. dominans*, and *Pelagostrobilidium* sp. when feeding on *G. smaydae* were measured. Expts 2, 3, and 4 were designed to measure the growth and ingestion rates of *O. marina*, *G. dominans*, and *Pelagostrobilidium* sp. as a function of prey concentration (**Table 4.3**).

In Expts 2 and 3, a dense culture of *O. marina* (or *G. dominans*) was transferred to a 270-mL PC bottle when the prey cells were no longer detectable. The bottle was placed on a shelf and incubated at 20°C under illumination of 20 μmol photons m^{-2} s^{-1} of cool white fluorescent light on a 14 :10 h Light-Dark cycle. In Expt 2, the abundance of *O. marina* in the bottle was determined every 2 d for ca. 1 week, and the experiment started when the growth rate of *O. marina* was almost zero. This preincubation process was done to minimize the possible residual growth resulting from the ingestion of prey during batch culture. In Expt 3, the abundance of *G. dominans* in the bottle was determined without preincubation because the growth rate of *G. dominans* became almost zero rapidly.

In Expt 4, two dense cultures of *Pelagostrobilidium* sp. were transferred to an 800-mL flask when the prey cells were no longer detectable. The cells in three 1-mL aliquots from the flask were counted using a compound microscope to determine the concentrations of predator cells. For each experiment, the initial concentrations of *O. marina*, *G. dominans*, or *Pelagostrobilidium* sp. (predator) and *G. smaydae* (prey) were established using an autopipette to deliver predetermined volumes of known cell concentrations to the bottles. Triplicate 42-mL PC experimental bottles (mixtures of predator and prey) and triplicate control bottles (prey only) were set up for each predator-prey combination. Triplicate control bottles containing only predators were also established at a single predator concentration. To obtain similar water conditions, the water of the predator culture was filtered through a 0.7-μm GF/F filter and then added to the prey-control bottles in the same amount as the volume of the predator culture added to the experimental bottles for each predator-prey combination. In addition, the water of the prey culture was filtered through a 0.7-μm GF/F filter and then added to the predator-control bottles in the same amount as the volume of the prey culture added into the experimental bottles. All the bottles were then filled to capacity with freshly filtered seawater and capped. To determine the actual predator and prey densities at the beginning of the experiment, a 5-mL aliquot was removed from each bottle, fixed with 5% Lugol's solution, and examined with a light microscope to determine predator and prey abundances by enumerating the cells in three 1-mL Sedgwick-Rafter chambers (SRCs). The bottles were refilled to capacity with F/2 medium (Guillard and Ryther 1962), capped, and placed on a shelf under the conditions described above. Dilution of the cultures associated with refilling the bottles was considered when the growth and ingestion rates were calculated. A 10 mL aliquot was taken from each bottle at 48 h (or 24 h for *Pelagostrobilidium* sp.) and fixed with 5% Lugol's solution, and then the abundances of predators and prey were determined by counting all or more than 300 cells in three 1-mL SRCs. The conditions of predators and prey were assessed using a dissecting microscope, as described above, prior to subsampling.

For each experiment, the initial concentrations of *O. marina*, *G. dominans*, or *Pelagostrobilidium* sp. (predator) and *G. smaydae* (prey) were

established using an autopipette to deliver predetermined volumes of known cell concentrations to the bottles. Triplicate 42-mL PC experimental bottles (mixtures of predator and prey) and triplicate control bottles (prey only) were set up for each predator-prey combination. Triplicate control bottles containing only predators were also established at a single predator concentration. To obtain similar water conditions, the water of the predator culture was filtered through a 0.7-μm GF/F filter and then added to the prey-control bottles in the same amount as the volume of the predator culture added to the experimental bottles for each predator-prey combination. In addition, the water of the prey culture was filtered through a 0.7-μm GF/F filter and then added to the predator-control bottles in the same amount as the volume of the prey culture added into the experimental bottles. All the bottles were then filled to capacity with freshly filtered seawater and capped. To determine the actual predator and prey densities at the beginning of the experiment, a 5-mL aliquot was removed from each bottle, fixed with 5% Lugol's solution, and examined with a light microscope to determine predator and prey abundances by enumerating the cells in three 1-mL Sedgwick-Rafter chambers (SRCs). The bottles were refilled to capacity with F/2 medium (Guillard and Ryther 1962), capped, and placed on a shelf under the conditions described above. Dilution of the cultures associated with refilling the bottles was considered when the growth and ingestion rates were calculated. A 10-mL aliquot was taken from each bottle at 48 h (or 24 h for *Pelagostrobilidium* sp.) and fixed with 5% Lugol's solution, and then the abundances of predators and prey were determined by counting all or more than 300 cells in three 1-mL SRCs. The conditions of predators and prey were assessed using a dissecting microscope, as described above, prior to subsampling.

The specific growth rates of a predator, μ (d^{-1}) was calculated as follows:

$$\mu\ (d^{-1}) = [\mathrm{Ln}\ (P_t / P_0)] / t \qquad (1)$$

, where P_0 and P_t are the concentrations of the predator at time (t) 0 and 48 h for *O. marina* and *G. dominans* or 24 h for *Pelagostrobilidium* sp.

The calculated growth rate was fitted to a modified Michaelis-Menten

equation:

$$\mu\ (d^{-1}) = \mu_{max}\ (x - x') / [K_{GR} + (x - x')] \qquad (2)$$

, where μ_{max} = the maximum specific growth rate (d^{-1}); x = prey concentration (cells mL^{-1} or ng C mL^{-1}), x' = threshold prey concentration (i.e., the prey concentration where $\mu = 0$), and K_{GR} = the prey concentration sustaining 1/2 μ_{max}. The data were iteratively fitted to the model using DeltaGraph (Red Rock Software Inc., Salt Lake, UT, USA).

The ingestion and clearance rates and mean prey concentrations were calculated using the equations of Frost (1972) and Heinbokel (1978). The incubation time for calculating the ingestion and clearance rates was the same as that for estimating the growth rate. The ingestion rate data (IRs, cells $predator^{-1}\ d^{-1}$ or ng C $predator^{-1}\ d^{-1}$) were fitted into a modified Michaelis-Menten equation:

$$IR = I_{max}(x) / [K_{IR} + (x)] \qquad (3)$$

, where I_{max} = the maximum ingestion rate (cells $predator^{-1}\ d^{-1}$ or ng C $predator^{-1}\ d^{-1}$), x = the prey concentration (cells mL^{-1} or ng C mL^{-1}), and K_{IR} = the prey concentration sustaining 1/2 I_{max}.

Table 4.3. Design of experiments. The numbers in the prey and predator columns are the actual initial densities (cells mL^{-1}) of the prey and predator. The values within parentheses in the predator columns are the predator densities in the control bottles.

Expt. No.	Prey		Predator	
	Species	Density	Species	Density
1	*Gymnodinium smaydae*	10,000	*Gyrodinium dominans*	2,000
			Gyrodinium moestrupii	200
			Oblea rotunda	250
			Oxyrrhis marina	2,000
			Pelagostrobilidium sp.	5
			Polykrikos kofoidii	70
2	*Gymnodinium smaydae*	44, 81, 275, 609, 1039, 1866, 3613, 6083, 8550	*Oxyrrhis marina*	12, 22, 53, 113, 228, 351, 549, 728, 880 (355)
3	*Gymnodinium smaydae*	24, 53, 95, 302, 685, 1272, 2462, 5653, 8805, 10317	*Gyrodinium dominans*	8, 9, 19, 38, 94, 184, 361, 586, 869, 1174 (384)
4	*Gymnodinium smaydae*	79, 132, 557, 937, 1092, 2953, 4821, 5712, 6181	*Pelagostrobilidium* sp.	11, 11, 25, 24, 36, 32, 34, 45, 46 (39)

4.2.4. Swimming speed of *Pelagostrobilidium* sp.

Prior to the present study, the swimming speed of *Pelagostrobilidium* sp. had not been measured, whereas those of *G. smaydae*, *O. marina*, and *G. dominans* have been provided (Lee et al. 2014a, Jeong et al. 2018a). Thus, the swimming speed of *Pelagostrobilidium* sp. was determined in the present study.

A culture of *Pelagostrobilidium* sp. satiated with *Prorocentrum cordatum* (~90,000 cells mL^{-1}) was transferred into a 270-mL flask. When the prey was undetectable, a 25-mL aliquot from the bottle was added to a 25-mL cell culture flask and allowed to acclimate for 30 min. The video camera focused on an individual field view of a single circle in the cell culture flask under a dissecting microscope at 20°C. *Pelagostrobilidium* sp. cells were then recorded swimming at a magnification of × 20 using a video analyzing system (SRD-1673DN; Samsung Techwin, Seongnam, Korea) and CCD camera (Sony DXC-C33; Sony co.). The swimming speeds of all the swimming cells viewed between 10 and 30 min were analyzed. The average swimming speed (n = 30) was calculated on the basis of the linear displacement of cells in 1 sec during a single-frame playback. This result was shown in the discussion section.

4.3. Results

4.3.1. Interactions between *Gymnodinium smaydae* and common heterotrophic protists

Among the tested heterotrophic protists, *G. dominans*, *G. moestrupii*, *O. marina*, and *Pelagostrobilidium* sp. were able to feed on *G. smaydae* (**Table 4.2**, **Figure 4.1**) but *P. kofoidii* and *O. rotunda* did not feed on this dinoflagellate. Cells of *P. kofoidii* rarely deployed a nematocyst-taeniocyst complex on the surface of *G. smaydae*, and no prey cells were engulfed (n > 100 cells). Moreover, *O. rotunda* did not even deploy a tow filament to *G. smaydae*.

Cells of *O. marina* engulfed *G. smaydae* cells (**Figure 4.2**). It took ca. 10–20 s for an *O. marina* cell to completely engulf a *G. smaydae* cell. Furthermore, *Pelagostrobilidium* sp. also engulfed *G. smaydae* cells (**Figure 4.2**). It took ca. 2 s for a *Pelagostrobilidium* sp. cell to completely engulf a *G. smaydae* cell.

Interestingly, *G. smaydae* cells deployed peduncles to *O. rotunda* cells, but prey materials were not observed being transferred from *O. rotunda* cells to *G. smaydae* cells (**Figure 4.3**). Some *O. rotunda* cells to which *G. smaydae* deployed a peduncle escaped from being ingested and moved away (**Figure 4.3**), whereas other *O. rotunda* cells to which *G. smaydae* deployed a peduncle became motionless (**Figure 4.3**).

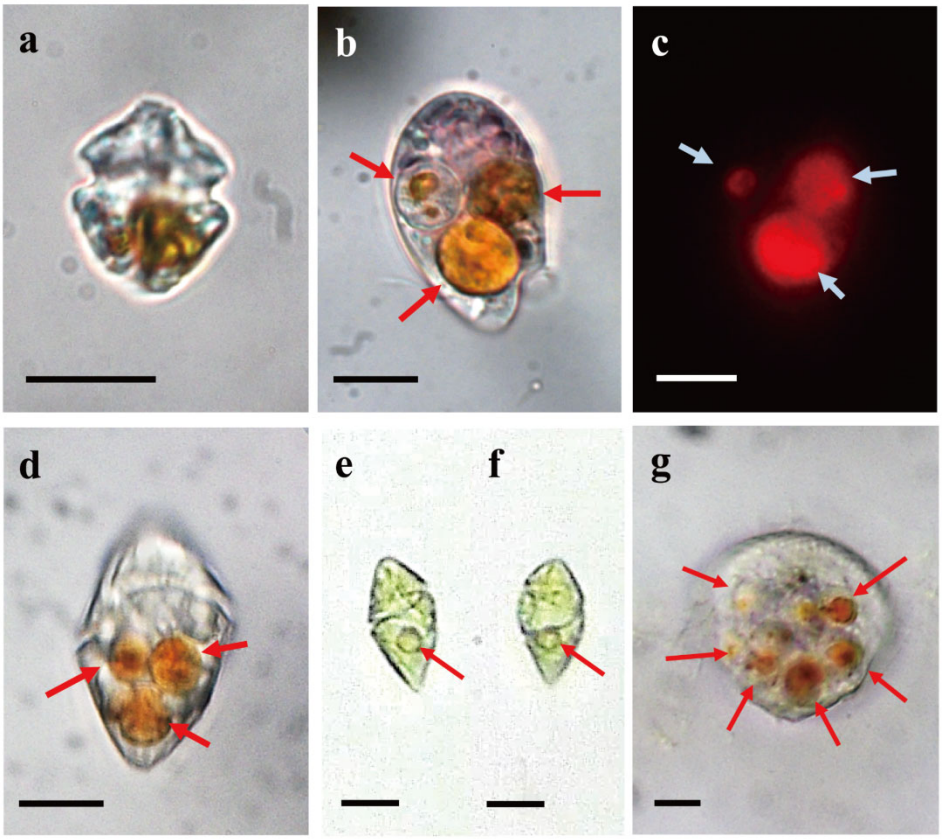

Figure 4.1. Heterotrophic protists fed on *Gymnodinium smaydae* (red arrows), taken using an epifluorescence microscope (Jeong and You et al. 2018). (a) Unfed *G. smaydae* cell. (b and c) The heterotrophic dinoflagellate *Oxyrrhis marina* cell containing three ingested *G. smaydae* cells observed using different lights and filter (b, no filter; and c, green filter). (d) The heterotrophic dinoflagellate *Gyrodinium dominans* cell containing three ingested *G. smaydae* cells. (e and f) The heterotrophic dinoflagellate *Gyrodinium moestrupii* cell containing one ingested *G. smaydae* cell. (g) The naked ciliate *Pelagostrobilidium* sp. cell containing several ingested *G. smaydae* cells. Scale bars = 10 μm.

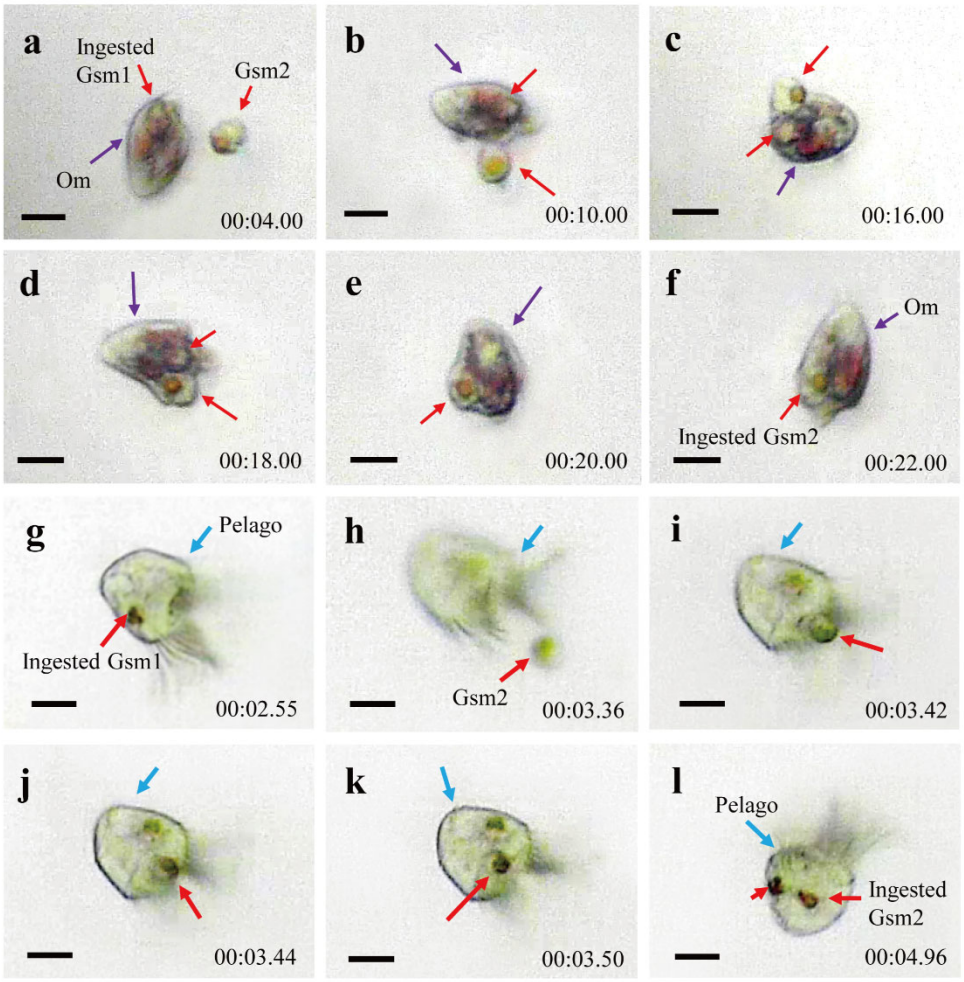

Figure 4.2. Feeding process of the heterotrophic dinoflagellate *Oxyrrhis marina* and the naked ciliate *Pelagostrobilidium* sp. on *Gymnodinium smaydae*, recorded using video microscopy (Jeong and You et al. 2018). (a–f) Feeding by *O. marina* (Om, purple arrows) on *G. smaydae* (Gsm, red arrows). An Om cell containing previously ingested Gsm cells fed on another Gsm cell. (g–l) Feeding by *Pelagostrobilidium* sp. (Pelago, blue arrows) on *G. smaydae* (Gsm). A Pelago cell containing a previously ingested Gsm cell fed on another Gsm cell. The numbers indicate min: sec.centisec. Scale bars = 10 μm for (a–f) and 20 μm for (g–l).

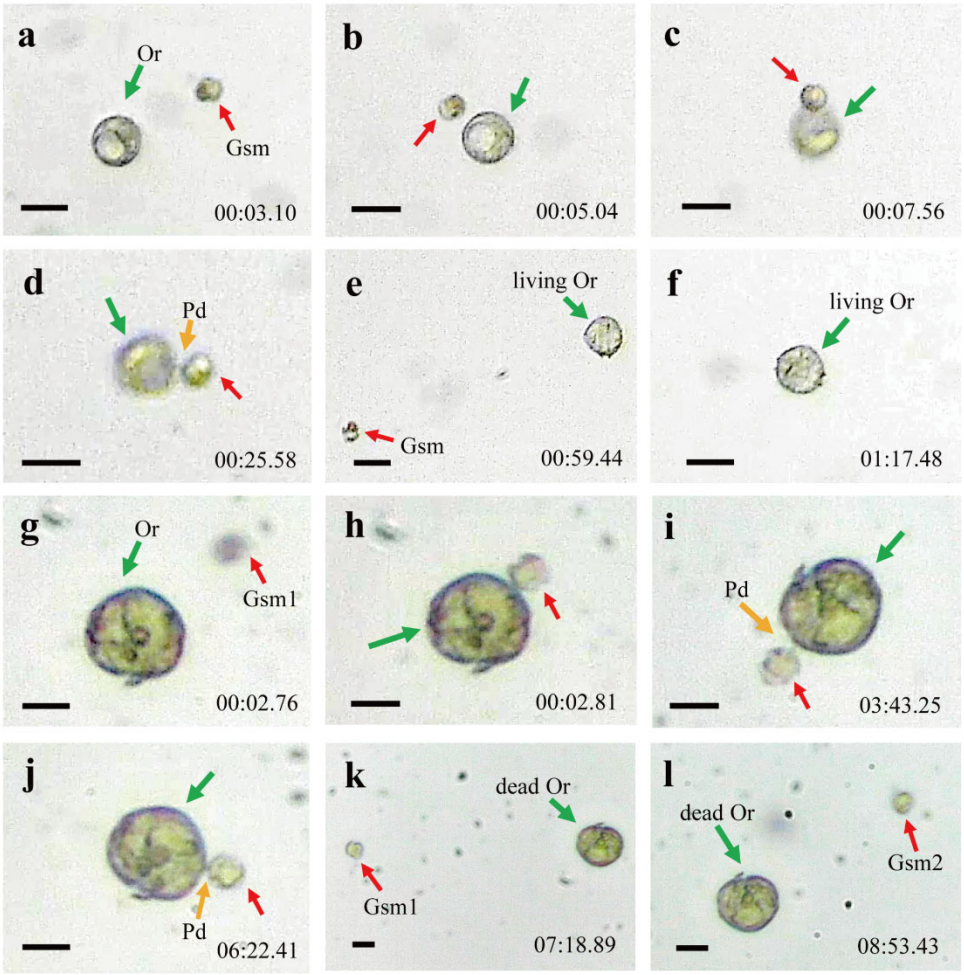

Figure 4.3. Process of *Gymnodinium smaydae* attacking the heterotrophic dinoflagellate *Oblea rotunda* recorded using video microscopy (Jeong and You et al. 2018). (a–f) A *Gymnodinium smaydae* (Gsm, red arrows) cell attacking *Oblea rotunda* (Or, green arrows) using a peduncle (Pd, orange arrows). The Or cell retreated after the attack was interrupted. (g–l) A *G. smaydae* (Gsm, red arrows) cell attacking *O. rotunda* (Or, green arrows) using a peduncle (Pd, orange arrows). The Or cell eventually became dead. The numbers indicate min:sec.centisec. Scale bars = 20 μm for (a–f) and 10 μm for (g–l).

4.3.2. Growth rates of heterotrophic protists with and without *Gymnodinium smaydae* and ingestion rates

With increasing mean prey concentration, the specific growth rates of *O. marina* on *G. smaydae* rapidly increased at prey concentrations ≤ 150 cells mL^{-1} (18 ng C mL^{-1}), but became saturated at higher prey concentrations (**Figure 4.4a**). The maximum growth rate (GR_{max}) of *O. marina* on *G. smaydae* was 0.411 d^{-1}. Furthermore, at the given mean prey concentrations, the specific growth rates of *G. dominans* on *G. smaydae* ranged from -0.104 to 0.114 d^{-1} (**Figure 4.4b**). However, the specific growth rates were not significantly affected by mean prey concentrations [ANOVA, F (10,22) = 0.395, p = 0.935]. Moreover, with increasing mean prey concentration, the specific growth rates of *Pelagostrobilidium* sp. on *G. smaydae* rapidly increased at prey concentrations ≤ 1,750 cells mL^{-1} (354 ng C mL^{-1}), but became saturated at higher prey concentrations (**Figure 4.4c**). However, all the growth rates of *Pelagostrobilidium* sp. on *G. smaydae* at the given prey concentrations were negative. The highest growth rate was -0.310 d^{-1}. Thus, *G. smaydae* did not support the positive growth of *Pelagostrobilidium* sp.

With increasing mean prey concentration, the ingestion rates of *O. marina* on *G. smaydae* rapidly increased at prey concentrations ≤650 cells mL^{-1} (78 ng C mL^{-1}; **Figure 4.5a**). The maximum ingestion rate (IR_{max}) of *O. marina* on *G. smaydae* was 0.27 ng C predator $^{-1}$ d^{-1} (2.3 cells $predator^{-1}$ d^{-1}). Furthermore, at the given mean prey concentrations, the ingestion rates of *G. dominans* on *G. smaydae* ranged from 0 to 0.04 ng C predator $^{-1}$ d^{-1} (**Figure 4.5b**). However, the ingestion rates were not significantly affected by mean prey concentrations [ANOVA, F (9,20) = 0.937, p = 0.516]. Moreover, with increasing mean prey concentration, the ingestion rates of *Pelagostrobilidium* sp. on *G. smaydae* rapidly increased at prey concentrations ≤ 1,750 cells mL^{-1} (354 ng C mL^{-1}; **Figure 4.5c**). The IR_{max} of *Pelagostrobilidium* sp. on *G. smaydae* was 6.91 ng C predator $^{-1}$ d^{-1} (57.6 cells $predator^{-1}$ d^{-1}).

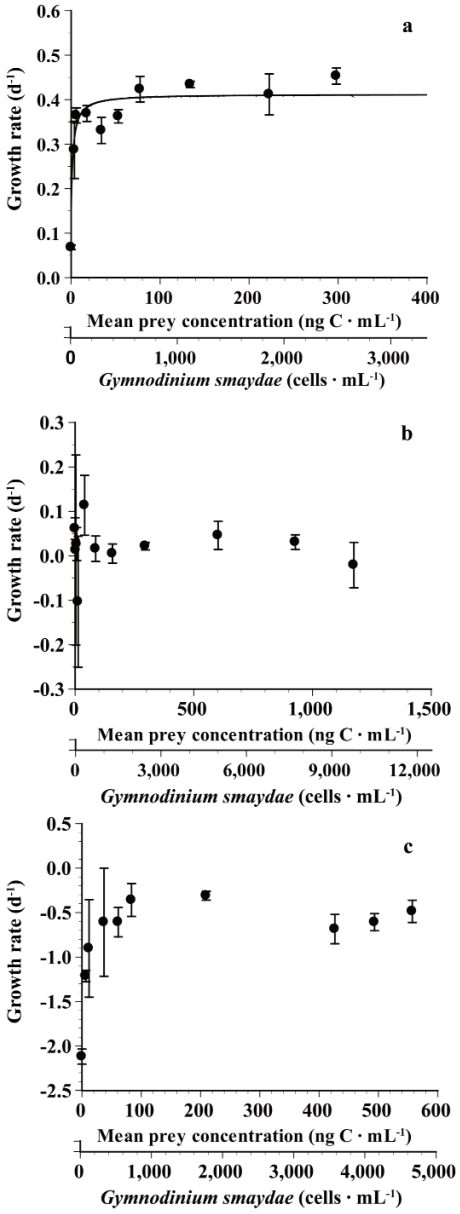

Figure 4.4. Specific growth rates of *Oxyrrhis marina* (a), *Gyrodinium dominans* (b), and *Pelagostrobilidium* sp. (c) on *Gymnodinium smaydae* as a function of mean prey concentration (x, ng C mL^{-1} or eaten *G. smaydae* cells mL^{-1}) (Jeong and You et al. 2018). The carbon content of *G. smaydae* is 0.12 ng C $cell^{-1}$. Symbols represent treatment means ±SE. The curve in (a) was fitted to the Michaelis-Menten equation (eq. 2) using all treatments in the experiment. Growth rate (GR, d^{-1}) = 0.411 {[x + 0.28] / [1.4 + (x + 0.28)]}, r^2 = 0.774.

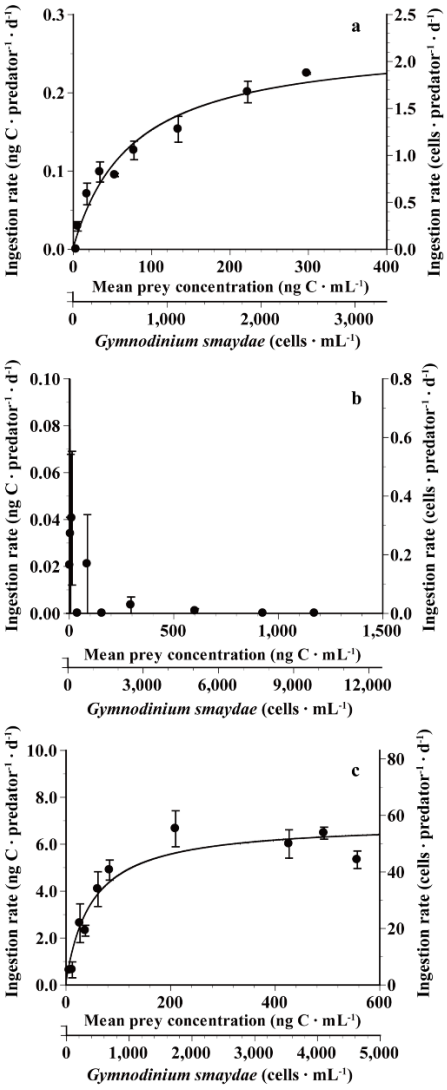

Figure 4.5. Ingestion rates by *Oxyrrhis marina* (a), *Gyrodinium dominans* (b), and *Pelagostrobilidium* sp. (c) on *Gymnodinium smaydae* as a function of mean prey concentration (x, ng C mL^{-1} or eaten *G. smaydae* cells mL^{-1}) (Jeong and You et al. 2018). The carbon content of *G. smaydae* is 0.12 ng C $cell^{-1}$. Ingestion rates in the left axis are expressed in terms of carbon content (ng C $predator^{-1}$ d^{-1}), while those in the right axis in terms of equivalent prey cell number (cells $predator^{-1}$ d^{-1}). Symbols represent treatment means ±SE. The curves in (a) and (c) were fitted to the Michaelis-Menten equation (eq. 3) using all treatments in the experiment. (a) Ingestion rate (IR, ng C $predator^{-1}$ d^{-1}) = 0.266 [(x) / (75.4 + x)], r^2 = 0.923. (c) Ingestion rate (IR, ng C $predator^{-1}$ d^{-1}) = 6.91 [(x) / (48.8 + x)], r^2 = 0.830 (x, ng C mL^{-1}).

4.4. Discussions

4.4.1. Interactions between *Gymnodinium smaydae* and common heterotrophic protists

Theoretically, in the population dynamics of a dinoflagellate, high growth but low mortality rates due to predation cause rapid increases in its cell abundance (Jeong et al. 2015). *G. smaydae* has the highest growth rate among the dinoflagellates (2.23 d^{-1}). The study clearly shows that 4 of 6 potential heterotrophic protistan predators feed on *G. smaydae*. Another MTDs *Paragymnodinium shiwhaense* and *Yihiella yeosuensis* also have high growth rates (1.10 and 1.32 d^{-1}; Yoo et al. 2010, Jang et al. 2017b). However, there are only a few heterotrophic protistan predators that are able to feed on *P. shiwhaense* and *Y. yeosuensis* (Jeong et al. 2017a, 2018a). Thus, the growth rate of *G. smaydae* could be lowered by common heterotrophic protistan predators, but those of the other MTDs may not be lowered. Predation by heterotrophic protists may change the dominant species among these dinoflagellates in natural environments.

To increase feeding efficiency, HTDs have different feeding mechanisms (e.g., Hansen and Calado 1999): engulfment feeding (Hansen 1991), pallium feeding (Jacobson and Anderson 1986), and peduncle feeding (Burkholder and Glasgow 1997). Moreover, as tools for capturing a moving prey cell, some HTDs have a nematocyst or a nematocyst-taeniocyst complex which can paralyze a prey cell (Westfall et al. 1983, Hoppenrath and Leander 2007). Interestingly, *G. smaydae* is not preyed upon by the nematocyst-taeniocyst complex bearing *P. kofoidii*, which is known to feed on diverse algal prey species and the mixotrophic ciliate *Mesodinium rubrum* (e.g., Matsuoka et al. 2000), and also has a considerable grazing impact on populations of the red tide dinoflagellate *Cochlodinium polykrikoides* (Lim et al. 2017). Furthermore, *G. smaydae* is not fed on by the pallium feeder *O. rotunda*, which is also known to feed on diverse algal prey species (e.g., Strom and Buskey 1993). When *G. smaydae* is provided, *O. rotunda* does not even deploy a tow filament, which is known to be used to capture prey cells (Strom and Buskey 1993). Thus, *P. kofoidii* and *O. rotunda* may have difficulty in anchoring small *G. smaydae* cells using a nematocyst-taeniocyst complex or

a tow filament. This evidence suggests that feeding mechanisms of predators may be critical in feeding on *G. smaydae* cells, and also *G. smaydae* may have an advantage over its competitors with minimizing grazing pressure by *P. kofoidii* or *O. rotunda*.

The kind of the heterotrophic protistan predators that are able to feed on *G. smaydae* is different from that on most other MTDs. Thus, the ecological niche of *G. smaydae* is different from that of other MTDs in marine ecosystems.

4.4.2. Growth and ingestion rates of common heterotrophic protists feeding on *Gymnodinium smaydae*

The present study clearly shows that *G. smaydae* prey supports the positive growth of only *O. marina*. Thus, when *G. smaydae* is abundant, *O. marina* is likely to be abundant, but *G. dominans*, *G. moestrupii*, and *Pelagostrobilidium* sp. may not be abundant.

The IR_{max} of *O. marina* on *G. smaydae* is the lowest among its IR_{max} on algal prey species, but it is comparable to that on the HTD prey species *Luciella masanensis*, *Pfiesteria piscicida*, and *Stoeckeria algicida*, as well as the heterotrophic nanoflagellate prey *Cafeteria* sp. (**Table 4.4**, **Figure 4.6a**). Therefore, *O. marina* may have more difficulty in feeding on *G. smaydae* than on other algal prey species, but can feed on heterotrophic protists with comparable difficulty. In addition, the GR_{max} of *O. marina* on *G. smaydae* is also lower than that of any other algal prey except for the haptophyte *Emiliania huxleyi*, which contains dimethylsulfoniopropionate and a toxic strain of *Karlodinium veneficum* (**Table 4.4**, **Figure 4.6b**). In contrast, the GR_{max} of *O. marina* on *G. smaydae* is greater than that on *L. masanensis*, and *S. algicida* (**Table 4.4**, **Figure 4.6b**). The size of *G. smaydae* is intermediate among the algal prey species for *O. marina* (**Figure 4.6a**, **b**). Thus, the size of *G. smaydae* is not likely to be responsible for the lowest IR_{max} and almost lowest GR_{max} among the algal prey species. The maximum swimming speed of *G. smaydae* is greater than that of the other algal prey species (**Table 4.4**); thus, the high motility of *G. smaydae* may make it more difficult for *O.*

marina to capture, handle, and engulf it, compared to other algal prey species (i.e., low ingestion rate). However, the ratio of GR_{max} relative to IR_{max} of *G. smaydae* is greater than those of other algal prey species. Therefore, once the *G. smaydae* cells are ingested by *O. marina* cells, the ingested prey cells may be more readily assimilated into the predator's body than those of other algal prey species.

Unlike *G. smaydae* prey, diverse algal prey species are known to support the positive growth of *G. dominans* (Nakamura et al. 1995, Yoo et al. 2010, 2013, Calbet et al. 2013). Furthermore, both *G. dominans* and *O. marina* are known to grow well on diverse algal prey species, such as the haptophyte *Isochrysis galbana*, the cryptophyte *Rhodomonas salina*, the chlorophyte *Dunaliella tertiolecta*, and the dinoflagellate *Amphidinium carterae* (Goldman et al. 1989, Nakamura et al. 1995, Jeong et al. 2001a, Kimmance et al. 2006, Calbet et al. 2013). Therefore, *G. smaydae* is an example of a prey species providing differential support to the growth of *O. marina* and *G. dominans*.

Although the highest growth rate of *Pelagostrobilidium* sp. on *G. smaydae* at the given prey concentrations is -0.31 d^{-1}, the specific growth rates of *Pelagostrobilidium* sp. at high prey concentrations are greater than those at low prey concentrations. The calculated daily carbon acquisition by *Pelagostrobilidium* sp. from *G. smaydae* (6.9 ng C) is ca. 330% of the body carbon of the predator. Thus, theoretically, if the growth efficiency of *Pelagostrobilidium* sp. on *G. smaydae* is assumed to be 30%, a *Pelagostrobilidium* cell should divide once per day. Thus, the growth efficiency of *Pelagostrobilidium* sp. on *G. smaydae* must be very low (possibly <10%). In this study, the maximum swimming speed of *Pelagostrobilidium* sp. was 3,500 μm s^{-1}, while the average (± SE) swimming speed (n = 30) was 765 (±162) μm s^{-1}. The maximum swimming speed of *Pelagostrobilidium* sp. is much greater than that of the other heterotrophic protist predators (**Table 4.5**). Thus, *Pelagostrobilidium* sp. is likely to spend a large amount of energy on searching and feeding prey cells.

In conclusion, the growth rate of the fast-growing *G. smaydae* may be lowered by some heterotrophic protists. In particular, *O. marina* may be an

effective predator on *G. smaydae*. However, the grazing impact of *O. marina* on populations of *G. smaydae* cannot be calculated at this moment, because data on the abundances of the predator and prey are not available. Thus, it would be worthwhile to investigate their abundance at sea.

Table 4.4. Comparison of growth and ingestion data for *Oxyrrhis marina*. Temperature (T, ℃) for maximum swimming speed (MSS, μm s^{-1}) measurement was 20℃ except for *Brachiomonas submarina, Eutreptiella gymnastica, Heterosigma akashiwo,* and *Karlodinium veneficum*. Data on T were not available for these algal prey species. AV in MSS data indicated average values.

Prey	ESD	MGR	K_{GR}	χ′	MIR	K_{IR}	MGR/MIR	T	MSS	Ref
Bacteria										
Mixed bacteria	< 1.0	0.59	11.50	1.63	0.07	44.00	8.5	20	-	1, 2
Diatom										
Phaeodactylum tricornutum	4.2	1.30			1.89		0.7	20	-	3
Chlorophyte									-	
Chlamydomonas spreta	6.2	0.53	387.00	146.00	1.97	338.25	0.3	21	-	4
Dunaliella primolecta (Fuller)	6.4	1.47	458.30	-22.00	1.10	126.78	1.3	21	-	4
Dunaliella tertiolecta	7.3	0.80			1.54		0.5	20	-	3
Dunaliella primolecta (351_FAR01)	8.0	0.50	91.80	46.20	1.22	4,538.00	0.4	20	-	2, 5
Dunaliella primolecta (45_BOG01)	8.0	0.77	49.40	21.30	2.30	19,300.00	0.3	20	-	2, 5
Brachiomonas submarina	10.5	0.73	40.80	57.60	1.29	146.19	0.6	21	115	4, 6
Euglenophyte										
Eutreptiella gymnastica	12.6	0.81	11.00	0.80	2.70	163.00	0.3	20	275	7, 8

Eustigmatophyte										
Nannochloropsis oculata	2.5	1.31	625.50	114.40	1.37	182.30	1.0	21	-	4
Prymnesiophyte										
Emiliania huxleyi	4.1	0.37			2.65		0.1	15	-	9
Isochrysis galbana	5.0	0.94	98.70	44.50	1.43	781.00	0.7	20	-	2, 5, 10
Raphidophyte										
Heterosigma akashiwo	11.5	1.43	104.00	8.00	1.25	704.00	1.1	20	361	11
Fibrocapsa japonica	20.4	0.72			1.18		0.6	20	-	12
Phototrophic dinoflagellate										
Azadinium cf. *poporum*	10.0	0.50	79.40	0.51	4.99	287.00	0.1	20	550	13
Mixotrophic dinoflagellate										
*Karlodinium veneficum*_NTX (MD5)	9.1	0.85			6.36		0.1	20	81[AV]	14
Amphidinium carterae	9.7	1.17	12.50	1.30	2.80	90.00	0.4	20	190	15
*Karlodinium veneficum*_TX (CCMP 2064)	10.5	0.25			2.36		0.1	20	81 [AV]	14
Gymnodinium smadyae	10.5	0.41	1.42	-0.28	0.27	75.40	1.5	20	707	16
Symbiodinium voratum	11.1	0.87	61.40	14.10	2.10	357.00	0.4	20	287	17, 18
Biecheleria cincta	12.2	0.49	5.67	1.38	0.35	9.22	1.4	20	691	18, 19
Gymnodinium aureolum	19.5	0.71	55.20	7.80	0.51	60.60	1.4	20	576	20

Heterotrophic dinoflagellate										
Luciella masanensis	13.5	0.04			0.07	132.00	0.6	20	680	21, 22
Pfiesteria piscicida	13.5	0.66	21.00	0.40	0.33	83.00	2.0	20	300 [AV]	21, 23
Stoeckeria algicida	13.9	0.22	64.00	-4.70	0.14	89.00	1.6	20	681	21, 24
Heterotrophic nanoflagellate										
Cafeteria sp.	3.5	0.19	0.48	0.06	0.29	455.00	0.6	20	-	25

ESD, equivalent spherical diameter (μm); MGR, maximum growth rate (μ_{max}, d^{-1}); K_{GR}, the prey concentration sustaining 1/2 μ_{max} (ng C mL^{-1}); χ', threshold prey concentration (the prey concentration where μ=0, ng C mL^{-1}); MIR, maximum ingestion rate (I_{max}, ng C $predator^{-1}$ day^{-1}); K_{IR}, the prey concentration sustaining 1/2 I_{max} (ng C mL^{-1}); T, temperature (°C) for MGR and MIR measurement; NTX, non-toxic; TX, toxic; MSS, maximum swimming speed (μm s^{-1}).

(1) Jeong et al. (2008); (2) Roberts et al. (2010); (3) Goldman et al. (1989); (4) Fuller (1990); (5) Montagnes et al. (2010); (6) Bauerfeind et al. (1986); (7) Jeong et al. (2011); (8) Throndsen (1973), Sommer (1988); (9) Strom et al. (2003); (10) Kimmance et al. (2006); (11) Jeong et al. (2003), Yamochi and Abe (1984); (12) Tillmann and Reckermann (2002); (13) Potvin et al. (2013); (14) Adolf et al. (2007), Sheng et al. (2010); (15) Jeong et al. (2001a), Kamykowski and McCollum (1986); (16) This study, Lee et al. (2014a); (17) Jeong at al. (2014); (18) Yoo et al. (2015); (19) Yoo et al. (2013); (20) Yoo et al. (2010), Jeong et al. (2010b); (21) Jeong et al. (2007); (22) Jeong et al. (2007a), Jang et al. (2016); (23) Jeong et al. (2006), Burkholder and Glasgow (1997); (24) Jeong et al. (2005c), Lim et al. (2014); (25) Jeong et al. (2007).

Table 4.5. Swimming speed of *Gymnodinium smaydae* and potential heterotrophic protistan predators. ASS, averaged swimming speed; MSS, maximum swimming speed.

Species	ASS (μm s^{-1})	MSS (μm s^{-1})	References
Gyrodinium dominans	299	440	Jeong at al. 2018
Gyrodinium moestrupii	405	880	Jeong et al. 2018a
Oblea rotunda	420	-	Buskey et al. 1993, Our unpublished data
Oxyrrhis marina	474	590	Jeong et al. 2018a
Polykrikos kofoidii	657	911	Jeong et al. 2002
Pelagostrobilidium sp.	765	3,500	This study
Gymnodinium smaydae	335	707	Lee et al. 2014a

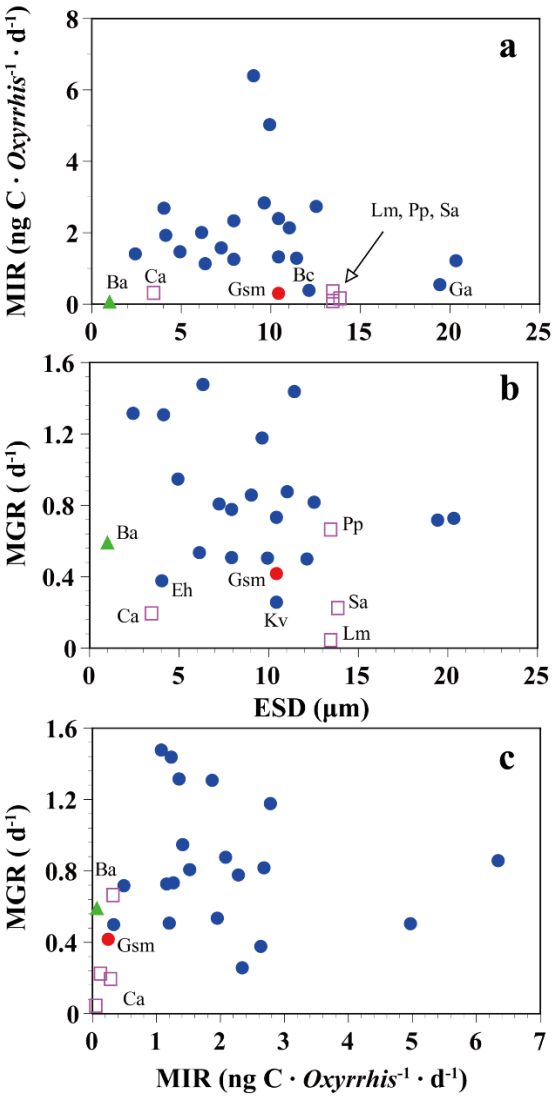

Figure 4.6. The maximum growth (MGR, d^{-1}) and ingestion rates (MIR, ng C $predator^{-1}$ d^{-1}) of *Oxyrrhis marina* on diverse prey species (Jeong and You et al. 2018). (a) MIRs and (b) MGRs of *O. marina* on bacteria (green triangle), algal prey (blue circles), heterotrophic nanoflagellates, and heterotrophic dinoflagellates (red squares) as a function of prey size (equivalent spherical diameter, ESD, lm). (c) MGRs of *O. marina* on the prey items as a function of MIRs: Bacteria (Ba), *Cafeteria* sp. (Ca), *Gymnodinium smaydae* (Gsm, red circle), *Biecheleria cincta* (Bc), *Luciella masanensis* (Lm), *Pfiesteria piscicida* (Pp), *Stoeckeria algicida* (Sa), *Gymnodinium aureolum* (Ga), *Emiliania huxleyi* (Eh) and *Karlodinium veneficum* (toxic strain, Kv). The rest of the algal prey species are provided in **Table 4.4**.

Chapter 5.
The extended prey spectrum of *Scrippsiella acuminata* and five *Scrippsiella* species lacking mixotrophic ability*

5.1. Introduction

Mixotrophy, a combination of autotrophy and heterotrophy, is observed in many marine flagellates, dinoflagellates, and ciliates (Stoecker et al. 1997, Burkholder et al. 2008, Esteban et al. 2010, Jeong et al. 2010b). Mixotrophs play diverse roles as primary producers, prey, and predators in marine ecosystems, whereas exclusively autotrophic organisms play the roles of primary producers and prey (Stoecker et al. 1997, Burkert et al. 2001, Burkholder et al. 2008, Jeong et al. 2012, 2016). Mixotrophy increases the growth rate of protists (Li et al. 2000, Smalley et al. 2003, Jeong et al. 2015, 2021, Ok et al. 2019, Kang et al. 2020, You et al. 2020b), causes horizontal gene transfer, and is the main driving force in the evolution of photosynthetic organisms (Tengs et al. 2000, Bhattacharya et al. 2004, Yoon et al. 2002, 2005, Wisecaver et al. 2013, Hehenberger et al. 2019). Therefore, understanding mixotrophy is of ecological and evolutionary importance.

Dinoflagellates are ubiquitous protists in marine environments (Jeong et al. 2013, Leles et al. 2019, Nishimura et al. 2020, Luo et al. 2021, Ok et al. 2021, Morquecho et al. 2022), and often form red tides or harmful algal blooms that can cause human diseases and massive mortality in shellfish, finfish, and mammals (Shumway 1990, Hallegraeff 1992, Flewelling et al. 2005, Shin et al. 2019, Sakamoto et al. 2021). Investigation of the trophic modes, growth and ingestion rates, and mortality rates due to predation of dinoflagellate species should be investigated to understand and predict the outbreak of dinoflagellate red tides (Franklin et al. 2006, Jeong et al. 2015). In the last three decades, many dinoflagellate species previously thought to

* This chapter has been published in Algae.
You, J. H., Ok, J. H.*, Kang, H. C., Park, S. A., Eom, S. H. & Jeong, H, J. 2023. Five phototrophic *Scrippsiella* species lacking mixotrophic ability and the extended prey spectrum of *Scrippsiella acuminata* (Thoracosphaerales, Dinophyceae). Algae, 38:111–126.

be autotrophs were reclassified as mixotrophs (Bockstahler and Coats 1993, Stoecker et al. 1997, Jeong 1999, Jeong et al. 2004, 2016), including many species that form red tides (Jeong et al. 2004, 2005a, b, c, Burkholder et al. 2008, Park et al. 2013a, Flynn et al. 2018). Approximately 90% of the dinoflagellates that form global red tides are mixotrophs (Jeong et al. 2021); however, less than 10% of the approximately 1,200 phototrophic dinoflagellates have been tested for mixotrophy (Stoecker et al. 1997, Jeong et al. 2004, 2005a, b, c, 2016, Park and Kim 2010b, Lee et al. 2014a, c, 2015, Lim et al. 2018b, 2019). Therefore, understanding the ecological and genetic characteristics and red tide dynamics of a phototrophic dinoflagellate species requires an examination of their mixotrophic ability. Moreover, the prey species of mixotrophic dinoflagellates should be identified.

Since the description of the genus *Scrippsiella* by Balech (1959) with the type species *S. sweeneyae*, 28 species have been formally described (Hoppenrath et al. 2014, Guiry and Guiry 2023). The species in the genus *Scrippsiella* have a global distribution; however, only *S. acuminata* (previously *S. trochoidea*) has caused red tides in the waters of many countries (Hallegraeff 1992, Pitcher et al. 2007, Pitcher and Joyce 2009, Soehner et al. 2012, Jeong et al. 2021). Red tides dominated by *Scrippsiella* spp. can cause fish mortality through hypoxia (Hallegraeff 1992); therefore, to minimize losses caused by *Scrippsiella* red tides, the ecophysiology and population dynamics of each *Scrippsiella* species should be understood (Jeong et al. 2015). Of the formally described and unidentified species in this genus, only *S. acuminata* and two unidentified *Scrippsiella* species have been confirmed to be mixotrophic (Jacobson and Anderson 1996, Jeong et al. 2005a, b, Coats et al. 2020). Therefore, the mixotrophic abilities of other *Scrippsiella* species should be investigated. *S. acuminata* cells have been reported to feed on the cyanobacterium *Synechococcus* sp., prymnesiophyte *Isochrysis galbana*, cryptophytes *Rhodomonas salina* and an unidentified species, raphidophyte *Heterosigma akashiwo*, and the phototrophic dinoflagellates *Amphidinium carterae* and *Prorocentrum cordatum* (Jeong et al. 2005a, b). Furthermore, an unidentified *Scrippsiella* sp., which was collected from the waters off Korea, has been reported to feed on the tintinnid ciliate *Helicostomella longa* using a feeding tube (Coats et al. 2020). Another unidentified *Scrippsiella* sp. isolated from West Boothbay Harbor, Maine,

USA was reported to possess food vacuoles (Jacobson and Anderson 1996). Heterotrophic bacteria are common in almost all marine ecosystems (Caron et al. 1982, Kjelleberg et al. 1987, Van Wambeke et al. 2000, Seong et al. 2006, Sanz-Sáez et al. 2020, Vijayan et al. 2022) and serve as prey for many mixotrophic dinoflagellates (Seong et al. 2006, Jeong et al. 2010b, 2012, Lee et al. 2014c, Millette et al. 2017). Thus, the ability of each *Scrippsiella* species to feed on heterotrophic bacteria warrants investigation.

In the present study, the mixotrophic abilities of five *Scrippsiella* species (*Scrippsiella donghaiensis* SDGJ1703, *S. lachrymosa* SLBS1703, *S. masanensis* SSMS0908, *S. plana* SSSH1009A, and *S. ramonii* VGO1053) were identified after they were provided 2-μm fluorescently labeled microspheres (FLM), fluorescently labeled heterotrophic bacteria (FLB), *Synechococcus* sp., and 12 microalgal species as potential prey. Whether *S. acuminata* STKP9909 can feed on FLM and FLB was also investigated. The present study provides a basis for understanding the ecological roles of these *Scrippsiella* species in marine ecosystems and their evolution within the genus *Scrippsiella*.

5.2. Materials and Methods

5.2.1. Preparation of experimental organisms

Scrippsiella acuminata STKP9909, *S. donghaiensis* SDGJ1703, *S. lachrymosa* SLBS1703, and *S. masanensis* SSMS0908 were isolated from the waters off Kunpho in September 1999, Gijang in March 2017, Busan in March 2017, and Masan in August 2009, respectively. A clonal culture of each of the four species was established using two serial single-cell isolations (**Table 5.1**; Kim et al. 2019, Lee et al. 2019c). To isolate and culture *S. plana* SSSH1009A, surface sediment samples were collected from Shiwha Bay, Korea, in September 2010 using an Ekman Grab (Wildco; Wildlife Supply Company, Buffalo, NY, USA) (**Table 5.1**). The collected sediments were stored at 4℃ in the dark and incubated as described by Jeong et al. (2014). A clonal culture of *S. plana* SSSH1009A was established using two serial single-cell isolations from the incubated sediment samples. A culture of *S. ramonii* VGO1053 that was originally collected from Ebro Delta in Spain was obtained from a culture collection at the Centro Oceanografico in Vigo (**Table 5.1**). All *Scrippsiella* cultures were transferred every two weeks in 250- or 800-mL flat culture flasks containing fresh F/2-Si medium (Guillard and Ryther 1962) and maintained in a 14 : 10 h Light-Dark cycle under 50–100 μmol photons m^{-2} s^{-1} from a cool-white fluorescent light at 20℃.

The microalgal species selected as potential prey were maintained under the same light and temperature conditions as the *Scrippsiella* species (**Table 5.2**). The cyanobacterium *Synechococcus* sp. was maintained under 5–10 μmol photons m^{-2} s^{-1} from cool-white fluorescent light with a 14 : 10 h Light-Dark cycle at 20℃.

Table 5.1. Culture conditions for the six *Scrippsiella* species used in this study. Equivalent spherical diameter (ESD, μm); water temperature (T, °C); salinity (S); not available, (-).

Organisms	Strain name	ESD	Location	Date	T	S
Scrippsiella lachrymosa	SLBS1703	17.7	Busan, Korea	March 2017	10.9	33.5
S. donghaiensis	SDGJ1703	19.4	Gijang, Korea	March 2017	13.2	33.9
S. masanensis	SSMS0908	22.0	Masan bay, Korea	August 2009	27.0	31.5
S. acuminata (= *S. trochoidea*)	STGP9909	22.8	Kunpho, Korea	September 1999	-	-
S. plana	SSSH1009A	24.9	Surface sediment in the Shiwha bay, Korea	September 2010	21.3	15.6
S. ramonii	VGO1053	25.5	Ebro Delta, Spain	-	-	-

Table 5.2. Culture conditions for the potential prey items offered to *Scrippsiella* species in feeding occurrence tests (Expts 1–4). Equivalent spherical diameter (ESD, μm); water temperature (T, ℃); salinity (S); initial prey concentration (IPC, cells mL^{-1}); not available, (-).

Organisms (strain name)	**ESD**	**Location**	**Date**	**T**	**S**
Microspheres	2.0				
Bacteria					
Heterotrophic bacteria	0.5-1.0	Each *Scrippsiella* culture	-	-	-
Synechococcus sp. (N54-2)	0.5-1.0	East China Sea	Jul 2005	25.5	33.2
Prymnesiophyte					
Isochrysis galbana (IG)	4.8	-	-	-	-
Prasinophyte					
Pyramimonas sp. (PSSH1204)	5.6	Shiwha bay, Korea	Apr 2012	-	-
Cryptophyte					
Teleaulax amphioxeia (TSGS0202)	5.6	Gomso bay, Korea	Feb 2002	7.8	30.1
Storeatula major (SSSH1103)	6.0	Shiwha bay, Korea	Mar 2011	4.3	19.1
Rhodomonas salina (RS)	8.8	-	-	-	-
Raphidophyte					
Heterosigma akashiwo (HAKS9905)	11.5	Kunsan, Korea	May 1999	16.0	27.7
Phototrophic dinoflagellate					
Heterocapsa rotundata (HRSH1201)	8.2	Shiwha bay, Korea	Jan 2012	0.2	31.0

Heterocapsa minima (HMMJ1604)	9.5	Mijo Port, Korea	Apr 2016	12.9	30.3
Amphidinium carterae (SIO PY-1)	9.7	USA	Nov 1985	-	-
Prorocentrum cordatum (PMKS9906)	12.1	Kunsan, Korea	Jun 1999	21.1	30.1
Prorocentrum donghaiense (PDYS1407)	13.3	Yeosu, Korea	Jul 2017	-	-
Prorocentrum micans (PMSH0910)	26.6	Shiwha bay, Korea	Oct 2009	16.8	27.0
Akashiwo sanguinea	30.8	-	-	-	-

5.2.2. Feeding occurrence test

Experiments 1–4 were designed to explore whether *S. donghaiensis* SDGJ1703, *S. lachrymosa* SLBS1703, *S. masanensis* SSMS0908, *S. plana* SSSH1009A, and *S. ramonii* VGO1053 could feed on the FLM (diameter = 2 μm; 18604 Fluoresbrite® YG Microspheres, Polysciences Inc., Warrington, PA, USA; Expt 1), FLB (Expt 2), *Synechococcus* sp. (Expt 3), or microalgal prey species (Expt 4). Whether *S. acuminata* STKP9909 can feed on the FLM and FLB was also investigated.

In Expt 1, approximately 3×10^7 FLM were added to a 30-mL polycarbonate (PC) rounded bottle containing either *S. acuminata*, *S. donghaiensis*, *S. lachrymosa*, *S. masanensis*, *S. plana*, or *S. ramonii*. One experimental bottle (one *Scrippsiella* species + FLM), one prey control bottle (FLM only), and one predator control bottle (one *Scrippsiella* species only) were included in each experimental run. The bottles were incubated on a plankton wheel rotating at 0.9 rpm (0.00017 × g) at 20℃ under a 14 : 10 h light-dark cycle (20 μmol photons m^{-2} s^{-1}). After 2 and 24 h of incubation, 3-mL aliquots were removed from each bottle and transferred to confocal dishes (SPL100350; SPL Life Sciences Co., Ltd., Pocheon, Korea). To observe *Scrippsiella* spp. feeding on the FLM, the protoplasm of 200 cells of each target *Scrippsiella* species was carefully observed under an inverted microscope (Zeiss Axiovert 200M; Carl Zeiss Ltd., Göttingen, Germany) and photographs were taken using a digital camera (Zeiss Axiocam 506; Carl Zeiss Ltd.) attached to the microscope at 1,000 × magnification.

To prepare for Expt 2, marine heterotrophic bacterial cells were obtained by filtering non-axenic cultures of *S. acuminata*, *S. donghaiensis*, *S. lachrymosa*, *S. masanensis*, *S. plana*, and *S. ramonii*. Aliquots of 300–2,000 mL from each *Scrippsiella* culture were serially filtered through 5.0-μm and 1.2-μm pore-sized filter papers (Merk Millipore, Burlington, MA, USA). The filtrates containing only bacterial cells were centrifuged at 3,000 rpm (2,063 × *g*) for 30 min at 4℃ (Labogene 1696R; Gyrozen Co., Gimpo, Korea) in Falcon tubes (Falcon; Corning, NY, USA). The centrifuged bacterial cells were fluorescently labeled with 5- (4, 6-dichlorotriazin-2-yl) amino fluorescein hydrochloride (D0531; Sigma-Aldrich, St. Louis, MO, USA)

according to the method of Sherr et al. (1987) and then stored in the dark at 4℃ until use. The FLB cells were resuspended in the culture medium using a sonicator (Bransonic cleaner 5510E-DTH, Danbury, CT, USA) for 10 min and then filtered through a 3-μm pore-sized filter paper (Merck Millipore) to remove aggregated bacterial cells. Each *Scrippsiella* spp. was tested using FLB collected from its own culture.

In Expts 2 and 3, approximately 3×10^7 FLB (Expt 2) or *Synechococcus* cells (Expt 3) were added to 30-mL PC rounded bottles containing each *Scrippsiella* species (**Table 5.3**). After 1 and 4 h of incubation, 3-mL aliquots were removed from each bottle, transferred into confocal dishes (SPL Life Sciences Co.), and carefully observed as described above.

In Expt 4, dense cultures of *S. donghaiensis*, *S. lachrymosa*, *S. masanensis*, *S. plana*, and *S. ramonii* were added to the wells of 6-well plates containing each algal prey species. Experimental well (one *Scrippsiella* species + one microalgal prey species), one prey control well (microalgal prey species only), and one predator control well (one *Scrippsiella* species only) were established, and the plate was cultured in a 14 :10 h Light-Dark cycle (20 μmol photons m^{-2} s^{-1}) at 20℃. After 2 h and 24 h of incubation, 3-mL aliquots were removed from each experimental well and transferred to confocal dishes (SPL Life Sciences Co.). The protoplasm of 200 cells of target *Scrippsiella* spp. was observed using an inverted microscope (Carl Zeiss) and photographed at 1,000 × magnification.

Table 5.3. Feeding occurrence results for the six *Scrippsiella* species tested.

Organisms	**ESD**	**IPC**	**Predator species**					
			S. acuminata	***S. donghaiensis***	***S. lachrymosa***	***S. masanensis***	***S. plana***	***S. ramonii***
Microspheres	2.0	1,000	Y*	N	N	N	N	N
Bacteria								
Heterotrophic bacteria	0.5-1.0	700–1,000	Y*	N	N	N	N	N
Synechococcus	1.0	1,000	Y[a,]*	N	N	N	N	N
Prymnesiophytes								
Isochrysis galbana	4.8	100–200	Y[b]	N	N	N	N	N
Prasinophytes								
Pyramimonas sp.	5.6	100	-	N	N	N	N	N
Cryptophytes								
Unidentified cryptophyte	5.6	100	Y[b]	-	-	-	-	-
Teleaulax amphioxeia	5.6	50–100	-	N	N	N	N	N
Storeatula major	6.0	50–100	-	N	N	N	N	N
Rhodomonas salina	8.8	30–50	Y[b]	N	N	N	N	N
Raphidophyte								
Heterosigma akashiwo	11.5	10–30	Y[b]	N	N	N	N	N

Phototrophic dinoflagellates								
Heterocapsa minima	8.2	60	-	-	-	N	N	N
Heterocapsa rotundata	9.5	50	-	N	N	-	-	-
Amphidinium carterae	9.7	30–60	Y[b]	N	N	N	N	N
Prorocentrum cordatum	12.1	13–30	Y[b]	N	N	N	N	N
Prorocentrum donghaiense	13.3	13–30	N[b]	N	N	N	N	N
Prorocentrum micans	26.6	2–5	N[b]	N	N	N	N	N
Akashiwo sanguinea	30.8	1–3	N[b]	N	N	N	N	N

Equivalent spherical diameter (ESD, μm); initial prey concentration (IPC, × 10^3 cells or particles mL^{-1}). The heterotrophic bacteria used in this study and *Synechococcus* sp. for *S. acuminata* used in Jeong et al. (2005a) were fluorescently labeled. The *Scrippsiella* species fed on prey (Y); the *Scrippsiella* species did not feed on prey (N); not available (-). Initial *Scrippsiella* concentrations were approximately 2,000–7,000 cells mL^{-1}. [a], rarely fed on the prey; [b], Jeong et al. (2005a); [c], Jeong et al. (2005b).

5.2.3. DNA sequencing and phylogenetic analysis

The LSU rDNA sequences of *S. acuminata* STKP9909, *S. donghaiensis* SDGJ1703, and *S. plana* SSSH1009A were not previously reported and that of *S. ramonii* VGO1053 was previously partially reported. To obtain these sequences, 1 μL from each culture was removed and added into 0.2-mL PCR tubes with 38.75 μL deionized sterile distilled water. Subsequently, a mixture of 1 μL dNTP mix, 0.25 μL F-StarTaq DNA polymerase, 5 μL 10X F-StarTaq buffer (BioFACT Co., Ltd., Daejeon, Korea), and 4 μL of each forward-reverse primer set needed for amplification of the LSU rDNA region (Set 1, ITSF2 and LSU500R; Set 2, D1R and 1483R) were added to the test tubes. The sequences of the primers used are as follows: ITSF2, 5′-TAC GTC CCT GCC CTT TGT AC-3′; D1R, 5′-ACC CGC TGA ATT TAA GCA TA-3′; LSU500R, 5′-CCC TCA TGG TAC TTG TTT GC-3′; 1483R, 5′-GCT ACT ACC ACC AAG ATC TGC-3′ (Scholin et al. 1994, Litaker et al. 2003, Daugbjerg et al. 2000). Polymerase chain reaction (PCR) was conducted using an AllInOne Cycler (Bioneer, Daejeon, Korea) under the same thermal conditions as described by You et al. (2023a). The PCR products were purified using an AccuPrep DNA Purification Kit (Bioneer) and then sequenced using an ABI 3730XL DNA Analyzer (Applied Biosystems, Foster City, CA, USA). Sequences were aligned and manually edited using ContigExpress (Infomax, Frederick, MD, USA).

For phylogenetic analysis, LSU rDNA sequences from 19 *Scrippsiella* spp. were obtained from this study and GenBank and aligned using MEGA v4 (Tamura et al. 2007). An LSU rDNA phylogenetic tree was constructed using Bayesian (the default GTR + G + I model in MrBayes v3.1; Ronquist and Huelsenbeck 2003) and maximum likelihood analyses (the default GTRGAMMA model in RAxML 7.0.3 program; Stamatakis 2006). The assumed empirical nucleotide frequencies of the LSU rDNA comprised a substitution rate matrix where A–C = 0.0344, A–G = 0.1778, A–T = 0.0562, C–G = 0.0163, C–T = 0.6361, and G–T = 0.0792. The rates were assumed to follow a gamma distribution with a shape parameter of 0.4747 for the variable sites. The proportion of the sites that were assumed to be invariable was 0.2041.

5.3. Results

5.3.1. Feeding occurrence of the *Scrippsiella* spp.

In Expt 1, the 2-µm FLM were found in the protoplasm of *S. acuminata* STKP9909 cells, although they were rarely observed (**Table 5.3**, **Figure 5.1**). However, no FLM were observed in the protoplasm of observed *S. donghaiensis* SDGJ1703, *S. lachrymosa* SLBS1703, *S. masanensis* SSMS0908, *S. plana* SSSH1009A, or *S. ramonii* VGO1053 cells (**Table 5.3**, **Figure 5.2**). Similarly, in Expt 2, FLBs were found in the protoplasm of *S. acuminata* STKP9909 cells, although they were rarely observed (**Table 5.3**, **Figure 5.3A–B**); however, *S. donghaiensis*, *S. lachrymosa*, *S. masanensis*, *S. plana*, and *S. ramonii* did not feed on FLB (**Table 5.3**; **Figure 5.3C–L**). Moreover, in Expt 3, *S. donghaiensis*, *S. lachrymosa*, *S. masanensis*, *S. plana*, and *S. ramonii* did not feed on *Synechococcus* sp. (**Table 5.3**).

In Expt 4, *S. donghaiensis*, *S. lachrymosa*, *S. masanensis*, *S. plana*, and *S. ramonii* did not feed on any of the microalgal prey species, which included the prymnesiophyte *Isochrysis galbana* (IG), prasinophyte *Pyramimonas* sp. (PSSH1204), cryptophytes *Teleaulax amphioxeia* (TSGS0202), *Storeatula major* (SSSH1103), *Rhodomonas salina* (RS), raphidophyte *Heterosigma akashiwo* (HAKS9905), and phototrophic dinoflagellates *Heterocapsa rotundata* (HRSH1201), *Heterocapsa minima* (HMMJ1604), *Amphidinium carterae* (SIO PY-1), *Prorocentrum cordatum* (PMKS9906), *Prorocentrum donghaiense* (PDYS1407), *Prorocentrum micans* (PMSH0910), and *Akashiwo sanguinea* (ASUSA) (**Table 5.3**, **Figure 5.4**). Furthermore, *S. donghaiensis*, *S. lachrymosa*, *S. masanensis*, *S. plana*, and *S. ramonii* did not show any attack behaviors toward the prey items, inhibit their swimming, or lyse the prey.

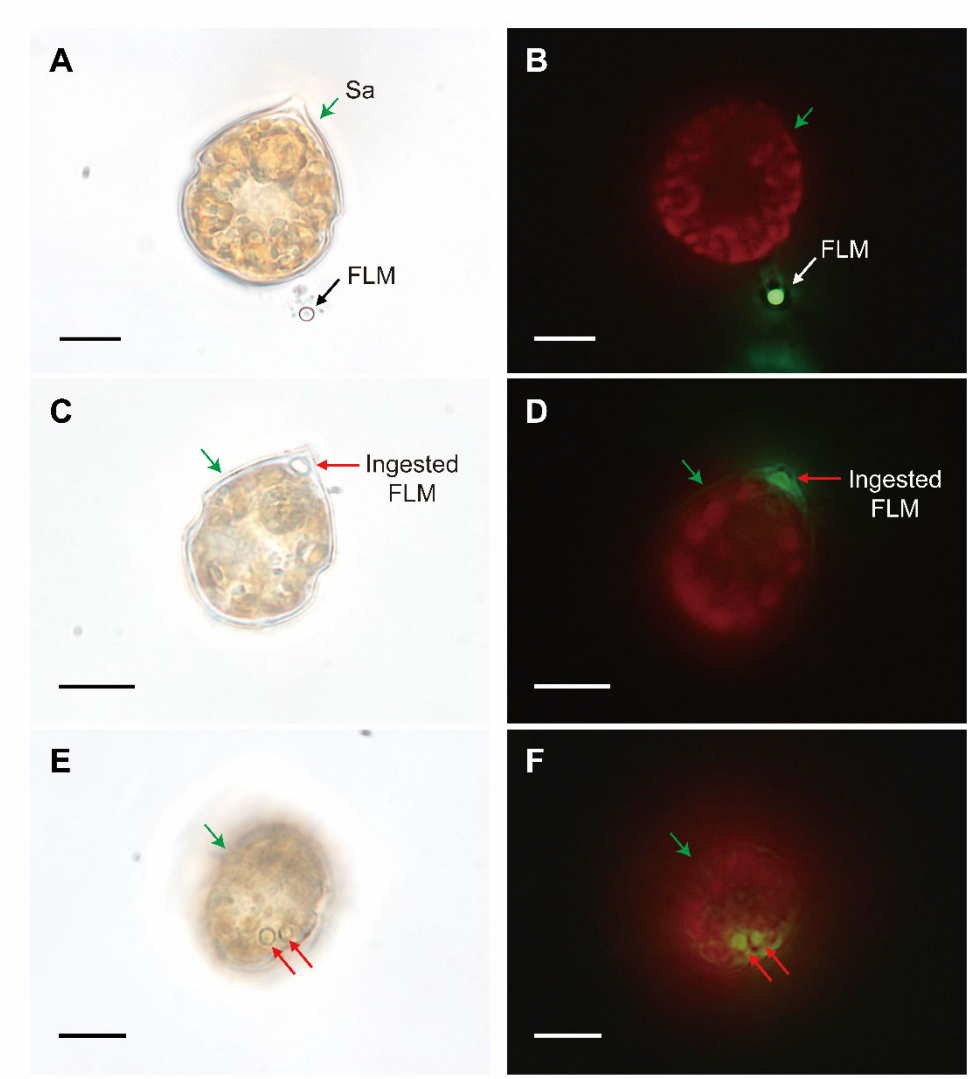

Figure 5.1. *Scrippsiella acuminata* STKP9909 (Sa) not fed (A–B) or fed (C–F) fluorescently labeled microspheres (FLM). Micrographs A, C, and E were taken under a light microscope and B, D, and F under an epifluorescence microscope. Green arrows indicate Sa cells, black and white arrows indicate not ingested FLM, and red arrows indicate ingested FLM within Sa cells. Scale bars represent: A–F, 10 μm

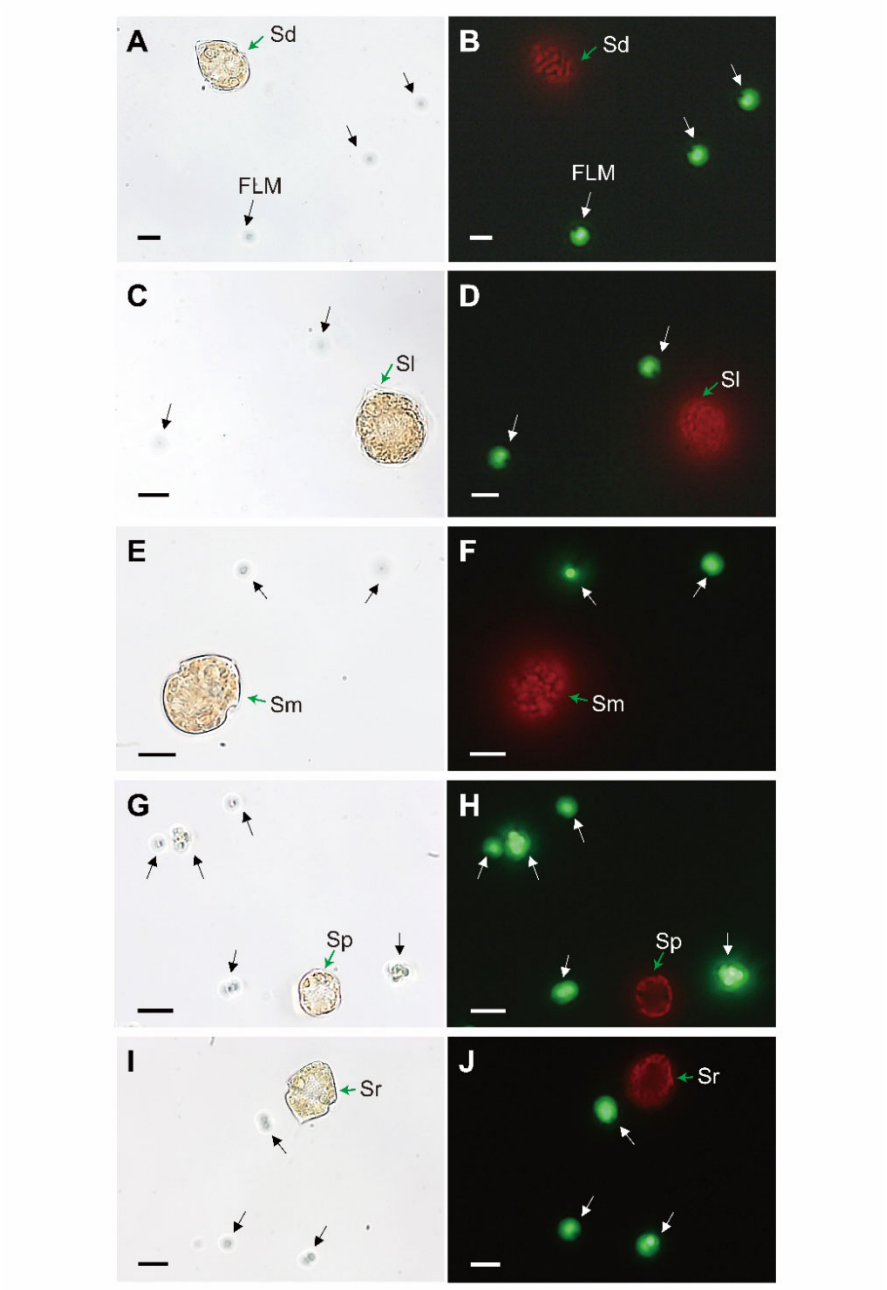

Figure 5.2. *Scrippsiella donghaiensis* SDGJ1703 (Sd; A–B), *S. lachrymosa* SLBS1703 (Sl; C–D), *S. masanensis* SSMS0908 (Sm; E–F), *S. plana* SSSH1009A (Sp; G–H), and *S. ramonii* VGO1053 (Sr; I–J), not fed fluorescently labeled microspheres (FLM). Micrographs A, C, E, G, and I were taken under a light microscope and those in B, D, F, H, and J under an epifluorescence microscope. Green arrows indicate *Scrippsiella* cells; Black or white arrows indicate not ingested FLM. Scale bars represent: A–J, 10 µm.

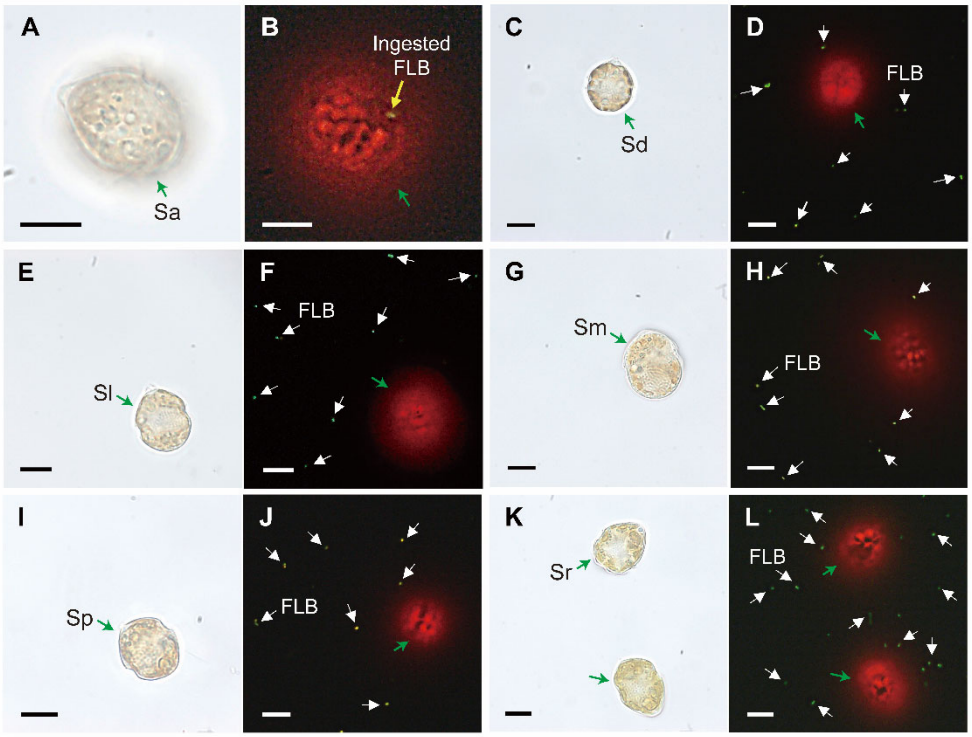

Figure 5.3. A *Scrippsiella acuminata* STKP9909 (Sa; A–B) cell feeding on the fluorescently labeled heterotrophic bacteria (FLB) and *S. donghaiensis* SDGJ1703 (Sd; C–D), *S. lachrymosa* SLBS1703 (Sl; E–F), *S. masanensis* SSMS0908 (Sm; G–H), *S. plana* SSSH1009A (Sp; I–J), and *S. ramonii* VGO1053 (Sr; K–L) not feeding on the FLB. Micrographs A, C, E, G, I, and K were taken under a light microscope and those in B, D, F, H, J, and L under an epifluorescence microscope. Green arrows, *Scrippsiella* cells; a yellow arrow, ingested FLB within a *Scrippsiella* cell; white arrows, not ingested FLB. Scale bars represent: A–L, 10 μm.

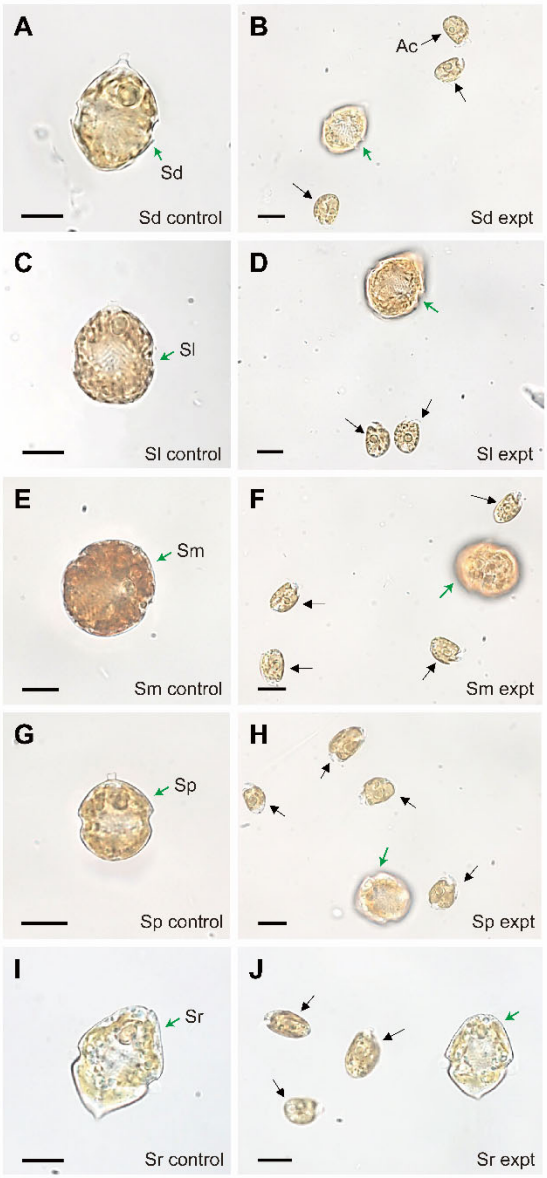

Figure 5.4. Cells of *Scrippsiella donghaiensis* SDGJ1703 (Sd; A–B), *S. lachrymosa* SLBS1703 (Sl; C–D), *S. masanensis* SSMS0908 (Sm; E–F), *S. plana* SSSH1009A (Sp; G–H), and *S. ramonii* VGO1053 (Sr; I–J), not feeding on the dinoflagellate *Amphidinium carterae* (Ac). A, C, E, G, and I, *Scrippsiella* cells without Ac (control). B, D, F, H, and J, *Scrippsiella* cells with Ac (expt). Green arrows indicate *Scrippsiella* cells and black arrows indicate Ac cells. Scale bars represent: A–J, 10 μm.

5.3.2. Phylogenetic analysis of *Scrippsiella* spp.

Four novel LSU rDNA sequences from *S. acuminata* STKP9909, *S. donghaiensis* SDGJ1703, *S. plana* SSSH1009A, and *S. ramonii* VGO1053 were obtained and deposited in GenBank under the accession numbers OQ266790, OQ266882, OQ266885, and OQ275008 for *S. acuminata* STKP9909, *S. donghaiensis* SDGJ1703, *S. plana* SSSH1009A, and *S. ramonii* VGO1053, respectively. A phylogenetic tree generated using LSU rDNA showed that *S. acuminata*, *S. lachrymosa*, and *S. ramonii* belong to a large clade along with *S. spinifera*, *S. kirschiae*, S. *trifida*, *S. bicarinata*, *S. erinacea*, *S. sweeneyae*, *Scrippsiella* sp. JKG47-2, *S. precaria*, and *S. irregularis* (**Figure 5.5**). This clade included not only the two mixotrophic species, *S. acuminata* STKP9909 and *Scrippsiella* sp. JKG47-2, but also *S. lachrymosa* and *S. ramonii*, which lack mixotrophic abilities. The clades that included *S. donghaiensis* SDGJ1703, *S. masanensis* SSMS0908, and *S. plana* SSSH1009A, which lack mixotrophic abilities, were divergent in the phylogenetic tree.

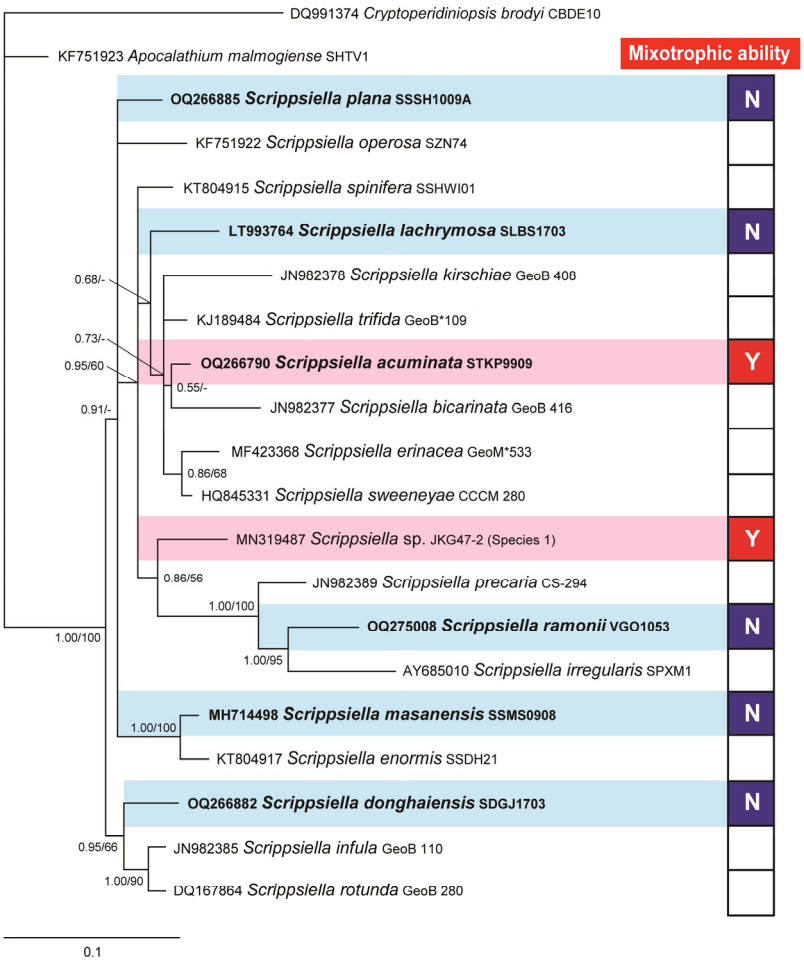

Figure 5.5. Consensus Bayesian tree based on 601-bp aligned positions of the large subunit regions from 19 species within the genus *Scrippsiella*. Sequences from *Cryptoperidiniopsis brodyi* and *Apocalathium malmogiense* were used as an outgroup. The number of character changes are proportional to branch lengths and indicate the maximum likelihood bootstrap values (right) and Bayesian posterior probability (left); posterior probabilities ≥ 0.5 are shown; the species names are followed by the strain names of each species. The species tested in this study are shown in bold. Red boxes (Y) indicate mixotrophic *Scrippsiella* species; blue boxes (N) indicate *Scrippsiella* species without mixotrophic ability; and white boxes represent *Scrippsiella* species that were not tested for mixotrophy. Data of the presence or absence of mixotrophic ability for species within the genus *Scrippsiella* were obtained from this study, Jeong et al. (2005a, b), and Coats et al. (2020).

5.4. Discussions

5.4.1. Lack of mixotrophy in five *Scrippsiella* species and phylogenetic analysis

The present study reports, for the first time, that *S. donghaiensis*, *S. lachrymosa*, *S. masanensis*, *S. plana*, and *S. ramonii* lack mixotrophic abilities. Previous studies reported that three *Scrippsiella* species, *S. acuminata* and two unidentified *Scrippsiella* spp. were mixotrophic (Jacobson and Anderson 1996, Jeong et al. 2005a, b, Coats et al. 2020). The results of the present study lower a proportion of mixotrophic species relative to the total *Scrippsiella* species tested for mixotrophy. In the phylogenetic tree based on LSU rDNA, the unidentified *Scrippsiella* species isolated from Korean waters was divergent from *S. acuminata*, indicating a distinct species. If the two unidentified *Scrippsiella* species from the United States and Korean waters are distinct from each other and from *S. acuminata*, the proportion of mixotrophic species relative to that of the total *Scrippsiella* species tested for mixotrophy is 38% (3 of 8 tested species). However, if the unidentified *Scrippsiella* species from the United States is *S. acuminata* or the unidentified *Scrippsiella* species from Korean waters, the proportion of the number of mixotrophic species relative to that of the total *Scrippsiella* species tested for mixotrophy is 29% (2 of 7 tested species). The mixotrophic abilities of species in the dinoflagellate genera *Alexandrium*, *Paragymnodinium*, and *Karenia* have also been reported (Lim et al. 2019b, Yokouchi et al. 2022, Ok et al. 2023) (**Table 5.4**). The proportion of mixotrophic species relative to the total species tested for mixotrophy was 44% (7 of 16 tested species) in the genus *Alexandrium*, 60% (3 of 5 tested species) in the genus *Paragymnodinium*, and 40% (2 of 5 tested species) in the genus *Karenia* (**Table 5.4**). Thus, the proportion of mixotrophic species in the genus *Scrippsiella* was slightly lower than that in the genera *Karenia* or *Alexandrium* and considerably lower than that in the genus *Paragymnodinium*. Among the formally described 34, 10, and 28 species in the genera *Alexandrium*, *Karenia*, and *Scrippsiella*, respectively, the mixotrophic abilities of 16, 5, and 6 species have been explored. Thus, the proportion of mixotrophic species relative to the total species tested for mixotrophy may be changed.

In the phylogenetic tree based on the LSU rDNA sequences of 19 *Scrippsiella* species, a large clade included *S. acuminata* and *Scrippsiella* sp. JKG47-2, which have mixotrophic abilities, and *S. lachrymosa* and *S. ramonii*, which lack mixotrophic abilities. However, three clades, *S. donghaiensis* SDGJ1703, *S. masanensis* SSMS0908, and *S. plana* SSSH1009A, that lack mixotrophic abilities diverged from the large clade. Thus, the ancestral species of *Scrippsiella* may have lacked feeding ability and acquired it later through evolution. However, to confirm this hypothesis, the mixotrophic abilities of other *Scrippsiella* spp. need to be examined.

5.4.2. The extended prey spectrum of *Scrippsiella acuminata*

Scrippsiella acuminata was able to feed on the cyanobacterium *Synechococcus* sp., a prymnesiophyte, cryptophytes, raphidophytes, and phototrophic dinoflagellates that were ≤ 12.1 μm in equivalent spherical diameter (Jeong et al. 2005a, b). The results of the present study expand the range of prey items of *S. acuminata* to include FLB. Heterotrophic bacteria are ubiquitous (Caron et al. 1982, Kjelleberg et al. 1987, Van Wambeke et al. 2000, Seong et al. 2006, Sanz-Sáez et al. 2020, Vijayan et al. 2022); thus, the ability of *S. acuminata* to feed on heterotrophic bacteria may be critical for the survival of this dinoflagellate species under conditions of inorganic nutrient depletion. Heterotrophic bacteria usually have high phosphorus : nitrogen ratios (Vadstein et al. 1988, Tezuka 1990) and some cyanobacteria can conduct nitrogen fixation (Mitsui et al. 1987, Zehr 2011). Therefore, *S. acuminata* may obtain phosphorus and nitrogen for their growth by feeding on heterotrophic bacteria and cyanobacteria in offshore or oceanic waters (Jeong et al. 2010b).

Scrippsiella acuminata has a global distribution and can cause red tides in many countries (Velikova et al. 1999, Moncheva et al. 2001, Pitcher et al. 2007, Gárate-Lizárraga et al. 2009, Kumar et al. 2018, Tsikoti and Genitsaris 2021, Jeong et al. 2021). However, *S. donghaiensis*, *S. lachrymosa*, *S. masanensis*, *S. plana*, or *S. ramonii*, which lack mixotrophic abilities, cause few or no red tides (Jang et al. 2022). Thus, the mixotrophic ability of *S. acuminata* may allow it to cause red tides in several marine ecosystems.

Scrippsiella acuminata is preyed upon by the common heterotrophic dinoflagellates *Oxyrrhis marina*, *Gyrodinium dominans*, *Polykrikos kofoidii*, *Oblea rotunda*, and *Pfiesteria piscicida*, ciliates *Tiarina fusus* and *Strombidinopsis* sp., copepods *Acartia omorii*, *Calanus helgolandicus*, *Calanus pacificus*, and *Temora longicornis*, and larvae of the mussel *Mytilus galloprovincialis* (Gill and Harris 1987, Hassett and Landry 1990, Jeong et al. 2002, 2004*a*, Shin et al. 2003, Kim et al. 2019). Thus, *S. acuminata* plays an ecological role as a primary producer and predator of heterotrophic bacteria, cyanobacteria, and diverse microalgae, and serves as a suitable prey item for many heterotrophic protists in marine ecosystems. *S. donghaiensis*, *S. lachrymosa*, and *S. masanensis* are also consumed by *O. marina*, *G. dominans*, *P. kofoidii*, *O. rotunda*, *P. piscicida*, and *Strombidinopsis* spp. (Kim et al. 2019). Thus, *S. donghaiensis*, *S. lachrymosa*, and *S. masanensis* may play ecological roles as primary producers and prey for heterotrophic protists in marine ecosystems, and owing to its mixotrophic ability, *S. acuminata* has a different ecological niche that of *S. donghaiensis*, *S. lachrymosa*, *S. masanensis*, *S. plana*, and *S. ramonii*.

Table 5.4. Number of species having or lacking the mixotrophic ability in the dinoflagellate genera *Scrippsiella*, *Alexandrium*, *Karenia*, and *Paragymnodinium*. [a], If the unidentified *Scrippsiella* species from USA is *S. acuminata* or the unidentified *Scrippsiella* species isolated from Korean waters, the number of *Scrippsiella* species tested for mixotrophic ability and those having the ability changes from 8 to 7 and from 3 to 2, respectively.

Genus	No. of the species tested for mixotrophic ability	No. of the species having mixotrophic ability	No. of the species lacking mixotrophic ability	References
Scrippsiella	7 or 8[a]	2 or 3[a]	5	This study; Jacobson and Anderson (1996); Jeong et al. (2005a, b)
Alexandrium	16	7	9	Jacobson and Anderson (1996); Jeong et al. (2005a, b); Yoo et al. (2009); Blossom et al. (2012), (2017); Lee et al. (2016); Lim et al. (2015), (2019a), (2005b)
Karenia	5	2	3	Jeong et al. (2005*a*); Glibert et al. (2009); Zhang et al. (2011); Ok et al. (2023)
Paragymnodinium	5	3	2	Yoo et al. (2010); Yokouchi et al. (2018), (2020); Yokouchi and Horiguchi (2021)

Chapter 6.
Development of an automatic system for cultivating useful mixotrophic and heterotrophic dinoflagellates on a 100-L scale*

6.1. Introduction

Dinoflagellates are ubiquitous and a major component of marine ecosystems (Jacobson and Anderson 1996, Glibert et al. 2012, Jeong et al. 2013, 2021, Sellers et al. 2014, Lee et al. 2021). They play diverse roles as primary producers, prey, predators, symbiotic partners, and parasites in marine ecosystems (Coats 1999, Jeong et al. 2010a, b, 2012, Davy et al. 2012, Park et al. 2013b, Spilling et al. 2018, Ok et al. 2021). Marine dinoflagellates are known to produce diverse useful products, such as omega-3, amino acids, pigments, and bioluminescent materials (Wynn and Ratledge 2005, Sugawara et al. 2007, Valiadi and Iglesias-Rodriguez 2013, Onodera et al. 2014, Jang et al. 2017a, Lim et al. 2018a, 2020, Park et al. 2021b). In addition, marine mixotrophic and heterotrophic dinoflagellates can sometimes have a considerable grazing impact on the prey population, and the grazing impact may sometimes be larger than that of metazooplankton (Lee et al. 2014b, Lim et al. 2017). Thus, the mixotrophic and heterotrophic dinoflagellates can be used as biological materials controlling red tides in the sea (Jeong et al. 2003, Lim et al. 2017). However, obtaining pure cultures of mixotrophic and heterotrophic dinoflagellates on a large scale is difficult, which may limit research and commercial utilization (Gupta et al. 2015, Jerney and Spilling 2018). Thus, developing an automatic or semi-automatic system for cultivating useful dinoflagellate species on a large scale is required.

---

* This chapter has been published in Algae.
Lim, A. S., Jeong, H. J.*, **You, J. H.** & Park, S. A. 2020. Semi-continuous cultivation of the mixotrophic dinoflagellate *Gymnodinium smaydae*, a new promising microalga for omega-3 production. Algae, 35:277–292.
You, J. H., Jeong, H. J.*, Kang, H. C., Ok, J. H., Park, S. A. & Lim, A. S. 2020. Feeding by common heterotrophic protist predators on seven *Prorocentrum* species. Algae, 35:61–78.
You, J. H., Jeong, H. J.*, Park, S. A., Ok, J. H., Kang, H. C., Eom, S. H. & Lim, A. S. 2022. Development of an automatic system for cultivating the bioluminescent heterotrophic dinoflagellate *Noctiluca scintillans* on a 100-liter scale. Algae, 37:149–161.

The cultivation of mixotrophic and heterotrophic dinoflagellates on a large scale is difficult due to their biological characteristics. When a relatively fast-growing alga is selected for culture, the total production cost will increase if the cost for media or carbon sources is high. For example, glucose has been used as an effective organic compound to enhance the growth and production of some microalgae (Li et al. 2007, Cheirsilp and Torpee 2012); however, glucose is expensive, sometimes accounting for 80% of the total medium cost (Li et al. 2007). Therefore, to reduce the total production cost, low-cost nutrient and carbon sources and cost-effective culture methods should be developed. Suitable algal prey cells present a good carbon source for mixotrophic and heterotrophic microalgae with high growth rates and useful materials, such as EPA or DHA contents. Based on this, it is beneficial to determine the optimal cultivation conditions for maximum mixotrophic microalgal growth. However, to cultivate useful mixotrophic and heterotrophic dinoflagellates in this way, it is necessary to consider the growth and ingestion rates of the predators for determining optimal prey amount and addition intervals, light and temperature conditions for the optimal growth of prey and predators, and optimal medium mixing methods that do not damage the cells and prevent prey and predators from being separated by water layer in a tank (Lim et al. 2020). Therefore, although the direct input of prey cells to cultivate predators is cost-effective, it is not easily used because both the biological conditions of prey and predators must be considered in advance.

The mixotrophic dinoflagellates *Gymnodinium smaydae* and *Biecheleria cincta* and the heterotrophic dinoflagellates *Gyrodinium dominans*, *Polykrikos kofoidii*, and *Noctiluca scintillans* are known as organisms producing useful materials, such as omega-3, or predators feeding on red tide-forming species *Amphidinium carterae*, *Alexandrim* spp., *Heterocapsa* spp., *Heterosigma akshiwo*, *Margelefidinium polykrikoides*, and *Prorocentrum* spp. (Mediodia and Catedral 1988; Honjo 1992; Kiϕrboe and Titelman 1998; Lindholm and Nummelin 1999; Matsuyama 1999; Townsend et al. 2001; Tomas and Smayda 2008; Kang et al. 2011, 2018; Lee et al. 2014a; McGillicuddy et al. 2014; Zhang et al. 2016; Lim et al. 2020; You et al. 2020a). However, the method for automatic cultivation of the mixotrophic and heterotrophic dinoflagellates has not yet been developed. Especially, *N. scintillans* is a bioluminescent organism and often causes red tides. Thus, *N.*

scintillans often causes a red ocean during the day and a glowing ocean at night. Red-tide patches containing *N. scintillans* provide a large-scale bright bioluminescence field when bioluminescent cells in the patches are hit by waves, swimming fish and mammals, moving boats, ships, and submarines (Tarasov 1956, Bityukov 1971, Hastings 1975, Morin 1983, Williams and Kooyman 1985, Rhor et al. 1998). Thus, many scientists wish to conduct research on large-scale cultures of *N. scintillans*. However, while it is easy to cultivate *N. scintillans* at scales < 1 L, large-scale cultivation (> 100 L) is challenging. This dinoflagellate swims slowly and usually stays near the surface (Kiϕrboe and Titelman 1998, Johnson and Shanks 2003). In large tanks, some prey (e.g., diatoms and eggs) tend to sink and accumulate at the bottom of the tanks, while others (e.g., nano-, micro-, and dinoflagellates) swim fast enough to escape being eaten by *N. scintillans*. The highest reported growth rate of *N. scintillans* is approximately 0.8 d^{-1} (Tada et al. 2004, Stauffer et al. 2017). However, the spatial separation between *N. scintillans* and its prey cells in large tanks inhibits the rapid growth of *N. scintillans*. In large tanks, dense prey should be supplied to surface waters where *N. scintillans* cells stay, or the waters where *N. scintillans* cells and prey cells co-exist should be mixed. Thus, it is necessary to develop an automatic system for cultivating *N. scintillans* on a large scale while overcoming these shortcomings.

In the present study, I developed a semi-continuous cultivation system on a 10-L scale for mixotrophic and heterotrophic dinoflagellates feeding on prey cells and scaled it up to a 100-liter automatic cultivation system with the newly developed software. Using these systems, the cultivation methods of the mixotrophic dinoflagellates *G. smaydae* and *B. cincta* and the heterotrophic dinoflagellates *G. dominans*, *P. kofoidii*, and *N. scintillans* were developed. I harvested 10-L dense cultures of *G. smaydae*, *B. cincta*, *G. dominans*, and *P. kofoidii* every 4–12 d using the 10-liter system. In addition, the fatty acid composition of *G. smaydae* was analyzed to track changes during semi-continuous cultivation using the system. Moreover, I harvested 100-L dense culture of *N. scintillans* every 10 d using the 100-liter system, and this culture was used for bioluminescence experiments. The results of this study provide insights into automatically producing pure mass cultures of mixotrophic and heterotrophic dinoflagellates.

6.2. Materials and Methods

6.2.1. Preparation of experimental organisms

A clonal culture of *Gymnodinium smaydae* GSSH1005, which was isolated from Shiwha Bay, Korea (37° 18′ N, 126° 36′ E), during May 2010 and established following two serial single-cell isolations (Kang et al. 2014, Lee et al. 2014a), was used. Approximately 90 mL of a dense culture (ca. 20,000 cells mL^{-1}) of *G. smaydae* were transferred every three days to a 270-mL flask of a fresh culture of *Heterocapsa rotundata* containing ca. 100,000 cells mL^{-1}. The flask was placed on a rotating wheel (0.00017 × g) at 20°C under an illumination of 20 μmol photons m^{-2} s^{-1} cool-white fluorescent light in a 14:10 h Light-Dark cycle. The culture of *H. rotundata* was placed on a shelf and maintained in 250-mL culture flasks containing a F/2-Si medium (Guillard and Ryther 1962).

A clonal culture of *Biecheleria cincta* BCSH1005 was originally isolated from Shiwha Bay in May 2010 when water temperature and salinity were 17.8℃ and 27.9, respectively. A dense culture (ca. 3,000 cells mL^{-1}) of *B. cincta* was transferred every week to a 270-mL culture flask containing a fresh culture of *Heterosigma akashiwo* HAKS9905 (ca. 30,000 cells mL^{-1}) in 0.2-μm filtered sea water. The flask was placed on a shelf at same conditions described above. The culture of *H. akashiwo* was placed on a shelf and maintained in 250-mL culture flasks containing a F/2-Si medium (Guillard and Ryther 1962).

A clonal culture of *Gyrodinium dominans* GDJG1907 was originally isolated from Jeongok, Korea in July 2019 when water temperature and salinity were 25.2℃ and 31.9, respectively. A dense culture (ca. 5,000 cells mL^{-1}) of *G. dominans* was transferred every week to a 270-mL culture flask containing a fresh culture of *Amphidinium carteare* (ca. 10,000–20,000 cells mL^{-1}) in 0.2-μm filtered sea water. The flask was placed on a rotating wheel (0.00017 × g) at same conditions described above. The culture of *A. carterae* was placed on a shelf and maintained in 250-mL culture flasks containing a F/2-Si medium (Guillard and Ryther 1962).

A clonal culture of *Polykrikos kofoidii* PKJH1607 was originally isolated

from Jangheung, Korea in July 2016 when water temperature and salinity were 23.6℃ and 26.4, respectively. A dense culture (ca. 100 cells mL^{-1}) of *P. kofoidii* was transferred every week to a 270-mL culture flask containing a fresh culture of *Alexandrium minutum* CCMP1888 (=*A. lusitanicum*) (ca. 5,000 cells mL^{-1}) in 0.2-μm filtered sea water. All flasks were placed on a rotating wheel (0.00017 × g) at same conditions described above. The culture of *A. minutum* was placed on a shelf and maintained in 250-mL culture flasks containing a F/2-Si medium (Guillard and Ryther 1962).

Cells of *Noctiluca scintillans* NSDJ2010 were isolated from plankton samples collected from surface waters off the coast of Dangjin, Korea, when the water temperature and salinity were 19.5℃ and 28.8, respectively. A clonal culture was established using two serial single-cell isolations and was grown on *Dunaliella salina* DSJH1710 (approximately 80,000 cells mL^{-1}) in 6-well plates. Cells of *D. salina* DSJH1710 were originally isolated from the coastal waters of Jinhae, Korea. As the abundance of *N. scintillans* increased, the cells were transferred to 50-mL and 250-mL plate flasks and 1-L polycarbonate (PC) bottles containing fresh prey. The 1-L PC bottles were placed on a rotating wheel (0.00017 × g) and incubated under same conditions mentioned above. The culture of *D. salina* was placed on a shelf and maintained in 800-mL culture flasks containing a F/2-Si medium (Guillard and Ryther 1962).

6.2.2. Design of a semi-continuous system for cultivating the mixotrophic and heterotrophic dinoflagellates on a 10-liter scale

A newly developed photo-bioreactor for semi-continuous culturing of mixotrophic dinoflagellates was used for this experiment (Jeong and Lim 2020, Lim and You et al. 2020). The bioreactor consisted of three 10-L vessels, two peristaltic pumps, and silicon tubing (Masterflex, Cole Parmer, IL, USA). Vessels containing the F/2 medium, prey, and predator were connected in series by the tubings. A peristaltic pump fed the F/2 medium into the prey vessel, and another pump fed the prey culture into the predator vessel (**Figure**

6.1). To avoid any potential countercurrent between the two vessels, the outlet nozzle of each vessel was designed to be positioned in the lower part of the vessel and the inlet nozzle was positioned in the upper part of the vessel (**Figure 6.1**). Filtered air was supplied into the vessel through a sparger for aeration, and was released via a hole in the lid of the vessel (**Figure 6.1**). LED lamps were fitted inside the vessel for illumination, and the temperature inside the vessel was continuously monitored (**Figure 6.1**).

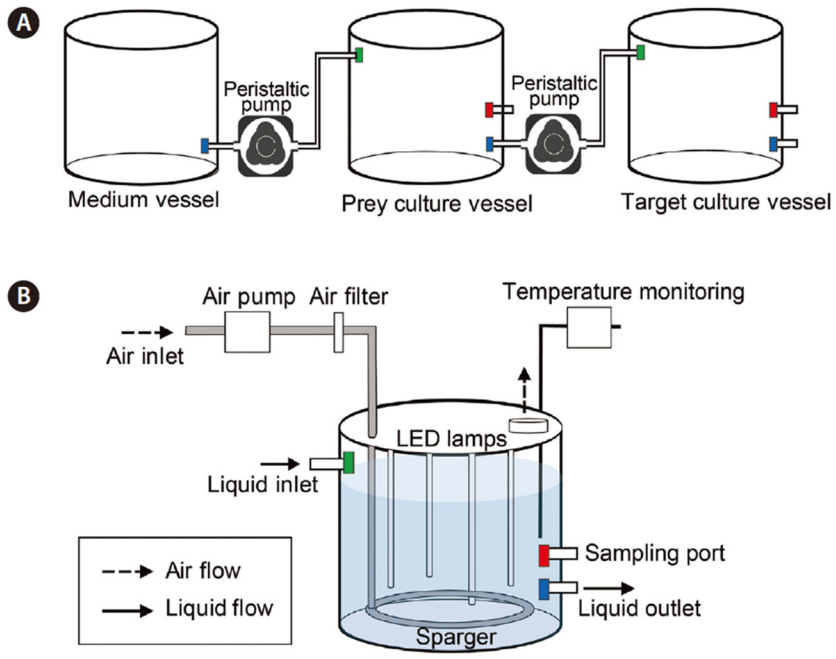

Figure 6.1. Schematic diagram of a cultivation system for mixotrophic dinoflagellates on a 10-L scale (A) and the culture vessels (B) used in the present study (Lim and You et al. 2020). Media and cultures exiting the vessel through the liquid outlet were transferred to the next vessel through the liquid inlet. Air was supplied to the vessels using an air pump with an air filter for aeration and was dispersed evenly in the culture by the sparger.

6.2.3. Cultivating the mixotrophic dinoflagellate *Gymnodinium smaydae* using the semi-continuous system on a 10-liter scale and lipid analysis

To optimize the growth of *G. smaydae*, the prey species were explored through the literature, and the growth and ingestion rates of *G. smaydae* feeding on the prey species were obtained. Based on the measured growth and ingestion rates of *G. smaydae* and the growth rate of the prey species, a suitable prey species was selected and used for the cultivation experiment of *G. smaydae*.

Semi-continuous cultivation of *G. smaydae* was conducted to test its potential for application in EPA and DHA production. The semi-continuous cultivation system was operated in a temperature-controlled chamber at 25 ± 1℃ under 50 μmol photons m^{-2} s^{-1} LED illumination and 14 : 10 h Light-Dark cycle, and the F/2 medium was also acclimated to this temperature. At the initial stage of operation, the medium vessel contained 10 L of fresh F/2 medium, the prey vessel contained 9 L of dense prey culture, and the predator vessel contained 3 L of dense *G. smaydae* culture. In this cultivation system, *H. rotundata* cultures in the prey vessel were automatically transferred to the *G. smaydae* culture vessel via a peristaltic pump (flow rate = 300 mL min^{-1}) for 10 min. Thus, a total of 3 L of the prey culture was transferred to the *G. smaydae* culture vessel every day. When the volume in the *G. smaydae* culture vessel reached 9 L, 6 L of the culture was transferred to the container and starved for 1 day under the same conditions. After starvation, *G. smaydae* cells were harvested by centrifugation (Labogene 1696R; Gyrozen Co., Gimpo, Korea) at 4,315 × g for 10 min and then stored at -70℃ in a deep freezer until analysis. Fatty acid contents of the sample were analyzed.

Simultaneously, F/2 medium from the medium vessel was transferred to the prey culture vessel using a peristaltic pump (flow rate = 2.1 mL min^{-1}) in continuous operation. Thus, a total of 3 L of the F/2 medium was transferred to the prey vessel every day. Fresh F/2 medium was added into the medium vessel as required. The flow rates of all pumps were calibrated before use.

To monitor *H. rotundata* density in the prey vessel, the culture was

homogenously and gently mixed by aeration through the sparger for 2 min (airflow rate = 1 L min^{-1}) before subsampling (**Figure 6.1**). Ten milliliter aliquots were sampled daily from the prey vessel through a sampling port and fixed with 5% acidic Lugol's solution. Moreover, to monitor *G. smaydae* and *H. rotundata* densities in the predator vessel, the culture was mixed as previously described, and 5-mL aliquots were subsampled before and after prey addition and fixed with 5% acidic Lugol's solution. All or > 200 cells of each species were counted in three 1-mL SRC chambers. The experiment continued for 43 d, and the pH was not controlled.

To analyze lipid contents of *G. smaydae* harvested during semi-cultivation for 43 d, dry biomass was obtained from lyophilizing frozen cell pellets using a freeze dryer (Bondiro, Ilshine, Dongducheon, Korea) at -110℃ under vacuum for 1 d. Total fatty acid methyl esters (FAMEs) were analyzed in 2-39 mg samples, after extraction from the lyophilized cells using the one-step hydrolysis, extraction, and methylation procedure described by Garcés and Mancha (1993). FAMEs were analyzed by gas chromatography (7890A; Agilent Technologies, Santa Clara, CA, USA). One microliter aliquots of the extracted FAMEs were injected into a capillary column (DB-23, Ser. No. US8897617H; 60 m × 0.25 mm, 0.25 μm film thickness) coupled with a flame ionization detector at a split ratio of 20 : 1. The temperature program was as follows: initial temperature 50℃ maintained for 1 min, increased to 130℃ at 15°C min^{-1}, increased to 170°C at 8°C min^{-1}, increased to 215℃ at 2°C min^{-1} and maintained for 10 min. The injector and detector temperatures were 250°C and 280°C, respectively. FAME peaks were identified by comparing the retention times of the samples with those of the reference standards (Supelco 37-component FAME mix; Supelco, Bellafonte, PA, USA). The fatty acid contents of *G. smaydae* and *H. rotundata* (n = 3) were expressed as means of the triplicates, except for daily prey supply samples.

6.2.4. Cultivating the mixotrophic dinoflagellate *Biecheleria cincta* using the semi-continuous system on a 10-liter scale

To optimize the growth of *B. cincta*, the prey species were explored through the literature, and the growth and ingestion rates of *B. cincta* feeding on the prey species were obtained. Based on the measured growth and ingestion rates of *B. cincta* and the growth rate of the prey species, a suitable prey species was selected and used for the cultivation experiment of *B. cincta*. Moreover, I chose 20℃ as the optimal temperature and 20–25 μmol photons m^{-2} s^{-1} as the optimal light intensity under a 14 : 10 h light : dark cycle for *B. cincta* and *H. akashiwo* (Kang et al. 2011).

At the beginning of the experiment, 10 L of F/2-Si medium was added to the medium vessel, 9 L of *H. akashiwo* culture (approximately 20,000 cells mL^{-1}) to the prey vessel, and 4.5 L of *B. cincta* culture (approximately 3,000 cells mL^{-1}) to the predator vessel. In this cultivation system, *H. akashiwo* cultures in the prey vessel were automatically transferred to the *B. cincta* culture vessel via a peristaltic pump (flow rate = 450 mL min^{-1}) for 10 min. Thus, a total of 4.5 L of the prey culture was transferred to the *B. cincta* culture vessel every 2 d. Simultaneously, F/2 medium from the medium vessel was transferred to the prey culture vessel using a peristaltic pump (flow rate = 1.56 mL min^{-1}) in continuous operation. Thus, a total of 4.5 L of the F/2 medium was transferred to the prey vessel every 2 d. Fresh F/2 medium was added into the medium vessel as required. When the volume in the *B. cincta* culture vessel reached 9 L, 4.5 L of the culture was transferred to the container and maintained under the same conditions. This procedure was repeated three times and the pH was not controlled. The flow rates of all pumps were calibrated before use.

To monitor *H. akashiwo* density in the prey vessel, the culture was homogenously and gently mixed by aeration through the sparger for 2 min (airflow rate = 1 L min^{-1}) before subsampling (**Figure 6.1**). Ten milliliter aliquots were sampled daily from the prey vessel through a sampling port and fixed with 5% acidic Lugol's solution. Moreover, to monitor *B. cincta* and *H. akashiwo* densities in the predator vessel, the culture was mixed as previously described, and 10-mL aliquots were subsampled before and after prey

addition and fixed with 5% acidic Lugol's solution. All or > 200 cells of each species were counted in three 1-mL SRC chambers at a magnification of 100 × or 200 ×.

6.2.5. Cultivating the heterotrophic dinoflagellate *Gyrodinium dominans* using the semi-continuous system on a 10-liter scale

To optimize the growth of *G. dominans*, the prey species were investigated through the literature or preliminary tests, and the growth and ingestion rates of *G. dominans* feeding on the prey species were obtained or estimated. Based on the growth and ingestion rates of *G. dominans* and the growth rate of the prey species, a suitable prey species was selected and used for the cultivation experiment of *G. dominans*. Moreover, I chose 20℃ as the optimal temperature and 20 μmol photons m^{-2} s^{-1} as the optimal light intensity under a 14 : 10 h Light-Dark cycle for *G. dominans* and *A. carterae* (You et al. 2020a).

At the beginning of the experiment, 10 L of F/2-Si medium was added to the medium vessel, 9 L of *A. carterae* culture (approximately 35,000 cells mL^{-1}) to the prey vessel, and 2 L of *G. dominans* culture (approximately 5,000 cells mL^{-1}) to the predator vessel. In this cultivation system, the *A. carterae* culture in the prey vessel was automatically transferred to the *G. dominans* culture vessel via a peristaltic pump (flow rate = 200 mL min^{-1}) for 10 min. Thus, a total of 2 L of the prey culture was transferred to the *G. dominans* culture vessel every day. Simultaneously, F/2 medium from the medium vessel was transferred to the prey culture vessel using a peristaltic pump (flow rate = 1.39 mL min^{-1}) in continuous operation. Thus, a total of 2 L of the F/2 medium was transferred to the prey vessel every day. Fresh F/2-Si medium was added into the medium vessel as required. When the volume in the *G. dominans* culture vessel reached 8 L, 6 L of the culture was transferred to the container and maintained under the same conditions. This procedure was repeated three times and the pH was not controlled. The flow rates of all pumps were calibrated before use.

To monitor *A. carterae* density in the prey vessel, the culture was homogenously and gently mixed by aeration through the sparger for 2 min

(airflow rate = 1 L min^{-1}) before subsampling (**Figure 6.1**). Ten milliliter aliquots were sampled daily from the prey vessel through a sampling port and fixed with 5% acidic Lugol's solution. Moreover, to monitor *G. dominans* and *A. carterae* densities in the predator vessel, the culture was mixed as previously described, and 10-mL aliquots were subsampled before and after prey addition and fixed with 5% acidic Lugol's solution. All or > 200 cells of each species were counted in three 1-mL SRC chambers at a magnification of 100 × or 200 ×.

6.2.6. Cultivating the heterotrophic dinoflagellate *Polykrikos kofoidii* using the semi-continuous system on a 10-liter scale

To optimize the growth of *P. kofoidii*, the prey species were explored through the literature or preliminary tests, and the growth and ingestion rates of *P. kofoidii* feeding on the prey species were obtained or estimated. Based on the growth and ingestion rates of *P. kofoidii* and the growth rate of the prey species, a suitable prey species was selected and used for the cultivation experiment of *P. kofoidii*. Moreover, I chose 20°C as the optimal temperature and 20–25 μmol photons m^{-2} s^{-1} as the optimal light intensity under a 14 : 10 h Light-Dark cycle for *P. kofoidii* and *A. minutum* (You et al. 2020a).

At the beginning of the experiment, 10 L of F/2-Si medium was added to the medium vessel, 8 L of *A. minutum* culture (approximately 15,000 cells mL^{-1}) to the prey vessel, and 3 L of *P. kofoidii* culture (approximately 250 cells mL^{-1}) to the predator vessel. In this cultivation system, the *A. minutum* culture in the prey vessel was automatically transferred to the *P. kofoidii* culture vessel via a peristaltic pump (flow rate = 300 mL min^{-1}) for 10 min. Thus, a total of 3 L of the prey culture was transferred to the *P. kofoidii* culture vessel every 3 d. Simultaneously, F/2 medium from the medium vessel was transferred to the prey culture vessel using a peristaltic pump (flow rate = 0.70 mL min^{-1}) in continuous operation. Thus, a total of 3 L of the F/2 medium was transferred to the prey vessel every 3 d. Fresh F/2 medium was added into the medium vessel as required. When the volume in the *P. kofoidii* culture vessel reached 9 L, 6 L of the culture was transferred to the container and maintained

under the same conditions. This procedure was repeated three times, and the pH was not controlled. The flow rates of all pumps were calibrated before use.

To monitor *A. minutum* density in the prey vessel, the culture was homogenously and gently mixed by aeration through the sparger for 2 min (airflow rate = 1 L min^{-1}) before subsampling (**Figure 6.1**). Ten milliliter aliquots were sampled daily from the prey vessel through a sampling port and fixed with 5% acidic Lugol's solution. Moreover, to monitor *P. kofoidii* and *A. minutum* densities in the predator vessel, the culture was mixed as previously described, and 10-mL aliquots were subsampled before and after prey addition and fixed with 5% acidic Lugol's solution. All or > 200 cells of each species were counted in three 1-mL SRC chambers at a magnification of 100 × or 200 ×.

6.2.7. Design of an automatic system for cultivating mixotrophic and heterotrophic dinoflagellates on a 100-liter scale

To develop an automatic system for cultivating *N. scintillans* on a 100-L scale, the optimal conditions, such as the optimal prey species supporting high growth rate, time intervals and volumes at which nutrients in the nutrient tank were supplied to the prey in the prey culture tank, time intervals and volumes at which the prey in the prey culture tank were supplied to *N. scintillans* in the predator culture tank, and light intensities supporting high growth rates of the prey and predators were investigated. Furthermore, the results of our previous studies on the development of a semi-continuous system of cultivating mixotrophic dinoflagellates on a 10-L scale were used to develop an automatic system for cultivating *N. scintillans* on a 100-L scale (Jeong and Lim 2020, Lim et al. 2020). In the automatic system for cultivating *N. scintillans* on a 100-L scale, a stirring subsystem was set up for mixing.

To establish an automatic system for cultivating *N. scintillans* on a 100-L scale, we developed hardware for cultivation and a system controller for controlling the entire system. With respect to hardware, I chose 200-L round

PC water tanks; LED lamps for illumination for prey and predators; spectrometers measuring light intensities; magnetic pumps for supplying large volumes of nutrients and prey as main pumps; diaphragm pumps to supply small volumes of nutrients and prey as support pumps; sensors measuring water temperature, salinity, pH, and dissolved oxygen (DO); air pumps; spargers; stirrers; low-speed motors mounted on each stirrer; weighing systems; and polyvinyl chloride or silicone pipes (**Figure 6.2**).

In this study, a software program was developed for use with the system controller (**Figure 6.3**). The program was designed to control and monitor the hardware of the automatic system. The program contained parts controlling temperature, light intensity, and Light-Dark cycling for prey and predators, as well as opening and closing of valves between the two tanks. Furthermore, it controlled the speed, time interval, and duration of the stirring subsystem; air volume, time interval, and duration of aeration; and time intervals of numerical data saving. Moreover, it monitored temperature, light intensities, Light-Dark cycle, elapsed time, functions operating in each tank, water quality of prey and predator cultures, volumes in the prey and predator culture tanks, and current system mode (i.e., automatic or manual mode).

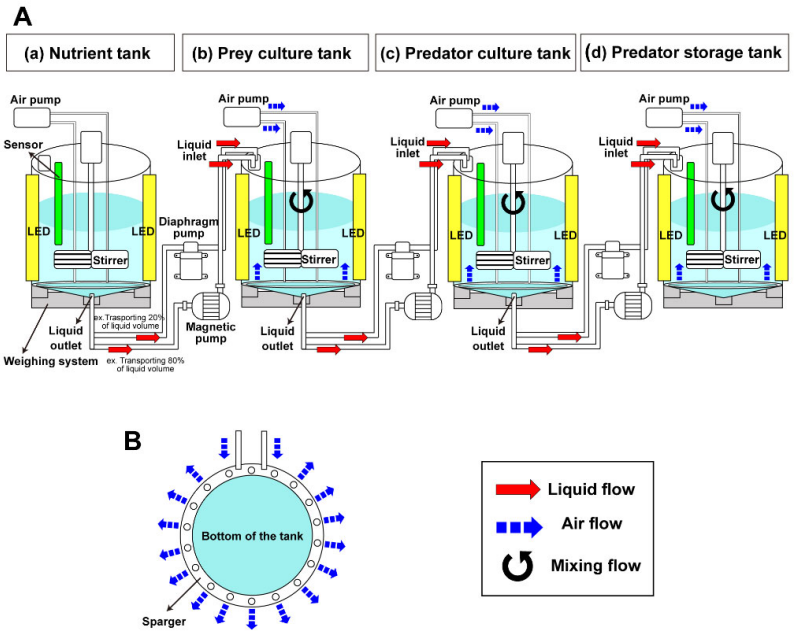

Figure 6.2. Schematic diagram of the automatic system for cultivating *Noctiluca scintillans* on a 100-L scale developed in this study (A). View of the sparger established on the bottom of each tank (B). LED, light-emitting diode. Red arrows indicate flows of liquid, blue broken arrows indicate air, and circle arrows indicate mixing. See the Materials and Methods section for details.

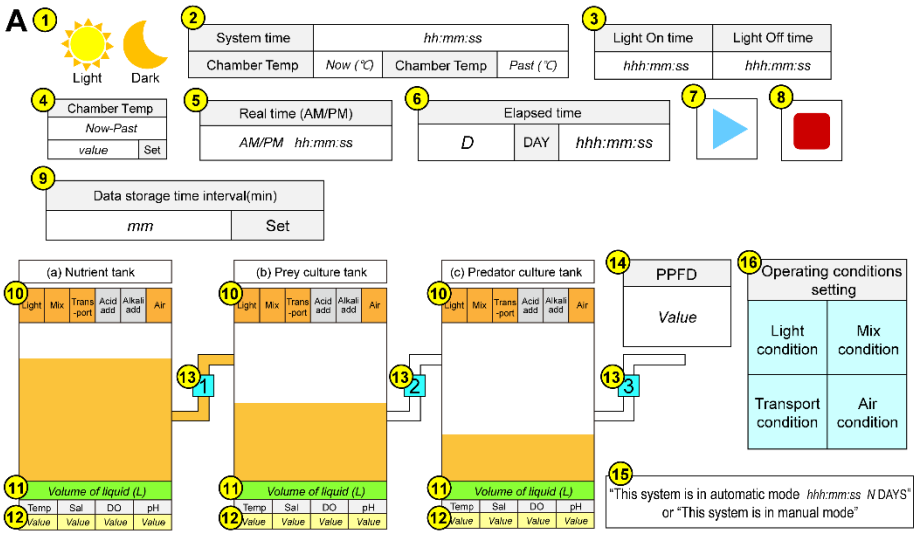

B

No.	Explanation
1	Light (LED on) and dark (LED off) display
2	System operation time and temperature in chamber display (current and last 1 minute data)
3	Light (LED on) : dark (LED off) cycle display
4	Temperature in chamber setting
5	Real time (AM/PM hour:minute:second) display
6	Elapsed time (days, hour:minute:second) display
7	Automatic mode start button
8	Automatic mode stop button
9	Numerical data saving time interval (minute) setting
10	Real-time operation of functions in each tank display (orange: operating, grey: standby)
11	Real-time volume of liquid (L, liters) in each tank display
12	Real-time water quality (temperature, salinity, dissolved oxygen, pH) in each tank display
13	Real-time operation of liquid transport in each tank display (orange: operating, white: standby)
14	Real-time light intensity (PPFD, μmol photons m^{-2} s^{-1}) irradiated to each tank display
15	Current system mode (automatic or manual) and elapsed time display
16	Operating conditions of Light source/Mix/Transport/Aeration in each tank setting

Figure 6.3. Schematic diagram of the program for operating the automatic system for cultivating *Noctiluca scintillans* on a 100-L scale developed in this study (A) and explanation of each part of the program (B). LED, light-emitting diode; PPFD, photosynthetic photon flux density. See the Materials and Methods section for details.

6.2.8. Cultivating *Noctiluca scintillans* on a 100-liter scale using the automatic system

To optimize the growth of *N. scintillans*, the prey species were explored through the literature or preliminary tests, and the growth and ingestion rates were estimated if *N. scintillans* fed on the potential prey species. Based on the calculated growth and ingestion rates of *N. scintillans* and the growth rate of the prey species, a suitable prey species was selected and used for the automatic cultivation experiment of *N. scintillans*. Moreover, after several preliminary tests, we chose 20℃ as the optimal temperature, 10–20 μmol photons m^{-2} s^{-1} for the optimal light intensity for *N. scintillans* and 300 μmol photons m^{-2} s^{-1} for *D. salina* under a 14 : 10 h Light-Dark cycle.

At the beginning of the experiment, 50 L of F/2-Si medium was added to the nutrient tank, 90 L of *D. salina* culture (approximately 120,000 cells mL^{-1}) to the prey culture tank, and 30 L of *N. scintillans* culture (approximately 25 cells mL^{-1}) to the predator culture tank. Every 2 d, the valves between the prey and predator culture tanks were opened to allow the prey to be transported, and subsequently the valves between the nutrient and prey culture tanks were opened to allow the medium to be transported. Every day, 10-mL aliquots were taken from the waters in the prey and predator culture tanks and fixed with 5% acidic Lugol's solution. In the prey culture tank, subsampling was performed both before and after the F/2-Si medium was added. Subsampling was also performed both before and after the prey culture was transported to the predator culture tank. All or > 200 cells of each species were counted in three 1-mL Sedgwick-Rafter chambers using inverted microscopes of 40 × or 100 × magnification. This procedure was repeated three times.

The specific growth rate of *N. scintillans* (μ, d^{-1}) was calculated as follows:

$$\mu = \frac{\ln(C_{t2}/C_{t1})}{t_2 - t_1}$$

, where Ct_1 and Ct_2 indicate the cell concentrations at time points t_1 (t = 0 d)

and t_2 (t = 1 d), respectively. The growth rates of *N. scintillans* were measured every day for 6 d during each experimental cultivation period.

The prey removal rate (%) of *N. scintillans* was calculated as follows:

$$\text{Prey removal rate (\%)} = \frac{P_{t1} - P_{t2}}{P_{t1}} \times 100$$

, where P_{t1} represents *D. salina* abundance (cells mL^{-1}) immediately after the culture was added to the predator culture tank, and P_{t2} represents the remaining *D. salina* abundance (cells mL^{-1}) 2 d after the culture was added to the predator culture tank. The prey removal rates of *N. scintillans* were measured every 2 d for six days6 d in each experimental cultivation period.

During the experimental cultivation periods, salinity, pH, and DO were monitored but not controlled. All cultivation periods were conducted under the same conditions as described above.

The bioluminescence capability of *N. scintillans* cultivated using the automatic mass cultivation system was tested when the volume of *N. scintillans* culture was 90 L in the predator culture tank. The *N. scintillans* culture was mechanically stimulated by placing the predator culture tank in the dark for 3 h. It was then stimulated using three air pumps (10 L min^{-1}) for aeration, and three spargers for even air distribution. During mechanical stimulation, bioluminescence images were captured using a Canon EOS R with a Canon RF 50 mm F1.2L lens (Canon, Tokyo, Japan) at aperture F2.2, shutter speed 8 s, and ISO200.

6.3. Results

6.3.1. Developed semi-continuous system for cultivating the mixotrophic and heterotrophic dinoflagellates on a 10-liter scale

The developed semi-continuous system consisted of two 10-L glass vessels (Hanil sci-med, Dajeon, Korea); one 10-L polycarbonate vessel; eight LED lamps (maximum 200 μmol photons m^{-2} s^{-1}); two peristaltic pumps; two air pumps; two spargers; two stirring subsytems each consisting of a stirrer equipped with a low-speed motor; two sensors for measuring water temperature; one timer; and silicone tubings (**Figure 6.4**). A temperature-controlled walk-in chamber enclosing all hardware parts could maintain a target temperature of 5–30℃.

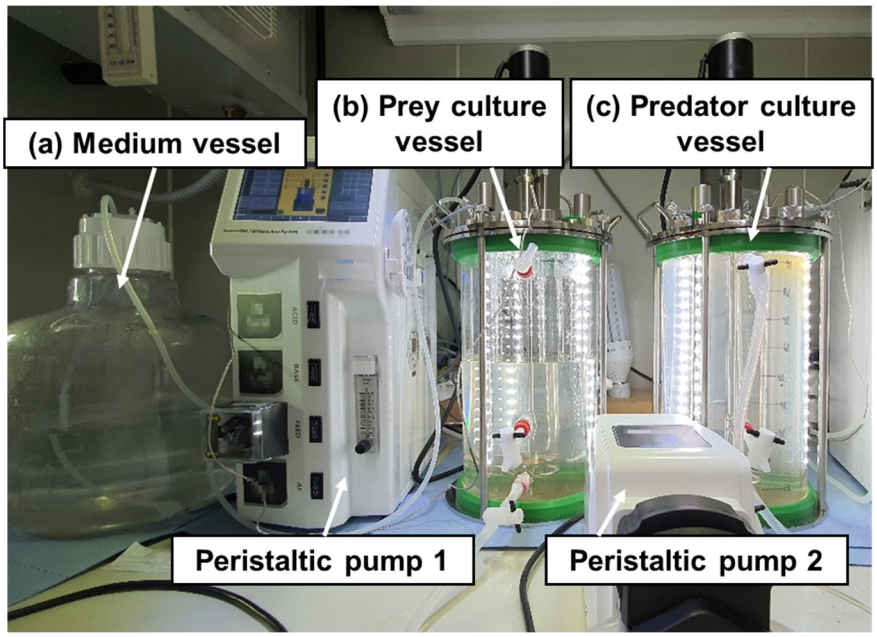

Figure 6.4. The developed semi-continuous cultivation system on a 10-L scale for mixotrophic and heterotrophic dinoflagellates. This system consisted of three 10-L water vessels: a medium PC vessel (a), a prey culture glass vessel (b), and a predator culture glass vessel (c). Two vessels were connected by silicone tubings and the liquid in the vessels was transferred using peristaltic pumps.

6.3.2. Cultivating *Gymnodinium smaydae* using the semi-continuous system on a 10-liter scale and lipid analysis

According to Lee et al. 2014a, the predator *G. smaydae* was able to feed on thecate dinoflagellates *Heterocapsa rotundata*, *Heterocapsa* sp., *H. triquetra*, and *Scrippsiella acuminata*. The maximum growth rates of *G. smaydae* on *H. rotundata*, *Heterocapsa* sp., *H. triquetra*, and *S. trochoidea* were 2.23, 1.76, 0.85, and 0.06 d^{-1}, respectively. Thus, *H. rotundata* was selected as the optimal prey species for cultivation of *G. smaydae*.

The different prey supply intervals (i.e., supplied daily, once every 2 d, and once for 4 d) during incubation did not affect the mixotrophic growth rate and fatty acid contents of *G. smaydae* (Lim et al. 2020). Thus, the prey for cultivation of *G. smaydae* in the semi-continuous system was supplied daily.

At the beginning of the 2-day cultivation experiment, 3 L of 9 L *H. rotundata* culture (approximately 150,000–160,000 cells mL^{-1}) in the prey culture vessel was transported to 3 L of *G. smaydae* culture (approximately 40,000–50,000 cells mL^{-1}) in the predator culture vessel. Subsequently, 3 L of *H. rotundata* culture in the prey culture vessel was transported to the predator culture vessel every day until *G. smaydae* culture in the predator culture vessel became 9 L.

This cultivation experiment was repeated three times (periods 1–3). At the beginning of each period (day 0), the abundance of *H. rotundata* in the prey culture vessel containing 9 L of prey culture was 1.39×10^9–1.4×10^9 cells (154,333–160,333 cells mL^{-1}) in periods 1–3 (**Figure 6.5**). Ten minutes later, 2 L of *H. rotundata* culture from the prey culture vessel was automatically transported to the predator culture vessel. Subsequently, 3 L of F/2-Si medium in the medium vessel was added to the prey culture vessel containing 7 L prey culture as a rate of 2.1 mL min^{-1} for 24 h in continuous operation; thus, the total volume of the prey culture became 9 L 1 d after the prey culture in the prey culture vessel was transferred to the predator culture vessel. One day later (day 1), *H. rotundata* in the prey culture vessel grew, and its abundance was 1.35×10^9–1.57×10^9 cells (149,667–174,000 cells mL^{-1}) in periods 1–3. This process was repeated on days 1–2.

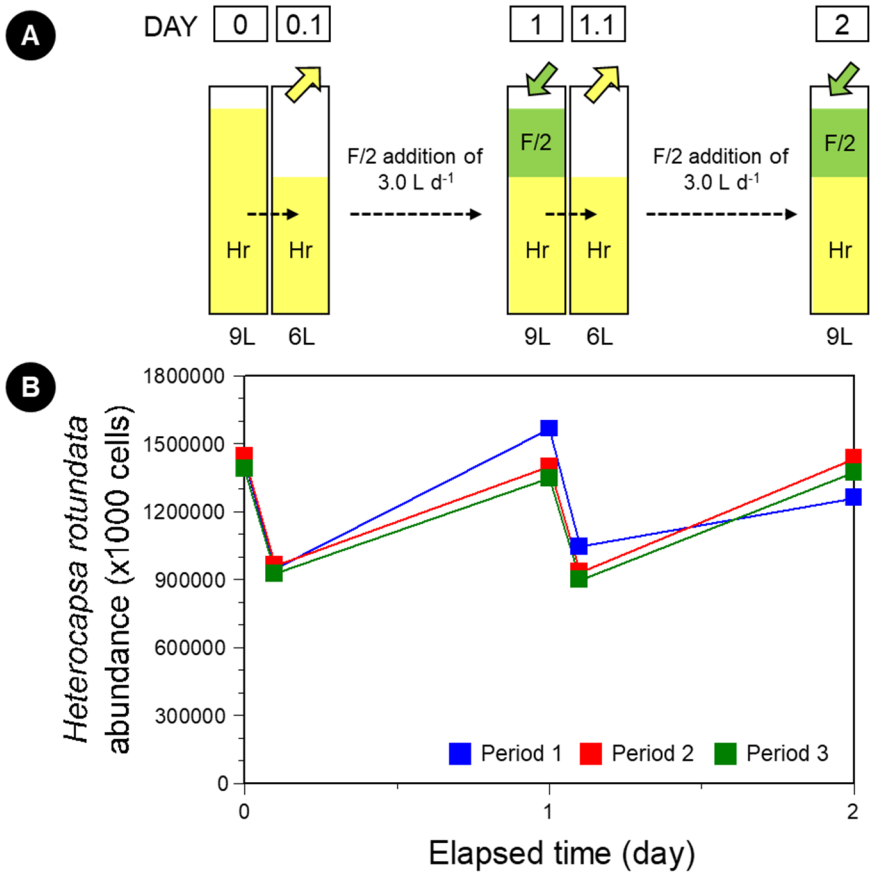

Figure 6.5. (A) Schematic diagram showing changes in water volume [*Heterocapsa rotundata* (Hr), F/2-Si (F/2) medium] in the prey culture vessel (Redrawn from Lim and You et al. 2020). Yellow (Hr) and green (F/2) arrows indicate inlet and outlet of water, respectively. (B) Changes in the abundance of Hr (cells in a total volume of culture) in the prey culture vessel as a function of elapsed incubation time. The data on the abundance of Hr were obtained by operating the system three times from day 0 to day 2. Blue, red, and green squares indicate periods 1, 2, and 3, respectively.

At the beginning of each period (day 0), the abundance of *H. rotundata* in the predator culture vessel containing 3 L predator culture was 19–61 cells mL^{-1} in periods 1–3 (**Figure 6.6**). Ten minutes later, 3 L of *H. rotundata* culture in the prey culture vessel was transported to the predator culture vessel (on day 0.1). The abundance of *H. rotundata* in the predator culture vessel immediately after the prey culture was added was 58,667–64,600 cells mL^{-1} in periods 1–3. Most *H. rotundata* cells in the predator culture vessel were eaten by *G. smaydae* cells 1 d later. On day 0, the abundance of *G. smaydae* in the predator culture vessel containing 3 L predator culture was 40,875–48,429 cells mL^{-1} in periods 1–3 (**Figure 6.6**). After 3 L of *H. rotundata* culture was transported to the predator culture vessel (on day 0.1), the abundance of *G. smaydae* in the predator culture vessel immediately after the prey culture was added was 16,737–21,467 cells mL^{-1} in periods 1–3. Cells of *G. smaydae* grew well on *H. rotundata* and the abundance of *G. smaydae* was 38,625–45,000 cells mL^{-1} on day 1 in periods 1–3. This process was repeated on days 1–2. The maximum abundance of *G. smaydae* in the predator culture vessel was 57,000 cells mL^{-1} during periods 1–3. The prey removal rate (%) by *G. smaydae* 1 d after prey cultures were added was 99.7–99.9 % in periods 1–3 (**Figure 6.6D**).

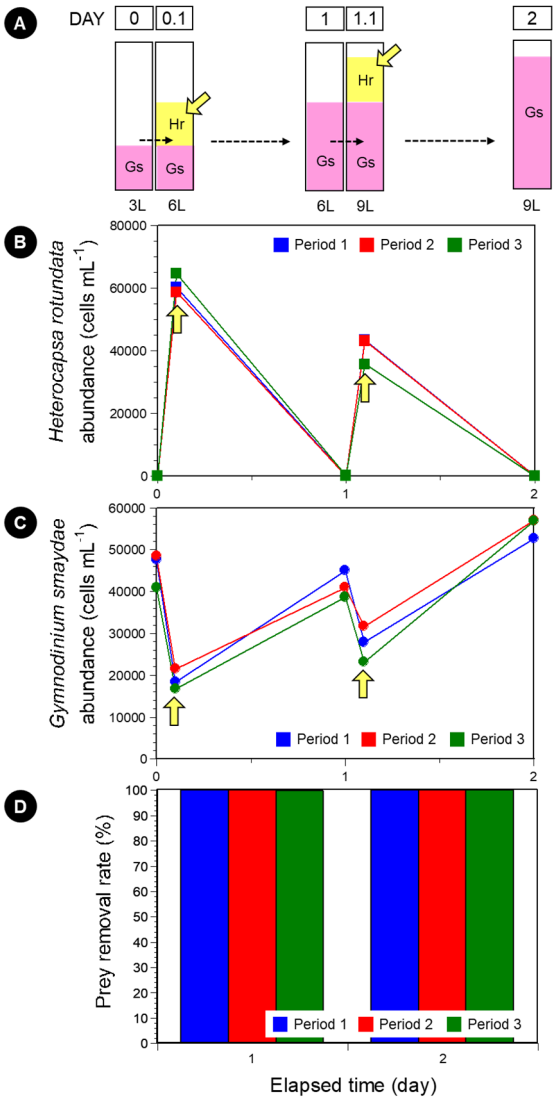

Figure 6.6. (A) Schematic diagram showing changes in water volume [*Heterocapsa rotundata* (Hr), *Gymnodinium smaydae* (Gs)] in the predator culture vessel (Redrawn from Lim and You et al. 2020). Yellow (Hr) arrows indicate input of prey culture. (B) Changes in the abundance of Hr (cells mL^{-1}) in the predator culture vessel as a function of elapsed incubation time. (C) Changes in the abundance of Gs (cells mL^{-1}) in the predator culture vessel as a function of elapsed incubation time. The data on the abundances of Hr (B) and Gs (C) were obtained by operating the system three times from day 0 to day 2. Blue, red, and green squares indicate periods 1, 2, and 3, respectively. Yellow arrows in (B) and (C) indicate the timing of Hr culture input. (D) The prey removal rate (%) in periods 1 (blue bars), 2 (red bars), and 3 (green bars).

In the semi-cultivation system, *G. smaydae* on *H. rotundata* was continuously cultivated for 43 d to track changes in abundance and fatty acid content, following the described method above (Lim and You et al. 2020; **Figure 6.7–6.9**).

In the system, on transferring 3 L of the *H. rotundata* culture to the *G. smaydae* culture vessel, the former's density in the *G. smaydae* culture vessel increased. However, it decreased to almost zero with increasing incubation time because of predation by *G. smaydae*. After prey addition, the density of *H. rotundata* in the *G. smaydae* culture vessel was maintained between 27,750 and 79.600 cells mL^{-1} (**Figure 6.7**). Moreover, before prey addition, the density of *G. smaydae* in the *G. smaydae* culture vessel was maintained above 30,000 cells mL^{-1}, except for the first day when *G. smaydae* was inoculated (**Figure 6.7**). The density of *G. smaydae* decreased temporarily immediately after prey addition, to as low as 3,500 cells mL^{-1} on the first day, before rapidly increasing to 30,700 cells mL^{-1} on the next day because of predation (**Figure 6.7**). The maximum density of *G. smaydae* in the vessel was recorded as 57,000 cells mL^{-1} and the average growth rate of *G. smaydae* during the experimental period was 0.72 d^{-1}. After starvation for 1 day, the density of *H. rotundata* in the *G. smaydae* culture vessel was < 10 cells mL^{-1} for most samples, whereas the density of *G. smaydae* ranged from 29,363–43,500 cells mL^{-1}.

In this semi-continuous cultivation system, the total fatty acid (TFA) content of *G. smaydae* in the harvested samples ranged from 52.80–65.24 mg g^{-1}, whereas the DHA content ranged between 23.74–30.98 mg g^{-1} (**Figure 6.8**). Moreover, the content of EPA and DHA together was 28.67–37.15 mg g^{-1} (**Figure 6.8**). DHA accounted for 45.0–47.5% of *G. smaydae* TFAs, averaging at 46.3%, whereas EPA and DHA together accounted for 54.2–56.9% of the TFAs (**Figure 6.9**).

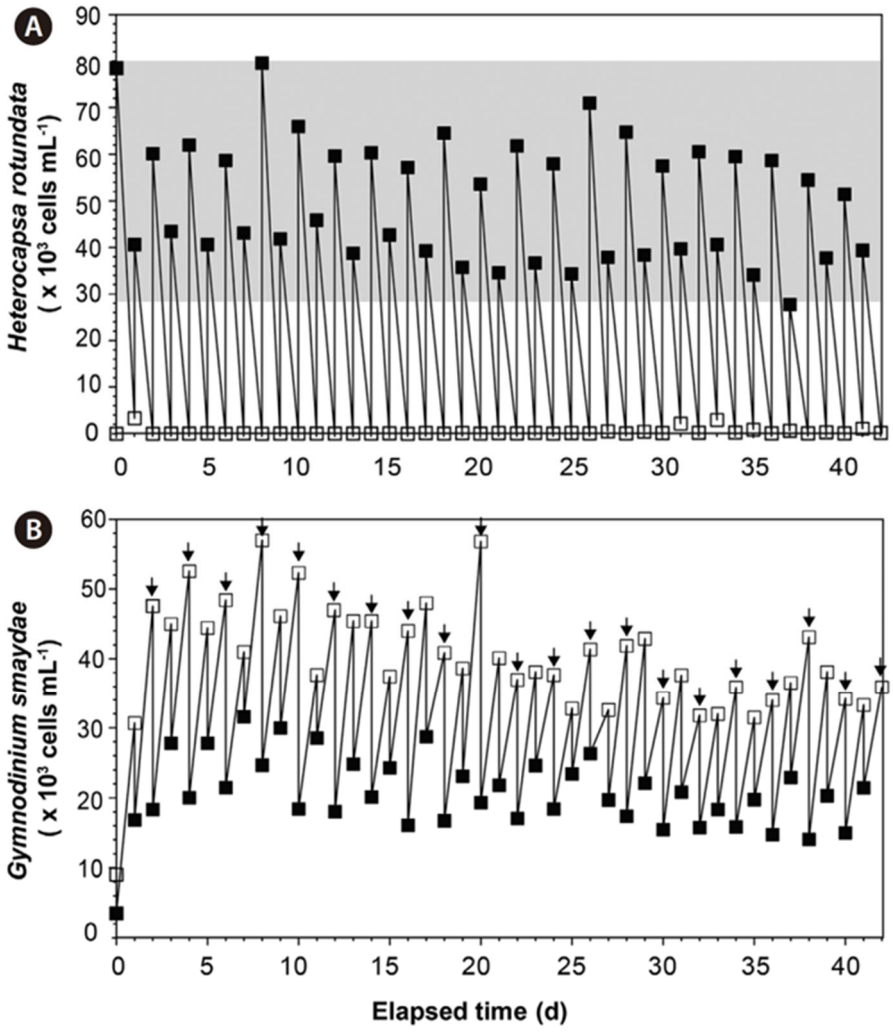

Figure 6.7. Changes in the densities (cells mL^{-1}) of *Heterocapsa rotundata* (A) and *Gymnodinium smaydae* (B) in the predator culture vessel of the semi-continuous cultivation system (Lim and You et al. 2020). The gray area in (A) indicates the range of *H. rotundata* density after feeding. An increase was observed in *H. rotundata* density owing to the daily addition of prey culture (3 L for 10 min), which then decreased because of predation by *G. smaydae* (A). Arrows in (B) indicate the day when the *G. smaydae* culture was transferred to the harvest container. Dilution of the *G. smaydae* culture occurred because of daily addition of prey culture (3 L for 10 min), but the density of *G. smaydae* increased after feeding on prey cells (B). Open and solid squares indicate the densities of *H. rotundata* and *G. smaydae* before and after prey culture addition, respectively.

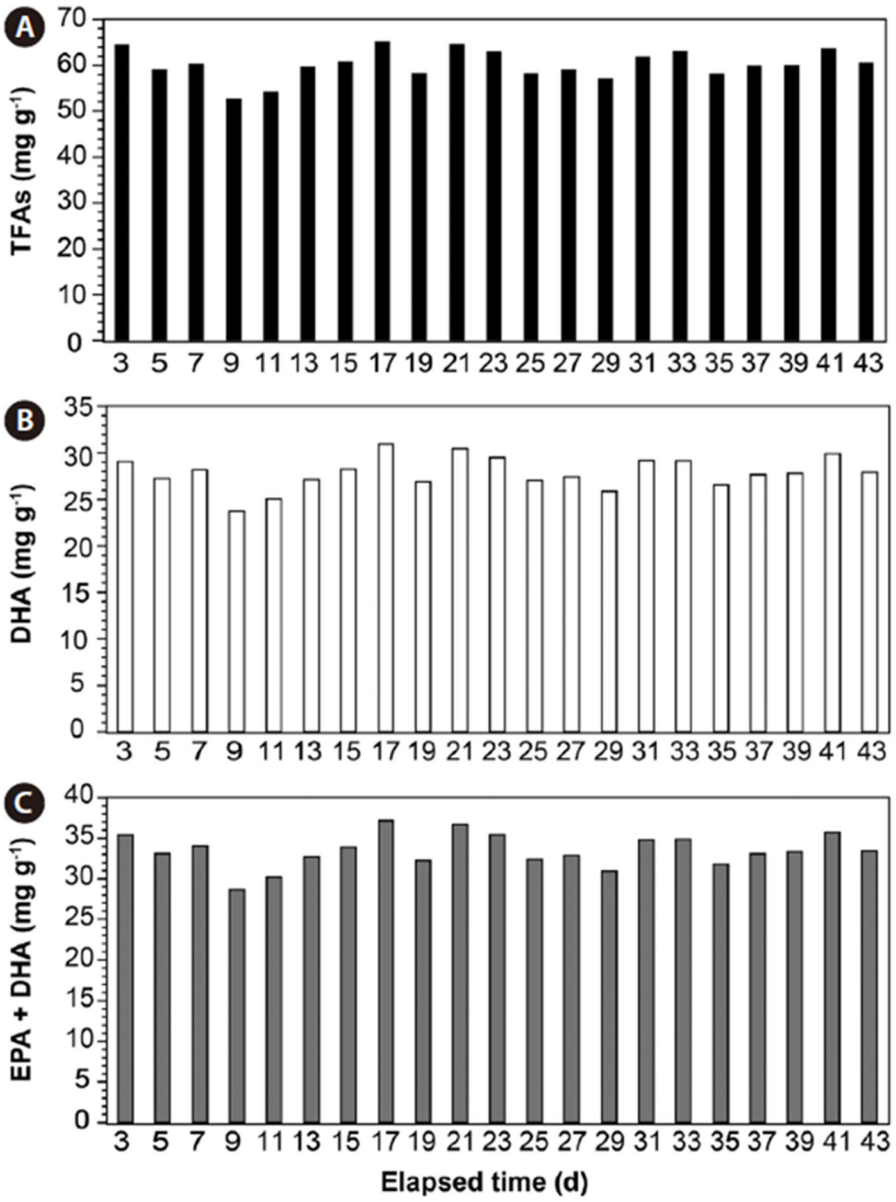

Figure 6.8. Contents (mg g^{-1}) of total fatty acids (TFAs) (A), docosahexaenoic acid (DHA) (B), and eicosapentaenoic acid (EPA) together with DHA (C) in *Gymnodinium smaydae* harvested using the semi-continuous cultivation system (Lim and You et al. 2020).

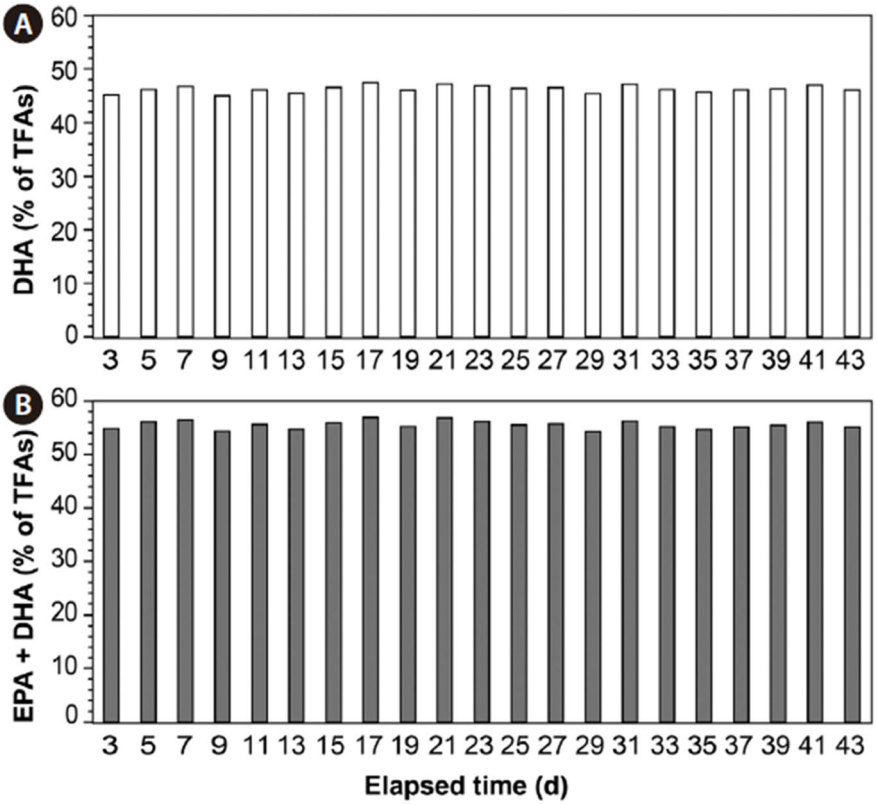

Figure 6.9. Percentage (%) of docosahexaenoic acid (DHA) (A) and eicosapentaenoic acid (EPA) together with DHA (B) in the total fatty acid (TFA) content of *Gymnodinium smaydae* harvested using the semi-continuous cultivation system (Lim and You et al. 2020).

6.3.3. Cultivating *Biecheleria cincta* using the semi-continuous system on a 10-liter scale

Kang et al. (2011) reported that the predator *B. cincta* was able to feed on *Isochrysis galbana*, *Teleaulax* sp., *Rhodomonas salina*, *Heterosigma akashiwo*, *Eutreptiella gymnastica*, *H. rotundata*, and *Amphidinium carterae*. The growth rates of *B. cincta* on *I. galbana*, *Teleaulax* sp., *R. salina*, *A. carterae*, *H. akashiwo*, *E. gymnastica* were 0.086, 0.157, 0.265, 0.229, 0.475, and 0.117 d^{-1}, respectively, at a single prey concentration. Therefore, *H. akashiwo* was selected as the optimal prey species for cultivation of *B. cincta*.

To determine the volume of the F/2–Si medium transported from the medium vessel to the prey culture vessel, as well as the volume of prey culture transported from the prey culture vessel to the predator culture vessel, the growth rate of *H. akashiwo* (ca. 0.5 d^{-1}) and the growth and ingestion rates of *B. cincta* feeding on *H. akashiwo* (0.3 d^{-1} and 3.0 *H. akashiwo* cells predator^{-1} d^{-1}, respectively) were used in this study (Kang et al. 2011, You et al. 2023a).

At the beginning of the 2-day cultivation experiment, 4.5 L of 9 L *H. akashiwo* culture (approximately 20,000–36,000 cells mL^{-1}) in the prey culture vessel was transported to 4.5 L of *B. cincta* culture (approximately 2,000–5,000 cells mL^{-1}) in the predator culture vessel. Subsequently, 4.5 L of *H. akashiwo* culture in the prey culture vessel was transported to the predator culture vessel every 2 d until *B. cincta* culture in the predator culture vessel became 9 L.

This cultivation experiment was repeated three times (periods 1–3). At the beginning of each period (day 0), the abundance of *H. akashiwo* in the prey culture vessel containing 9 L of prey culture was 1.8×10^8–3.3×10^8 cells (20,000–36,500 cells mL^{-1}) in periods 1–3 (**Figure 6.10**). Ten minutes later, 4.5 L of *H. akashiwo* culture from the prey culture vessel was automatically transported to the predator culture vessel. Subsequently, 4.5 L of F/2-Si medium in the medium vessel was added to the prey culture vessel containing 4.5 L prey culture as a rate of 1.56 mL min^{-1} for 48 h in continuous operation; thus, the total volume of the prey culture became 9 L 2 d after the prey culture in the prey culture vessel was transferred to the predator culture

vessel. Two days later (day 2), *H. akashiwo* in the prey culture vessel grew, and its abundance was 2.8×10^8–3.6×10^8 cells (31,286–39,600 cells mL^{-1}) in periods 1–3.

At the beginning of each period (day 0), the abundance of *H. akashiwo* in the predator culture vessel containing 4.5 L predator culture was 17–385 cells mL^{-1} in periods 1–3 (**Figure 6.11**). Ten minutes later, 4.5 L of *H. akashiwo* culture in the prey culture vessel was automatically transported to the predator culture vessel (on day 0.1). The abundance of *H. akashiwo* in the predator culture vessel immediately after the prey culture was added was 9,733–20,400 cells mL^{-1} in periods 1–3. Most *H. akashiwo* cells in the predator culture vessel were eaten by *B. cincta* cells 2 d later. On day 0, the abundance of *B. cincta* in the predator culture vessel containing 4.5 L predator culture was 2,310–4,483 cells mL^{-1} in periods 1–3 (**Figure 6.11**). After 4.5 L of *H. akashiwo* culture was transported to the predator culture vessel (on day 0.1), the abundance of *B. cincta* in the predator culture vessel immediately after the prey culture was added was 1,263–2,150 cells mL^{-1} in periods 1–3. Cells of *B. cincta* grew well on *H. akashiwo* and the abundance of *B. cincta* was 3,417–5,170 cells mL^{-1} on day 2 in periods 1–3. The maximum abundance of *B. cincta* in the predator culture vessel was 5,170 cells mL^{-1} during periods 1–3. The prey removal rate (%) by *B. cincta* 2 d after prey cultures were added was 96–100% in periods 1–3 (**Figure 6.11D**).

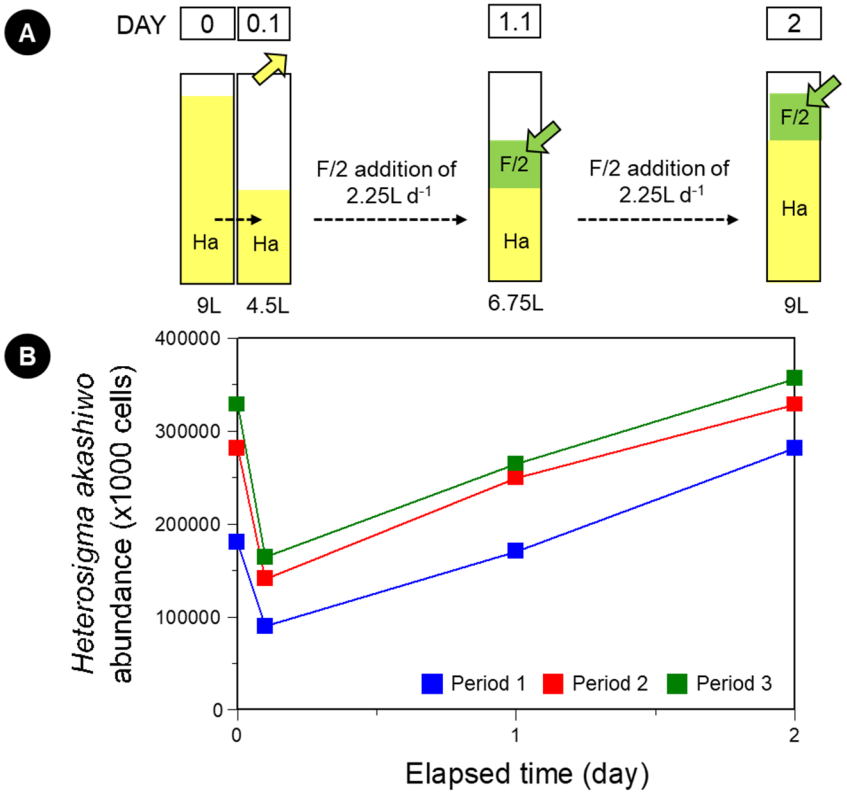

Figure 6.10. (A) Schematic diagram showing changes in water volume [*Heterosigma akashiwo* (Ha), F/2-Si (F/2) medium] in the prey culture vessel. Yellow (Ha) and green (F/2) arrows indicate inlet and outlet of water, respectively. (B) Changes in the abundance of Ha (cells in a total volume of culture) in the prey culture vessel as a function of elapsed incubation time. The data on the abundance of Ha were obtained by operating the system three times from day 0 to day 2. Blue, red, and green squares indicate periods 1, 2, and 3, respectively.

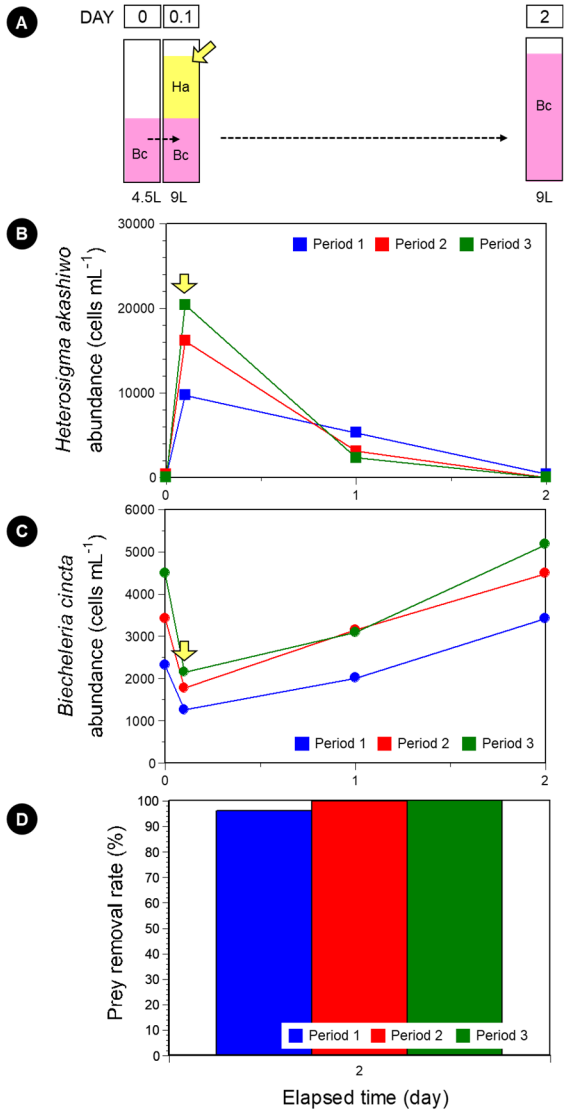

Figure 6.11. (A) Schematic diagram showing changes in water volume [*Heterosigma akashiwo* (Ha), *Biecheleria cincta* (Bc)] in the predator culture vessel. Yellow (Ha) arrows indicate input of prey culture. (B) Changes in the abundance of Ha (cells mL^{-1}) in the predator culture vessel as a function of elapsed incubation time. (C) Changes in the abundance of Bc (cells mL^{-1}) in the predator culture vessel as a function of elapsed incubation time. The data on the abundances of Ha (B) and Bc (C) were obtained by operating the system three times from day 0 to day 2. Blue, red, and green squares indicate periods 1, 2, and 3, respectively. Green arrows in (B) and (C) indicate the timing of Ha culture input. (D) The prey removal rate (%) in periods 1 (blue bars), 2 (red bars), and 3 (green bars).

6.3.4. Cultivating *Gyrodinium dominans* using the semi-continuous system on a 10-liter scale

In preliminary test, *G. dominans* was able to feed on seven *Prorocentrum* species, such as *P. cordatum*, *P. triestinum*, *P. donghaiense*, *P. rhathymum*, *P. micans*, *P. lima*, and *P. hoffmanianum*, and *A. carterae*. At a single high prey concentration of 2,870 ng C mL^{-1}, the specific growth and ingestion rates of *G. dominans* on *A. carterae* were 0.870 d^{-1} and 0.03 ng C $predator^{-1}$ d^{-1} (7.5 cells $predator^{-1}$ d^{-1}) with the autotrophic growth rate of *A. carterae*, 0.49 d^{-1}. At single high mean prey concentrations of 2,450–2,779 ng C mL^{-1}, the specific growth rates of *G. dominans* on *P. donghaiense*, *P. triestinum*, and *P. cordatum* were 0.871, 0.850, and 0.759 d^{-1}, respectively; those on *P. rhathymum*, *P. micans*, and *P. hoffmannianum* were 0.499, 0.206, and 0.153 d^{-1}, respectively, but that on *P. lima* was -0.193 d^{-1}. At single high mean prey concentrations of 2,450–2,779 ng C mL^{-1}, the ingestion rates of *G. dominans* on *P. rhathymum* and *P. lima* were 4.0 and 3.3 ng C $predator^{-1}$ d^{-1}, respectively, and those on *P. donghaiense* and *P. cordatum* were both 1.1 ng C $predator^{-1}$ d^{-1}; however, those on *P. triestinum*, *P. micans*, and *P. hoffmannianum* were 0.9, 0.7, and 0.5 ng C $predator^{-1}$ d^{-1}, respectively. Autotrophic growth rates of *P. cordatum*, *P. donghaiensis*, *P. triestinum*, *P. rhathymum*, *P. micans*, *P. lima*, and *P. hoffmannianum* were 0.358, 0.164, 0.155, 0.108, 0.375, 0.068, and -0.032 d^{-1}. In addition, other prey species of *G. dominans* were explored in the literature (**Table 6.1**). Therefore, *A. carterae* was selected as the optimal prey species for cultivation of *G. dominans* due to the higher autotrophic growth rate of *A. carterae* and the growth and ingestion rates of *G. dominans*.

Table 6.1. Comparison of growth and ingestion rates of *Gyrodinium dominans* feeding on prey species. ESD, equivalent spherical diameter (μm); GR, growth rate (μ, d^{-1}); MGR, maximum growth rate (μ, day^{-1}); IR, ingestion rate (ng C $predator^{-1}$ day^{-1}); MIR, maximum ingestion rate (I_{max}, ng C $predator^{-1}$ day^{-1}).

Prey	ESD	GR(*MGR)	IR(*MIR)	Reference
Chlorophyte				
Chlorella sapsulata	4.2	0.34		Nakamura et al. 1995
Nephroselmis aff. *rotunda*	4.5	0.46		Nakamura et al. 1995
Dunaliella tertiolecta [1]	6.5	0.57	0.67	Calbet et al. 2013
Dunaliella tertiolecta [2]	8.5	0.09		Naustvoll 2000
Pyramimonas parkeae	10.5	0.06		Nakamura et al. 1995
Cryptophyte				
Rhodomonas cf. *baltica*	6.4	0.26		Naustvoll 2000
Rhodomonas salina	6.5	0.34	**1.17***	Calbet et al. 2013
Diatom				
Thalassiosira sp.	5.4	0.64		Nakamura et al. 1995
Skeletonema costatum [1]	5.6	0.22		Nakamura et al. 1995
Skeletonema costatum [2]	6.8	0.05		Naustvoll 2000
Navicula sp.	9.7	0.03		Naustvoll 2000
Ditylum brightwelli	43.1	0.21		Naustvoll 2000
Dinoflagellate				

Amphidinium carterae	8.4	0.87	0.03	This study
Heterocapsa triquetra [1]	10.9	1.21		Naustvoll 2000
Symbiodinium voratum	11.1	**0.61***	**1.90***	Jeong et al. 2014
Gymnodinium galatheanum	11.5	0.45		Naustvoll 2000
Prorocentrum triestinum	11.8	**0.22***	**0.45***	This study
Prorocentrum cordatum [1]	12.1	**1.13***	**1.20***	Kim and Jeong 2004
Prorocentrum cordatum [2]		**0.80**	**1.51**	This study
Biecheleria cincta	12.2	0.07	0.13	Yoo et al. 2013
Prorocentrum donghaiense	13.3	**-0.05***	**1.19***	This study
Prorocentrum cordatum [3]	13.6	0.50		Naustvoll 2000
Heterocapsa triquetra [2]	14.9	**0.44***	**3.56***	Anderson and Menden-Deur 2017
Heterocapsa triquetra [3]	15.3	**0.47***	**2.45***	Nakamura et al. 1995
Scrippsiella acuminata	16.3	0.32		Nakamura et al. 1995
Karenia mikimotoi [1]	16.8	0.42		Nakamura et al. 1995
Gymnodinium aureolum	19.5	**0.92***	**2.00***	Yoo et al. 2010
Karenia mikimotoi [2]	22.1	0.02		Naustvoll 2000
Prorocentrum micans [1]	23.8	0.01		Naustvoll 2000
Prorocentrum micans [2]	24.3	0.06		Nakamura et al. 1995
Prorocentrum cf. *rhathymum*	25.3	**0.18***	**0.36***	This study
Prorocentrum micans [3]	26.0	-0.13	0.00	This study

Prorocentrum lima	37.1	0.07	2.10	This study
Prorocentrum hoffmannianum	43.4	0.02	0.00	This study
Euglenophyte				
Eutreptiella gymnastica	12.6	**1.13***	**2.70***	Jeong et al. 2011
Prymnesiophyte				
Isochrysis galbana	4.2	0.41		Nakamura et al. 1995
Gephyrocapsa oceanica	4.7	0.37		Nakamura et al. 1995
Emiliania huxleyi	6.4	0.02		Naustvoll 2000
Chrysochromulina polylepis	6.9	0.13		Naustvoll 2000
Raphidophyte				
Heterosigma akashiwo	10.6	0.13		Nakamura et al. 1995
Chattonella marina	26.3	0.40		Nakamura et al. 1995
Chattonella antiqua [1]	35.3	0.07		Nakamura et al. 1995
Chattonella antiqua [2]	35.3	0.44	2.20	Nakamura et al. 1992
Naked ciliate				
Mesodinium rubrum	22.0	**0.48***	**0.55***	Lee et al. 2014a

Considering the growth rates of *G. dominans* on *A. carterae* and that of *A. carterae*, the volume of the F/2-Si medium transported from the medium vessel to the prey culture vessel, as well as the volume of prey culture transported from the prey culture vessel to the predator culture vessel, were determined.

At the beginning of the 3-day cultivation experiment, 2 L of 9 L *A. carterae* culture (approximately 40,000–130,000 cells mL^{-1}) in the prey culture vessel was transported to 2 L of *G. dominans* culture (approximately 7,000–10,000 cells mL^{-1}) in the predator culture vessel. Subsequently, 2 L of *A. carterae* culture in the prey culture vessel was transported to the predator culture vessel every day until *G. dominans* culture in the predator culture vessel became 8 L.

This cultivation experiment was repeated three times (periods 1–3). At the beginning of each period (day 0), the abundance of *A. carterae* in the prey culture vessel containing 9 L of prey culture was 3.9×10^8–1.1×10^9 cells (43,400–127,667 cells mL^{-1}) in periods 1–3 (**Figure 6.12**). Ten minutes later, 2 L of *A. carterae* culture from the prey culture vessel was automatically transported to the predator culture vessel. Subsequently, 2 L of F/2-Si medium in the medium vessel was added to the prey culture vessel containing 7.0 L prey culture as a rate of 1.39 mL min^{-1} for 24 h in continuous operation; thus, the total volume of the prey culture became 9 L 1 d after the prey culture in the prey culture vessel was transferred to the predator culture vessel. One day later (day 1), *A. carterae* in the prey culture vessel grew, and its abundance was 5.2×10^8–1.3×10^9 cells (57,750–148,667 cells mL^{-1}) in periods 1–3. This process was repeated on days 1–2 and days 2–3.

At the beginning of each period (day 0), the abundance of *A. carterae* in the predator culture vessel containing 2 L predator culture was 34–88 cells mL^{-1} in periods 1–3 (**Figure 6.13**). Ten minutes later, 2 L of *A. carterae* culture in the prey culture vessel was automatically transported to the predator culture vessel (on day 0.1). The abundance of *A. carterae* in the predator culture vessel immediately after the prey culture was added was 23,444–57,750 cells mL^{-1} in periods 1–3. Most *A. carterae* cells in the predator culture vessel were eaten by *G. dominans* cells one day later. On day 0, the abundance

of *G. dominans* in the predator culture vessel containing 2 L predator culture was 7,008–10,275 cells mL^{-1} in periods 1–3 (**Figure 6.13**). After 2 L of *A. carterae* culture was transported to the predator culture vessel (on day 0.1), the abundance of *G. dominans* in the predator culture vessel immediately after the prey culture was added was 2,092–5,167 cells mL^{-1} in periods 1–3. Cells of *G. dominans* grew well on *A. carterae* and the abundance of *G. dominans* was 4,467–13,150 cells mL^{-1} on day 1 in periods 1–3. This process was repeated on days 1–2 and days 2–3. The maximum abundance of *G. dominans* in the predator culture vessel was 17,361 cells mL^{-1} during periods 1–3. The prey removal rate (%) by *G. dominans* 1 d after prey cultures were added was 99% in periods 1–3 (**Figure 6.13D**).

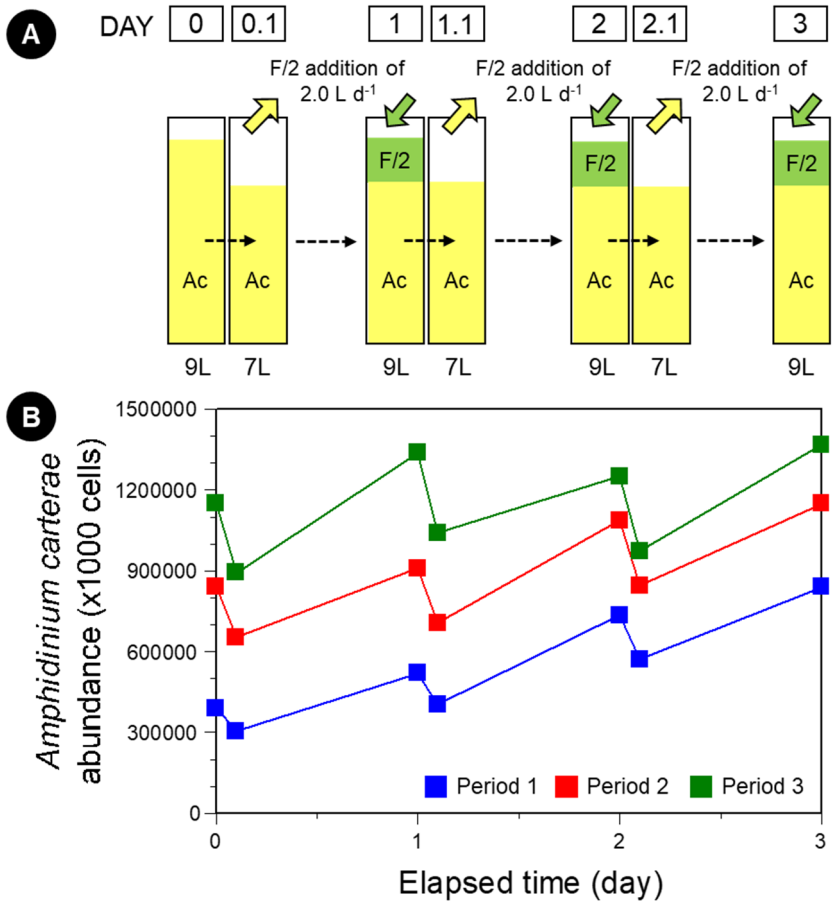

Figure 6.12. (A) Schematic diagram showing changes in water volume [*Amphidinium carterae* (Ac), F/2-Si (F/2) medium] in the prey culture vessel. Yellow (Ac) and green (F/2) arrows indicate inlet and outlet of water, respectively. (B) Changes in the abundance of Ac (cells in a total volume of culture) in the prey culture vessel as a function of elapsed incubation time. The data on the abundance of Ac were obtained by operating the system three times from day 0 to day 3. Blue, red, and green squares indicate periods 1, 2, and 3, respectively.

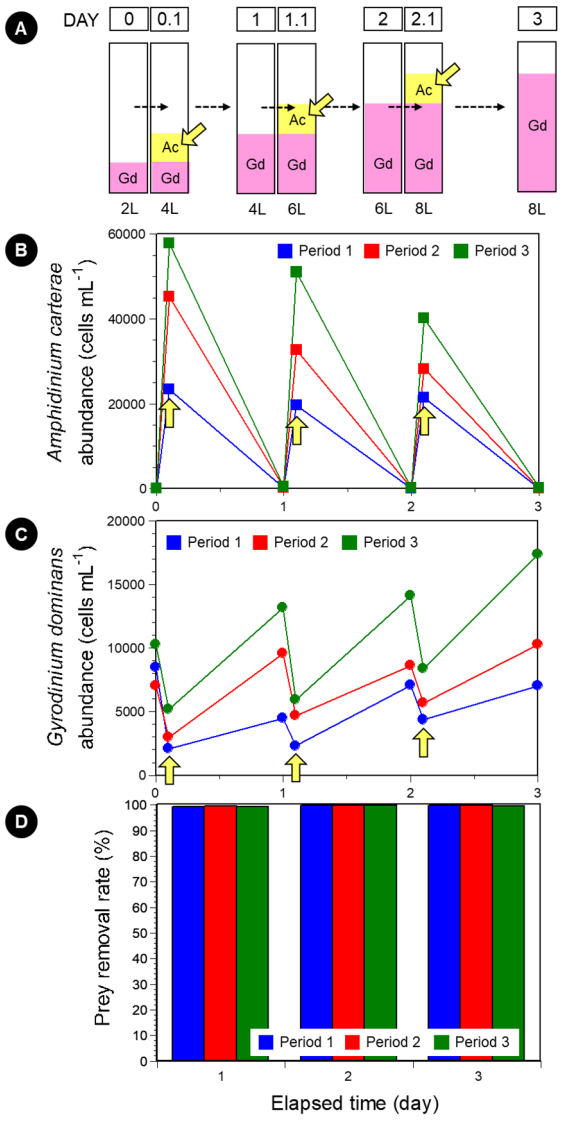

Figure 6.13. (A) Schematic diagram showing changes in water volume [*Amphidinium carterae* (Ac), *Gyrodinium dominans* (Gd)] in the predator culture vessel. Yellow (Ac) arrows indicate input of prey culture. (B) Changes in the abundance of Ac (cells mL^{-1}) in the predator culture vessel as a function of elapsed incubation time. (C) Changes in the abundance of Gd (cells mL^{-1}) in the predator culture vessel as a function of elapsed incubation time. The data on the abundances of Ac (B) and Gd (C) were obtained by operating the system three times from day 0 to day 3. Blue, red, and green squares indicate periods 1, 2, and 3, respectively. Yellow arrows in (B) and (C) indicate the timing of Ac culture input. (D) The prey removal rate (%) in periods 1 (blue bars), 2 (red bars), and 3 (green bars).

6.3.5. Cultivating *Polykrikos kofoidii* using the semi-continuous system on a 10-liter scale

In preliminary test, *P. kofoidii* was able to feed on seven *Prorocentrum* species, such as *P. cordatum*, *P. triestinum*, *P. donghaiense*, *P. rhathymum*, *P. micans*, *P. lima*, and *P. hoffmanianum*.

At single high mean prey concentrations of 1,442–1,965 ng C mL^{-1}, the specific growth rate of *P. kofoidii* on *P. hoffmannianum* was 0.160 d^{-1}, but those on *P. donghaiense*, *P. lima*, *P. rhathymum*, and *P. triestinum* ranged from -0.272 to -0.071 d^{-1}. The specific growth rates of *P. kofoidii* on *P. cordatum* and *P. micans* at 1,467–2,303 ng C mL^{-1} were -0.363 and -0.042 d^{-1}, respectively (Kim and Jeong 2004). At single high mean prey concentrations of 1,442–1,965 ng C mL^{-1}, the ingestion rate of *P. kofoidii* on *P. hoffmannianum* was 7.3 ng C $predator^{-1}$ d^{-1}, those on *P. lima* and *P. rhathymum* were 4.2–4.7 ng C $predator^{-1}$ d^{-1}, and those on *P. donghaiense* and *P. triestinum* were 0.8–1.0 ng C $predator^{-1}$ d^{-1}. The ingestion rates of *P. kofoidii* on *P. cordatum* and *P. micans* at 1,467–2,303 ng C mL^{-1} were 0.4 and 4.1 ng C $predator^{-1}$ d^{-1}, respectively (Kim and Jeong 2004). Autotrophic growth rates of *P. donghaiensis*, *P. triestinum*, *P. rhathymum*, *P. lima*, and *P. hoffmannianum* were 0.299, 0.228, -0.023, 0.007, and 0.375, 0.068, and -0.049 d^{-1}. In addition, other prey species of *P. kofoidii* were explored in the literature (**Table 6.2**). Therefore, *A. minutum* CCMP1888 was selected as the optimal prey species for cultivation of *P. kofoidii* due to the higher autotrophic growth rate of *A. minutum* and the growth and ingestion rates of *P. kofoidii*.

Table 6.2. Comparison of growth and ingestion rates of *Polykrikos kofoidii* feeding on prey species. ESD, equivalent spherical diameter (μm); GR, growth rate (μ, d^{-1}); IR, ingestion rate (ng C $predator^{-1}$ d^{-1}).

Prey	ESD	GR	IR	Reference
Amphidinium carterae	9.8	0.10		Jeong et al. 2001a
Symbiodinium voratum	11.1	0.04	10.0	Jeong et al. 2014
Prorocentrum triestinum	11.8	-0.071	1.0	This study (You et al. 2020a)
Prorocentrum cordatum	12.2	-0.363	0.4	Kim and Jeong 2004
Prorocentrum donghaiense	13.3	-0.272	0.8	This study (You et al. 2020a)
Scrippsiella lachrymosa	17.7	0.52	9.4	Kim et al. 2019
Gymnodinium impudicum	17.8	0.06	5.4	Jeong et al. 2001b
Scrippsiella donghaiensis	19.4	-0.03	4.5	Kim et al. 2019
Gymnodinium aureolum	19.5	0.11	2.3	Yoo et al. 2010
Alexandrium minutum CCMP1888	20.4	0.77	11.1	Kang et al. 2018
Scrippsiella masanensis	22.0	-0.05	10.4	Kim et al. 2019
Scrippsiella acuminata	22.8	0.97	16.6	Jeong et al. 2001b
Prorocentrum rhathymum	25.4	-0.122	4.7	This study (You et al. 2020a)
Prorocentrum micans	26.0	-0.042	4.1	Kim and Jeong 2004
Ostreopsis cf. ovata	26.4	0.72	33.3	Yoo et al. 2015
Prorocentrum micans	26.6	0.06	4.6	Jeong et al. 2001b
Tripos furca	29.0	0.35	9.8	Jeong et al. 2001b

Alexandrium tamarense	31.2	1.01	26.2	Kang et al. 2018
Gymnodinium catenatum	33.0	1.12	17.1	Jeong et al. 2001b
Prorocentrum lima	37.1	-0.192	4.2	This study (You et al. 2020a)
Lingulodinium polyedrum	38.2	0.83	24.4	Jeong et al. 2001b
Prorocentrum hoffmannianum	43.4	0.160	7.3	This study (You et al. 2020a)

Considering the growth rates of *P. kofoidii* on *A. minutum* and that of *A. minutum* (ca. 0.2 d^{-1}), the volume of the F/2-Si medium transported from the medium vessel to the prey culture vessel, as well as the volume of prey culture transported from the prey culture vessel to the predator culture vessel, were determined.

At the beginning of the 6-day cultivation experiment, 3 L of 8 L *A. minutum* culture (approximately 13,000–15,000 cells mL^{-1}) in the prey culture vessel was transported to 3 L of *P. kofoidii* culture (approximately 250–550 cells mL^{-1}) in the predator culture vessel. Subsequently, 3 L of *A. minutum* culture in the prey culture vessel was transported to the predator culture vessel every 3 d until *P. kofoidii* culture in the predator culture vessel became 9 L.

This cultivation experiment was repeated three times (periods 1–3). At the beginning of each period (day 0), the abundance of *A. minutum* in the prey culture vessel containing 8 L of prey culture was 1.1×10^8–1.2×10^8 cells (13,483–15,053 cells mL^{-1}) in periods 1–3 (**Figure 6.14**). Ten minutes later, 3 L of *A. minutum* culture from the prey culture vessel was automatically transported to the predator culture vessel. Subsequently, 3 L of F/2-Si medium in the medium vessel was added to the prey culture vessel containing 5 L prey culture as a rate of 0.70 mL min^{-1} for 72 h in continuous operation; thus, the total volume of the prey culture became 8 L 3 d after the prey culture in the prey culture vessel was transferred to the predator culture vessel. Three days later (day 3), *A. minutum* in the prey culture vessel grew, and its abundance was 9.8×10^7–1.2×10^8 cells (12,300–15,462 cells mL^{-1}) in periods 1–3. This process was repeated on days 3–6.

At the beginning of each period (day 0), the abundance of *A. minutum* in the predator culture vessel containing 3 L predator culture was 0–20 cells mL^{-1} in periods 1–3 (**Figure 6.15**). Ten minutes later, 3 L of *A. minutum* culture in the prey culture vessel was automatically transported to the predator culture vessel (on day 0.1). The abundance of *A. minutum* in the predator culture vessel immediately after the prey culture was added was 6,483–7,783 cells mL^{-1} in periods 1–3. Most *A. minutum* cells in the predator culture vessel were eaten by *P. kofoidii* cells 3 d later. On day 0, the abundance of *P. kofoidii* in

the predator culture vessel containing 3 L predator culture was 256–547 cells mL^{-1} in periods 1–3 (**Figure 6.15**). After 3 L of *A. minutum* culture was transported to the predator culture vessel (on day 0.1), the abundance of *P. kofoidii* in the predator culture vessel immediately after the prey culture was added was 110–208 cells mL^{-1} in periods 1–3. Cells of *P. kofoidii* grew well on *A. minutum* and the abundance of *P. kofoidii* was 423–511 cells mL^{-1} on day 3 in periods 1–3. This process was repeated on days 3–6. The maximum abundance of *P. kofoidii* in the predator culture vessel was 875 cells mL^{-1} during periods 1–3. The prey removal rate (%) by *P. kofoidii* 3 d after prey cultures were added was 99–100% in periods 1–3 (**Figure 6.15D**).

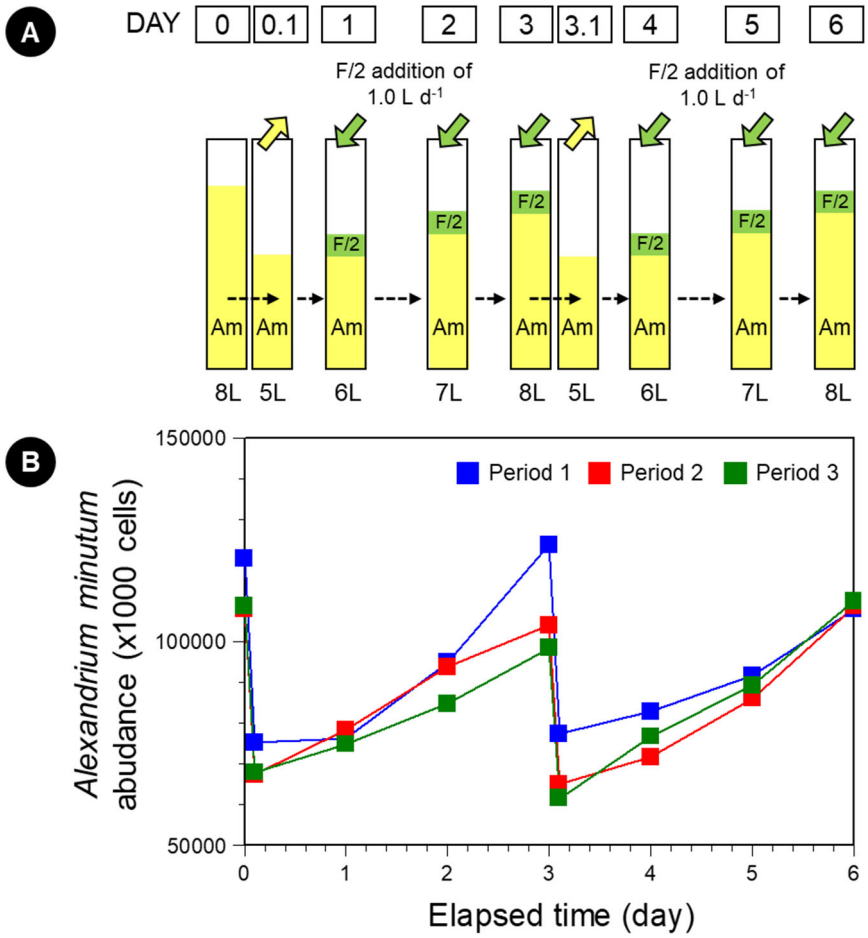

Figure 6.14. (A) Schematic diagram showing changes in water volume [*Alexandrium minutum* (Am), F/2-Si (F/2) medium] in the prey culture vessel. Yellow (Am) and green (F/2) arrows indicate inlet and outlet of water, respectively. (B) Changes in the abundance of Am (cells in a total volume of culture) in the prey culture vessel as a function of elapsed incubation time. The data on the abundance of Am were obtained by operating the system three times from day 0 to day 6. Blue, red, and green squares indicate periods 1, 2, and 3, respectively.

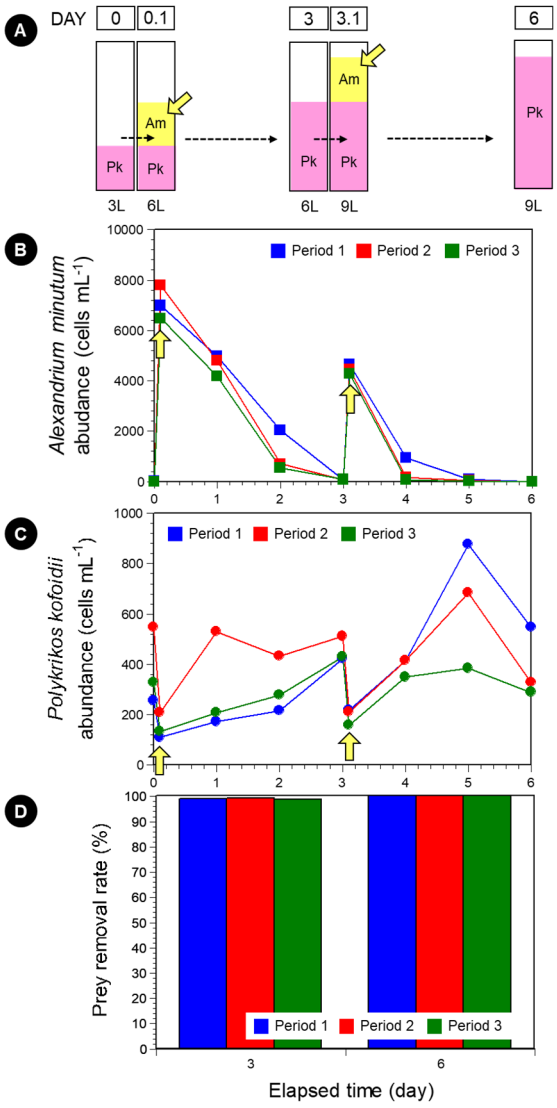

Figure 6.15. (A) Schematic diagram showing changes in water volume [*Alexandrium minutum* (Am), *Polykrikos kofoidii* (Pk)] in the predator culture vessel. Yellow (Am) arrows indicate input of prey culture. (B) Changes in the abundance of Am (cells mL^{-1}) in the predator culture vessel as a function of elapsed incubation time. (C) Changes in the abundance of Pk (cells mL^{-1}) in the predator culture vessel as a function of elapsed incubation time. The data on the abundances of Am (B) and Pk (C) were obtained by operating the system three times from day 0 to day 6. Blue, red, and green squares indicate periods 1, 2, and 3, respectively. Yellow arrows in (B) and (C) indicate the timing of Am culture input. (D) The prey removal rate (%) in periods 1 (blue bars), 2 (red bars), and 3 (green bars).

6.3.6. Developed hardware and software of the automatic system for cultivating the mixotrophic and heterotrophic dinoflagellates on a 100-liter scale

The hardware components of the automatic system were successfully established based on the design and results of several trials (**Figure 6.16**). The hardware consisted of four 200-L PC water tanks; eight full spectrum LED lamps (maximum 1,000 μmol photons m^{-2} s^{-1}; Full spectrum LED lamp; Yunlighting, Namyangju, Korea); four spectrometers (UM-2280; OtO Photonics Inc., Hsinchu, Taiwan); four magnetic pumps (NH-100PX; Panworld Co., Ltd., Tokyo, Japan); four diaphragm pumps (KM212; Cheonsei Co., Ltd., Ansan, Korea); four sensors measuring water temperature (℃), salinity, pH, and DO (Aqua TROLL 500; In-Situ Inc., Fort Collins, CO, USA); four air pumps (maximum 10 L min^{-1}); four spargers; four stirring subsystems each consisting of a stirrer equipped with a low-speed motor (maximum 100 rpm); four weighing systems (HBS-200, CI-600; CAS Co., Ltd., Yangju, Korea); and polyvinyl chloride or silicone pipes (**Figure 6.16**). A temperature-controlled walk-in chamber enclosing all hardware parts could maintain a temperature between 15 and 25℃.

When the valves between the prey and predator culture tanks were opened, predetermined volume (L) of the prey culture in the prey culture tank was transported to the predator culture tank at a rate of 10 L min^{-1}. Subsequently, when the valves between the nutrient tank and prey culture tank were opened, predetermined volume of the nutrient medium in the nutrient tank was transported to the prey culture tank at a rate of 10 L min^{-1}. Prior to opening the valves, the culture in the prey culture tank was mixed using a stirrer at a rate of 5 rpm for 2 min to homogenize prey abundance. This minimized the difference in the abundances of the remaining and transported prey.

Cells of prey species, such as *D. salina*, tended to stay near the bottom of the prey culture tank, and thus, mixing was necessary. To mix the cultures in the prey culture tank, air was automatically supplied to the bottom of the tank at a predetermined rate (L min^{-1}) using an air pump and a sparger for predetermined time (min) and interval. Additionally, the culture was able to

be automatically mixed using a stirrer at a predetermined rate (rpm) for predetermined time (min) and interval. Mixing was required to prevent the predator cells from being separated from the prey cells in the predator culture tank. To mix the culture in the predator culture tank, air was automatically supplied to the bottom of the tanks and a stirrer was automatically operated at described above.

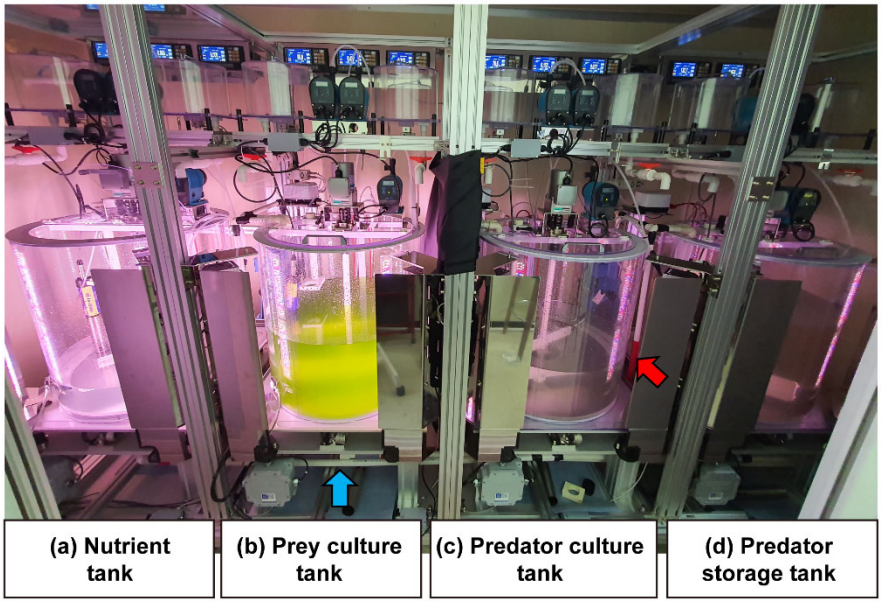

Figure 6.16. Hardware apparatus of the automatic system for cultivating *Noctiluca scintillans* on a 100-L scale developed in this study. This system consisted of four 200-L PC water tanks: a nutrient tank (a), a prey culture tank (b), a predator culture tank (c), and a predator storage tank (d). Two tanks were connected by silicone (red arrow) or PVC pipes (blue arrow).

The system controller program was designed to control, adjust, and monitor the hardware functions (**Figure 6.17**). The program can automatically adjust and control the temperature in the chamber as well as various functions of the hardware (light source operation, mix operation, pump operation, and aeration operation), and save numerical data (volume, light intensity, water temperature, salinity, pH, and DO in each tank) measured in real time at a set time interval. In addition, it is possible to monitor the current system operation status (automatic or manual mode), incubation period (elapsed time), and environmental changes of cultures in each tank (water temperature, salinity, pH, DO, and light intensity) in real time (**Figure 6.17**).

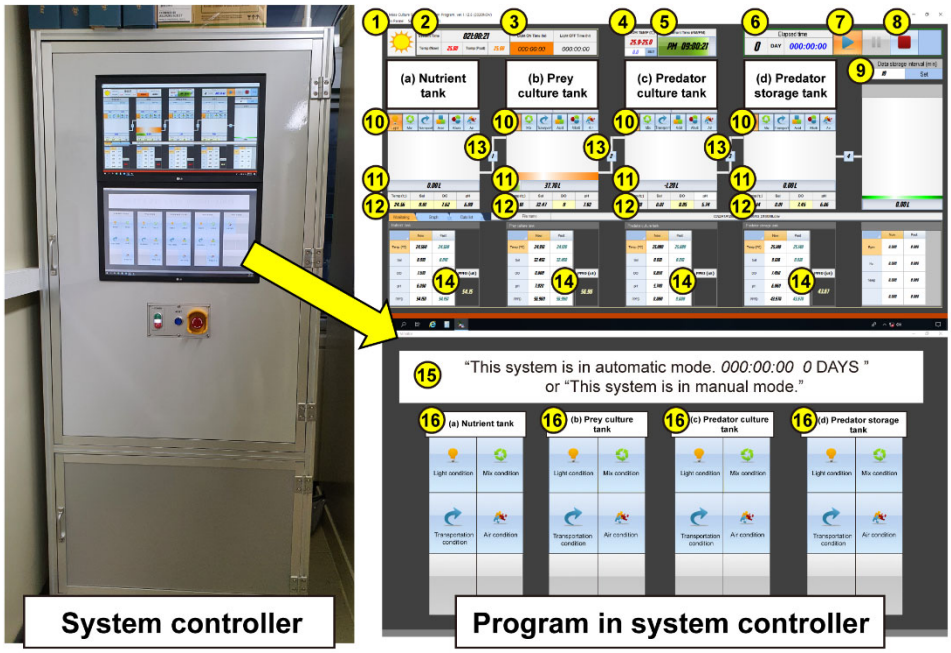

Figure 6.17. System controller and program for operating the automatic system for cultivating *Noctiluca scintillans* on a 100-L scale developed in this study. Explanation of functions of each part is provided in **Figure 6.3**.

6.3.7. Operation of the automatic system for cultivating *Noctiluca scintillans* on a 100-liter scale

Before the beginning of the operation, 50 L of F/2-Si medium was added to the nutrient tank, 90 L of *D. salina* culture (approximately 120,000 cells mL^{-1}) to the prey culture tank, and 30 L of *N. scintillans* culture (approximately 25 cells mL^{-1}) to the predator culture tank. When the automatic system of cultivating *N. scintillans* on a 100-L scale was operated in automatic mode, the hardware and software of the system controller worked as follows. A predetermined volume (20 L) of *D. salina* culture in the prey culture tank was transported to the predator culture tank. The prey culture tank was then refilled to capacity with nutrient medium in the nutrient tank. The prey culture tank was maintained at a constant volume (90 L). Subsequently, in the predator culture tank, the volume of the *N. scintillans* culture gradually increased with the addition of *D. salina* culture. Thus, when *N. scintillans* culture in the predator culture tank reached a predetermined volume (90 L), some of the volume (70 L) was transported to the predator storage tank. And then, 10 L of 0.2-μm filtered sea water was manually added to the remaining *N. scintillans* culture (20 L) in the predator culture tank. Thus, the *N. scintillans* culture in the predator culture tank became 30 L and was semi-continuously cultivated by repeating the above process using this automatic mass cultivation system. Seventy L of *N. scintillans* culture in the predator storage tank was maintained with adding 30 L of *D. salina* culture.

The transport of the nutrient medium, *D. salina* culture, and *N. scintillans* culture were conducted through two-stage pumping systems. All transportation was performed automatically at set times. In addition, *N. scintillans* and *D. salina* cultures were mixed for a set time (2 min) before being transported and continuously mixed during transport to the next tank using stirrers equipped with a low-speed motor at a predetermined speed (5 rpm).

Meanwhile, to suspend cells of *D. salina* in the prey culture tank, the culture was aerated with a predetermined air volume (9 L min^{-1}) for a set time (10 min) and at a set time interval (twice every day) using an air pump and a sparger; and mixed with a stirrer at a predetermined speed (5 rpm) for a set

time (10 min) and at a set time interval (twice every day). In addition, to prevent spatial separation of *D. salina* cells and *N. scintillans* cells by depth in the predator culture tank, the culture was aerated with a predetermined air volume (9 L min^{-1}) for a set time (10 min) and at a set time interval (twice every day) using an air pump and a sparger; and mixed with a stirrer at a predetermined speed (5 rpm) for a set time (10 min) and at a set time interval (once every 2 h).

Each tank was irradiated with predetermined light intensities, 20 μmol photons m^{-2} s^{-1} for *N. scintillans* and 300 μmol photons m^{-2} s^{-1} for *D. salina*, for a set duration (a 14 : 10 h Light-Dark cycle). The light intensities were measured using spectrometers and monitored and controlled by the program in real time.

In addition, the elapsed time in automatic mode, water quality of cultures in each tank (water temperature, salinity, pH, and DO), and liquid volumes of each tank were measured in real time.

6.3.8. Cultivating *Noctiluca scintillans* on a 100-liter scale using the automatic system

Among the tested dinoflagellates *Lingulodinium polyedra*, *Scrippsiella acuminata*, *Prorocentrum cordatum*, *Amphidinium carterae*, *Heterocapsa steinii*, *Alexandrium tamarense*, and *A. minutum* (previously *A. lusitanicum*), and the chlorophyte *D. salina* in screening tests using 6-well plates, *D. salina* was selected as the optimal prey to support the high growth of *N. scintillans*.

The light intensity supporting the high growth rate of *D. salina* was 300 μmol photons m^{-2} s^{-1} in a 14 : 10 h Light-Dark cycle, whereas that supporting the high growth rate of *N. scintillans* was 20 μmol photons m^{-2} s^{-1} in a 14 : 10 h Light-Dark cycle. LED lamps were used because they provided the target light intensity for a long time, and the heat from the LED lamp was lower than that from other light sources such as fluorescent lamps and halogen lamps.

To determine the volume of the F/2-Si medium transported from the nutrient tank to the prey culture tank, as well as the volume of prey culture transported from the prey culture tank to the predator culture tank, the growth rate of *D. salina* and the growth and ingestion rates of *N. scintillans* feeding on *D. salina* were measured in our preliminary test. The growth rate of *D. salina* in a stationary stage was 0.1–0.2 d^{-1} and the growth and ingestion rates of *N. scintillans* feeding on *D. salina* were 0.6 d^{-1} and 2,725 cells $predator^{-1}$ d^{-1}, respectively. Furthermore, when *N. scintillans* was manually cultivated with *D. salina*, *D. salina* cultures with an abundance of > 100,000 cells mL^{-1} were required to maintain the abundance of *N. scintillans* at 10–20 cells mL^{-1}. Thus, in this automatic system, the abundance of *D. salina* in the prey culture tank was maintained at > 100,000 cells mL^{-1}. At the beginning of the 6-day cultivation experiment, 20 L of 90 L *D. salina* culture (approximately 120,000 cells mL^{-1}) in the prey culture tank was transported to 30 L of *N. scintillans* culture (approximately 25 cells mL^{-1}) in the predator culture tank. Subsequently, 20 L of *D. salina* culture in the prey culture tank was transported to the predator culture tank every 2 d until *N. scintillans* culture in the predator culture tank became 90 L.

This cultivation experiment was repeated three times (periods 1–3). At the beginning of each period (day 0), the abundance of *D. salina* in the prey culture tank containing 90 L of prey culture was 111,500–122,333 cells mL^{-1} in periods 1–3 (**Figure 6.18**). Ten minutes later, 20 L of *D. salina* culture from the prey culture tank was automatically transported to the predator culture tank. Subsequently, 20 L of F/2-Si medium in the nutrient tank was added to the prey culture tank containing 70 L prey culture (on day 0.1); thus, the total volume of the prey culture became 90 L. Thus, due to dilution, the abundance of *D. salina* in the prey culture tank decreased to 86,660–96,500 cells mL^{-1} in periods 1–3. Two days later (day 2), *D. salina* in the prey culture tank grew, and its abundance was 113,660–126,330 cells mL^{-1} in periods 1–3. This process was repeated on days 2–4 and days 4–6.

At the beginning of each period (day 0), the abundance of *D. salina* in the predator culture tank containing 30 L predator culture was 100–170 cells mL^{-1} in periods 1–3 (**Figure 6.19**). Ten minutes later, 20 L of *D. salina* culture in the prey culture tank was automatically transported to the predator culture

tank (on day 0.1). The abundance of *D. salina* in the predator culture tank immediately after the prey culture was added was 44,000–47,800 cells mL^{-1} in periods 1–3. Most *D. salina* cells in the predator culture tank were eaten by *N. scintillans* cells 2 d later. On day 0, the abundance of *N. scintillans* in the predator culture tank containing 30 L predator culture was 25–33 cells mL^{-1} in periods 1–3 (**Figure 6.19**). After 20 L of *D. salina* culture was transported to the predator culture tank (on day 0.1), the abundance of *N. scintillans* in the predator culture tank immediately after the prey culture was added was 10–12 cells mL^{-1} in periods 1–3. Cells of *N. scintillans* grew well on *D. salina* and the abundance of *N. scintillans* was 16–26 cells mL^{-1} on day 2 in periods 1–3. This process was repeated on days 2–4 and days 4–6. The maximum abundance of *N. scintillans* in the predator culture tank was 45 cells mL^{-1} during periods 1–3.

The average and maximum growth rates of *N. scintillans* in periods 1–3 was 0.29–0.35 and 0.62–0.90 d^{-1}, respectively. The prey removal rate (%) by *N. scintillans* 2 d after prey cultures were added was 98–99% in periods 1–3 (**Figure 6.19D**).

Several single prey cells were observed inside the protoplasm of *N. scintillans* cells 1 h after the addition of prey cells, while packages of aggregated prey cells were observed 6 h later (**Figure 6.20**). Most *N. scintillans* cells contained single prey cells or packages of aggregated prey cells 48 h later. In addition, cells of *N. scintillas* fed on *D. salina* in the predator culture tank produced bright bioluminescence after mechanical stimulation (**Figure 6.21**).

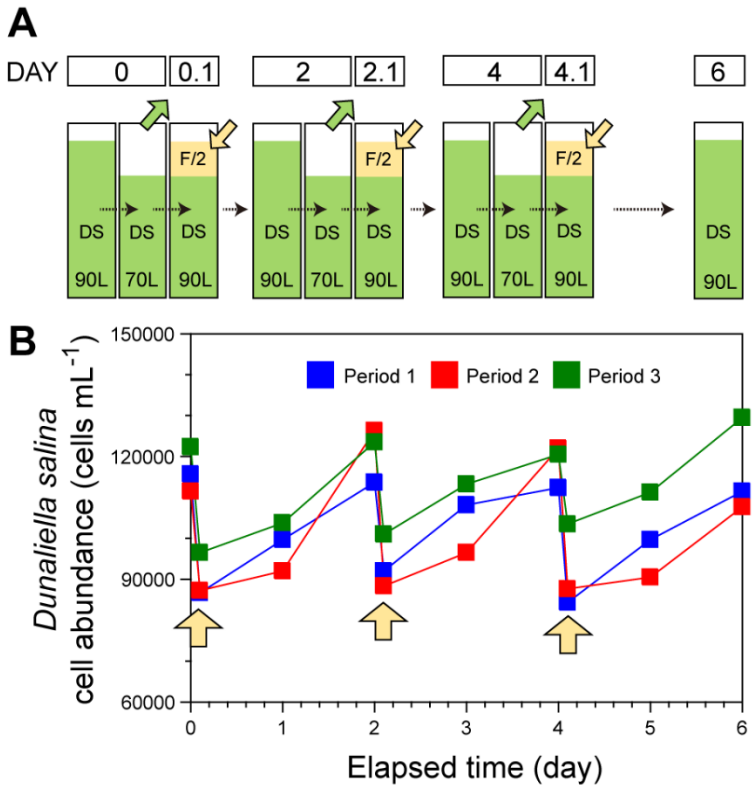

Figure 6.18. (A) Schematic diagram showing changes in water volume [*Dunaliella salina* (DS), F/2-Si (F/2) medium] in the prey culture tank. Green (DS) and yellow (F/2) arrows indicate inlet and outlet of water, respectively. (B) Changes in the abundance of DS (cells mL^{-1}) in the prey culture tank as a function of elapsed incubation time. The data on the abundance of DS were obtained by operating the system three times from day 0 to day 6. Blue, red, and green squares indicate periods 1, 2, and 3, respectively. Yellow arrows indicate the timing of F/2 medium input.

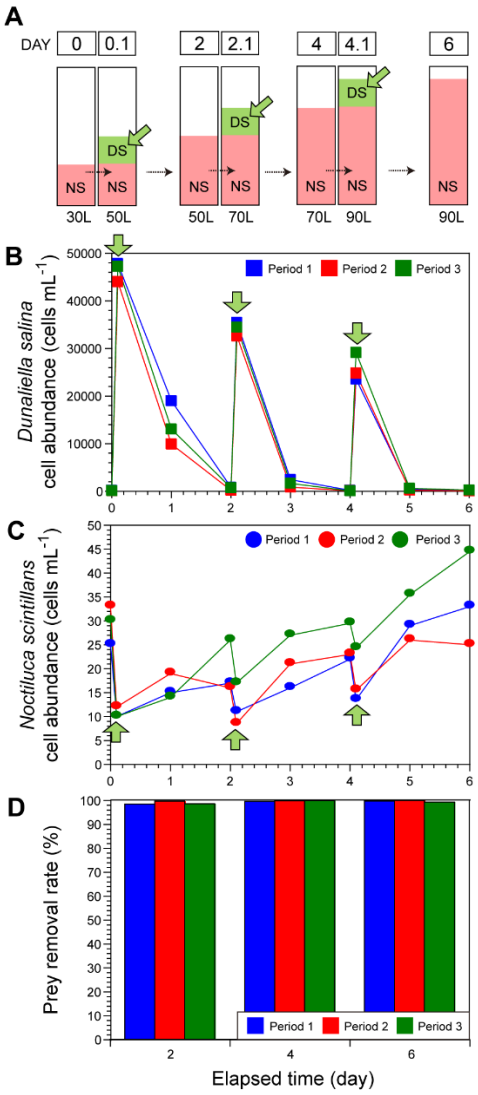

Figure 6.19. (A) Schematic diagram showing changes in water volume [*Dunaliella salina* (DS), *Noctiluca scintillans* (NS)] in the predator culture tank. Green (DS) arrows indicate input of prey culture. (B) Changes in the abundance of DS (cells mL^{-1}) in the predator culture tank as a function of elapsed incubation time. (C) Changes in the abundance of NS (cells mL^{-1}) in the predator culture tank as a function of elapsed incubation time. The data on the abundances of DS (B) and NS (C) were obtained by operating the system three times from day 0 to day 6. Blue, red, and green squares indicate periods 1, 2, and 3, respectively. Green arrows in (B) and (C) indicate the timing of DS culture input. (D) The prey removal rate (%) in periods 1 (blue bars), 2 (red bars), and 3 (green bars).

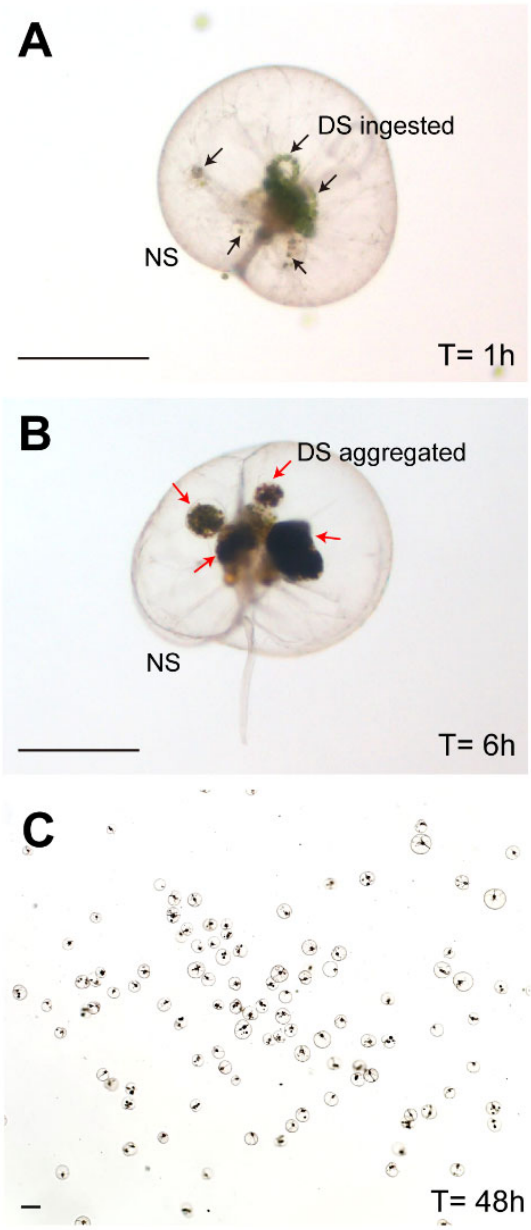

Figure 6.20. *Noctiluca scintillans* (NS) with ingested *Dunaliella salina* (DS) cells cultivated in the automatic system on a 100-L scale. (A) An NS cell with ingested single DS cells (black arrows) after 1 h of incubation. (B) An NS cell with packages containing aggregated prey cells (red arrows) after 6 h of incubation. (C) Many NS cells with ingested single DS cells or packages containing aggregated prey cells after 48 h incubation. Scale bars represent: 200 µm.

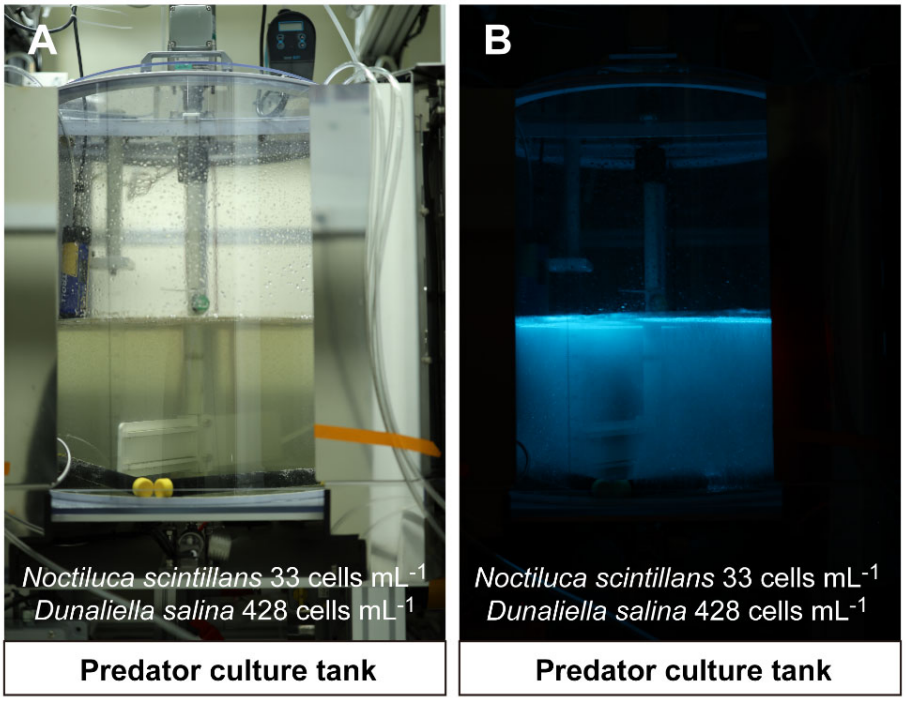

Figure 6.21. Photographs of the predator culture tank containing 90-L *Noctiluca scintillans* culture (abundance = 33 cells mL^{-1}) and some remaining *Dunaliella salina* cells (428 cells mL^{-1}) under the light (A) and dark (B) conditions. Aeration produced bright bioluminescence of *N. scintillans* in (B).

6.4. Discussions

6.4.1. Developed a semi-continuous system for cultivating the mixotrophic and heterotrophic dinoflagellates and cultivation of them using the system

In this study, a newly developed semi-continuous cultivation system could continuously produce dense *G. smaydae* cultures with high DHA and omega-3 contents and useful predators *B. cincta*, *G. dominans*, and *P. kofoidii* feeding on red tide species (**Table 6.3**).

Obtaining approximately 10 L of a pure microalgal culture is a critical step in omega-3 content, pigment, and transcriptome analyses. I successfully developed a 10-L culture system that could continuously produce heathy *G. smaydae*, *B. cincta*, *G. dominans*, and *P. kofoidii*. The system design allowed transferring a known volume of the prey culture from the prey vessel to the predator vessel, while adding the exact same volume of fresh medium to the prey culture vessel. Therefore, using this system, dense *G. smaydae B. cincta*, *G. dominans*, and *P. kofoidii* cultures could be harvested every 2 d, 2 d, 3 d, and 6 d. Based on the operation of culture systems producing 10 L of pure microalga cultures, scaled-up culture systems capable of producing larger culture volumes for commercial utilization can be developed.

Obtaining sufficient quantities of seed culture (20–25% of the final culture) for inoculation is critical step in the scaling up process (Rawat et al. 2013). This is the first study on semi-continuous cultivation of dinoflagellates using mixotrophy and an automatic system. Almost all previous studies on culturing dinoflagellates have focused on their autotrophic or heterotrophic growth (Jiang et al. 1999, Jiang and Chen 2000, Fuentes-Grunewald et al. 2016, Assuncao et al. 2017). The effects of nutrients, light, and salinity on the growth and contents of compounds of interest in autotrophic dinoflagellate cultures have been investigated suing phototrophic reactors (Camacho et al. 2007, Gallardo-Rodriguez et al. 2007, 2010, Benstein et al. 2014, Wang et al. 2015, Fuentes-Grunewald et al. 2016). An automatic system has already been developed for culturing the heterotrophic dinoflagellate *C. cohnii* (De Swaaf et al. 2003). The growth rates and biomass of mixotrophic dinoflagellates are

generally higher under mixotrophic conditions (i.e., with added prey) (Li et al. 1999, Jeong et al. 2015). *Karlodinium veneficum* and *Effrenium voratum* (previously *Symbiodinium voratum*) are known mixotrophic dinofalgellates, and their mixotrophic growth rates are considerably higher than their phototrophic growth rates (Li et al. 1999, Yoo et al. 2009, Jeong et al. 2012). Furthermore, the EPA content of *K. veneficum* fed with *Storeatula major* was greater than that of *K. veneficum* without added prey (Adolf et al. 2007). Thus, mixotrophy can be employed for higher production of biomass and biological materials by microalgae in comparison with autotrophy. Furthermore, mixotrophy may lower energy costs because dinoflagellates require lower light intensities for growth, as compared with when they are grown autotrophically (Li et al. 1999, Kim et al. 2008, Lim et al. 2019b). For culturing mixotrophic dinoflagellates, an arrangement for supplying prey is required to be added to a system for culturing autotrophic dinoflagellates. However, such as an addition would be beneficial because mixotrophy yields considerably higher growth rates and biomass of mixotrophic dinoflagellates.

6.4.2. Developed an automatic system for cultivating the mixotrophic and heterotrophic dinoflagellates on a 100-liter scale and cultivation of *Noctiluca scintillans* using the system

In the present study, the newly developed automatic system for cultivating useful *N. scintillans* could continuously produce 100 L of dense *N. scintillans* culture every 10 d (**Table 6.3**). Prior to the present study, there were no reports on the development of automatic systems for cultivating *N. scintillans*. Thus, the newly developed automatic system for cultivating *N. scintillans* will enable scientists to conduct diverse experiments that require large volumes of *N. scintillans*. I am currently conducting experiments to test whether the bioluminescence of *N. scintillans* in several 10-L tanks can be detected remotely using drones or aircraft. For these experiments, several hundred liters of pure *N. scintillans* culture were needed simultaneously, and the newly developed automatic system provides this.

In the present study, the highest abundance of cultivated *N. scintillans*

using the newly developed automatic system was 45 cells mL^{-1}. In general, the highest abundance of *N. scintillans* when manually cultivated was < 20 cells mL^{-1}. When the newly developed automatic system was used, 98–99% of prey cells in the predator culture tank were eliminated by *N. scintillans* after 2 d of incubation. Furthermore, the maximum growth rate of *N. scintillans* in the predator culture tank in periods 1–3 was 0.62–0.90 d^{-1}, which was similar or higher than that of *N. scintillans* when manually cultivated (Jeong 1995, Tada et al. 2004, Stauffer et al. 2017). Thus, supplying a designated amount of prey culture at a designated interval may help *N. scintillans* feed on prey cells effectively and support high maximum growth rates of *N. scintillans*. This newly developed automatic system for cultivating *N. scintillans* can significantly reduce labor costs, as only 1–2 people may be needed to produce several tons of *N. scintillans* culture.

Mixing cultures using air pumps and spargers for air supply and stirrers prevents predator cells from separating from the prey cells in the predator tank. However, strong mixing often causes high turbulence, which can inhibit the growth of dinoflagellates (Thomas and Gibson 1990a, b, Berdalet 1992). Therefore, the rates, durations, and time intervals of air supply or stirring at which cultures are well mixed without harming prey and predator cells should be standardized. The high growth rates of *N. scintillans* and *D. salina* in the predator culture tank indicates that the rates, durations, and time intervals of air supply using a sparger and a stirrer selected in this study were suitable and safe.

The light intensity illuminating the predator culture tank was selected to be 20 μmol photons m^{-2} s^{-1}, whereas that illuminating the prey culture tank was 300 μmol photons m^{-2} s^{-1}. High light intensity sometimes causes active swimming of prey cells; thus, it is critical to choose a light intensity at which prey cells survive, but swim slowly, and are easily eaten by predator cells. The light intensity of 20 μmol photons m^{-2} s^{-1} was ideal for the survival and weak swimming of *D. salina* and active ingestion by *N. scintillans*. A light intensity of 20 μmol photons m^{-2} s^{-1} was used in the experiments on feeding by other heterotrophic dinoflagellates, such as *G. dominans*, *Oxyrrhis marina*, *P. kofoidii*, and *Stoeckeria changwonensis* (Lee et al. 2014c, Lim et al. 2014, Jeong et al. 2018a, c, You et al. 2020a, Eom et al. 2021, Park et al. 2021a).

This 100-liter-scaled automatic system can be used as a unit, and several units can be combined to obtain a larger volume of *N. scintillans* cultures. Furthermore, a one-ten- or one-hundred-ton-scaled automatic system can be established based on this unit.

The newly developed automatic system for cultivating *N. scintillans* on a 100-L scale can be applied to cultivate other heterotrophic dinoflagellates or mixotrophic dinoflagellates. However, prey species supporting a high growth rate of a target heterotrophic or mixotrophic dinoflagellate should be selected. Furthermore, the growth rates of the optimal prey and also the target predator feeding on the prey should be determined. Based on the growth rates of the prey species and target dinoflagellate, the time interval and duration at which the valves between the nutrient tank and the prey culture tank, or between the prey culture tank and the predator culture tank open should be modified. Furthermore, suitable rates, durations, and time intervals of air supply using an air pump and a sparger, and those of mixing using a stirrer supporting the high growth of the predators in the predator culture tank should be chosen. Moreover, light intensities that support high growth of predators should be selected. The conditions for the target predator and its prey can be set up by changing the parameters in the program of the system controller in this study.

Table 6.3. The usefulness of the mixotrophic and heterotrophic dinoflagellates used in this study.

Species	Usefulness
Gymnodinium smaydae	● It was able to feed on species potentially forming red tides, such as the dinoflagellates *Heterocapsa* spp. and the *Scrippsiella acuminata*, and grew optimally with *Heterocapsa* spp. (Lee et al. 2014a). ● It was found to be rich in omega-3 fatty acids. Especially, the DHA content of *G. smaydae* on *H. rotundata* was 21 mg g^{-1} dry weight, accounting for 43% of the total fatty acid content (Lim et al. 2020).
Biecheleria cincta	● It was able to feed on species forming red tides, such as *Isochrysis galbana*, *Teleaulax* sp., *Rhodomonas salina*, *Heterosigma akashiwo*, *Eutreptiella gymnastica*, *H. rotundata*, and *Amphidinium carterae*, and grew optimally with *H. akashiwo* (Kang et al. 2011).
Gyrodinium dominans	● It fed on red tide species, such as *Prorocentrum* spp., *Alexandrium* spp., and *Scrippsiella* spp. (Kang et al. 2018, Kim et al. 2019, This study)
Polykrikos kofoidii	● It fed on *Prorocentrum* spp., *Alexandrium* spp., and *Scrippsiella* spp. potentially forming red tides (Kang et al. 2018, Kim et al. 2019, This study).
Noctiluca scintillans	● It fed on diverse prey, including phytoplankton, heterotrophic protists, and eggs of metazoans. ● It is a heterotrophic dinoflagellate that causes red-colored oceans during the day (red tides) and glowing oceans at night (bioluminescence).

Chapter 7. Overall conclusions

Investigating the growth and distribution of mixotrophic dinoflagellates is an important step to better understand and conserve marine ecosystems. Furthermore, mixotrophic and heterotrophic dinoflagellates have the ability to produce useful substances and control red tide species. However, they have not yet been extensively studied or commercially utilized due to difficulties in large-scale cultivation. This thesis revealed the ecological and physiological characteristics of mixotrophic dinoflagellates and developed an automatic cultivation system for them using their ecophysiological characteristics.

To understand the distribution mechanism of mixotrophic dinoflagellates, Chapters 2–5 explained effects of warming, prey, and predators on the distributions of the mixotrophic dinoflagellates *Biecheleria cincta* and *Gymnodinium smaydae*, as well as phototrophic dinoflagellates *Scrippsiella* spp. Among approximately 1,200 phototrophic dinoflagellates, 10 species have been investigated for their mixotrophic growth rates as a function of water temperature. Of the 10 species, *G. smaydae* and *B. cincta* were the sixth and tenth, respectively. Among the 370 genera of dinoflagellates, 4 genera have been explored for mixotrophic abilities at the genus level. Of the 4 genera, the genus *Scrippsiella* was the fourth.

The mixotrophic dinoflagellate *B. cincta* was mainly present in summer and autumn in Korean coastal waters. Furthermore, the presence and distribution of *B. cincta* were predicted to decrease in summer and autumn when the water temperature increased by up to 6℃ in Korean waters. In laboratory experiments, *B. cincta* grew with the prey *Heterosigma akashiwo* at 15–25℃, but did not grow without prey at all tested water temperatures. Thus, the combined effects of the water temperature and prey *H. akashiwo* on the growth rates of *B. cincta* could explain the current presence of *B. cincta* in Korean coastal waters and the predicted distribution change when the water temperature increases by up to 6℃. The impact of predators on the growth rate of *B. cincta* was investigated in a previous study and thus was not investigated in this thesis. *B. cincta* is known to be eaten by common

heterotrophic protists *Gyrodinium* spp., *Oxyrrhis marina*, *Polykrikos kofoidii*, and *Strobilidium* sp. and result in high growth rates of the ciliate *Strobilidium* sp. and the dinoflagellate *O. marina* (Yoo et al. 2013).Therefore, the narrow distribution of *B. cincta* in Korean coastal waters could be explained not only by high mortality rates caused by predators but also by the preference of *B. cincta* for the water temperatures of summer and autumn (**Table 7.1**).

Another mixotrophic dinoflagellate *G. smaydae* showed a wide spatial distribution in spring, summer, and autumn in Korean coastal waters. Its presence was predicted to decrease only in summer if the water temperature increased by approximately 6℃. In laboratory experiments, *G. smaydae* grew with the prey *Heterocapsa rotundata* at 10–32℃ but did not grow without prey at all tested water temperatures. Thus, the distribution of *G. smaydae* may be altered by the combied effects of the water temperature and prey *H. rotundata*. The combined effects can explain the presence of *G. smaydae* in Korean coastal waters and the predicted distribution change during the summer when the water temperature rises by up to 6℃. Meanwhile, *G. smaydae* was eaten by common heterotrophic protists *O. marina*, *Gyrodinium* spp., and *Pelagostrobilidium* sp. *G. smaydae* resulted in positive growth rates of heterotrophic dinoflagellates *O. marina* and *G. dominans* but a negative growth rate of the ciliate *Pelagostrobilidium* sp. However, the growth rates of *O. marina* and *G. dominans* feeding on *G. smaydae* were lower than those feeding on other prey species, as inferred from a literature survey. Thus, *G. smaydae* may not be the preferred prey for supporting the high growth of predators. Therefore, the wide distribution of *G. smaydae* in Korean coastal waters could be explained not only by low mortality rates owing to predators but also by the wide temperature range for its growth or survival (**Table 7.2**).

Two mixotrophic dinoflagellates, *B. cincta* and *G. smaydae*, showed different distributions in Korean coastal waters, although they had similar cell size and showed the global distribution patterns (**Figure 7.1**, Vaulot et al. 2022). In Korean waters, *B. cincta* was detected in fewer stations (13 stations) than *G. smaydae* (24 stations). *B. cincta* feeds on various prey species belonging to diverse classes but has a lower growth rate in the presence of optimal prey than *G. smaydae*. *B. cincta* grew mixotrophically at a narrow temperature range of 15–25℃. Additionally, *B. cincta* supported the high

growth rates of diverse protozoan predators feeding on it. However, *G. smaydae* feeds on thecate-prey species belonging to only one class but has higher growth rates on the prey than *B. cincta*. *G. smaydae* grew mixotrophically at a wide temperature range of 10–32℃. *G. smaydae* also supported the low growth rates of its protozoan predators. Therefore, the population of *B. cincta* is expected to rapidly decline, even with temporary increases in Korean coastal waters, because of its low growth rates and high mortality rates owing to predation. In contrast, *G. smaydae* may maintain an increased population longer in Korean coastal waters because of its high growth rates and low mortality rates owing to predation. In addition, *B. cincta* grew at a relatively narrow temperature range but *G. smaydae* grew at a wide temperature range. These can partially explain the relatively narrow distribution of *B. cincta* compared with that of *G. smaydae* along the Korean coast. However, because they are mixotrophic species, their growth rates may also be affected by other factors, such as the light intensity and nutrients. Therefore, research on these factors on growth of *B. cincta* and *G. smaydae* is required to explain the reasons for their different distributions.

Table 7.1. Overall ecophysiological characteristics of *Biecheleria cincta* in Chapters 2–3.

	Explanation
Temperature	● The positive mixotrophic growth rates occurred at 15–25℃. ● Optimal temperatures for growth with and without prey were 25 and 15℃, although all growth rates without prey were negative. ● It may not survive in the West and South Seas in summer and autumn if the water temperature was increased.
Prey	● It fed on diverse algal prey species in equivalent spherical diameter < 12.6 μm, except for diatom (Kang et al. 2011). ● The maximum growth rates of *B. cincta* WCSH0906 with and without the optimal prey *Heterosigma akashiwo* were 0.50 and 0.04 d^{-1}, respectively (Kang et al. 2011). ● As a function of water temperature, the maximum growth rates of *B. cincta* BCSH1005 with and without the prey *H. akashiwo* were 0.26 and -0.09 d^{-1}, respectively.
Predator	● It had diverse heterotrophic protistan predators, such as *Gyrodinium* spp., *Oxyrrhis marina*, and *Polykrikos kofoidii*, and the ciliate *Strobilidium* sp. (Yoo et al. 2013). ● It supported high growth rates of the ciliate *Strobilidium* sp. and the dinoflagellate *O. marina* but low growth rate of the dinoflagellate *Gyrodinium dominans* (Yoo et al. 2013).
Distribution	● It was detected at 13 stations among 27 stations in Korean coastal waters. ● It was found throughout all four seasons: 3 stations in spring, 8 stations in summer, 5 stations in autumn, and one station in winter in Korean coastal waters. ● Its distribution was predicted to decrease in summer and autumn under ocean warming conditions.

Table 7.2. Overall ecophysiological characteristics of *Gymnodinium smaydae* in Chapters 2–4.

	Explanation
Temperature	● The positive mixotrophic growth occurred at 10–32℃. ● Optimal temperatures for growth with and without prey were 25 and 20℃, although all growth rates without prey were negative. ● It may not survive in the West and South Seas in summer if the water temperature was increased.
Prey	● It fed on only thecate dinoflagellates *Heterocapsa* spp. and *Scrippsiella acuminata* (Lee et al. 2014a). ● The maximum growth rate of *G. smaydae* with the optimal prey *H. rotundata* was 2.23 d^{-1} (Lee et al. 2014a). ● As a function of water temperature, the maximum growth rates of *G. smaydae* with and without the prey *H. rotundata* were 1.55 and -0.05 d^{-1}, respectively.
Predator	● It had some heterotrophic protistan predators, such as *Gyrodinium* spp. and *Oxyrrhis marina*, and the ciliate *Pelagostrobilidium* sp. (Jeong and You et al. 2018). ● It supported positive growth rates of the dinoflagellates *O. marina* and *G. dominans* but negative growth rate of the ciliate *Pelagostrobilidium* sp. (Jeong and You et al. 2018). ● It may not be the preferred prey for supporting high growth of predators.
Distribution	● It was detected at 24 stations among 27 stations in Korean coastal waters (Lee and You et al. 2020). ● It was found throughout all four seasons: 10 stations in spring, 21 stations in summer, 10 stations in autumn, and one station in winter in Korean coastal waters. ● Its distribution was predicted to decrease in summer under ocean warming conditions (+4 and +6℃).

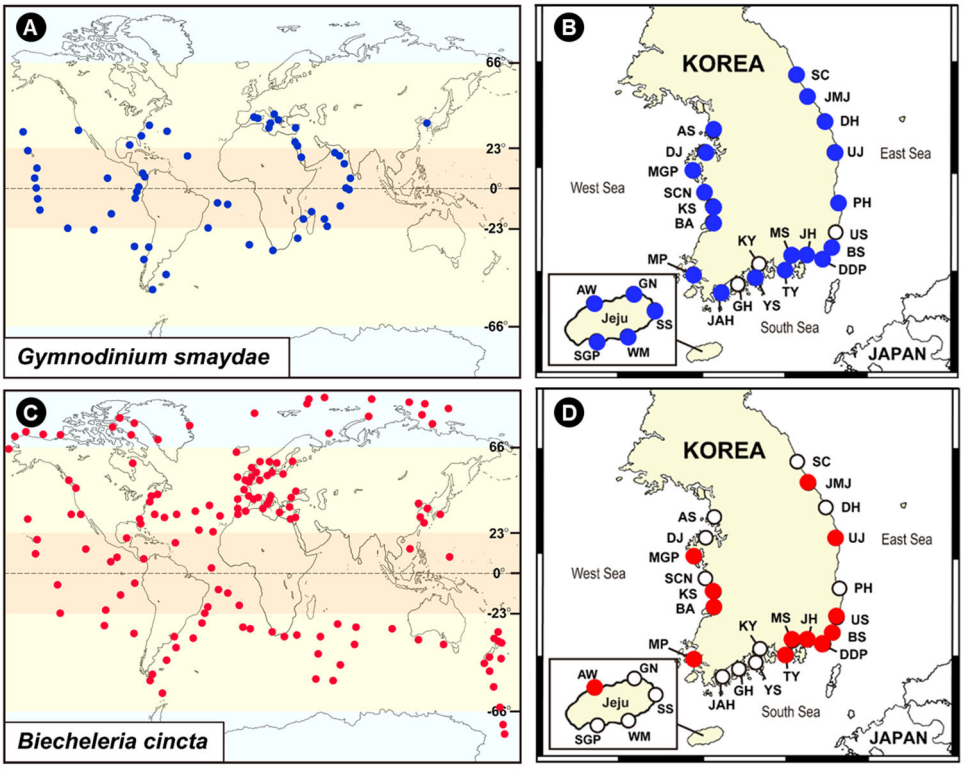

Figure 7.1. Global distributions and distributions in Korean coastal waters of mixotrophic dinoflagellates *Gymnodinium smaydae* (A, B) and *Biecheleria cincta* (C, D). Data on global distributions were obtained using a method of DNA metabarcoding from metaPR2 (Vaulot et al. 2022) and data on distributions in Korean coastal waters from this study.

Among the six *Scrippsiella* species (i.e., *S. acuminata*, *S. donghaiensis*, *S. lachrymosa*, *S. masanensis*, *S. plana*, and *S. ramonii*), *S. donghaiensis* and *S. lachrymosa* showed seasonal distributions along the Korean coast through their field observations, suggesting that water temperature might influence their distribution (Kim 2019, Lee et al. 2019c). However, *S. masanensis* did not show seasonality in Korean waters through its field observation, suggesting that other environmental factors might affect its distribution (Kim 2019). *S. acuminata* has a broad global distribution and is known as euryhaline and eurythermal species (Braarud 1951, Tian et al. 2021). In Chapter 5, the impact of potential prey species on the growth of five *Scrippsiella* species was investigated; however, the prey species did not affect their growth or survival due to their lacking mixotrophic ability. However, the prey spectrum of *S. acuminata* was expanded. Thus, the growth and survival of *S. acuminata* will be affected by prey availability. Moreover, Kim et al. (2019) investigated the mortality of *Scrippsiella* spp. owing to predators, and found that each *Scrippsiella* species affected the growth rate of its predators differently. Therefore, the effect of warming, prey, and predators on *Scrippsiella* spp. can partially explain the different global and local distributions of these species (**Table 7.3**). However, to accurately describe the distributions of the six *Scrippsiella* species, the growth rate of each species as fuctions of nutrient concentrations, light, and water temperature should be investigated in a laboratory. Currently, most studies focus on the growth rate of *S. acuminata*.

Automatic methods and systems for cultivating the mixotrophic dinoflagellates *G. smaydae* and *B. cincta*, as well as heterotrophic dinoflagellates *P. kofoidii*, *G. dominans*, and *N. scintillans* were discussed in Chapter 6, all of which could enrich human life. Mixotrophic and heterotrophic dinoflagellates are known to produce useful materials, such as omega-3, pigment, toxins, and bioluminescence, and have a higher grazing impact than metazooplankton, allowing them to control the population dynamics of red tide-forming phytoplankton. However, the mass cultivation of these organisms is difficult, limiting their research and commercial use. Therefore, to utilize them for research or commercial purposes, an automated mass cultivation system was developed in Chapter 6. Additionally, the methods of cultivating the mixotrophic and heterotrophic dinoflagellates

were investigated, as presented in **Table 7.4**. Automatically mass-cultivated cultures of mixotrophic or heterotrophic dinoflagellates can be used for various experiments. Notably, whether the bioluminescence of the heterotrophic dinoflagellate *N. scintillans* can be remotely detected using drones was investigated. This experiment required a large volume of *N. scintillnas* cultures produced under identical conditions, which was made possible by the developed automatic system.

In this doctoral thesis, I explored the effects of warming (i.e., a physical factor) as well as prey and predators (i.e., biological factors) on the distributions of marine mixotrophic dinoflagellates. Furthermore, I developed new automatic cultivation system for mixotrophic and heterotrophic dinoflagellates. Thus, this thesis contributes to an enhanced understanding of the distributions of mixotrophic dinoflagellates, which in turn provides a deeper understanding of the structure and function of marine ecosystems. Moreover, this thesis makes an academic contribution to the scientific community by enabling diverse experiments that require large volumes of dinoflagellate cultures in the future.

Table 7.3. Overall ecophysiological characteristics of *Scrippsiella* spp. in Chapter 5.

	Explanation
Temperature and distribution	● *Scrippsiella lachrymosa*, *S. donghaiensis*, and *S. masanensis* may prefer water temperatures in spring, summer, and autumn to early winter, respectively (Kim 2019). ● *S. acuminata* is an eurythermal species (Braarud 1951, Tian et al. 2021) and has sometimes cuased red tides globally.
Prey	● *Scrippsiella donghaiensis*, *S. lachrymosa*, *S. plana*, *S. masanensis*, and *S. ramonii* lacked the mixotrophic ability when common prey items were added. ● Mixotrophic *S. acuminata* was discovered to feed on heterotrophic bacteria and beads (diameter= 2 μm), as well as the cyanobacterium and algal prey species in ESD ≤ 12. 1 μm (Jeong et al. 2005a, b; this study).
Predator	● *Scrippsiella acuminata*, *S. donghaiensis*, *S. lachrymosa*, and *S. masanensis* had diverse heterotrophic protistan predators, such as *Pfiesteria piscicida*, *Gyrodinium* dominans, *Oxyrrhis marina*, *Oblea rotunda*, and *Polykrikos kofoidii*, and the ciliate *Strombidinopsis* sp. (Kim et al. 2019). ● The growth rates of *G. dominans* and *P. kofoidii* were different when they fed on the four *Scrippsiella* species, *S. acuminata*, *S. donghaiensis*, *S. lachrymosa*, and *S. masanensis*, respectively (Kim et al. 2019).

Table 7.4. The automatic cultivation methods of the mixotrophic and heterotrophic dinoflagellates using developed cultivation systems in Chapter 6 of this thesis.

Species	Automatic cultivation method
Gymnodinium smaydae	● Optimal prey: *Heterocapsa rotundata* ● Optimal temperature: 25℃ ● Optimal light intensity: 50 μmol photons m^{-2} s^{-1} ● Prey addition interval: Daily ● Prey addition amount: 3 L (60,000 cells mL^{-1}) of prey to 3–6 L (40,000–50,000 cells mL^{-1}) of *G. smaydae*
Biecheleria cincta	● Optimal prey: *Heterosigma akashiwo* ● Optimal temperature: 20℃ ● Optimal light intensity: 20 μmol photons m^{-2} s^{-1} ● Prey addition interval: Two days ● Prey addition amount: 4.5 L (10,000–20,000 cells mL^{-1}) of prey to 4.5 L (2,000–5,000 cells mL^{-1}) of *B. cincta*
Gyrodinium dominans	● Optimal prey: *Amphidinium carterae* ● Optimal temperature: 20℃ ● Optimal light intensity: 20 μmol photons m^{-2} s^{-1} ● Prey addition interval: Daily ● Prey addition amount: 2 L (20,000–60,000 cells mL^{-1}) of prey to 2–6 L (5,000–15,000 cells

	mL^{-1}) of *G. dominans*
Polykrikos kofoidii	● Optimal prey: *Alexandrium minutum* CCMP1888 ● Optimal temperature: 20℃ ● Optimal light intensity: 20 μmol photons m^{-2} s^{-1} ● Prey addition interval: Three days ● Prey addition amount: 3 L (6,000–8,000 cells mL^{-1}) of prey to 2–6 L (200–600 cells mL^{-1}) of *P. kofoidii*
Noctiluca scintillans	● Optimal prey: *Dunaliella salina* ● Optimal temperature: 20℃ ● Optimal light intensity: 10–20 μmol photons m^{-2} s^{-1} ● Prey addition interval: Two days ● Prey addition amount: 20 L (40,000–50,000 cells mL^{-1}) of prey to 30–70 L (10–35 cells mL^{-1}) of *N. scintillans*

Bibliography

Adolf, J. E., Place, A. R., Stoecker, D. K. & Harding, L. W. Jr. 2007. Modulation of polyunsaturated fatty acids in mixotrophic *Karlodinium veneficum* (Dinophyceae) and its prey, Storeatula major (Cryptophyceae). J. Phycol., 43:1259–1270.

Adolf, J. E., Stoecker, D. K. & Harding, L. W. Jr. 2006. The balance of autotrophy and heterotrophy during mixotrophic growth of *Karlodinium micrum* (Dinophyceae). J. Plankton Res. 28:737–751.

Allen, J. R., Roberts, T. M., Loeblich, III A. R. & Klotz, L. C. 1975. Characterization of the DNA from the dinoflagellate *Crypthecodinium cohnii* and implications for nuclear organization. Cell, 6:161–169

Assunção, J., Guedes, A. C. & Malcata, F. X. 2017. Biotechnological and pharmacological applications of biotoxins and other bioactive molecules from dinoflagellates. Mar. Drugs, 15:393.

Baek, S. H., Shimode, S. & Kikuchi, T. 2008 Growth of dinoflagellates, *Ceratium furca* and *Ceratium fusus* in Sagami Bay, Japan: the role of temperature, light intensity and photoperiod. Harmful Algae, 7:163–173.

Balech, E. 1959. Two new genera of dinoflagellates from California. Biol. Bull. 116:195–203.

Balzano, S., Gourvil, P., Siano, R., Chanoine, M., Marie, D., Lessard, S., Sarno, D., Vaulot, D. 2012 Diversity of cultured photosynthetic flagellates in the northeast Pacific and Arctic Oceans in summer. Biogeosciences, 9:4553–4571.

Band-Schmidt, C. J., Morquecho, L., Lechuga-Devéze, C. H. & Anderson, D. M. 2004. Effects of growth medium, temperature, salinity and seawater source on the growth of *Gymnodinium catenatum* (Dinophyceae) from Bahía Concepción, Gulf of California, Mexico. J. Plankton Res., 26:1459–1470.

Benstein, R. M., Çebi, Z., Podola, B. & Melkonian, M. 2014. Immobilized growth of the peridinin-producing marine dinoflagellate *Symbiodinium* in a simple biofilm photobioreactor. Mar. Biotechnol., 16:621–628.

Berdalet, E. 1992. Effects of turbulence on the marine dinoflagellate *Gymnodinium nelsonii*. J. Phycol., 28:267–272.

Berge, T. & Hansen, P. J. 2016. Role of the chloroplasts in the predatory dinoflagellate *Karlodinium armiger*. Mar. Ecol. Prog. Ser., 549:41–54.

Berge, T., Hansen, P. J. & Moestrup, Ø. 2008. Prey size spectrum and bioenergetics of the mixotrophic dinoflagellate *Karlodinium armiger*. Aquat. Microb. Ecol. 50:289–299.

Berthold, D. E., de la Rosa, N., Engene, N., Jayachandran, K., Gantar, M., Laughinghouse, H. D. & Shetty, K. G. 2020. Omega-7 producing alkaliphilic diatom *Fistulifera* sp. (Bacillariophyceae) from Lake Okeechobee, Florida. Algae, 35:91–106.

Bhattacharya, D., Yoon, H. S. & Hackett, J. D. 2004. Photosynthetic eukaryotes unite: endosymbiosis connects the dots. Bioessays 26:50–60.

Bityukov, E. P. 1971. Bioluminescence in the wake current in the Atlantic Ocean and Mediterranean Sea. Okean, 11:127–133.

Blasco, D. 1978. Observations on the diel migration of marine dinoflagellates off the Baja California coast. Mar. Biol., 46:41–47.

Blossom, H. E., Bædkel, T. D., Tillmann, U. & Hansen, P. J. 2017. A search for mixotrophy and mucus trap production in *Alexandrium* spp. and the dynamics of mucus trap formation in *Alexandrium pseudogonyaulax*. Harmful Algae, 64:51–62.

Blossom, H. E., Daugbjerg, N. & Hansen, P. J. 2012. Toxic muspecies *Temcus traps*: a novel mechanism that mediates prey uptake in the mixotrophic dinoflagellate *Alexandrium pseudogonyaulax*. Harmful Algae, 17:40–53.

Bockstahler, K. R. & Coats, D. W. 1993. Grazing of the mixotrophic dinoflagellate *Gymnodinium sanguineum* on ciliate populations of Chesapeake Bay. Mar. Biol., 116:477–487.

Box, G. E. 1949. A general distribution theory for a class of likelihood criteria. Biometrika, 36: 317–346.

Brierley, A. S. & Kingsford, M. J. 2009. Impacts of climate change on marine organisms and ecosystems. Curr. Biol., 19:R602–R614.

Burkert, U., Hyenstrand, P., Drakare, S. & Blomqvist, P. 2001. Effects of the mixotrophic flagellate *Ochromonas* sp. on colony formation in *Microcystis aeruginosa*. Aquat. Ecol., 35:11–17.

Burkholder, J. M. & Glasgow, H. B. 1997. *Pfiesteria piscicida* and other *Pfiesreria*-like dinoflagellates: Behavior, impacts, and environmental controls. Limnol. Oceanogr., 42:1052–75.

Burkholder, J. M., Glasgow, H. B. Jr. & Hobbs, C. W. 1995. Fish kills linked to a toxic ambush-predator dinoflagellate: distribution and environmental conditions. Mar. Ecol. Prog. Ser., 124:43–61.

Burkholder, J. M., Glibert, P. M. & Skelton, H. M. 2008. Mixotrophy, a major mode of nutrition for harmful algal species in eutrophic waters. Harmful Algae, 8:77–93.

Buskey, E. J. 1995. Growth and bioluminescence of *Noctiluca scintillans* on varying algal diets. J. Plankton Res., 17:29–40.

Buskey, E. J., Strom, S. & Coulter, C. 1992. Biolumiscence of heterotrophic dinoflagellates from Texas coastal waters. J. Exp. Mar. Biol. Ecol., 159:37–49.

Camacho, F. G., Rodríguez, J. G., Mirón, A. S., García, M. C. C., Belarbi, E. H., Chisti, Y. & Grima, E. M. 2007. Biotechnological significance of toxic marine dinoflagellates. Biotechnol. Adv., 25:176–194.

Carlos, A. A., Baillie, B. K., Maruyama, T. 2000. Diversity of dinoflagellate symbionts (zooxanthellae) in a host individual. Mar. Ecol. Prog. Ser., 195:93–100.

Caron, D. A. 2016. Mixotrophy stirs up our understanding of marine food webs. Proc. Natl. Acad. Sci. U. S. A. 113:2806–2808.

Caron, D. A., Davis, P. G., Madin, L. P. & Sieburth, J. M. 1982. Heterotrophic bacteria and bacterivorous protozoa in oceanic macroaggregates. Science, 218:795–797.

Calbet, A., Isari, S., Martínez, R. A., Saiz, E., Garrido, S., Peters, J., Borrat, R. M. & Alcaraz, M. 2013. Adaptations to feast and famine in different strains of the marine heterotrophic dinoflagellates *Gyrodinium dominans* and *Oxyrrhis marina*. Mar. Ecol. Prog. Ser., 483:67–84.

Campbell, L., Olson, R. J., Sosik, H. M., Abraham, A., Henrichs, D. W., Hyatt, C. J. & Buskey, E. J. 2010. First harmful *Dinophysis* (Dinophyceae, Dinophysiales) bloom in the US is revealed by automated imaging flow cytometry. J. Phycol., 46:66–75.

Cheirsilp, B. & Torpee, S. 2012. Enhanced growth and lipid production of microalgae under mixotrophic culture condition: effect of light

intensity, glucose concentration and fed-batch cultivation. Bioresour. Technol., 110:510–516.

Chua, E. T. & Schenk, P. M. 2017. A biorefinery for Nannochloropsis induction, harvesting, and extraction of EPArich oil and high-value protein. Bioresour. Technol., 244:1416–1424.

Claessens, M., Wickham, S. A., Post, A. F. & Reuter, M. 2008. Ciliate community in the oligotrophic Gulf of Aqaba, Red Sea. Aquat. Microb. Ecol., 53:181–190.

Coats, D. W. 1999. Parasitic life styles of marine dinoflagellates. J. Eukaryot. Microbiol., 46:402–409.

Coats, D. W., Choi, J., Jung, J. H., Kim, Y. O., Lu, Y. & Nielsen, L. T. 2020. Mixotrophic scrippsielloid dinoflagellates prey on tintinnid ciliates. Aquat. Ecosyst. Health Manag., 23:69–78.

Cox, P. M., Betts, R. A., Jones, C. D., Spall, S. A. & Totterdell, I. J. 2000. Acceleration of global warming due to carbon-cycle feedbacks in a coupled climate model. Nature, 408:184–187.

Coyne, K. J., Salvitti, L. R., Mangum, A. M., Ozbay, G., Main, C. R., Kouhanestani, Z. M. & Warner, M. E. 2021. Interactive effects of light, CO_2 and temperature on growth and resource partitioning by the mixotrophic dinoflagellate, *Karlodinium veneficum*. PloS one, 16:e0259161.

Cuellar-Bermudez, S. P., Aguilar-Hernandez, I., Cardenas-Chavez, D. L., Ornelas-Soto, N., Romero-Ogawa, M. A. & Parra-Saldivar, R. 2015. Extraction and purification of high-value metabolites from microalgae: essential lipids, astaxanthin and phycobiliproteins. Microb. Biotechnol., 8:190–209.

Daugbjerg, N., Hansen, G., Larsen, J. & Moestrup, Ø. 2000. Phylogeny of some of the major genera of dinoflagellates based on ultrastructure and partial LSU rDNA sequence data, including the erection of three new genera of unarmoured dinoflagellates. Phycologia, 39:302–317.

Davy, S. K., Allemand, D. & Weis, V. M. 2012. Cell biology of cnidarian-dinoflagellate symbiosis. Microbiol. Mol. Biol. Rev., 76:229–261.

De Swaaf, M. E., Sijtsma, L. & Pronk, J. T. 2003. High-celldensity fed-batch cultivation of the docosahexaenoic acid producing marine alga *Crypthecodinium cohnii*. Biotechnol. Bioeng., 81:666–672.

Dhanya, B. S., Sowmiya, G., Jeslin, J., Chamundeeswari, M. & Verma, M. L. 2020. Algal biotechnology: a sustainable route for omega-3 fatty acid production. In Alam M. A., Xu, J. -L. & Wang, Z. (Eds.) Microalgae Biotechnology for Food, Health and High Value Products. Springer, Singapore, pp. 125–145.

Ding, Y., Ren, G., Zhao, Z., Xu, Y., Luo, Y., Li, Q. & Zhang, J. 2007. Detection, causes and projection of climate change over China: an overview of recent progress. Adv. Atmos. Sci., 24:954–971.

Dodge, J. D. & Priddle, J. 1987. Species composition and ecology of dinoflagellates from the Southern Ocean near South Georgia. J. Plankton Res. 9:685–697.

Doughman, S. D., Krupanidhi, S. & Sanjeevi, C. B. 2007. Omega-3 fatty acids for nutrition and medicine: considering microalgae oil as a vegetarian source of EPA and DHA. Curr. Diabetes Rev., 3:198–203.

Dunn, O. J. 1961. Multiple comparisons among means. J. Am. Stat. Assoc., 56:52–64.

Dunstan, G. A., Volkman, J. K., Jeffrey, S. W. & Barrett, S. M. 1992. Biochemical composition of microalgae from the green algal classes Chlorophyceae and Prasinophyceae. 2. Lipid classes and fatty acids. J. Exp. Mar. Biol. Ecol., 161:115–134.

Eom, S. H., Jeong, H. J., Ok, J. H., Park, S. A., Kang, H. C., You, J. H., Lee, S. Y., Yoo, Y. D., Lim, A. S. & Lee, M. J. 2021. Interactions between common heterotrophic protists and the dinoflagellate *Tripos furca*: implication on the long duration of its red tides in the South Sea of Korea in 2020. Algae, 36:25–36.

Esteban, G. F., Fenchel, T. & Finlay, B. J. 2010. Mixotrophy in ciliates. Protist 161:621–641.

Ethier, S., Woisard, K., Vaughan, D. & Wen, Z. 2011. Continuous culture of the microalgae *Schizochytrium limacinum* on biodiesel-derived crude glycerol for producing docosahexaenoic acid. Bioresour. Technol., 102:88–93.

Fagan, T., Hastings, J. W. & Morse, D. 1998. The phylogeny of glyceraldehyde-3-phosphate dehydrogenase indicates lateral gene transfer from cryptomonads to dinoflagellates. J. Mol. Evol., 47:633–639.

Fajardo, A. R., Cerdán, L. E., Medina, A. R., Fernández, F. G. A., Moreno, P. A. G. & Grima, E. M. 2007. Lipid extraction from the microalga *Phaeodactylum tricornutum*. Eur. J. Lipid Sci. Technol., 109:120–126.

Fan, K. W., Jiang, Y., Faan, Y. -W. & Chen, F. 2007. Lipid characterization of mangrove thraustochytrid-*Schizochytrium mangrovei*. J. Agric. Food Chem., 55:2906–2910.

Flewelling, L. J., Naar, J. P., Abbott, J. P., Baden, D. G., Barros, N. B., Bossart, G. D., Bottein, M.-Y. D., Hammond, D. G., Haubold, E. M., Heil, C. A., Henry, M. S., Jacocks, H. M., Leighfield, T. A., Pierce, R. H., Pitchford, T. D., Rommel, S. A., Scott, P. S., Steidinger, K. A., Truby, E. W., Van Dolah, F. M. & Landsberg, J. H. 2005. Red tides and marine mammal mortalities. Nature, 435:755–756.

Flynn, K. J., Mitra, A., Anestis, K., Anschütz, A. A., Calbet, A., Ferreira, G. D., Gypens, N., Hansen, P. J., John, U., Martin, J. L., Mansour, J. S., Maselli, M., Medić, N., Norlin, A., Not, F., Pitta, P., Romano, F., Saiz, E., Schneider, L. K., Stolte, W. & Traboni, C. 2019. Mixotrophic protists and a new paradigm for marine ecology: where does plankton research go now? J. Plankton Res., 41:375–391.

Flynn, K. J., Mitra, A., Glibert, P. M. & Burkholder, J. M. 2018. Mixotrophy in harmful algal blooms: by whom, on whom, when, why, and what next. *In* Gilbert, P. M., Berdalet, E., Burford, M. A., Picher, G. C. & Zhou, M. (Eds.) Global Ecology and Oceanography of Harmful Algal Blooms. Springer, Cham, pp. 113–132.

Franklin, D. J., Cedrés, C. M. M. & Hoegh-Guldberg, O. 2006. Increased mortality and photoinhibition in the symbiotic dinoflagellates of the Indo-Pacific coral *Stylophora pistillata* (Esper) after summer bleaching. Mar. Biol., 149:633–642.

Frost, B. W. 1972. Effects of size and concentration of food particles on the feeding behavior of the marine planktonic copepod *Calanus pacificus*. Limnol. Oceanogr., 17:805–815.

Fuentes-Grünewald, C., Bayliss, C., Fonlut, F. & Chapuli, E. 2016. Long-term dinoflagellate culture performance in a commercial photobioreactor: *Amphidinium carterae* case. Bioresour. Technol., 218:533–540.

Gallardo-Rodríguez, J. J., García, M. D. C. C., Camacho, F. G., Mirón, A. S., Belarbi, E. H. & Grima, E. M. 2007. New culture approaches for

yessotoxin production from the dinoflagellate *Protoceratium reticulatum*. Biotechnol. Prog., 23:339–350.

Gallardo-Rodríguez, J. J. G., Mirón, A. S., Camacho, F. G., García, M. C. C., Belarbi, E. H. & Grima, E. M. 2010. Culture of dinoflagellates in a fed-batch and continuous stirred tank photobioreactors: growth, oxidative stress and toxin production. Process Biochem., 45:660–666.

Gallardo-Rodríguez, J., Sánchez-Mirón, A., García-Camacho, F., López-Rosales, L., Chisti, Y. & Molina-Grima, E. 2012. Bioactives from microalgal dinoflagellates. Biotechnol. Adv., 30:1673–1684.

Games, P. A. & Howell, J. F. 1976. Pairwise multiple comparison procedures with unequal n's and/or variances: a Monte Carlo study. J. Stat. Educ., 1:113–125.

Gao, K., Helbling, E. W., Häder, D. P. & Hutchins, D. A. 2012. Responses of marine primary producers to interactions between ocean acidification, solar radiation, and warming. Mar. Ecol. Prog. Ser., 470:167–189.

Gárate-Lizárraga, I., Band-Schmidt, C. J., López-Cortés, D. J. & del Socorro Muñetón-Gómez, M. 2009. Bloom of *Scrippsiella trochoidea* (Gonyaulacaceae) in a shrimp pond in the southwestern Gulf of California, Mexico. Mar. Pollut. Bull., 58:145–149.

Garcés, R. & Mancha, M. 1993. One-step lipid extraction and fatty acid methyl esters preparation from fresh plant tissues. Anal. Biochem., 211:139–143.

Gérikas Ribeiro, C., dos Santos, A. L., Gourvil, P., Le Gall, F., Marie, D., Tragin, M., Probert, I. & Vaulot, D. 2020. Culturable diversity of Arctic phytoplankton during pack ice melting. Elem. Sci. Anth., 8:6.

Gill, C. W. & Harris, R. P. 1987. Behavioural responses of the copepods *Calanus helgolandicus* and *Temora longicornis* to dinoflagellate diets. J. Mar. Biolog. Assoc. U. K., 67:785–801.

Glasgow, H. B. Jr., Burkholder, J. M., Schmechel, D. E., Tester, P. A. & Rublee, P. A. 1995. Insidious effects of a toxic estuarine dinoflagellate on fish survival and human health. J. Toxicol. Environ. Health 46:501–522.

Glibert, P. M., Burkholder, J. M. & Kana, T. M. 2012. Recent insights about relationships between nutrient availability, forms, and stoichiometry, and the distribution, ecophysiology, and food web effects of pelagic and benthic *Prorocentrum* species. Harmful Algae, 14:231–259.

Glibert, P. M., Burkholder, J. M., Kana, T. M., Alexander, J., Skelton, H. & Shilling, C. 2009. Grazing by *Karenia brevis* on *Synechococcus* enhances its growth rate and may help to sustain blooms. Aquat. Microb. Ecol., 55:17–30.

Goldman, J. C., Dennett, M. R. & Gordin, H. 1989. Dynamics of herbivorous grazing by the heterotrophic dinoflagellate *Oxyrrhis marina*. J. Plankton Res., 11:391–407.

Gómez, F. & Gast, R. J. 2018. Dinoflagellates *Amyloodinium* and *Ichthyodinium* (Dinophyceae), parasites of marine fishes in the South Atlantic Ocean. Dis. Aquat. Org., 131:29–37.

Grzebyk, D. & Berland, B. 1996. Influences of temperature, salinity and irradiance on growth of *Prorocentrum minimum* (Dinophyceae) from the Mediterranean Sea. J. Plankton Res., 18:1837–1849.

Guillard, R. R. L. & Ryther, J. H. 1962. Studies of marine planktonic diatoms. I. *Cyclotella nana* Hustedt and *Detonula confervacea* (Cleve) Grun. Can. J. Microbiol., 8:229–239.

Guiry, M. D. & Guiry, G. M. 2023. AlgaeBase. World-wide electronic publication, National University of Ireland, Galway. Available from: https://www.algaebase.org. Accessed Apr 1, 2023.

Gunstone, F. D. 1996. Fatty acid and lipid chemistry. Blackie Academic, London, 263 pp.

Gupta, A., Barrow, C. J. & Puri, M. 2012. Omega-3 biotechnology: thraustochytrids as a novel source of omega-3 oils. Biotechnol. Adv., 30:1733–1745.

Gupta, P. L., Lee, S. -M. & Choi, H. J. 2015. A mini review: photobioreactors for large scale algal cultivation. World J. Microbiol. Biotechnol., 31:1409–1417.

Ha, K., Kim, H. -W. & Joo, G. -J. 1998. The phytoplankton succession in the lower part of hypertrophic Nakdong River (Mulgum), South Korea. Hydrobiologia 369–370:217–227.

Hahm, D., Rhee, T. S., Kim, H. C., Jang, C. J., Kim, Y. S. & Park, J. H. 2019. An observation of primary production enhanced by coastal upwelling in the southwest East/Japan Sea. J. Mar. Syst., 195:30–37.

Hallegraeff, G. M. 1992. Harmful algal blooms in the Australian region. Mar. Pollut. Bull., 25:186–190.

Han, I. S. & Lee, J. S. 2020. Change the annual amplitude of sea surface temperature due to climate change in a recent decade around the Korean Peninsula. J. Korean Soc. Mar., 26:233–241.

Hand, W. G., Collard, P. A. & Davenport, D. 1965. The effects of temperature and salinity change on swimming rate in the dinoflagellates, *Gonyaulax* and *Gyrodinium*. Biol. Bull. 128:90–101.

Hansen, P. J. 1991. Quantitative importance and trophic role of heterotrophic dinoflagellates in a coastal pelagial food web. Mar. Ecol. Prog. Ser., 73:253–61.

Hansen, P. J. 1992. Prey size selection, feeding rates and growth dynamics of heterotrophic dinoflagellates with special emphasis on *Gyrodinium spirale*. Mar. Biol., 114:327–334.

Hansen, P. J. 2011. The role of photosynthesis and food uptake for the growth of marine mixotrophic dinoflagellates. J. Eukaryot. Microbiol., 58:203–214.

Hansen, P. J. & Calado, A. J. 1999. Phagotrophic Mechanisms and Prey Selection in Free-living Dinoflagellates. J. Eukaryot. Microbiol., 46:382–389.

Hansen, P. J. & Nielsen, T. G. 1997. Mixotrophic feeding of *Fragilidium subglobosum* (Dinophyceae) on three species of *Ceratium*: effects of prey concentration, prey species and light intensity. Mar. Ecol. Prog. Ser., 147:187–196.

Harrison, P. J., Furuya, K., Glibert, P. M., Xu, J., Liu, H. B., Yin, K., Lee, J. H. W., Anderson, D. M., Gowen, R., Al-Azri, A. R. & Ho, A. Y. T. 2011. Geographical distribution of red and green *Noctiluca scintillans*. Chin. J. Oceanol. Limnol., 29:807–831.

Harvey, E. L., Jeong, H. J. & Menden-Deuer, S. 2013. Avoidance and attraction: Chemical cues influence predator-prey interactions of planktonic protists. Limnol. Oceanogr., 58:1176–1184.

Hasle, G. R. 1950. Phototactic vertical migration in marine dinoflagellates. Oikos, 2:162–175.

Hassett, R. P. & Landry, M. R. 1990. Effects of diet and starvation on digestive enzyme activity and feeding behavior of the marine copepod *Calanus pacificus*. J. Plankton Res., 12:991–1010.

Hastings, J. W. 1975. Dinoflagellate bioluminescence: molecular mechanisms and circadian control. *In* Lo Cicero, V. R. (Ed.) Proc. First

Int. Conf. Toxic Dinoflagellate Blooms, The Massachusetts Science and Technology Foundation, Wakefield, pp. 235–248.

Hehenberger, E., Gast, R. J. & Keeling, P. J. 2019. A kleptoplastidic dinoflagellate and the tipping point between transient and fully integrated plastid endosymbiosis. Proc. Natl. Acad. Sci. U.S.A., 116:17934–17942.

Heinbokel, J. F. 1978. Studies on the functional role of tintinnids in the Southern California Bight. I. Grazing and growth rates in laboratory cultures. Mar. Biol., 47:177–89.

Hinder, S. L., Hays, G. C., Edwards, M., Roberts, E. C., Walne, A. W. & Gravenor, M. B. 2012. Changes in marine dinoflagellate and diatom abundance under climate change. Nature Climate Change 2:271–275.

Holm-Hansen, O. 1969. Algae: amounts of DNA and organic carbon in single cells. Science, 163: 87–88.

Holmes, M. J., Brust, A. & Lewis, R. J. 2014. Dinoflagellate toxins: an overview. In Botana, L. M. (Ed.) Seafood and Freshwater Toxins: Pharmacology, Physiology, and Detection. 3rd ed. CRC Press, Boca Raton, FL, pp. 3–38.

Hoppenrath, M. & Leander, B. S. 2007. Morphology and Phylogeny of the Pseudocolonial Dinoflagellates *Polykrikos lebourae* and *Polykrikos herdmanae* n. sp. Protist, 158:209–227.

Hoppenrath, M., Murray, S. A., Chomérat, N. & Horiguchi, T. 2014. *Marine benthic dinoflagellates: unveiling their worldwide biodiversity*. Schweizerbart Science Publishers, Stuttgart, 276 pp.

Horrocks, L. A. & Yeo, Y. K. 1999. Health benefits of docosahexaenoic acid (DHA). Pharmacol. Res., 40:211–225.

IPCC. 2007. Climate change 2007: the physical science basis. Contribution of Working Group I to the Fourth Assessment Report of the Intergovernmental Panel on Climate Change. IPCC Secretariat, Geneva, Switzerland.

IPCC. 2013. Climate change 2013: the physical science basis. Contribution of Working Group I to the Fifth Assessment Report of the Intergovernmental Panel on Climate Change. Cambridge Univ. Press, Cambridge, UK.

IPCC. 2021. Climate Change 2021: The Physical Science Basis. Contribution of Working Group I to the Sixth Assessment Report of the

Intergovernmental Panel on Climate Change Cambridge Univ. Press, Cambridge, UK. In Press

Jacobson, D. M. & Anderson, D. M. 1986. Thecate heterophic dinoflagellates: Feeding behavior and mechanisms. J. Phycol., 22:249–258.

Jacobson, D. M. & Anderson, D. M. 1996. Widespread phagocytosis of ciliates and other protists by marine mixotrophic and heterotrophic thecate dinoflagellates. J. Phycol., 32:279–285.

Jakobsen, H. H., Hansen, P. J. & Larsen, J. 2000. Growth and grazing responses of two chloroplast-retaining dinoflagellates: effect of irradiance and prey species. Mar. Ecol. Prog. Ser., 201:121–128.

Jang, S. H. & Jeong, H. J. 2020. Spatio-temporal distributions of the newly described mixotrophic dinoflagellate *Yihiella yeosuensis* (Suessiaceae) in Korean coastal waters and its grazing impact on prey populations. Algae, 35:45–59.

Jang, S. H., Jeong, H. J. & Kwon, J. E. 2017a. High contents of eicosapentaenoic acid and docosahexaenoic acid in the mixotrophic dinoflagellate *Paragymnodinium shiwhaense* and identification of putative omega-3 biosynthetic genes. Algal Res., 25:525–537.

Jang, S. H., Jeong, H. J., Kwon, J. E. & Lee, K. H. 2017b. Mixotrophy in the newly described dinoflagellate *Yihiella yeosuensis*: a small, fast dinoflagellate predator that grows mixotrophically, but not autotrophically. Harmful Algae, 62:94–103.

Jang, S. H., Jeong, H. J., Moestrup, Ø., Kang, N. S., Lee, S. Y., Lee, K. H. & Seong, K. A. 2017c. *Yihiella yeosuensis* gen. et sp. nov. (Suessiaceae, Dinophyceae), a novel dinoflagellate isolated from the coastal waters of Korea. J. Phycol., 53:131–145.

Jang, S. H., Jeong, H. J. & Yoo, Y. D. 2018. *Gambierdiscus jejuensis* sp. nov., an epiphytic dinoflagellate from the waters of Jeju Island, Korea, effect of temperature on the growth, and its global distribution. Harmful Algae, 80:149–157.

Jang, S. H., Lim, P., Torano, O., Neave, E. F., Seim, H. & Marchetti, A. 2022. Protistan communities within the Galápagos Archipelago with an emphasis on micrograzers. Front. Mar. Sci., 9:811979.

Jeong, H. J. 1995. The interactions between microzooplanktonic grazers and dinoflagellates causing red tides in the open coastal waters off southern

California. Ph.D. dissertation, University of California, San Diego, U. S. A.

Jeong, H. J. 1999. The ecological roles of heterotrophic dinoflagellates in marine planktonic community. J. Eukaryot. Microbiol. 46:390–396.

Jeong, H. J. 2022. Marine Ecology. Seoul National University Press, 336 pp. [in Korean].

Jeong, H. J. & Lim, A. S. 2020. Method and system for continuous mass culture for mixotrophic dinoflagellates. Patent no. KR102064718B1. Korean Intellectual Property Office, Daejeon.

Jeong, H. J., Ha, J. H., Park, J. Y., Kim, J. H., Kang, N. S., Kim, S., Kim, J. S., Yoo, Y. D. & Yih, W. 2006. Distribution of the heterotrophic dinoflagellate *Pfiesteria piscicida* in Korean waters and its consumption of mixotrophic dinoflagellates, raphidophytes and fish blood cells. Aquat. Microb. Ecol., 44:263–278.

Jeong, H. J., Ha, J. H., Yoo, Y. D., Park, J. Y., Kim, J. H., Kang, N. S., Kim, T. H., Kim, H. S. & Yih, W. 2007. Feeding by the *Pfiesteria*-like heterotrophic dinoflagellate *Luciella masanensis*. J. Eukaryot Microbiol., 54:231–241.

Jeong, H. J., Jang, S. H., Moestrup, Ø., Kang, N. S., Lee, S. Y., Potvin, É. & Noh, J. H. 2014. *Ansanella granifera* gen. et sp. nov. (Dinophyceae), a new dinoflagellate from the coastal waters of Korea. Algae, 29:75–99.

Jeong, H. J., Kang, H., Shim, J. H., Park, J. K., Kim, J. S., Song, J. Y. & Choi, H. J. 2001a. Interactions among the toxic dinoflagellate *Amphidinium carterae*, the heterotrophic dinoflagellate *Oxyrrhis marina*, and the calanoid copepods *Acartia* spp. Mar. Ecol. Prog. Ser., 218:77–86.

Jeong, H. J., Kang, H. C., Lim, A. S., Jang, S. H., Lee, K., Lee, S. Y., Ok, J. H., You, J. H., Kim, J. H., Lee, K. H., Park, S. A., Eom, S. H., Yoo, Y. D. & Kim, K. Y. 2021. Feeding diverse prey as an excellent strategy of mixotrophic dinoflagellates for global dominance. Sci. Adv., 7:eabe4214.

Jeong, H. J., Kang, H. C., You, J. H. & Jang, S. H. 2018a. Interactions between the newly-described small and fast-swimming mixotrophic dinoflagellate *Yihiella yeosuensis* and common heterotrophic protists. J. Eukaryot. Microbio., 65:612–626.

Jeong, H. J., Kim, J. S., Lee, K. H., Seong, K. A., Yoo, Y. D., Kang, N. S., Kim, T. H., Song, J. Y. & Kwon, J. E. 2017a. Differential interactions

between the nematocyst-bearing mixotrophic dinoflagellate *Paragymnodinium shiwhaense* and common heterotrophic protists and copepods: killer or prey. Harmful Algae, 62:37–51.

Jeong, H. J., Kim, S. K., Kim, J. S., Kim, S. T., Yoo, Y. D. & Yoon, J. Y. 2001b. Growth and grazing rates of the heterotrophic dinoflagellate *Polykrikos kofoidii* on red-tide and toxic dinoflagellates. J. Eukaryot. Microbio., 48:298–308.

Jeong, H. J., Lee, K. H., Yoo, Y. D., Kang, N. S. & Lee, K. 2011. Feeding by the newly described, nematocyst-bearing heterotrophic dinoflagellate *Gyrodiniellum shiwhaense*. J. Eukaryot. Microbiol., 58:511–524.

Jeong, H. J., Lee, K. H., Yoo, Y. D., Kang, N. S., Song, J. Y., Kim, T. H., Seong, K. A., Kim, J. S. & Potvin, E. 2018b. Effects of light intensity, temperature, and salinity on the growth and ingestion rates of the red-tide mixotrophic dinoflagellate *Paragymnodinium shiwhaense*. Harmful Algae, 80:46–54.

Jeong, H. J., Lim, A. S., Franks, P. J. S., Lee, K. H., Kim, J. H., Kang, N. S., Lee, M. J., Jang, S. H., Lee, S. Y., Yoon, E. Y., Park, J. Y., Yoo, Y. D., Seong, K. A., Kwon, J. E. & Jang, T. Y. 2015. A hierarchy of conceptual models of red-tide generation: nutrition, behavior, and biological interactions. Harmful Algae, 47:97–115.

Jeong, H. J., Lim, A. S., Lee, K., Lee, M. J., Seong, K. A., Kang, N. S., Jang, S. H., Lee, K. H., Lee, S. Y., Kim, M. O., Kim, J. H., Kwon, J. E., Kang, H. C., Kim, J. S., Yih, W. H., Shin, K., Jang, P. K., Ryu, J. -H., Kim, S. Y., Park, J. Y. & Kim, K. Y. 2017b. Ichthyotoxic *Cochlodinium polykrikoides* red tides offshore in the South Sea, Korea in 2014: I. Temporal variations in three-dimensional distributions of red-tide organisms and environmental factors. Algae, 32:101–130.

Jeong, H. J., Ok, J. H., Lim, A. S., Kwon, J. E., Kim, S. J. & Lee, S. Y. 2016. Mixotrophy in the phototrophic dinoflagellate *Takayama helix* (family Kareniaceae): predator of diverse toxic and harmful dinoflagellates. Harmful Algae, 60:92–106.

Jeong, H. J., Park, J. Y., Nho, J. H., Park, M. O., Ha, J. H., Seong, K. A., Lee, K. Y. & Yih, W. 2005a. Feeding by red–tide dinoflagellates on the cyanobacterium *Synechococcus*. Aquat. Microb. Ecol., 41: 131–143.

Jeong, H. J., Seong, K. A., Yoo, Y. D., Kim, T. H., Kang, N. S., Kim, S., Park, J. Y., Kim, J. S., Kim, G. H. & Song, J. Y. 2008. Feeding and

grazing impact by small marine heterotrophic dinoflagellates on heterotrophic bacteria. J. Eukaryot. Microbio., 55:271–288.

Jeong, H. J., Song, J. Y., Lee, C. H. & Kim, S. T. 2004. Feeding by larvae of the mussel *Mytilus galloprovincialis* on red-tide dinoflagellates. J. Shellfish Res., 23:185–195.

Jeong, H. J., Yoo, Y. D., Kang, N. S., Lim, A. S., Seong, K. A., Lee, S. Y., Lee, M. J., Lee, K. H., Kim, H. S., Shin, W., Nam, S. W., Yih, W. H. & Lee, K. 2012. Heterotrophic feeding as a newly identified survival strategy of the dinoflagellate *Symbiodinium*. Proc. Natl. Acad. Sci. U. S. A. 109:12604–12609.

Jeong, H. J., Yoo, Y. D., Kang, N. S., Rho, J. R., Seong, K. A., Park, J. W., Nam, G. S. & Yih, W. 2010a. Ecology of *Gymnodinium aureolum*. I. Feeding in western Korean waters. Aquat. Microb. Ecol., 59:239–255.

Jeong, H. J., Yoo, Y. D., Kim, J. S., Seong, K. A., Kang, N. S. & Kim, T. H. 2010b. Growth, feeding and ecological roles of the mixotrophic and heterotrophic dinoflagellates in marine planktonic food webs. Ocean Sci. J., 45:65–91.

Jeong, H. J., Yoo, Y. D., Lee, K. H., Kim, T. H., Seong, K. A., Kang, N. S., Lee, S. Y., Kim, J. S., Kim, S. & Yih, W. H. 2013. Red tides in Masan Bay, Korea in 2004–2005: I. Daily variations in the abundance of red-tide organisms and environmental factors. Harmful Algae, 30(Suppl. 1):S75–S88.

Jeong, H. J., Yoo, Y. D., Park, J. Y., Song, J. Y., Kim, S. T., Lee, S. H., Kim, K. Y., Yih, W. 2005b. Feeding by phototrophic red–tide dinoflagellates: five species newly revealed and six species previously known to be mixotrophic. Aquat. Microb. Ecol., 40:133–150.

Jeong, H. J., Yoo, Y. D., Seong, K. A., Kim, J. H., Park, J. Y., Kim, S. H., Lee, S. H., Ha, J. H., Yih, W. 2005c. Feeding by the mixotrophic red–tide dinoflagellate *Gonyaulax polygramma*: mechanisms, prey species, effects of prey concentration, and grazing impact. Aquat. Microb. Ecol. 38: 249–257.

Jeong, H. J., Yoon, J. Y., Kim, J. S., Yoo, Y. D. & Seong, K. A. 2002. Growth and grazing rates of the prostomatid ciliate *Tiarina fusus* on red-tide and toxic algae. Aquat. Microb. Ecol., 28:289–297.

Jeong, H. J., You, J. H., Lee, K. H., Kim, S. J. & Lee, S. Y. 2018c. Feeding by common heterotrophic protists on the mixotrophic alga

Gymnodinium smaydae (Dinophyceae), one of the fastest growing dinoflagellates. J. Phycol. 54:734–743.

Jerney, J. & Spilling, K. 2018. Large scale cultivation of microalgae: open and closed systems. *In* Spilling, K. (Ed.) *Biofuels from Algae: Methods and Protocols*. Humana Press, New York, NY, pp. 1–8.

Jiang, Y. & Chen, F. 2000. Effects of temperature and temperature shift on docosahexaenoic acid production by the marine microalge *Crypthecodinium cohnii*. J. Am. Oil Chem. Soc., 77:613–617.

Jiang, Y., Chen, F. & Liang, S. Z. 1999. Production potential of docosahexaenoic acid by the heterotrophic marine dinoflagellate *Crypthecodinium cohnii*. Process Biochem., 34:633–637.

Jiang, Y., Fan, K. W., Tsz-Yeung Wong, R. & Chen, F. 2004. Fatty acid composition and squalene content of the marine microalga *Schizochytrium mangrovei*. J. Agric. Food Chem., 52:1196–1200.

Johnson, K. B. & Shanks, A. L. 2003. Low rates of predation on planktonic marine invertebrate larvae. Mar. Ecol. Prog. Ser., 248:125–139.

Johnson, M. D. 2011. The acquisition of phototrophy: adaptive strategies of hosting endosymbionts and organelles. Photosynth Res., 107:117–132.

Johnson, M. D. 2015. Inducible mixotrophy in the dinoflagellate *Prorocentrum minimum*. J. Eukaryot. Microbiol. 62:431–443.

Kamiyama, T. & Matsuyama, Y. 2005. Temporal changes in the ciliate assemblage and consecutive estimates for their grazing effect during the course of a *Heterocapsa circularisquama* bloom. J. Plankton Res., 27:303–311.

Kamykowski, D. 1981. Laboratory experiments on the diurnal vertical migration of marine dinoflagellates through temperature gradients. Mar. Biol., 62:57–64

Kamykowski, D. & McCollum, S. A. 1986. The temperature acclimatized swimming speed of selected marine dinoflagellates. J. Plankton Res., 8:275–287.

Kamykowski, D & Zentara, S. J. 1977. The diurnal vertical migration of motile phytoplankton through temperature gradients. Limnol. Oceanogr., 22:148–151.

Kang, H. C., Jeong, H. J., Kim, S. J., You, J. H. & Ok, J. H. 2018. Differential feeding by common heterotrophic protists on 12 different *Alexandrium* species. Harmful Algae, 78:106–117.

Kang, H. C., Jeong, H. J., Lim, A. S., Ok, J. H., You, J. H., Park, S. A., Lee, S. Y. & Eom, S. H. 2020. Effects of temperature on the growth and ingestion rates of the newly described mixotrophic dinoflagellate *Yihiella yeosuensis* and its two optimal prey species. Algae, 35:263–275.

Kang, H. C., Jeong, H. J., Ok, J. H., You, J. H., Jang, S. H., Lee, S. Y., Lee, K. H., Park, J. Y. & Rho, J. R. 2019. Spatial and seasonal distributions of the phototrophic dinoflagellate *Biecheleriopsis adriatica* (Suessiaceae) in Korea: quantification using qPCR. Algae, 34:111–126.

Kang, N. S., Jeong, H. J., Moestrup, Ø., Lee, S. Y., Lim, A. S., Jang, T. Y., Lee, K. H., Lee, M. J., Jang, S. H., Potvin, É., Lee, S. K. & Noh, J. H. 2014. *Gymnodinium smaydae* n. sp., a new planktonic phototrophic dinoflagellate from the coastal waters of western Korea: morphology and molecular characterization. J. Eukaryot. Microbiol., 61:182–203.

Kang, N. S., Jeong, H. J., Yoo, Y. D., Yoon, E. Y., Lee, K. H., Lee, K. & Kim, G. 2011. Mixotrophy in the newly described phototrophic dinoflagellate *Woloszynskia cincta* from western Korean waters: feeding mechanism, prey species and effect of prey concentration. J. Eukaryot. Microbiol., 58:152–170.

Kang, N. S., Lee, K. H., Jeong, H. J., Yoo, Y. D., Seong, K. A., Potvin, É., Hwang, Y. G. & Yoon, E. Y. 2013. Red tides in Shiwha Bay, western Korea: a huge dike and tidal power plant established in a semi-enclosed embayment system. Harmful Algae, 30:S114–S130.

Keeling, P. J. & Palmer, J. D. 2008. Horizontal gene transfer in eukaryotic evolution. Nat. Rev. Genet., 9:605–618.

Khan, M. I., Shin, J. H. & Kim, J. D. 2018. The promising future of microalgae: current status, challenges, and optimization of a sustainable and renewable industry for biofuels, feed, and other products. Microb. Cell Fact., 17:36.

Kibbe, W. A. 2007. OligoCalc: an online oligonucleotide properties calculator. Nucleic Acids Res. 35(Suppl. 2):W43–W46.

Kibler, S. R., Litaker, R. W., Holland, W. C., Vandersea, M. W. & Tester, P. A. 2012. Growth of eight *Gambierdiscus* (Dinophyceae) species: Effects of temperature, salinity and irradiance. Harmful Algae, 19:1–14.

Kim, D. I., Matsuyama, Y., Nagasoe, S., Yamaguchi, M., Yoon, Y. H., Oshima, Y., Imada, N. & Honjo, T. 2004. Effects of temperature, salinity and irradiance on the growth of the harmful red tide dinoflagellate *Cochlodinium polykrikoides* Margalef (Dinophyceae). J. Plankton Res., 26:61–66.

Kim, H. Y. & Park, K. A. 2018. Comparison of sea surface temperature from oceanic buoys and satellite microwave measurements in the western coastal region of Korean Peninsula. J. Korean Earth Sci. Soc., 39:555–567.

Kim, J. H., Kang, E. J., Park, M. G., Lee, B. G. & Kim, K. Y. 2011. Effects of temperature and irradiance on photosynthesis and growth of a green-tide-forming species (*Ulva linza*) in the Yellow Sea. J. Appl. Phycol., 23:421–432.

Kim, J. S. & Jeong, H. J. 2004. Feeding by the heterotrophic dinoflagellates *Gyrodinium dominans* and *G. spirale* on the red-tide dinoflagellate *Prorocentrum minimum*. Mar. Ecol. Prog. Ser., 280:85–94.

Kim, S., Kang, Y. G., Kim, H. S., Yih, W., Coats, D. W. & Park, M. G. 2008. Growth and grazing responses of the mixotrophic dinoflagellate *Dinophysis acuminata* as functions of light intensity and prey concentration. Aquat. Microb. Ecol., 51:301–310.

Kim, S. J., Jeong, H. J., Kang, H. C., You, J. H. & Ok, J. H. 2019. Differential feeding by common heterotrophic protists on four *Scrippsiella* species of similar size. J. Phycol. 55:868–881.

Kimmance, S. A., Atkinson, D. & Montagnes, D. J. 2006. Do temperature–food interactions matter? Responses of production and its components in the model heterotrophic flagellate *Oxyrrhis marina*. Aquat. Microb. Ecol., 42:63–73.

Kimor, B. 1979. Predation by *Noctiluca miliaris* Souriray on *Acartia tonsa* Dana eggs in the inshore waters of southern California. Limnol. Oceanogr., 24:568–572.

Kiϕrboe, T. & Titelman, J. 1998. Feeding, prey selection and prey encounter mechanisms in the heterotrophic dinoflagellate *Noctiluca scintillans*. J. Plankton Res., 20:1615–1636.

Kjelleberg, S., Hermansson, M., Mårdén, P. & Jones, G. W. 1987. The transient phase between growth and nongrowth of heterotrophic

bacteria, with emphasis on the marine environment. Annu. Rev. Microbiol., 41:25–49.

Koprivnikar, J., Lim, D., Fu, C. & Brack, S. H. 2010. Effects of temperature, salinity, and pH on the survival and activity of marine cercariae. Parasitol. Res., 106:1167–1177.

Kruskal, W. H. & Wallis, W. A. 1952. Use of ranks in one–criterion variance analysis. J. Am. Stat. Assoc., 47:583–621.

Kudela, R. M. & Gobler, C. J. 2012. Harmful dinoflagellate blooms caused by *Cochlodinium* sp.: global expansion and ecological strategies facilitating bloom formation. Harmful Algae, 14:71–86.

Laabir, M., Jauzein, C., Genovesi, B., Masseret, E., Grzebyk, D., Cecchi, P., Vaquer, A., Perrin, Y. & Collos, Y. 2011. Influence of temperature, salinity and irradiance on the growth and cell yield of the harmful red tide dinoflagellate *Alexandrium catenella* colonizing Mediterranean waters. J. Plankton Res., 33:1550–1563.

LaJeunesse, T. C., Parkinson, J. E., Gabrielson, P. W., Jeong, H. J., Reimer, J. D., Voolstra, C. R. & Santos, S. R. 2018. Systematic revision of Symbiodiniaceae highlights the antiquity and diversity of coral endosymbionts. Curr. Biol., 28:2570–2580.

Lalli, C. & Parsons, T. R. 1997. Biological oceanography: an introduction (2nd ed) The Open University, Elsevier Butterworth-Heinemann, Oxford.

Lee, B. I., Kim, S. K., Kim, J. H., Kim, H. S., Kim, J. I., Shin, W., Rho, J. R. & Yih, W. 2019a. Intraspecific variations in macronutrient, amino acid, and fatty acid composition phytoof mass-cultured *Teleaulax amphioxeia* (Cryptophyceae) strains. Algae, 34:163–175.

Lee, E. Y. & Park, K. 2019. Change in the recent warming trend of sea surface temperature in the East Sea (Sea of Japan) over decades (1982–2018). Remote Sens., 11:2613.

Lee, H. G., Kim, H. M., Min, J., Park, C., Jeong, H. J., Lee, K. & Kim, K. Y. 2020a. Quantification of the paralytic shellfish poisoning dinoflagellate *Alexandrium* species using a digital PCR. Harmful Algae, 92:101726.

Lee, J. C., Kim, D. H. & Kim, J. C. 2003. Observations of coastal upwelling at Ulsan in summer 1997. J. Korean Soc. Oceanogr., 38:122–134.

Lee, K. H., Jeong, H. J., Jang, T. Y., Lim, A. S., Kang, N. S., Kim, J. H., Kim, K. Y., Park, K. T. & Lee, K. 2014a. Feeding by the newly described

mixotrophic dinoflagellate *Gymnodinium smaydae*: Feeding mechanism, prey species, and effect of prey concentration. J. Exp. Mar. Bio. Ecol., 459:114–125.

Lee, K. H., Jeong, H. J., Kwon, J. E., Kang, H. C., Kim, J. H., Jang, S. H., Park, J. Y., Yoon, E. Y. & Kim, J. S. 2016. Mixotrophic ability of the phototrophic dinoflagellates *Alexandrium andersonii*, *A. affine*, and *A. fraterculus*. Harmful Algae, 59:67–81.

Lee, K. H., Jeong, H. J., Lee, K. T., Franks, P. J. S., Seong, K. A., Lee, S. Y., Lee, M. J., Jang, S. H., Potvin, E., Lim, A. S., Yoon, E. Y., Yoo, Y. D., Kang, N. S. & Kim, K. Y. 2019b. Effects of warming and eutrophication on coastal phytoplankton production. Harmful Algae, 81:106–118.

Lee, K. H., Jeong, H. J., Yoon, E. Y., Jang, S. H., Kim, H. S. & Yih, W. H. 2014b. Feeding by common heterotrophic dinoflagellates and a ciliate on the red-tide ciliate *Mesodinium rubrum*. Algae, 29:153–163.

Lee, M. J., Jeong, H. J., Kim, J. S., Jang, K. K., Kang, N. S., Jang, S. H., Lee, H. B., Lee, S. B., Kim, H. S. & Choi, C. H. 2017a. Ichthyotoxic *Cochlodinium polykrikoides* red tides offshore in the South Sea, Korea in 2014: III. Metazooplankton and their grazing impacts on red-tide organisms and heterotrophic protists. Algae, 32:285–308.

Lee, M. J., Jeong, H. J., Lee, K. H., Jang, S. H., Kim, J. H. & Kim, K. Y. 2015. Mixotrophy in the nematocyst-taeniocyst complex–bearing phototrophic dinoflagellate *Polykrikos hartmannii*. Harmful Algae, 49:124–134.

Lee, S. K., Jeong, H. J., Jang, S. H., Lee, K. H., Kang, N. S., Lee, M. J., Potvin, É. 2014c. Mixotrophy in the newly described dinoflagellate *Ansanella granifera*: feeding mechanism, prey species, and effect of prey concentration. Algae, 29:137–152.

Lee, S. Y., Jeong, H. J. & Lajeunesse, T. C. 2020b. *Cladocopium infistulum* sp. nov. (Dinophyceae), a thermally tolerant dinoflagellate symbiotic with giant clams from the western Pacific Ocean. Phycologia, 59:515–526.

Lee, S. Y., Jeong, H. J., Kang, H. C., Ok, J. H., You, J. H., Park, S. A. & Eom, S. H. 2021. Comparison of the spatial-temporal distributions of the heterotrophic dinoflagellates *Gyrodinium dominans*, *G. jinhaense*, and *G. moestrupii* in Korean coastal waters. Algae, 36:37–50.

Lee, S. Y., Jeong, H. J., Kim, S. J., Lee, K. H. & Jang, S. H. 2019c. *Scrippsiella masanensis* sp. nov. (Thoracosphaerales, Dinophyceae), a phototrophic dinoflagellate from the coastal waters of southern Korea. Phycologia, 58:287–299.

Lee, S. Y., Jeong, H. J., Kwon, J. E., You, J. H., Kim, S. J., Ok, J. H., Kang, H. C. & Park, J. Y. 2019d. First report of the photosynthetic dinoflagellate *Heterocapsa minima* in the Pacific Ocean: morphological and genetic characterizations and the nationwide distribution in Korea. Algae, 34:7–21.

Lee, S. Y., Jeong, H. J., Ok, J. H., Kang, H. C. & You, J. H. 2020b. Spatial-temporal distributions of the newly described mixotrophic dinoflagellate *Gymnodinium smaydae* in Korean coastal waters. Algae, 35:225–236.

Lee, S. Y., Jeong, H. J., Seong, K. A., Lim, A. S., Kim, J. H., Lee, K. H., Lee, M. J. & Jang, S. H. 2017b. Improved real-time PCR method for quantification of the abundance of all known ribotypes of the ichthyotoxic dinoflagellate *Cochlodinium polykrikoides* by comparing 4 different preparation methods. Harmful Algae, 63:23–31.

Lee, S. Y., Jeong, H. J., You, J. H. & Kim, S. J. 2018. Morphological and genetic characterization and the nationwide distribution of the phototrophic dinoflagellate *Scrippsiella lachrymosa* in the Korean waters. Algae, 33:21–35.

Leu, S. & Boussiba, S. 2014. Advances in the production of high-value products by microalgae. Ind. Biotechnol., 10:169–183.

Levene, H. 1960. Robust tests for equality of variances. In: Olkins I (ed) Contributions to probability and statistics: Essays in honor of Harold Hotelling, Stanford University Press, Redwood City, CA, pp 279–292.

Levitus, S., Antonov, J. & Boyer, T. 2005. Warming of the world ocean, 1955–2003. Geophys. Res. Lett., 32.

Lewis, J., Kennaway, G., Franca, S. & Alverca, E. 2001. Bacterium-dinoflagellate interactions: investigative microscopy of *Alexandrium* spp. (Gonyaulacales, Dinophyceae). Phycologia, 40:280–285.

Li, A., Stoecker, D. K. & Adolf, J. E. 1999. Feeding, pigmentation, photosynthesis and growth of the mixotrophic dinoflagellate *Gyrodinium galatheanum*. Aquat. Microb. Ecol., 19:163–176.

Li, A., Stoecker, D. K. & Coats, D. W. 2000. Mixotrophy in *Gyrodinium galatheanum* (Dinophyceae): grazing responses to light intensity and inorganic nutrients. J. Phycol., 36:33–45.

Li, X., Xu, H. & Wu, Q. 2007. Large-scale biodiesel production from microalga *Chlorella protothecoides* through heterotrophic cultivation in bioreactors. Biotechnol. Bioeng., 98:764–771.

Liang, Y., Sarkany, N., Cui, Y., Yesuf, J., Trushenski, J. & Blackburn, J. W. 2010. Use of sweet sorghum juice for lipid production by *Schizochytrium limacinum* SR21. Bioresour. Technol., 101:3623–3627.

Lim, A. S., Jeong, H. J., Jang, T. Y., Yoo, Y. D., Kang, N. S., Yoon, E. Y. & Kim, G. H. 2014. Feeding by the newly described heterotrophic dinoflagellate *Stoeckeria changwonensis*: a comparison with other species in the family Pfiesteriaceae. Harmful Algae, 36:11–21.

Lim, A. S., Jeong, H. J., Kim, J. H. & Lee, S. Y. 2015a. Description of the new phototrophic dinoflagellate *Alexandrium pohangense* sp. nov. from Korean coastal waters. Harmful Algae, 46:49–61.

Lim, A. S., Jeong, H. J., Kim, J. H., Jang, S. H., Lee, M. J. & Lee, K. 2015b. Mixotrophy in the newly described dinoflagellate *Alexandrium pohangense*: a specialist for feeding on the fast-swimming ichthyotoxic dinoflagellate *Cochlodinium polykrikoides*. Harmful Algae, 49:10–18.

Lim, A. S., Jeong, H. J., Kim, S. J. & Ok, J. H. 2018a. Amino acids profiles of six dinoflagellate species belonging to diverse families: possible use as animal feeds in aquaculture. Algae, 33:279–290.

Lim, A. S., Jeong, H. J. & Ok, J. H. 2019a. Five *Alexandrium* species lacking mixotrophic ability. Algae, 34:289–301.

Lim, A. S., Jeong, H. J., Ok, J. H. & Kim, S. J. 2018b. Feeding by the harmful phototrophic dinoflagellate *Takayama tasmanica* (Family Kareniaceae). Harmful Algae, 74:19–29.

Lim, A. S., Jeong, H. J., Ok, J. H., You, J. H., Kang, H. C., Kim, S. J. 2019b. Effects of light intensity and temperature on growth and ingestion rates of the mixotrophic dinoflagellate *Alexandrium pohangense*. Mar. Biol., 166:1–11.

Lim, A. S., Jeong, H. J., Seong, K. A., Lee, M. J., Kang, N. S., Jang, S. H., Lee, K. H., Park, J. Y., Jang, T. Y. & Yoo, Y. D. 2017. Ichthyotoxic *Cochlodinium polykrikoides* red tides offshore in the South Sea, Korea

in 2014: II. Heterotrophic protists and their grazing impacts on red-tide organisms. Algae, 32:199–222.

Lim, A. S., Jeong, H. J., You, J. H. & Park, S. A. 2020. Semi-continuous cultivation of the mixotrophic dinoflagellate *Gymnodinium smaydae*, a new promising microalga for omega-3 production. Algae, 35:277–292.

Lim, P. T., Leaw, C. P., Usup, G., Kobiyama, A., Koike, K. & Ogata, T. 2006. Effects of light and temperature on growth, nitrate uptake, and toxin production of two tropical dinoflagellates: *Alexandrium tamiyavanichii* and *Alexandrium minutum* (dinophyceae). J. Phycol., 42:786–799.

Litaker, R. W., Vandersea, M. W., Kibler, S. R., Reece, K. S., Stokes, N. A., Steidinger, K. A., Millie, D. F., Bendis, B. J., Pigg, R. J. & Tester, P. A. 2003. Identification of *Pfiesteria piscicida* (dinophyceae) and *Pfiesteria*-like organisms using internal transcribed spacer-specific PCR assays. J. Phycol., 39:754–761.

Löder, M. G. J., Kraberg, A. C., Aberle, N., Peters, S. & Wiltshire, K. H. 2012. Dinoflagellates and ciliates at Helgoland roads, North Sea. Helgol. Mar. Res., 66:11–23.

López-Rosales, L., Gallardo-Rodríguez, J., Sánchez-Mirón, A., Cerón-García, M., Belarbi, E., García-Camacho, F. & Molina-Grima, E. 2014. Simultaneous effect of temperature and irradiance on growth and okadaic acid production from the marine dinoflagellate *Prorocentrum belizeanum*. Toxins, 6:229–253.

Luo, Z., Wang, N., Mohamed, H. F., Liang, Y., Pei, L., Huang, S. & Gu, H. 2021. *Amphidinium stirisquamtum* sp. nov. (Dinophyceae), a new marine sand-dwelling dinoflagellate with a novel type of body scale. Algae, 36:241–261.

Luo, Z., Yang, W., Xu, B. & Gu, H. 2013. First record of *Biecheleria cincta* (Dinophyceae) from Chinese coasts, with morphological and molecular characterization of the strains. Chin. J. Oceanol. Limnol., 31:835–845.

Magaña, H. A. & Villareal, T. A. 2006. The effect of environmental factors on the growth rate of *Karenia brevis* (Davis) G. Hansen and Moestrup. Harmful Algae, 5:192–198

Mann, H. B. & Whitney, D. R. 1947. On a test of whether one of two random variables is stochastically larger than the other. Ann. Math. Stat., 5:0–60.

Mansour, M. P., Frampton, D. M. F., Nichols, P. D., Volkman, J. K. & Blackburn, S. I. 2005. Lipid and fatty acid yield of nine stationary-phase microalgae: applications and unusual C24-C28 polyunsaturated fatty acids. J. Appl. Phycol., 17:287–300.

Marine Environment Information System (MEIS). http://www.meis.go.kr. Accessed 05 March 2020.

Martins, D. A., Custódio, L., Barreira, L., Pereira, H., Ben-Hamadou, R., Varela, J. & Abu-Salah, K. M. 2013. Alternative sources of n-3 long-chain polyunsaturated fatty acids in marine microalgae. Mar. Drugs, 11:2259–2281.

Matsubara, T., Nagasoe, S., Yamasaki, Y., Shikata, T., Shimasaki, Y., Oshima, Y. & Honjo, T. 2007. Effects of temperature, salinity, and irradiance on the growth of the dinoflagellate *Akashiwo sanguinea*. J. Exp. Mar. Biol. Ecol., 342:226–230.

Matsuoka, K., Cho, H. J. & Jacobson, D. M. 2000. Observations of the feeding behavior and growth rates of the heterotrophic dinoflagellate *Polykrikos kofoidii* (Polykrikaceae, Dinophyceae). Phycologia, 39:82–86.

Matsuoka, K., Iizuka, S., Takayama, H., Honjyo, T., Fukuyo, Y. & Ishimaru, T. 1989. Geographic distribution of *Gymnodinium nagasakiense* Takayama et Adachi around west Japan. In: Okaichi T, Anderson DM, Nemoto T (ed) Red Tides: Biology, Environmental Science and Toxicology, Elsevier, New York, pp 101–104.

Medlin, L., Elwood, H. J., Stickel, S. & Sogin, M. L. 1988. The characterization of enzymatically amplified eukaryotic 16S-like rRNA-coding regions. Gene, 71:491–499.

Menden-Deuer, S. & Lessard, E. J. 2000. Carbon to volume relationships for dinoflagellates, diatoms, and other protist plankton. Limnol. Oceanogr., 45:569–579.

Menden-Deuer, S. & Montalbano, A. L. 2015. Bloom formation potential in the harmful dinoflagellate *Akashiwo sanguinea*: clues from movement behaviors and growth characteristics. Harmful Algae, 47:75–85.

Menden-Deuer, S., Lessard, E. J., Satterberg, J. & Grünbaum, D. 2005. Growth rates and starvation survival of three species of the pallium-feeding, thecate dinoflagellate genus *Protoperidinium*. Aquat. Microb. Ecol., 41:145–152.

Mendes, A., Reis, A., Vasconcelos, R., Guerra, P. & da Silva, T. L. 2009. *Crypthecodinium cohnii* with emphasis on DHA production: a review. J. Appl. Phycol., 21:199–214.

Millette, N. C., Pierson, J. J., Aceves, A. & Stoecker, D. K. 2017. Mixotrophy in *Heterocapsa rotundata*: a mechanism for dominating the winter phytoplankton. Limnol. Oceanogr., 62:836–845.

Mitsui, A., Cao, S., Takahashi, A. & Arai, T. 1987. Growth synchrony and cellular parameters of the unicellular nitrogen-fixing marine cyanobacterium, *Synechococcus* sp. strain Miami BG 043511 under continuous illumination. Physiol. Plant., 69:1–8.

Miyaguchi, H., Fujiki, T., Kikuchi, T., Kuwahara, V. S. & Toda, T. 2006. Relationship between the bloom of *Noctiluca scintillans* and environmental factors in the coastal waters of Sagami Bay, Japan. J. Plankton Res., 28:313–324.

Mobin, S. & Alam, F. 2017. Some promising microalgal species for commercial applications: a review. Energy Procedia, 110:510–517.

Moestrup, Ø., Lindberg, K. & Daugbjerg, N. 2009. Studies on woloszynskioid dinoflagellates IV: The genus *Biecheleria* gen. nov. Phycol. Res., 57:203–220.

Moline, M. A., Claustre, H., Frazer, T. K., Schofield, O. & Vernet, M. 2004. Alteration of the food web along the Antarctic Peninsula in response to a regional warming trend. Glob. Chang. Biol., 10:1973–1980.

Moncheva, S., Gotsis-Skretas, O., Pagou, K. & Krastev, A. 2001. Phytoplankton blooms in Black Sea and Mediterranean coastal ecosystems subjected to anthropogenic eutrophication: similarities and differences. Estuar. Coast. Shelf Sci., 53:281–295.

Morin, J. G. 1983. Coastal bioluminescence: patterns and functions. Bull. Mar. Sci., 33:787–817.

Morton, S. L., Norris, D. R. & Bomber, J. W. 1992. Effect of temperature, salinity and light intensity on the growth and seasonality of toxic dinoflagellates associated with ciguatera. J. Exp. Mar. Biol. Ecol., 157:79–90.

Morquecho, L., Gárate-Lizárraga, I. & Gu, H. 2022. Morphological and molecular characterization of the genus *Coolia* (Dinophyceae) from Bahía de La Paz, southwest Gulf of California. Algae, 37:185–204.

Nagasoe, S., Kim, D. I., Shimasaki, Y., Oshima, Y., Yamaguchi, M. & Honjo, T. 2006. Effects of temperature, salinity and irradiance on the growth of the red-tide dinoflagellate *Gyrodinium instriatum* Freudenthal et Lee. Harmful Algae, 5:20–25.

Nakamura, Y. 1998. Growth and grazing of a large heterotrophic dinoflagellate, *Noctiluca scintillans*, in laboratory cultures. J. Plankton Res., 20:1711–1720.

Nakamura, Y., Suzuki, S. Y. & Hiromi, J. 1995. Growth and grazing of a naked heterotrophic dinoflagellate, *Gyrodinium dominans*. Aquat. Microb. Ecol., 9:157–64.

National Institute of Biological Resources. 2020. *Heterocapsa triquetra* (Ehrenberg) Stein 1883. Available from: https://species.nibr.go.kr/geo/html/index.do?ktsn=120000012982. Accessed Jul 14, 2020.

National Institute of Fisheries Science. 2020. Red-tide information system. Available from: http://www.nifs.go.kr/portal/external/environment/redtide/index.jsp. Accessed Jul 14, 2020.

Naustvoll, L. J. 2000. Prey size spectra in naked heterotrophic dinoflagellates. Phycologia, 39:448–455.

Nielsen, M. V. 1996. Growth and chemical composition of the toxic dinoflagellate *Gymnodinium galatheanum* in relation to irradiance, temperature and salinity. Mar. Ecol. Prog. Ser., 136:205–211.

Ning, Y. & Liu, X. 2020. *Enteromorpha* hydrolysate as carbon source for fatty acids production of microalgae *Schizochytrium* sp. Energy, 203:117900.

Nishitani, G., Nagai, S., Sakiyama, S. & Kamiyama, T. 2008. Successful cultivation of the toxic dinoflagellate *Dinophysis caudata* (Dinophyceae). Plank. Benth. Res., 3:78–85.

Nitschke, M. R., Davy, S. K., Cribb, T. H. & Ward, S. 2015. The effect of elevated temperature and substrate on free-living *Symbiodinium* cultures. Coral Reefs 34:161–171.

NOAA National Centers for Environmental information. 2022. Climate at a Glance: Global Time Series. https://www.ncdc.noaa.gov/cag/. Accessed Apr 12, 2022

Ogata, T., Ishimaru, T. & Kodama, M. 1987. Effect of water temperature and light intensity on growth rate and toxicity change in *Protogonyaulax tamarensis*. Mar. Biol., 95:217–220.

Ok, J. H., Jeong, H. J., Kang, H. C., Park, S. A., Eom, S. H., You, J. H. & Lee, S. Y. 2021. Ecophysiology of the kleptoplastidic dinoflagellate *Shimiella gracilenta*: I. spatiotemporal distribution in Korean coastal waters and growth and ingestion rates. Algae, 36:263–283.

Ok, J. H., Jeong, H. J., Kang, H. C., Park, S. A., Eom, S. H., You, J. H. & Lee, S. Y. 2022. Ecophysiology of the kleptoplastidic dinoflagellate *Shimiella gracilenta*: II. Effects of temperature and global warming. Algae, 37:49–62.

Ok, J. H., Jeong, H. J., Lim, A. S. & Lee, K. H. 2017. Interactions between the mixotrophic dinoflagellate *Takayama helix* and common heterotrophic protists. Harmful Algae, 68:178–91.

Ok, J. H., Jeong, H. J., Lim, A. S., Kang, H. C., You, J. H., Park, S. A. & Eom, S. H. 2023. Lack of mixotrophy in three *Karenia* species and the prey spectrum of *Karenia mikimotoi* (Gymnodiniales, Dinophyceae). Algae, 38:39–55.

Ok, J. H., Jeong, H. J., Lim, A. S., You, J. H., Kang, H. C., Kim, S. J. & Lee, S. Y. 2019. Effects of light and temperature on the growth of *Takayama helix* (Dinophyceae): mixotrophy as a survival strategy against photoinhibition. J. Phycol. 55:1181–1195.

Ono, K., Khan, S. & Onoue, Y. 2000. Effects of temperature and light intensity on the growth and toxicity of *Heterosigma akashiwo* (Raphidophyceae). Aquac. Res., 31:427–433.

Onodera, K. -I., Konishi, Y., Taguchi, T., Kiyoto, S. & Tominaga, A. 2014. Peridinin from the marine symbiotic dinoflagellate, *Symbiodinium* sp., regulates eosinophilia in mice. Mar. Drugs, 12:1773–1787.

Paliwal, C., Mitra, M., Bhayani, K., Bharadwaj, S. V. V., Ghosh, T., Dubey, S. & Mishra, S. 2017. Abiotic stresses as tools for metabolites in microalgae. Bioresour. Technol., 244:1216–1226.

Park, J., Jeong, H. J., Yoo, Y. D. & Yoon, E. Y. 2013a. Mixotrophic dinoflagellate red tides in Korean waters: distribution and ecophysiology. Harmful Algae, 30(Suppl 1):S28–S40.

Park, K. A. & Kim, K. R. 2010a. Unprecedented coastal upwelling in the East/Japan Sea and linkage to long-term large-scale variations. Geophys. Res. Lett., 37.

Park, M. G. & Kim, M. 2010b. Prey specificity and feeding of the thecate mixotrophic dinoflagellate *Fragilidium duplocampanaeforme*. J. Phycol., 46:424–432.

Park, M. G., Kim, S., Shin, E. Y., Yih, W. & Coats, D. W. 2013b. Parasitism of harmful dinoflagellates in Korean coastal waters. Harmful Algae, 30:S62–S74.

Park, M. G., Lee, H., Kim, K. Y. & Kim, S. 2011. Feeding behavior, spatial distribution and phylogenetic affinities of the heterotrophic dinoflagellate *Oxyphysis oxytoxoides*. Aquat. Microb. Ecol., 62:279–287.

Park, S. A., Jeong, H. J., Ok, J. H., Kang, H. C., You, J. H., Eom, S. H. & Park, E. C. 2021a. Interactions between the kleptoplastidic dinoflagellate *Shimiella gracilenta* and several common heterotrophic protists. Front. Mar. Sci., 8:738547.

Park, S. A., Jeong, H. J., Ok, J. H., Kang, H. C., You, J. H., Eom, S. H., Yoo, Y. D. & Lee, M. J. 2021b. Bioluminescence capability and intensity in the dinoflagellate *Alexandrium* species. Algae, 36:299–314.

Park, W. K., Moon, M., Shin, S. -E., Cho, J. M., Suh, W. I., Chang, Y. K. & Lee, B. 2018. Economical DHA (docosahexaenoic acid) production from *Aurantiochytrium* sp. KRS101 using orange peel extract and low cost nitrogen sources. Algal Res., 29:71-79.

Patil, V., Källqvist, T., Olsen, E., Vogt, G. & Gislerød, H. R. 2007. Fatty acid composition of 12 microalgae for possible use in aquaculture feed. Aquac. Int., 15:1–9.

Petchey, O. L., McPhearson, P. T., Casey, T. M. & Morin, P. J. 1999. Environmental warming alters food-web structure and ecosystem function. Nature, 402:69–72.

Pillai, K. C. S. 1955. Some new test criteria in multivariate analysis. Ann. Math. Stat., 26:117–121.

Pistevos, J. C., Nagelkerken, I., Rossi, T., Olmos, M. & Connell, S. D. 2015. Ocean acidification and global warming impair shark hunting behaviour and growth. Sci. Rep., 5:1–10.

Pitcher, G. C. & Joyce, L. B. 2009. Dinoflagellate cyst production on the southern Namaqua shelf of the Benguela upwelling system. J. Plankton Res., 31:865–875.

Pitcher, G. C., Cembella, A. D., Joyce, L. B., Larsen, J., Probyn, T. A. & Sebastián, C. R. 2007. The dinoflagellate *Alexandrium minutum* in Cape Town harbour (South Africa): bloom characteristics, phylogenetic analysis and toxin composition. Harmful Algae, 6:823–836.

Pleissner, D. & Eriksen, N. T. 2012. Effects of phosphorous, nitrogen, and carbon limitation on biomass composition in batch and continuous flow cultures of the heterotrophic dinoflagellate *Crypthecodinium cohnii*. Biotechnol. Bioeng., 109:2005–2016.

Poole, H. H. & Atkins, W. R. G. 1929. Photo-electric measurements of submarine illumination throughout the year. J. Mat. Biol. Assoc. U. K., 16:297–324.

Rawat, I., Kumar, R. R., Mutanda, T. & Bux, F. 2013. Biodiesel from microalgae: a critical evaluation from laboratory to large scale production. Appl. Energy, 103:444–467.

Richardson, K., Beardall, J. & Raven, J. A. 1983. Adaptation of unicellular algae to irradiance: an analysis of strategies. New Phytol., 93:157–191.

Rohr, J., Latz, M. I., Fallon, S., Nauen, J. C. & Hendricks, E. 1998. Experimental approaches towards interpreting dolphin-stimulated bioluminescence. J. Exp. Biol., 201:1447–1460.

Ronquist, F. & Huelsenbeck, J. P. 2003. MRBAYES 3: Bayesian phylogenetic inference under mixed models. Bioinformatics, 19:1572–1574.

Sakamoto, S., Lim, W. A., Lu, D., Dai, X., Orlova, T. & Iwataki, M. 2021. Harmful algal blooms and associated fisheries damage in East Asia: current status and trends in China, Japan, Korea and Russia. Harmful Algae, 102:101787.

Sanz-Sáez, I., Salazar, G., Sánchez, P., Lara, E., Royo-Llonch, M., Sà, E. L., Lucena, T., Pujalte, M. J., Vaqué, D., Duarte, C. M., Gasol, J. M., Pedrós-Alió, C., Sánchez, O. & Acinas, S. G. 2020. Diversity and distribution of marine heterotrophic bacteria from a large culture collection. BMC Microbiol., 20:207.

Scholin, C. A., Herzog, M., Sogin, M. & Anderson, D. M. 1994. Identification of group-and strain-specific genetic markers for globally distributed

Alexandrium (Dinophyceae). ii. sequence analysis of a fragment of the LSU rRNA gene. J. Phycol., 30:999–1011.

Seip, K. L. & Reynolds, C. S. 1995. Phytoplankton functional attributes along trophic gradient and season. Limnol. Oceanogr., 40:589–597.

Sellers, C. G., Gast, R. J. & Sanders, R. W. 2014. Selective feeding and foreign plastid retention in an Antarctic dinoflagellate. J. Phycol., 50:1081–1088.

Seo, H. -S., Jeong, Y. -H. & Kim, D. -S. 2020. A study on the characteristics of summer water temperature fluctuations by spectral analysis in coast of Korea in 2016. J. Korean Soc. Mar. Environ. Saf. 26:186–194.

Seong, K. A., Jeong, H. J., Kim, S., Kim, G. H. & Kang, J. H. 2006. Bacterivory by co-occurring red-tide algae, heterotrophic nanoflagellates, and ciliates. Mar. Ecol. Prog. Ser., 322:85–97.

Shapiro, S. S. & Wilk, M. B. 1965. An analysis of variance test for normality (complete samples). Biometrika, 52:591–611.

Sherr, B. F., Sherr, E. B. & Fallon, R. D. 1987. Use of monodispersed, fluorescently labeled bacteria to estimate *in situ* protozoan bacterivory. Appl. Environ. Microbiol., 53:958–965.

Sherr, E. B. & Sherr, B. F. 2007. Heterotrophic dinoflagellates: a significant component of microzooplankton biomass and major grazers of diatoms in the sea. Mar. Ecol. Prog. Ser., 352:187–197.

Shields, J. D. 1994. The parasitic dinoflagellates of marine crustaceans. Annu. Rev. Fish. Dis., 4:241–271.

Shimizu, Y. 1996. Microalgal metabolites: a new perspective. Annu. Rev. Microbiol., 50:431–465.

Shin, K., Jang, M. -C., Jang, P. -K., Ju, S. -J., Lee, T. -K. & Chang, M. 2003. Influence of food quality on egg production and viability of the marine planktonic copepod *Acartia omorii*. Prog. Oceanogr., 57:265–277.

Shumway, S. E. 1990. A review of the effects of algal blooms on shellfish and aquaculture. J. World Aquac. Soc., 21:65–104.

Shumway, S. E., Burkholder, J. M. & Morton, S. L. 2018. *Harmful algal blooms: a compendium desk reference*. John Wiley & Sons, Hoboken, NJ, 667 pp.

Shumway, S. E., Burkholder, J. M. & Springer, J. 2006. Effects of the estuarine dinoflagellate *Pfiesteria shumwayae* (Dinophyceae) on

survival and grazing activity of several shellfish species. Harmful Algae, 5:442–458.

Siano, R., Kooistra, W. H., Montresor, M. & Zingone, A. 2009. Unarmoured and thin-walled dinoflagellates from the Gulf of Naples, with the description of *Woloszynskia cincta* sp. nov. (Dinophyceae, Suessiales). Phycologia, 48:44–65.

Skovgaard, A. 1996. Mixotrophy in *Fragilidium subglobosum* (Dinophyceae): growth and grazing responses as functions of light intensity. Mar. Ecol. Prog. Ser., 143:247–253.

Skovgaard, A. 2000. A phagotrophically derivable growth factor in the plastidic dinoflagellate *Gyrodinium resplendens* (Dinophyceae). J. Phycol., 36:1069–1078.

Skovgaard, A., Karpov, S. A. & Guillou, L. 2012. The parasitic dinoflagellates *Blastodinium* spp. inhabiting the gut of marine, planktonic copepods: morphology, ecology, and unrecognized species diversity. Front. Microbiol., 3:305.

Smalley, G. W., Coats, D. W. & Stoecker, D. K. 2003. Feeding in the mixotrophic dinoflagellate *Ceratium furca* is influenced by intracellular nutrient concentrations. Mar. Ecol. Prog. Ser., 262:137–151.

Smayda, T. J. 1997. Harmful algal blooms: their ecophysiology and general relevance to phytoplankton blooms in the sea. Limnol. Oceanogr., 42:1137–1153.

Smith, K. F., Rhodes, L., Harwood, D. T., Adamson, J., Moisan, C., Munday, R. & Tillmann, U. 2016. Detection of *Azadinium poporum* in New Zealand: the use of molecular tools to assist with species isolations. J. Appl. Phycol., 28:1125–1132.

Soehner, S., Zinssmeister, C., Kirsch, M. & Gottschling, M. 2012. Who am I-and if so, how many? Species diversity of calcareous dinophytes (Thoracosphaeraceae, Peridiniales) in the Mediterranean Sea. Org. Divers. Evol., 12:339–348.

Spilling, K., Olli, K., Lehtoranta, J., Kremp, A., Tedesco, L., Tamelander, T., Klais, R., Peltonen, H. & Tamminen, T. 2018. Shifting diatom: dinoflagellate dominance during spring bloom in the Baltic Sea and its potential effects on biogeochemical cycling. Front. Mar. Sci., 5:327.

Staehr, P. A. & Sand-Jensen, K. A. J. 2006. Seasonal changes in temperature and nutrient control of photosynthesis, respiration and growth of natural phytoplankton communities. Freshwater Biol., 51:249–262.

Stamatakis, A. 2006. RaxML-VI-HPC: maximum likelihood-based phylogenetic analyses with thousands of taxa and mixed models. Bioinformatics, 22:2688–2690.

Stauffer, B. A., Gellene, A. G., Rico, D., Sur, C. & Caron, D. A. 2017. Grazing of the heterotrophic dinoflagellate *Noctiluca scintillans* on dinoflagellate and raphidophyte prey. Aquat. Microb. Ecol., 80:193–207.

Stoecker, D. K. 1999. Mixotrophy among Dinoflagellates. J. Eukaryot. Microbiol. 46:397-401.

Stoecker, D. K. & Sanders, N. K. 1985. Differential grazing by *Acartia tonsa* on a dinoflagellate and a tintinnid. J. Plankton Res., 7:85–100.

Stoecker, D. K., Hansen, P. J., Caron, D. A. & Mitra, A. 2017. Mixotrophy in the marine plankton. Annu. Rev. Mar. Sci., 9:311–335.

Stoecker, D. K., Li, A., Coats, D. W., Gustafson, D. E. & Nannen, M. K. 1997. Mixotrophy in the dinoflagellate *Prorocentrum minimum*. Mar. Ecol. Prog. Ser., 152:1–12.

Strom, S. L. & Buskey, E. J. 1993. Feeding, growth, and behavior of the thecate heterotrophic dinoflagellate *Oblea rotunda*. Limnol. Oceanogr., 38:965–977.

Sugawara, T., Yamashita, K., Sakai, S., Asai, A., Nagao, A., Shiraishi, T., Imai, I. & Hirata, T. 2007. Induction of apoptosis in DLD-1 human colon cancer cells by peridinin isolated from the dinoflagellate, *Heterocapsa triquetra*. Biosci. Biotechnol. Biochem., 71:1069–1072.

Sweeney, B. M. 1971. Laboratory studies of a green *Noctiluca* from New Guinea. J. Phycol., 7:53–58.

Tada, K., Pithakpol, S. & Montani, S. 2004. Seasonal variation in the abundance of *Noctiluca scintillans* in the Seto Inland Sea, Japan. Plankton Biol. Ecol., 51:7–14.

Tamura, K., Dudley, J., Nei, M. & Kumar, S. 2007. MEGA4: molecular evolutionary genetics analysis (MEGA) software version 4.0. Mol. Biol. Evol., 24:1596–1599.

Tan, C. H., Show, P. L., Chang, J. -S., Ling, T. C. & Lan, J. C. -W. 2015. Novel approaches of producing bioenergies from microalgae: a recent review. Biotechnol. Adv., 33:1219– 1227.

Tang, E. P. Y. 1996. Why do dinoflagellates have lower growth rates? J. Phycol., 32:80-84.

Tarasov, N. I. 1956. *Marine luminescence*. *Naval Oceanographic Office, Report No. NOOT-21*. National Space Technology Laboratories Station, Bay St. Louis, MO, 183 pp.

Taylor, F. J. R., Hoppenrath, M. & Saldarriaga, J. F. 2008. Dinoflagellate diversity and distribution. Biodivers. Conserv., 17:407–418.

Tett, P. B. 1971. The relation between dinoflagellates and the bioluminescence of sea water. J. Mar. Biol. Assoc. U. K., 51:183–206.

Tezuka, Y. 1990. Bacterial regeneration of ammonium and phosphate as affected by the carbon: nitrogen: phosphorus ratio of organic substrates. Microb. Ecol., 19:227–238.

Thomas, W. H. & Gibson, C. H. 1990a. Effects of small-scale turbulence on microalgae. J. Appl. Phycol., 2:71–77.

Thomas, W. H. & Gibson, C. H. 1990b. Quantified small-scale turbulence inhibits a red tide dinoflagellate, *Gonyaulax polyedra* Stein. Deep Sea Res. Part A Oceanogr. Res. Pap., 37:1583–1593.

Thompson, P. A., Guo, M. X., Harrison, P. J. & Whyte, J. N. C. 1992. Effects of variation in temperature. II. On the fatty acid composition of eight species of marine phytoplankton. J. Phycol., 28:488–497.

Tillmann, U. & Hoppenrath, M. 2013. Life cycle of the pseudocolonial dinoflagellate *Polykrikos kofoidii* (Gymnodiniales, Dinoflagellata). J. Phycol., 49:298–317.

Torres-Tiji, Y., Fields, F. J. & Mayfield, S. P. 2020. Microalgae as a future food source. Biotechnol. Adv., 41:107536.

Trenberth, K. E., Jones, P. D., Ambenje, P., Bojariu, R., Easterling, D., Tank, A. K., Parker, D., Rahimzadeh, F., Renwick, J. A., Rusticucci, M., Soden, B. & Zhai, P. 2007. “Observations: surface and atmospheric climate change” in Climate Change 2007: The Physical Science Basis. Contribution of Working Group 1 to the 4th Assessment Report of the Intergovernmental Panel on Climate Change, Cambridge University Press, Cambridge, pp 235–336.

Tsikoti, C. & Genitsaris, S. 2021. Review of harmful algal blooms in the coastal Mediterranean Sea, with a focus on Greek waters. Diversity, 13:396.

Tukey, J. W. 1953. The problem of multiple comparisons. In: Braun HI (ed) The Collected Works of John W. Tukey, Volume VIII, Multiple Comparisons: 1948–1983, Chapman and Hall, London, pp 1–300.

Turkoglu, M. 2013. Red tides of the dinoflagellate *Noctiluca scintillans* associated with eutrophication in the Sea of Marmara (the Dardanelles, Turkey). Oceanologia, 55:709–732.

Turner, J. T. 2006. Harmful algae interactions with marine planktonic grazers. Ecological Studies, 189:259–270.

Turner, J. T. & Borkman, D. G. 2005. Impact of zooplankton grazing on *Alexandrium* blooms in the offshore Gulf of Maine. Deep-Sea Res. (2 Top. Stud. Oceanogr.), 52:2801–2816.

Turner, J. T., Doucette, G. J., Powell, C. L., Kulis, D. M., Keafer, B. A. & Anderson, D. M. 2000. Accumulation of red tide toxins in larger size fractions of zooplankton assemblages from Massachusetts Bay, USA. Mar. Ecol. Prog. Ser., 203:95–107.

Turner, J. T., Roncalli, V., Ciminiello, P., Dell'Aversano, C., Fattorusso, E., Tartaglione, L., Carotenuto, Y., Romano, G., Esposito, F., Miralto, A. & Ianora, A. 2012. Biogeographic effects of the Gulf of Mexico red tide dinoflagellate *Karenia brevis* on Mediterranean copepods. Harmful Algae, 16:63–73.

Uhlig, G. & Sahling, G. 1990. Long-term studies on *Noctiluca scintillans* in the German Bight population dynamics and red tide phenomena 1968–1988. Neth. J. Sea Res., 25:101–112.

Vadstein, O., Jensen, A., Olsen, Y. & Reinertsen, H. 1988. Growth and phosphorus status of limnetic phytoplankton and bacteria. Limnol. Oceanogr., 33:489–503.

Valiadi, M., de Rond, T., Amorim, A., Gittins, J. R., Gubili, C., Moore, B. S., Iglesias-Rodriguez, D. & Latz, M. I. 2019. Molecular and biochemical basis for the loss of bioluminescence in the dinoflagellate *Noctiluca scintillans* along the west coast of the USA. Limnol. Oceanogr., 64:2709–2724.

Valiadi, M. & Iglesias-Rodriguez, D. 2013. Understanding bioluminescence in dinoflagellates: how far have we come? Microorganisms, 1:3–25.

Valiadi, M. & Iglesias-Rodriguez, M. D. 2014. Diversity of the luciferin binding protein gene in bioluminescent dinoflagellates: insights from a new gene in *Noctiluca scintillans* and sequences from Gonyaulacoid genera. J. Eukaryotic Microbiol., 61:134–145.

Van Wambeke, F., Christaki, U., Bianchi, M., Psarra, S. & Tselepides, A. 2000. Heterotrophic bacterial production in the Cretan Sea (NE Mediterranean). Prog. Oceanogr., 46:205–216.

Vaulot, D., Sim, C. W. H., Ong, D., Teo, B., Biwer, C., Jamy, M. & Lopes dos Santos, A. 2022. metaPR2: a database of eukaryotic 18S rRNA metabarcodes with an emphasis on protists. Mol. Ecol. Resour., 22:3188–3201.

Vijayan, J., Ammini, P. & Nathan, V. K. 2022. Diversity pattern of marine culturable heterotrophic bacteria in a region with coexisting upwelling and mud banks in the southeastern Arabian Sea. Environ. Sci. Pollut. Res., 29:3967–3982.

Volkman, J. K., Jeffrey, S. W., Nichols, P. D., Rogers, G. I. & Garland, C. D. 1989. Fatty acid and lipid composition of 10 species of microalgae used in mariculture. J. Exp. Mar. Biol. Ecol., 128:219–240.

Wang, S., Chen, J., Li, Z., Wang, Y., Fu, B., Han, X. & Zheng, L. 2015. Cultivation of the benthic microalga *Prorocentrum lima* for the production of diarrhetic shellfish poisoning toxins in a vertical flat photobioreactor. Bioresour. Technol., 179:243–248.

Watts, P. C., Martin, L. E., Kimmance, S. A., Montagnes, D. J. & Lowe, C. D. 2010. The distribution of *Oxyrrhis marina*: a global disperser or poorly characterized endemic?. J. Plankton Res., 33:579–589.

Welch, B. L. 1947. The generalization of ‘student’s’ problem when several different population variances are involved. Biometrika, 34:28–35.

Westfall, J. A., Bradbury, P. C. & Townsend, J. W. 1983. Ultrastructure of the dinoflagellate *Polykrikos*. I. Development of the nematocyst-taeniocyst complex and morphology of the site for extrusion. J. Cell Sci., 63:245-61.

Whittington, J., Sherman, B., Green, D. & Oliver, R. L. 2000. Growth of *Ceratium hirundinella* in a subtropical Australian reservoir: the role of vertical migration. J. Plankton Res., 22:1025–1045.

Wiklund, A. K. E., Dahlgren, K., Sundelin, B. & Andersson, A. 2009. Effects of warming and shifts of pelagic food web structure on benthic

productivity in a coastal marine system. Mar. Ecol. Prog. Ser., 396:13–25.

Williams, T. M. & Kooyman, G. L. 1985. Swimming performance and hydrodynamic characteristics of harbor seals *Phoca vitulina*. Physiol. Zool., 58:576–589.

Wisecaver, J. H., Brosnahan, M. L. & Hackett, J. D. 2013. Horizontal gene transfer is a significant driver of gene innovation in dinoflagellates. Genome Biol. Evol., 5:2368–2381.

Wolny, J. L., Scott, P. S., Tustison, J. & Brooks, C. R. 2015. Monitoring the 2007 Florida east coast *Karenia brevis* (Dinophyceae) red tide and neurotoxic shellfish poisoning (NSP) event. Algae, 30:49–58.

Wynn, J. P. & Ratledge, C. 2005. Oils from microorganisms. *In* Shahidi, F. (Ed.) *Bailey's Industrial Oil and Fat Products*. John Wiley & Sons, Hoboken, NJ, pp. 121–153.

Xu, N., Duan, S., Li, A., Zhang, C., Cai, Z. & Hu, Z. 2010. Effects of temperature, salinity and irradiance on the growth of the harmful dinoflagellate *Prorocentrum donghaiense* Lu. Harmful Algae, 9:13–17.

Yokouchi, K., Onuma, R. & Horiguchi, T. 2018. Ultrastructure and phylogeny of a new species of mixotrophic dinoflagellate, *Paragymnodinium stigmaticum* sp. nov. (Gymnodiniales, Dinophyceae). Phycologia 57:539–554.

Yokouchi, K., Suzuki, K. & Horiguchi, T. 2022. Comparative analyses of nutritional strategies among the species within the genus *Paragymnodinium* (Gymnodiniales, Dinophyceae). J. Phycol., 58:490–501.

Yongmanitchai, W. & Ward, O. P. 1991. Growth of and omega-3 fatty acid production by *Phaeodactylum tricornutum* under different culture conditions. Appl. Environ. Microbiol., 57:419–425.

Yoo, Y. D., Jeong, H. J., Kang, N. S., Song, J. Y., Kim, K. Y., Lee, G. & Kim, J. 2010. Feeding by the Newly Described Mixotrophic Dinoflagellate *Paragymnodinium shiwhaense*: Feeding Mechanism, Prey Species, and Effect of Prey Concentration. J. Eukaryot. Microbiol., 57:145–158.

Yoo, Y. D., Jeong, H. J., Kim, M. S., Kang, N. S., Song, J. Y., Shin, W., Kim, K. Y. & Lee, K. 2009. Feeding by phototrophic red-tide dinoflagellates on the ubiquitous marine diatom *Skeletonema costatum*. J. Eukaryot. Microbiol., 56:413–420.

Yoo, Y. D., Jeong, H. J., Lee, S. Y., Yoon, E. Y., Kang, N. S., Lim, A. S., Lee, K. H., Jang, S. H., Park, J. Y. & Kim, H. S. 2015. Feeding by heterotrophic protists on the toxic dinoflagellate *Ostreopsis* cf. *ovata*. Harmful Algae, 49:1–9.

Yoo, Y. D., Seong, K. A., Kim, J. S., Nam, S. W., Jeong, H. J., Rho, J. R., Yih, W. H. & Kim, H. S. 2018. Mixotrophy in the sand-dwelling dinoflagellate *Thecadinium kofoidii*. Mar. Biol. Res. 14:165–172.

Yoo, Y. D., Yoon, E. Y., Lee, K. H., Kang, N. S. & Jeong, H. J. 2013. Growth and ingestion rates of heterotrophic dinoflagellates and a ciliate on the mixotrophic dinoflagellate *Biecheleria cincta*. Algae, 28:343–354.

You, J. H., Jeong, H. J., Kang, H. C., Ok, J. H., Park, S. A., Lim, A. S. 2020a. Feeding by common heterotrophic protist predators on seven *Prorocentrum* species. Algae, 35:61–78.

You, J. H., Jeong, H. J., Lim, A. S., Ok, J. H. & Kang, H. C. 2020b. Effects of irradiance and temperature on the growth and feeding of the obligate mixotrophic dinoflagellate *Gymnodinium smaydae*. Mar. Biol., 167:1–13.

You, J. H., Jeong, H. J., Ok, J. H., Kang, H. C., Park, S. A., Eom, S. H., Lee, S. Y. & Kang, N. S. 2023a. Effects of temperature on the autotrophic and mixotrophic growth rates of the dinoflagellate *Biecheleria cincta* and its spatiotemporal distributions under current temperature and global warming conditions. Mar. Biol., 170:15.

You, J. H., Jeong, H. J., Park, S. A., Ok, J. H., Kang, H. C., Eom, S. H. & Lim, A. S. 2022. Development of an automatic system for cultivating the bioluminescent heterotrophic dinoflagellate *Noctiluca scintillans* on a 100-liter scale. Algae, 37:149–161.

You, J. H., Ok, J. H., Kang, H. C., Park, S. A., Eom, S. H. & Jeong, H. J. 2023b. Five phototrophic *Scrippsiella* species lacking mixotrophic ability and the extended prey spectrum of *Scrippsiella acuminata* (Thoracosphaerales, Dinophyceae). Algae, 38:111–126.

Zehr, J. P. 2011. Nitrogen fixation by marine cyanobacteria. Trends. Microbiol., 19:162–173.

Zhang, S., Liu, H., Guo, C. & Harrison, P. J. 2016. Differential feeding and growth of *Noctiluca scintillans* on monospecific and mixed diets. Mar. Ecol. Prog. Ser., 549:27–40.

Zhang, Q., Yu, R., Song, J., Yan, T., Wang, Y. & Zhou, M. 2011. Will harmful dinoflagellate *Karenia mikimotoi* grow phagotrophically? Chin. J. Oceanol. Limnol., 29:849–859.

Zhang, Z., Green, B. R. & Cavalier-Smith, T. 1999. Single gene circles in dinoflagellate chloroplast genomes. Nature, 400:155–159.

Abstract in Korean

온난화, 먹이, 포식자가 혼합영양성 와편모류의 한국 연안 분포에 미치는 영향과 100리터급 와편모류 자동배양시스템 개발

혼합영양성 와편모류는 해양 생태계의 중요한 구성 요소이고, 일차생산자, 먹이, 포식자 및 공생체로써 전지구적인 생물지구화학적 순환에 관여한다. 그들은 때때로 플랑크톤 군집에서 우위를 차지하여 적조 혹은 유해 조류 대번성을 일으킨다. 그러므로 이들의 개체군 동태는 이들의 먹이와 포식자의 개체군 동태와 관련이 깊다. 따라서 혼합영양성 와편모류의 분포를 이해하는 것은 생태적으로도, 상업적으로도 중요하다. 지구 온난화가 지속되면 혼합영양성 와편모류의 분포는 변할 것으로 예상된다. 이들의 분포 변화는 이들의 먹이와 포식자의 분포에 영향을 줄 것이다. 따라서 한 혼합영양성 와편모류의 분포를 예측하기 위해서는 이들의 성장과 사망에 영향을 주는 요소들이 연구되어야 한다. 혼합영양성 와편모류의 분포에 영향을 주는 주요 생태학적 요인으로는 먹이 또는 영양염, 광량, 수온, 염분, 그리고 포식자 등이 있다. 본 연구에서는 생태생리학적 특성이 서로 다른 두 혼합영양성 와편모류 *Gymnodinium smaydae*와 *Biecheleria cincta*, 그리고 광영양성 와편모류인 *Scrippsiella* 종들을 대상으로 온난화, 먹이, 포식자의 영향이 조사되었다. 더불어 혼합영양성 및 종속영양성 와편모류의 생태생리학적 특성을 기반으로 이들을 연속적으로 자동 배양할 수 있는 새로운 시스템을 개발하였다.

제2장에서는 혼합영양성 와편모류 *B. cincta*와 *G. smaydae*의 현재 한국 연안에서의 분포를 알아내고 이를 이용하여 온난화 조건에서의 분포 변화 예측을 위해, 2015-2018년 동안 한국 연안의 27개 정점에서 채집한 표층수를 양적 실시간 중합효소 연쇄반응법 (quantitative real-time polymerase chain reaction)을 이용하여 분석하였다. 그리고 현장 관측 결과를 활용하여 현재의 수온에서 2, 4, 6도가 상승할 때의 분포 변화를 예측하였다. 2015-2018년 동안 *B. cincta*는 27개의 정점 중 13개의 정점에서 검출되었으며, 사계절 내내 출현하였으나 여름에 가장 많은 정점(8개의 정점)에서 출현하였다. 그러나 *B. cincta*가 가장 높은 농도로 출현한 것은 가을이었고, 수온은 25.1도였다. 반면 *G. smaydae*는 27개의 정점 중 24개의 정점에서

검출되었으며, 사계절 내내 출현하였으나 여름에 가장 많은 정점(21개의 정점)에서 출현하였다. 또한 *G. smaydae*가 가장 높은 농도로 출현한 것도 여름이었고, 수온은 23.8도였다. 수온 상승으로 인한 분포 변화를 예측했을 때, *B. cincta*는 여름에는 2, 4, 6도가 상승했을 때, 가을에는 6도가 상승했을 때 일부 정점에서 생존할 수 없을 것으로 예상되었다. 그러나 *G. smaydae*는 여름에만 2, 4, 6도 상승했을 때 일부 지점에서 생존할 수 없을 것으로 예상되었다. 결과적으로 *B. cincta*는 한국 연안에서 *G. smaydae*보다 출현 분포가 좁았고, *G. smaydae*에 비해 수온의 변화에 더 취약한 것으로 예측되었다.

제3장에서는 혼합영양성 와편모류 *B. cincta*와 *G. smaydae*의 온난화에 대한 영향을 알아보기 위해, 다양한 수온 조건에서의 두 종의 독립영양 및 혼합영양 성장률과 섭식률을 측정하였다. 혼합영양 성장률과 섭식률을 측정하기 위해, *B. cincta*는 침편모조류 *Heterosigma akashiwo*를, *G. smaydae*는 와편모류 *Heterocapsa rotundata*를 먹이로써 사용하였다. 5-35도의 수온에서 *B. cincta*와 *G. smaydae*는 먹이 없이는 모두 성장하지 못했다. 그러나, 먹이가 있을 때, *B. cincta*는 15-25도의 수온에서, *G. smaydae*는 10-32도의 수온에서 성장이 가능하였다. 또한 두 종 모두 25도에서 가장 높은 성장률을 보여주었다. 따라서 *B. cincta*의 생존수온범위는 현장에서 *B. cincta*가 *G. smaydae*에 비해 좁은 분포를 가지고, 수온의 변화에 취약한 것을 설명한다. 즉, 제3장의 결과는 제2장의 두 종의 현장 분포 결과를 뒷바침한다.

제4장에서는 혼합영양성 와편모류 *G. smaydae*의 포식자에 대한 영향을 알아보기 위해, 해양에 흔히 존재하는 종속영양성 원생생물 포식자가 혼합영양성 와편모류인 *G. smaydae*를 먹는 지에 대해 조사하였다. 실험 결과, *Oxyrrhis marina*, *Gyrodinium dominans*, *G. moestrupii*, 그리고 *Pelagostrobilidium* sp.가 *G. smaydae*를 섭식할 수 있었다. 그러나 *Polykrikos kofoidii*와 *Oblea rotunda*는 *G. smaydae*를 섭식하지 못했다. 또한, *G. smaydae*는 포식자 *O. marina*와 *G. dominans*의 성장을 가능하게 했지만, 두 포식자의 성장률은 다른 먹이종을 섭식할 때보다 낮았다. 따라서 *O. marina*와 *G. dominans*는 *G. smaydae*의 효과적인 포식자일 수는 있지만, *G. smaydae*는 다른 먹이종에 비해 포식자의 높은 성장률을 지원하는 먹이는 아닐 것으로 판단되었다. *B. cincta*의 포식자는 기존 연구에서 밝혀져있는데, *B.*

*cincta*는 포식자 *O. marina*와 *Strobilidium* sp.의 비교적 높은 성장률을 지원하는 먹이종으로 알려져있다. 따라서 *G. smaydae*의 개체군 동태는 *B. cincta*에 비해 포식자 *O. marina*의 개체군 동태에 적은 영향을 줄 것이다.

제5장에서는 광영양성 와편모류 *Scrippsiella* spp.의 먹이 가용성에 대한 영향을 알아보기 위해, 15개의 먹이 종류를 투입하여 *S. donghaiensis*, *S. lachrymosa*, *S. masanensis*, *S. plana*, *S. ramonii*의 혼합영양성 능력을 조사하였다. 또한, 혼합영양성 와편모류 *S. acuminata*가 형광으로 표지된 미세입자와 종속영양성 박테리아를 섭식할 수 있는 지 조사하였다. 와편모류 속 *Scrippsiella*의 종은 바다에서 흔하게 발견되고 때때로 해로운 적조를 일으킨다. *Scrippsiella* 종의 성장에 영향을 미치는 요인인 빛, 수온, 포식자 등과 관련된 연구는 꾸준히 진행되어 왔으나, 혼합영양성 능력과 먹이의 가용성에 대한 연구는 많지 않았다. 제5장의 실험 결과, 5개의 *Scrippsiella* 종은 어떠한 잠재적 먹이도 섭식하지 않았으며, 따라서 이는 혼합영양성 능력의 결여를 나타내었다. 그러나 *S. acuminata*는 형광으로 표지된 미세입자와 종속영양성 박테리아를 모두 섭식하였고, 이로 인해 *S. acuminata*의 섭식이 가능한 먹이 범위가 확장되었다. 결론적으로, 혼합영양성 실험이 된 *Scrippsiella* 종의 총 수 대비 혼합영양성 종의 비율이 100%에서 20-38%로 낮아졌다. 혼합영양성 능력을 가진 *S. acuminata*는 *S. donghaiensis*, *S. lachrymosa*, *S. masanensis*, *S. plana*, *S. ramonii*와는 다른 생태적 지위를 차지할 것이다.

제6장에서는 혼합영양성 종인 *G. smaydae*와 *B. cincta*, 그리고 종속영양성 와편모류 *G. dominans*, *P. kofoidii*, *Noctiluca scintillans*의 배양의 자동화 방법과 시스템을 개발하였다. 혼합영양성과 종속영양성 와편모류는 유용한 물질의 생산과 천적에 대한 개체수 조절 능력으로 인해 가치가 있다. 실험에 사용된 종 모두 적조 종을 섭식하여 개체수를 제어할 수 있거나 오메가3, 발광물질 등 유용한 물질을 생산함으로써 유용성이 입증된 종이다. 그러나 그들의 생태생리학적 특성으로 인해 배양이 어려워 연구 및 상업적 응용이 제한되어 왔다. 따라서 유용한 혼합영양성 및 종속영양성 생물을 배양하기 위해서는 공학적인 기술과 함께 생태생리학적 특성을 근본적으로 이해하는 것이 중요하다. 이러한 시스템을 개발하기 위해 예비 실험 또는 문헌 고찰을 통해 최적의 먹이 종을 선택하고, 또한 각 포식자의 성장률 및 섭식율을 조사하였다.

더불어, 먹이와 그 먹이를 섭식하는 포식자의 성장률을 고려하여 먹이 투입 간격과 투입량을 결정하였다. 10리터 규모에서 100리터 규모의 자동화 시스템으로 확장하기 위해 새롭게 개발된 소프트웨어를 도입하였다. 개발된 시스템은 *G. smaydae*, *B. cincta*, *G. dominans*, *P. kofoidii*, *N. scintillans*를 자동으로 연속 배양하는 데에 성공하였다. 이렇게 동일한 환경에서 오염없이 생산된 대량의 배양체는 다양한 방면의 응용 연구 및 상업화를 수월하게 할 것이다.

본 학위논문에서는 전반적으로, 현장 관측과 실내 실험을 통해 주요 생태학적 요인인 온난화, 먹이, 그리고 포식자가 혼합영양성 와편모류에게 미치는 영향을 연구하였다. 이 와편모류들은 그 생태학적 요인들에 대해 다르게 반응하였고, 이것은 해양 생태계에서 그들의 분포와 생태학적 지위가 다른 것을 설명할 수 있었다. 게다가, 와편모류의 생태생리학적 특성을 기반으로 자동으로 대량 배양하는 시스템을 개발하여 미래에 다양한 종류의 실험을 가능하게 하였다. 결과적으로, 본 학위논문은 혼합영양성 와편모류의 생태학적 그리고 생리학적 특징을 연구함으로써 해양생태계의 구조와 기능을 더 잘 이해하게 하고, 나아가 연구 및 상업적 목적으로 그들을 활용하는 데에 기여하였다.

주요어 : 기후변화, 대량배양, 생태생리학, 영양방식, 원생생물, 적조, 플랑크톤, 해양생태계

학 번 : 2017-22349

Acknowledgement

2017년에 입학하여 약 7년간의 학위과정을 마치고, 박사학위논문을 제출하게 되었습니다. 저의 학위논문은 제 곁에 있는 많은 분들의 도움과 지지 덕분에 완성될 수 있었습니다. 이 소중한 순간을 함께 나눌 수 있는 이 자리를 빌려 감사의 말씀을 전합니다.

서울대학교 플랑크톤 연구실을 설립해주신 심재형 교수님께 깊은 감사를 드립니다. 교수님께서 이끌어 주신 플랑크톤 연구는 우리나라 해양학 발전에 큰 역할을 하였으며, 덕분에 저는 꿈꾸던 해양학자가 되는 길을 걸을 수 있었습니다.

항상 휴일없이 밤낮으로 아낌없는 지도와 가르침을 주셨던 저의 은사님 이신 정해진 교수님께 감사드립니다. 교수님께서는 학생이 성장하는 것을 보는 것이 가장 큰 기쁨이라며 항상 연구실 문을 열어 두시고 격려와 함께 많은 기회와 지원을 아끼지 않으셨습니다. 또한 학문적인 것뿐만 아니라 삶을 살아가는 지혜도 알려주셨으며, 학자로도 인격자로도 성장할 수 있도록 도와주셨습니다. 교수님께는 어떠한 표현도 부족하지만, 감사하고 존경합니다. 인간적으로는 항상 주위의 모든 사람에게 감사함을 가지고 겸손해야 하며, 학자로서는 연구를 통해 세상과 소통해야 한다고 하셨던 가르침, 잊지 않고 마음에 새겨 두도록 하겠습니다.

바쁘신 일정에도 저의 학위논문 심사를 위해 시간을 할애해주시고 더 깊이 있는 학문적 고찰을 도와주신 서울대학교 김종성 교수님, 황청연 교수님, 조형택 교수님, 군산대학교 노정래 교수님께 감사의 인사를 드립니다. 또한 저에게 해양학이라는 학문의 길을 열어 주시고 다양한 분야를 가르쳐 주신 군산대학교 최문술 교수님, 조수근 교수님, 김영식 교수님, 이기영 교수님, 이원호 교수님, 김형섭 교수님께도 감사드립니다.

학위과정 동안 선배님들의 많은 가르침과 조언에 큰 도움을 받았습니다. 기초부터 꼼꼼하게 가르쳐 주신 생태바이오적조 연구실 선배님들께도 감사의 인사를 전합니다. 많은 실험들에 참여하게 해주시고, 지금도 여전히 논문에 대해 아낌없는 조언을 주시는 임안숙 교수님, 다양한 데이터 분석 방법을 가르쳐 주시고 모르는 부분들에 대해서 꼼꼼하게 설명해주신 이승연 박사님, 실험뿐만 아니라 생활

방면에서도 세심하게 챙겨 주신 이경하 박사님, 연구에 대한 열정으로 제가 생각하지 못했던 새로운 방면을 제시해 주셨던 장세현 교수님께 감사드립니다. 또한 항상 웃는 모습과 따뜻한 목소리로 후배들을 격려하고 지지하며, 열정 가득한 모습으로 후배들에게 모범이 되었던 옥진희 박사님께 감사합니다. 그리고 학위과정동안 함께 동고동락하여 힘들 때도 서로 격려해주고 함께 성장해온 동료와 후배들 모두 감사합니다. 동기로 입학하였지만 실험실이 낯선 저에게 정신적으로도 큰 힘이 되어주고 학문적으로도 모범이 되어준 선배 같은 강희창 박사님, 항상 먼저 나서서 도와주고 고민해주던 박상아, 어려운 상황에서도 꿋꿋하게 함께 해주던 엄세희, 모두 감사합니다. 그리고 제가 연구에 몰두할 수 있게 도와주신 김은지 선생님에게도 감사합니다. 여러분이 있어 제가 이 시간을 무사히 보내며 마칠 수 있었습니다. 저 또한 여러분과 같은 좋은 선배, 동료, 후배가 되도록 노력하겠습니다.

고등학교 시절부터 항상 제 힘이 되어주고 무조건적으로 절 응원해주는 친구들, 김소현, 최선아, 이자연, 박미소에게도 감사의 인사를 전합니다. 또한 학부시절부터 함께하여, 지금은 멀리 떨어져 있지만 잊지 않고 꼬박꼬박 안부를 물어주는 우리 동기들, 주소연, 김지민, 김소연, 이조은, 강명지에게 고마움을 전합니다. 여러분이 있어 항상 든든했고 흔들리지 않을 수 있었습니다.

마지막으로 사랑하는 제 가족들에게 이 학위논문을 바칩니다. 항상 저를 믿고 제가 하고자 하는 일들을 응원하고 사랑해 주셔서 감사합니다. 바람이 불고 때로는 비가 와도 베풀어 주신 사랑으로 무사히 꺾이지 않고 여기까지 올 수 있었습니다. 하나라도 저에게 더 해주고 싶어하셨던 그 모습들을 기억합니다. 아버지, 어머니, 그리고 오빠. 인생의 선배이자 동반자, 그리고 친구로서 따뜻한 격려를 해주고 쓴 소리도 마다하지 않아 주셔서 덕분에 길을 잃어버리지 않고, 항상 웃으면서 생활할 수 있었습니다. 또 멀리서도 항상 제 건강부터 챙겨 주신 할머니, 작은 아버지, 외삼촌께도 감사인사를 전합니다.

박사학위 논문을 마치며, 이것은 끝이 아닌 새로운 시작임을 잘 알고 있습니다. 이 감사의 마음을 잊지 않고, 더욱 학문에 정진하도록 하겠습니다. 감사합니다.